The Role of β-cell Glutamate Receptors in Pancreatic Endocrine Function and in the Pathogenesis of Type 1 Diabetes Mellitus

Louis Dwomoh

Department of Biological, Biomedical and Analytical Sciences

University of the West of England, Bristol

November, 2016

A thesis submitted in partial fulfilment of the requirements of the University of the West of England, Bristol for the degree of Doctor of Philosophy

This research was carried out

in collaboration with the University of Bristol

Acknowledgements

My deepest gratitude goes to my Director of Studies, Professor Aniko Varadi for believing in me from the beginning and for her encouragement, constructive criticisms, support, inspiration and motherly advice throughout my PhD. I could not have made it this far without her. I would also like to thank Professor Richard Luxton (second supervisor) for his support. My outmost thanks also goes to the Faculty of Applied Sciences, UWE Bristol and the Graduate School for funding my PhD. I hope they find it a worthwhile investment.

At the University of Bristol, I would like to thank Professor Elek Molnar (second supervisor) for allowing me to use his laboratory for some of my experiments and also for his suggestions and comments throughout my PhD. I would also like to thank Dr. Garry Whitehead and Dr. Alexandra Spittle for their support and for putting up with me in their laboratory.

I would also like to thank Professor Colin Dayan (Cardiff University) for providing us with patient samples for this research and also thank the patients who agreed have their samples taken for this research.

At the University of the West of England, I would like to thank Marian Manso, Dr. Shavanthi Rajatileka, Dr. Man-Kim Cheung, Dr. Emmanuel Adukwu, Paul Deanne and Carolyn Morgan for their support and encouragement in my times of need.

Finally, I would like to thank my mum for putting up with me during all those moments when I was in the worsts of moods. She always found a way to cheer me up!

Abstract

Background: Kainate receptors (KARs) are one of the three classes of ionotropic glutamate receptors (iGluRs) expressed primarily in the central nervous system (CNS) where they mediate information transfer and neurotransmitter release. Very little is known about native KARs and their interacting partners outside the CNS.

Aim: The aim of this study was to investigate systematically the molecular composition and functional properties of KARs in pancreatic endocrine cells and also to investigate the role of KARs in the pathogenesis of T1DM.

Methods: The presence of KAR subunits was investigated in pancreatic clonal β-cells (MIN6 and INS-1), α-cells (α-TC) and primary rat islets of Langerhans using RT-PCR and immunoblotting. The effect of KAR activation on intracellular calcium concentration and insulin secretion in MIN6 was investigated using FURA-2AM epifluorescence imaging and Mercodia insulin assay respectively. The effect of glutamate, kainate and glutamate transporter inhibitor (dihydrokainic acid) on survival and viability of INS-1, α-TC and neuroblastoma cells (SH-SY5Y) was investigated using MTT cell viability assay. The presence of autoantibodies against GluR subunits in serum of T1DM patients and controls was investigated using ELISA and immunoblotting.

Results: RT-PCR identified mRNAs for GluK2-5 KAR subunits in clonal β-and α-cells and all five subunits (GluK1-5) in primary rat islets of Langerhans. The presence of these subunits was confirmed using immunoblotting with GluK2/3 and GluK5 antibodies. In addition, auxiliary KAR subunits Neto 1 and Neto 2 were also identified in all cell types. FURA-2AM epifluorescence imaging of cultured MIN6 β-cells showed that activation of KARs with kainate induced significant increase in intracellular calcium concentration. Kainate also induced increased insulin secretion in MIN6 and INS-1 cells. These effects of kainate were blocked by KAR antagonist (NBQX; 30μM) but not by an antagonist (GYKI-53655 hydrochloride; 100μM) of other iGluRs. Chronic exposure to kainate (0.1-0.5mM), glutamate (0.25-12mM) and dihydrokainic acid (0.1mM) cause significantly reduced viability of pancreatic endocrine and neuronal cells. ELISA and immunoblotting showed that serum of T1DM patients and non-diabetic controls react against components of synaptosomal plasma membrane and also against overexpressed GluR subunits.

Conclusion: Together, these results indicate that a range of functional KAR subunits and their interacting proteins are expressed in the endocrine pancreas. These KAR subunits identified could assemble as homomeric or heteromeric channels in both β-and α-cells of the pancreas. The activation of these receptors is likely to have an impact on pancreatic hormone secretion and viability of endocrine cells in the islets of Langerhans. Much work ought to be carried out to optimise the methods for identification of autoantibodies against GluR subunits in serum of T1DM patients. This will help to understand the potential role of GluRs in the pathogenesis of T1DM.

Posters, presentations and publications

- Dwomoh, L., Spittle, A., Whitehead, G., Dayan, C., Luxton, R., Molnar, E. Varadi, A. Expression and function of kainate receptor subunits in pancreatic endocrine cells. **Poster presentation.** UWE CRIB Annual Meeting (January 11, 2013).

- Dwomoh, L., Spittle, A., Whitehead, G., Dayan, C., Luxton, R., Molnar, E. Varadi, A. The role of β-cell glutamate receptors (GluRs) in the development of type 1 diabetes mellitus (T1DM). **Conference presentation.** Postgraduate Research Conference. UWE (April 28, 2013).

- Dwomoh, L., Spittle, A., Whitehead, G., Dayan, C., Luxton, R., Molnar, E. Varadi, A. The role of β-cell glutamate receptors (GluRs) in the development of type 1 diabetes mellitus (T1DM). **Conference presentation.** Postgraduate Summer School. UWE (July 11, 2013).

- Dwomoh, L., Spittle, A., Whitehead, G., Dayan, C., Luxton, R., Molnar, E. Varadi, A. Expression and function of kainate receptor subunits in pancreatic endocrine cells. **Poster presentation.** UWE CRIB Annual Meeting (January 14, 2014).

- Dwomoh, L., Spittle, A., Whitehead, G., Dayan, C., Luxton, R., Molnar, E. Varadi, A. Type 1 Diabetes: when savoury taste goes wrong. **Conference presentation.** Postgraduate Research Conference. UWE (June 27, 2014).

- Dwomoh, L., Spittle, A., Whitehead, G., Dayan, C., Molnar, E. Varadi, A. (2014) Kainate Receptors (KARs) in pancreatic endocrine cells. **Conference Paper**: Islet Study Group Meeting 2014, Lausanne, Switzerland. September 12-14, 2014.

- Dwomoh, L., Spittle, A., Whitehead, G., Dayan, C., Molnar, E. Varadi, A. (2015) Molecular composition, function and physiology of Kainate Receptors (KARs) in pancreatic endocrine cells. **Conference Paper**: The 15th annual FEBS Young Scientists' Forum (YSF) and the 40th Congress of The Federation of European Biochemical Societies (FEBS), Berlin, Germany. July 2-9, 2015.

- Dwomoh, L., Spittle, A., Whitehead, G., Dayan, C., Molnar, E. Varadi, A. (2015) Molecular composition, function and physiology of Kainate Receptors (KARs) in pancreatic endocrine cells. *FEBS Journal* 282(SUPPL. 1):137-138. **Conference proceedings.**

Abbreviations

- α-TC16: α-TC1 clone 6
- 3D: Three-dimensional
- *3xTgAD:* triple-transgenic mouse model of Alzheimer's Disease
- 7TM: Seven α-helical transmembrane domains
- AD: Alzheimer's Disease
- ADA: American Diabetes Association
- ADAM10: A disintegrin and metalloprotease 10
- ADP: Adenosine diphosphate
- AMPARs: (S)-2-amino-3-(3-hydroxy-5-methyl-4-isoxazolyl) propionic acid receptors
- ANOVA: Analysis of variance
- ANKI: Ankyrin-l
- APS: Ammonium Persulfate
- ATD: Amino terminal domain
- ATP: Adenosine triphosphate
- Aβ: Amyloid beta
- BASP1: Brain acid soluble protein 1
- BSA: Bovine serum albumin
- BTB: Broad-complex, Tramtrack, Bric-a-Brac
- CA3: *cornus ammonis* region III
- $CaCl_2.6H_2O$: Calcium chloride hexahydrate
- CaMKII: Ca^{2+}/calmodulin-dependent protein kinase II
- cAMP: Cyclic adenosine monophosphate
- CAPS: N-cyclohexyl-3-aminopropanesulfonic acid

- CASK: Calcium/calmodulin-dependent serine protein kinase
- CCR5: Chemokine receptor type 5
- CD: Cluster of differentiation
- CCD: Charge-coupled device
- cDNA: Complementary deoxyribonucleic acid
- cGMP: Cyclic guanosine monophosphate
- CNQX: 6-cyano-7-nitroquinoxaline-2,3-dione
- CNS: Central nervous system
- CSF: Cerebrospinal fluid
- CTD: Carboxyl-terminal domain
- CTLA-4: Cytotoxic T-lymphocyte-associated protein 4
- CTSH: Cathepsin H
- CUB: Complement C1r/C1s, Uegf, Bmp1
- DDBJ: DNA Data Bank of Japan
- DEPC: diethylpyrocarbonate
- DHK: Dihydrokainic acid
- DHPG: 3,5-dihydroxyphenylglycine
- DLK1: Delta-like 1 homolog
- DM: Diabetes mellitus
- DMEM: Dulbecco's modified eagle medium
- DMSO: Dimethyl sulfoxide
- DNA: Deoxyribonucleic acid
- dNTP: Deoxynucleotide triphosphate
- dT: Deoxy-thymine
- EAAT2: Excitatory amino acid transporter 2

- ECF: Extracellular fluid
- EDTA: Ethylenediaminetetraacetic acid
- ELISA: Enzyme-linked immunosorbent assay
- EMBL: European Molecular Biology Laboratory
- EPSC: Excitatory postsynaptic current
- ER: Endoplasmic reticulum
- ER-α: Oestrogen receptor alpha
- FCS: Foetal calf serum
- Fura-2AM: Fura-2-Acetoxymethyl ester
- g: gram
- GABA: Gamma-aminobutyric acid
- GAD65: Glutamic acid decarboxylase 65
- GDM: Gestational diabetes mellitus
- GIT: gastrointestinal tract
- GluA: AMPAR subunit
- GluK: KAR subunit
- GluN: NMDAR subunit
- GluRs: Glutamate receptors
- GLT: Glutamate transporter
- GLUT : Glucose transporter
- GPCR: G Protein-Coupled Receptor
- GPRC5B: G Protein-Coupled Receptor, Class C, Group 5, Member B
- *GRIK*: glutamate receptor, ionotropic, kainate
- GRIP: Glutamate receptor-interacting protein
- GSIS: Glucose-stimulated insulin secretion

- GWAS: Genome-wide association studies
- HBSS: Hank's Balanced Salt Solution
- HCl: Hydrochloric acid
- HEK293: Human embryonic kidney 293
- HEPES: 4-(2-hydroxyethyl)-1-piperazineethanesulfonic acid
- HHEX: Haematopoietically expressed homeobox
- HIP14: Huntingtin-interacting protein 14
- HLA: Human leukocyte antigen
- hPSC: Human pluripotent stem cells
- HRP: Horseradish peroxidase
- IA-2: Insulinoma antigen 2
- IDF: International Diabetes Federation
- IFIH1: Interferon-Induced Helicase C Domain-Containing Protein 1
- IgE: Immunoglobulin E
- IgG: Immunoglobulin G
- IGF-1: Insulin-like growth factor 1
- iGluR: ionotropic glutamate receptor
- KARs: Kainate receptors
- K_{ATP}: ATP-sensitive potassium channels
- KCl: Potassium chloride
- kDa: Kilodalton
- Kg: Kilogram
- KH_2PO_4: Potassium dihydrogen phosphate
- Kip27: Kinase interacting protein 27

- KRB: Kreb's Ringer Bicarbonate Buffer
- LBD: Ligand binding domain
- LDLa: Low-density lipoprotein receptor domain class A
- LTP: Long-term potentiation
- $MgCl_2.6H_2O$: Magnesium chloride hexahydrate
- MBS: Membrane binding solution
- MEM mixture: Minimum essential medium
- mEPSC: Miniature excitatory postsynaptic currents
- mGlu: Metabotropic receptor subunit
- mGluRs: Metabotropic receptors
- mM: millimolar
- mmol/L: Millimoles per litre
- MODY: Maturity-onset diabetes of the young
- MPSS: Massively parallel signature sequencing
- mRNA: Messenger ribonucleic acid
- MSG: Monosodium glutamate
- mTOR: Mechanistic target of rapamycin
- MTT: 3-(4,5-Dimethyl-2-thiazolyl)-2,5-diphenyl-2H-tetrazolium bromide
- Na_2HPO_4: Sodium hydrogen phosphate
- $NaHCO_3$: Sodium hydrogen carbonate
- NaCl: Sodium chloride
- NBQX: 2,3-Dioxo-6-nitro-1,2,3,4-tetrahydrobenzo[f]quinoxaline-7-sulfonamide
- NCBI: National Center for Biotechnology Information
- Neto: Neuropilin and tolloid-like
- Ngn3: neurogenin 3

- NMDARs: N-methyl-D-aspartate receptors
- NTD: N-terminal domain
- OCD: Obsessive compulsive disorder
- PAGE: Polyacrylamide gel electrophoresis
- Pax4: Paired box gene 4
- PBS: Phosphate-buffered saline
- PCA: Paraneoplastic cerebellar ataxia
- PCR: Polymerase chain reaction
- Pdx1: Pancreatic and duodenal homeobox 1
- PDZ: Post synaptic density protein (PSD95), Drosophila disc large tumour suppressor (Dlg1), and zonula occludens-1 protein (zo-1)
- PEI: polyethylenimine
- PICK1: Protein interacting with PRKCA 1
- PKA: Protein kinase A
- PKC: Protein kinase C
- PLL: Poly-L-lysine
- ρmol/L: Picomole per litre
- PMP: Pancreatic multipotent progenitor
- PMSF: Phenylmethanesulfonylfluoride
- PP: Pancreatic polypeptide
- PPARG: Peroxisome proliferator-activated receptor gamma
- PRKCA 1: Protein Kinase C, Alpha 1
- PSD-95: Post synaptic density protein-95
- PTPN22: Protein tyrosine phosphatase, non-receptor type 22

- PTX: pertussis toxin
- PVDF: Polyvinylidene difluoride
- Rab3a: RAS-associated protein
- RIPA: Radioimmunoprecipitation assay
- RKK: Alpha2 integrin-specific motif
- RNA: Ribonucleic acid
- ROI: Region of interest
- ROS: Reactive oxygen species
- RP: reserved pools
- RPM: Revolutions per minute
- RPMI-1640: Roswell Park Memorial Institute-1640
- RRP: readily releasable pool
- RT: Reverse transcriptase
- RT: Room temperature
- sAHP: slow after-hyperpolarization currents
- SAP-102: Synapse-associated protein-102
- SAP-97: Synapse-associated protein-97
- SDS: Sodium dodecyl sulfate
- SEM: Standard error of means
- SENP-1: Sentrin-specific protease 1
- SLC30A8: Solute carrier family 30 (zinc transporter), member 8
- SLE: Systemic lupus erythematosus
- SNAP25: Synaptosomal-Associated Protein, 25kDa
- SNP: Single nucleotide polymorphism
- SPM: Synaptosomal plasma membrane

- STAT4: Signal transducer and activator of transcription 4
- SUMO: Small ubiquitin-like modifier
- T1DM: Type 1 diabetes mellitus
- T2DM: Type 1 diabetes mellitus
- TAE: Tris-acetate-EDTA
- TBS-T: Tris-buffered saline-tween
- TCA: Tricarboxylic acid cycle
- TCF7L2: Transcription Factor 7-Like 2
- TEMED: Tetramethylethylenediamine
- TIF: Tagged image format
- TLE: Temporal lobe epilepsy
- TMB: 3,3′,5,5′-tetramethylbenzidine
- TMD: Transmembrane domain
- U/ml: Units per millilitre
- v/v: Volume per volume
- VDCCs: Voltage-dependent calcium channels
- VFD: Venus flytrap domain
- VGLUT: Vesicular glutamate transporter
- w/v: Weight per volume
- ZnT8: Insulin and zinc transporter 8
- α-KG: α-ketoglutarate
- µg: Microgram
- µL: Microlitre
- µM: Micromolar

Table of Contents

Table of Figures

1. Thesis Introduction

2. Kainate receptors in pancreatic endocrine cells

3. <u>Role of GluRs in autoimmune T1DM</u>

Table of Tables

1. Thesis Introduction

2. Kainate Receptors in Pancreatic Endocrine Cells

3. Role of GluRs in autoimmune T1DM

Chapter One

Thesis Introduction

1.1. β-cell physiology

1.1.1. *Pancreatic anatomy*

The pancreas is located in the upper part of the abdominal region, behind the stomach. The pancreas belongs to both the digestive (exocrine) and endocrine systems because it secretes digestive enzymes responsible for digestion of food, particularly lipids and also secretes hormones that control metabolism throughout the body. In an average adult human, the pancreas weighs 60g to 100g (Dolensek *et al*., 2015). The exocrine part of the pancreas is made up of acinar and duct cells and associated nerves, vessels and connective tissues. Acinar cells make up about 95% of the pancreatic mass and are responsible for synthesis and secretion of the bulk of digestive enzymes in the small intestine including pancreatic lipase, amylase and trypsinogen (Weir and Bonner-Weir, 2013). The ducts add bicarbonate and mucus to the secreted enzymes and then empty these into the duodenum of the small intestines (Dolensek *et al*., 2015). The endocrine part of the pancreas is made up of the islets of Langerhans which make up 1-2% of the total pancreatic mass. In humans, the pancreas contains about 1 million pancreatic islets with an average diameter of about 200 μM (Rorsman and Braun, 2013). Islet cells consist of five distinct specialised cells namely insulin-secreting beta cells beta cells (β-cells), glucagon-secreting alpha cells (α-cells), somatostatin-secreting delta cells (δ-cells), pancreatic polypeptide-secreting PP cells and ghrelin-producing cells. β-cells make up majority of pancreatic endocrine cells. They make up 50-70% of islets in humans and 60-80% of rodent total islet cell mass. α-cells and δ-cells comprise about 30% and 10% of human islets and 15%

and 5% of rodent islets respectively (Kim *et al*., 2009; Dolensek *et al*., 2015). Also, islets receive about a tenth of the total blood supply to the pancreas, though they comprise only 1-2% of the total pancreatic mass (Rorsman and Braun, 2013). This underscores the importance of islet function in the body.

There are a number of differences and similarities in the anatomy of human and rodent islets of Langerhans. First, in rodents, islets consist of a core of β-cells surrounded by a region of α-cells and other islet subtypes and there is a clear demarcation between these two regions (Pfeifer *et al*., 2015). However, in human islets, this clear demarcation is not present and β-cells and non-β-cells lie next to each other in a fashion that enhances paracrine actions in human islets (Rorsman and Braun, 2013; Bosco *et al*., 2010). Also, though the diameter of human pancreatic lobules is larger relative to that of rodents, the diameters of individual rodent and human islets are comparable (Dolensek *et al*., 2015). Also, while only few and discreet regions of human islets are innervated, rodent islets are densely supplied with nerves (Rodriguez-Diaz *et al*., 2011; Pfeifer *et al*., 2015). However, distribution of autonomic nerves is similar in islets of mice and human (Dolensek *et al*., 2015).

In spite of some of these differences, rodents particularly mice, remain the most studied organism in pancreatic endocrine research and most of the findings from mice research are translated or extrapolated to humans.

1.1.2. *β-cell generation, development and programming*

During foetal development, β-cells are mostly produced as result of adult stem cell or progenitor cell differentiation in a process termed β-cell neogenesis (Miyatsuka, 2015).

These progenitor or stem cells are thought to be present in the spleen, bone marrow, and also in pancreatic acinar cells (Ding *et al*., 2013; Miyatsuka, 2015). In humans, islets are found to be fully organised and stain positive for insulin, somatostatin, pancreatic polypeptide, glucagon and ghrelin by about 3 months into foetal development (Levetan, 2010). Formation and proliferation of β-cells during pancreatic development is controlled and influenced by transcription factors and cell-cycle regulators including the cell cycle inhibitor p16, Kip27, cyclin D1, cyclin D2 and cyclin D3 (Vetere *et al*., 2014). Also, eostrogen receptor-α (ER-α) has recently been shown to regulate β-cell proliferation during development as well as following injury (Yuchi *et al*., 2015). After birth, β-cell production (regeneration) is a result of replication by already-existing differentiated β-cells (Miyatsuka, 2015).

Furthermore, β-cell mass is thought to expand significantly by replication from birth to early stages of infancy in both rodents and human after which there is decline in replication at rates of 10% per day during the first three years of neonatal life and then to 3% during adult lives (Mezza and Kulkarni, 2014; Cnop *et al*., 2011). However, in both physiological and pathological conditions, the rate of β-cell replication is significantly increased to compensate for a prevailing condition. In addition to a number of cell cycle regulators, some conditions stimulate changes in β-cell replication and β-cell mass in both humans and rodents. These conditions include peripheral insulin resistance (Cerf, 2013; Sharma *et al,*. 2015), injury to the pancreas (Brereton *et al*., 2014), hyperglycaemia (Sharma *et al,*. 2015), gestation/pregnancy (Toselli *et al*., 2014), obesity (Linnemann *et al*., 2014), ageing (Vetere *et al*., 2014). Also, hormones including insulin (Cerf *et al*., 2013), prolactin (Hussain *et al*., 2016) and some incretin hormones (Hussain *et al*., 2016) stimulate and increase β-cell replication in both human and rodents. A recently-

discovered gene, betatrophin has also been shown to specifically induce β-cell proliferation and expansion of β-cell mass significantly when overexpressed in rodents (Yi *et al*., 2013).

In summary, β-cell replication and β-cell mass exhibit a dynamic characteristic whereby their rate is dependent on the prevailing situation to maintain effective metabolic control in the body.

1.1.3. *β-cell mass in health and in disease*

The β-cell mass of adults is thought to be influenced significantly by a fine balance between β-cell differentiation, proliferation, size, survival and death (Vetere *et al*., 2014). The most important pathological condition that alters β-cell mass is diabetes mellitus (DM). Existing evidence indicate that an average non-diabetic adult human can survive and carry out normal glycaemic function with only half the amount of the individual's β-cell mass (Ashcroft and Rorsman, 2012; Menge *et al*., 2008). Studies have also established that loss of β-cell mass in T2DM patients involve mechanisms including apoptosis, ER stress (Costes *et al*., 2013) as well as glucotoxicity and lipotoxicity (Shimo *et al*., 2015). Reduced β-cell mass may also be due to 'wearing out' of the cells as result of increased production of insulin subsequent to peripheral insulin resistance. The loss of β-cell mass in T2DM has also been recently attributed to Nkx6.1- and Pdx1-induced loss of β-cell identity (Spijker *et al*., 2015). In both *in vivo* and *in vitro* human studies, induction of diabetes resulted in β-cells becoming bi-hormonal (exhibiting characteristic of and secreting glucagon in addition to insulin) under the influence of β-cell transcription factors namely Nkx6.1- and Pdx1 (Spijker *et al*., 2013). All of these observations

underscore the suggestion that reduction in β-cell mass in T2DM is as important an episode just as reduced β-cell function.

However, it remains unclear whether reduction in β-cell mass in T2DM patients is entirely as a result of persistent hyperglycaemia or whether some individuals may have started life with reduced β-cell mass.

In T1DM, it is generally acknowledged that only about 10-20% of β-cell mass remains at the time of diagnosis (Crevecoeur *et al*., 2015). Loss in β-cell mass is thought to occur mainly due to the immune system recognising β-cells as foreign and attacking them, thereby causing a pathological loss of insulin-producing β-cells (Mannering *et al*., 2016). In addition to loss of β-cell mass, T1DM also presents with reduced or loss of β-cell function (Herold *et al*., 2015).

Persistent β-cell function has been reported in diabetic patients to suggest that β-cells may be capable to restoring a fraction of their function in pathological situations. The presence of residual β-cell mass and insulin secretion has been reported in individuals who have had insulin-dependent diabetes for 50 years or more (Keenan *et al*., 2010) and also in T1DM patients (Oram *et al*., 2015). These residual β-cells in T1DM could be the result of regeneration from other islet subtypes or could have been due to the fact that not all β-cells are killed during development of the disease.

1.1.4. *β-cell regeneration in health and in disease*

The generally-accepted concept is that β-cells are generated from stem/progenitor cells during pancreatic development (Miyatsuka, 2015). In addition, β-cells undergo replication in postnatal life in order to regulate and maintain β-cell mass and function

(Taylor *et al*., 2015). In pathological conditions such as in diabetes and injury to the pancreas, there is significant loss of β-cells, resulting in metabolic derangements. In spite of several therapeutic approaches to diabetes, the permanent and ideal 'cure' for the condition will involve replacing the lost β-cells in order to restore endocrine function for a maximum duration. For example, transplantation of cadaveric islets as a 'cure' for T1DM has been shown to be significantly effective at making the islet recipient become insulin independent for 5 years and over (Bellin *et al*., 2012). However, the difficulties in obtaining enough cadaveric pancreases coupled with surgical complications have posed significant limitations to this method. This has therefore necessitated much investigation into mechanisms via which β-cells can be generated *in vivo* or *in vitro* from stem cells or pre-existing pancreatic exocrine or from non-β-cells of the endocrine pancreas. This will not only be a very significant contribution to finding a permanent solution for treating diabetes; it will also present an unlimited source of β-cells for research and drug discovery. The quest for this method of β-cells regeneration follows the successful generation of cortical neurons and astrocytes (Pasca *et al*., 2015; Merkle *et al*., 2015) and cardiomyocytes (Fuerstenau-Sharp *et al*., 2015) among others from human pluripotent stem cells.

Previous studies using genetic marking of β-cells in mice have argued against the theory of β-cell neogenesis or regeneration (Dor *et al*., 2004). This study refuted the idea of regeneration and suggested that the major source of new β-cells during post-natal and adult life is replication of pre-existing β-cells. Several studies have however reported of successes in mechanisms and procedures of β-cells regeneration from stem cells and non-β-cell sources (Pagliuca *et al*., 2014; Ye *et al*., 2015).

During pancreatic development, the transcription factor Pax4 significantly controls the conversion of progenitor cells into different subtypes of endocrine cells. Using pancreatic cells from mice, it has been observed that α-cells rapidly undergo reprogramming and re-differentiation into insulin-secreting β-cells under the control of ectopic expression of Pax4. These α-cells were found to arise from the duct lining of the pancreas and expressed transcription factors including neurogenin 3 (Ngn3) (Collombat *et al* 2009). This study suggests the possibility that in addition to islet transplantation; an individual's pre-existing α-cells and progenitor cells could be genetically manipulated to produce new β-cells as a relatively permanent approach to managing diabetes. This has been corroborated by other studies (Thorel *et al*., 2010; Ye *et al*., 2015; Chung *et al*., 2010).

In another study, millions of functional human pancreatic β-cells were generated *in vitro* from human pluripotent stem cells (hPSC) using multiple signalling pathways in a scalable 3D cell culture system. In response to high glucose challenge, the generated β-cells recorded an increased Ca^{2+} influx and were able to package and secrete insulin in mechanisms similar to those observed in β-cells from adult humans (Pagliuca *et al*., 2014). The study also proposed a method of β-cell transplantation whereby the cells could be protected from the recipient's immune system to prevent rejection.

It has also been observed that in adult mouse models of diabetes, there is a significant proliferation of pancreatic multipotent progenitor (PMP) cells. Under diabetic conditions, the differentiation of the PMPs is significantly biased towards insulin-positive cells which are capable of secreting insulin (Razavi *et al*., 2015).

These studies and others present a positive indication that β-cell neogenesis or regeneration could be utilised in the near future as a potent procedure to generate enough cells either inside or outside diabetic patients for therapeutic and research purposes.

1.2. Glucose Homeostasis

1.2.1. *Regulation of glucose level in the blood*

Glucose is the main substrate for the production of energy in cells and tissues. Maintenance of glucose level in a very narrow range in blood is of significant importance since elevated or severely reduced levels of glucose could lead to several complications including lethal brain damage and diabetes mellitus (Cantley and Ashcroft, 2015). In addition to intestinal absorption of glucose during the postprandial state, glucose is produced endogenously by the liver via the breakdown of stored glycogen (glycogenolysis), and also by synthesis of glucose from sources such as glycerol, lactate and amino acids (gluconeogenesis) (Guemes *et al*., 2015). Current evidence also points to a role of the kidney in the synthesis of glucose though it is suggested that this role is required particularly in periods of extreme starvation (Andrianesis and Doupis, 2013).

Glucose is transported unbound in blood, and with the exception of the period shortly after birth, the concentration of blood glucose is kept tightly at a physiological range of 3.9-5.5 mmol/L. This range is maintained by a balance between glucose absorption/production and utilisation, made possible by the action of hormones including insulin, glucagon, epinephrine, norepinephrine, cortisol and growth hormone (Guemes *et al*., 2015). When blood glucose levels deviate from the physiological range in certain situations (particularly in postprandial states), the level is rapidly reverted to normal through the action of hormones that suppress endogenous glucose production and increase glucose usage by the muscles, liver and adipose tissue (Giugliano *et al*., 2008). Under physiological conditions, insulin regulates blood glucose concentrations mostly during the post-prandial state whereas glucagon, epinephrine, norepinephrine, cortisol and growth hormone play their roles particularly in the fasting state (Guemes *et al*., 2015).

In spite of the rigid control of blood glucose, the levels may fall or rise drastically under certain physiological and pathological conditions including pregnancy and diabetes mellitus. The brain, which depends permanently on blood glucose for energy consumes about 120 g of glucose per day (van Praag *et al*., 2014). Blood glucose levels below 3 mmol/L presents with hypoglycaemic coma whiles levels below 2.4 mmol/L results in functional neurological impairments and neuronal death (Yeo and Sawdon, 2013). Moreover, at blood glucose levels of 1.1 mmol/L and below, there is irreversible damage to the very vulnerable regions of the brain (Languren *et al*., 2013; Timon *et al*., 2015). Such low levels of glucose in blood can be as result of excessive insulin administration, insulinomas or medications (Martin-Timon *et al*., 2015).

On the other hand, sustained rise in blood glucose (hyperglycaemia) results in short-term effects such as ketosis or long-term effects including severe organ complications as result of micro- and macro-vascular injury. These complications include cardiovascular accidents, stroke, nephropathy, retinal damage and neuropathy (Downs and Faulkner, 2015).

Complications associated with aberrant blood glucose concentrations underscore the importance of effective regulation of glucose metabolism, utilisation and concentration in blood.

1.2.2. *Mechanisms of blood glucose regulation*

Several factors affect the concentration of glucose in blood. Of these, two hormones; insulin and glucagon play the most significant roles in glucose regulation.

1.2.2a. *Role of glucagon in regulation of blood glucose concentration*

Glucagon is a 29-amino acid hormone secreted from α-cells of the pancreas. This hormone ensures a sustained level of glucose in blood during fasting conditions by promoting glucose synthesis in the liver (Campbell and Drucker, 2015). Under conditions where blood glucose levels fall, there is increased secretion of glucagon from α-cells. This results in increased endogenous glucose via glycogenolysis and synthesis of glucose from amino acids and other substrates (Gylfe and Gilon, 2014). The liver is the major site of the physiological actions of glucagon. This is evidenced by the observation that the liver is exposed to 2-3 times higher concentrations of glucagon than any other organ (Edgerton and Cherrington, 2013). Three major mechanisms have been suggested for mediation of glucagon secretion and response during hypoglycaemia. First, reduced blood glucose attenuates the direct inhibitory effect of glucose on α-cell secretion of glucagon (Gylfe and Gilon, 2014). This is not thought to be a major mechanism since exposing isolated α-cell to low glucose *in vitro* does not result in significant release of glucagon (Franklin *et al*., 2005; Gylfe, 2013). Second, the paracrine effect of β-cells that results in inhibition of glucagon from α-cells is attenuated during hypoglycaemia. This mechanism is supported by reports that circulating insulin in T1DM patients inhibits glucagon secretion from α-cells (Unger and Cherrington, 2012; Campbell and Drucker, 2015). This mechanism could also explain why in humans with early-onset T1DM where there is significant reduction in endogenous insulin secretion, there is normal glucagon response

in hypoglycaemic conditions (Campbell and Drucker, 2015). This is however counteracted by reports of early loss of glucagon response to hypoglycaemia in adolescents with T1DM (Siafarikas *et al*., 2012; Campbell and Drucker, 2015). Third, the CNS is thought to act directly on α-cells to facilitate secretion of glucagon during hypoglycaemic states (Lamy *et al*., 2015). This autonomic activation of glucagon secretion is made possible by three inputs namely: parasympathetic nerves, sympathetic nerves (Taborsky and Mundinger, 2012; Gotoh *et al*., 2013) and circulating level of epinephrine (De Marinis *et al*., 2010). Studies have shown that pharmacological or surgical manipulations of these three inputs results in attenuation or significant reduction of glucagon secretion *in vivo* (Taborsky *et al*., 2012; Paranjape *et al*., 2010).

1.2.2b. *Role of insulin in regulation of blood glucose concentration*

Insulin, a 51-amino acid peptide is produced in the β-cells of the pancreas. The peptide is initially synthesised as preproinsulin, cleaved into proinsulin which later matures into two components; insulin and C-peptide. Many factors are known to influence insulin biosynthesis. The single most significant physiological process that stimulates transcription and translation of the insulin gene and RNA respectively is metabolism of glucose (Fu *et al*., 2013; Cantley and Ashcroft, 2015). In response to increased blood glucose following food ingestion and absorption, insulin is secreted in two phases and binds to insulin receptors expressed on liver, muscle and fat cells (Newsholme *et al*., 2014). The main function of insulin is to reduce glucose concentration in blood by three distinct mechanisms. The first involves stimulation of peripheral glucose uptake by adipose tissue and muscle. This ensures that glucose is used as a major energy source in these cells thereby lowering the concentration of glucose in blood (Newsholme *et al*.,

2014). Through the paracrine effect of insulin, the second mechanism involves suppression of endogenous glucose synthesis/production by the liver both directly and indirectly. The direct effect of insulin on the liver involves inhibition of hepatic glucose production via attenuation of glycogenolysis and gluconeogenesis (Lee *et al*., 2016). This process is responsible for suppressing up to 80% of hepatic glucose production (Herring *et al*., 2014). Indirectly, insulin reduces glucose synthesis by inhibiting the secretion of glucagon from α-cells as well as reducing the concentration of blood lipids and glycerol available for gluconeogenesis (Rojas and Schwartz, 2014). The third mechanism through which insulin decreases blood glucose is through promotion of hepatic glycogenesis in which glucose is converted into its storage molecule, glycogen (Newsholme *et al*., 2014). Homeostasis of blood glucose by insulin, glucagon and other hormones is illustrated in Figure 1.1.

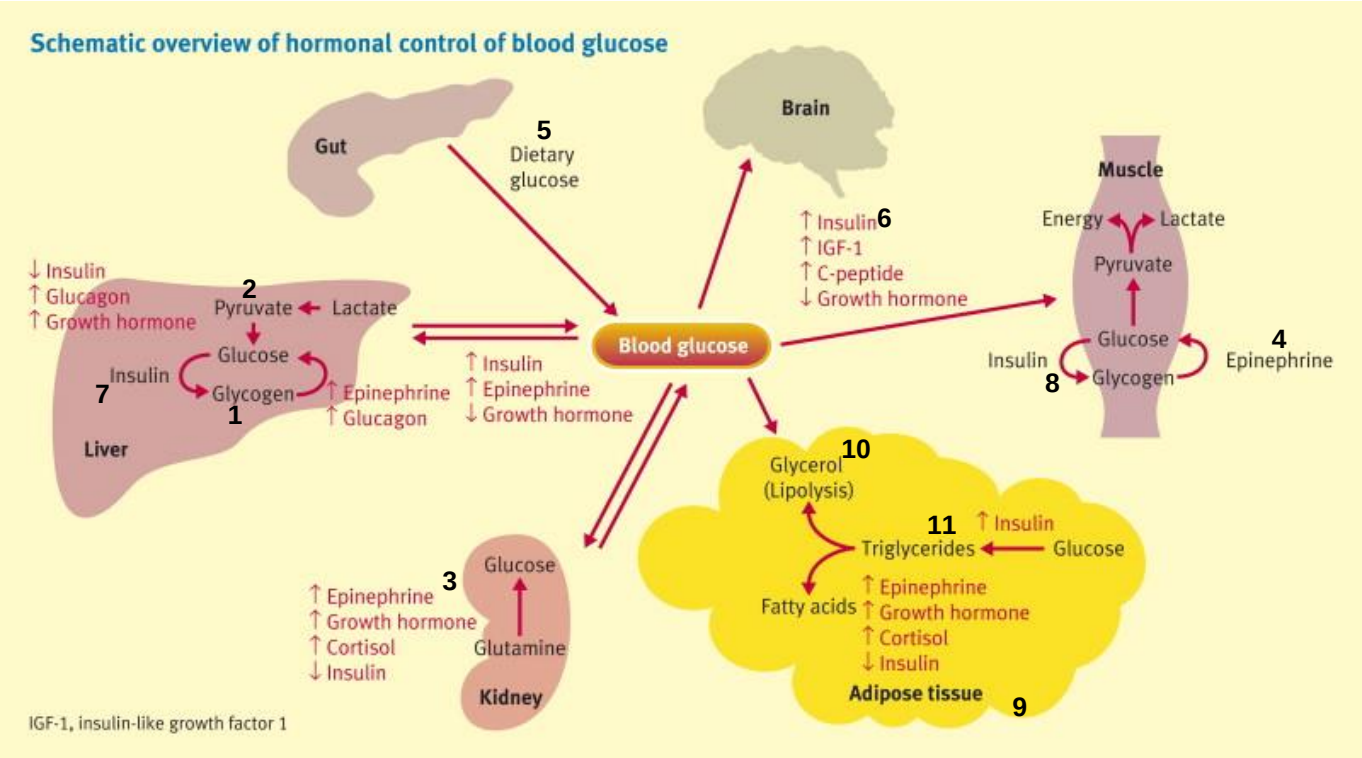

Figure 1.1. Glucose homeostasis. During fasting state, reduced blood glucose stimulates release of glucagon which stimulates conversion of glycogen to glucose in the liver **(1)** and also promotes gluconeogenesis using non-carbohydrates sources as well as pyruvate **(2)**. Epinephrine, growth hormone and cortisol also stimulate gluconeogenesis in the kidney using glutamine **(3)**. Reduced blood glucose in the muscle stimulates epinephrine-induced conversion of glucose from glycogen **(4)**. In the fed state **(5)**, insulin is secreted from β-cells via mechanisms including control from the central nervous system **(6)**. Insulin reduces blood glucose by inhibiting gluconeogenesis and glycogenolysis in the liver. It also enhances glycogenesis in the liver **(7)** and muscle tissue **(8)**. In addition, insulin enhances uptake of glucose by the muscle and adipose tissue **(9)**. Insulin also reduces the rate of lipolysis **(10)** and increase synthesis of fatty acids and triglycerides **(11)**. Yeo and Sawdon (2013). *Image used with copyright permission from Medicine Publishing Company Limited (2016).*

1.2.3. *Mechanism of glucose-stimulated insulin secretion*

Secretion of insulin from β-cells is stimulated by increase in blood concentration of amino acids, fatty acids and more significantly glucose following ingestion and absorption of food. In both humans and rodents, studies have shown that glucose elicits a higher insulin response relative to other nutrients. In humans for example, oral administration of 75 g of glucose results in about tenfold increase in plasma insulin relative to the basal insulin level (from 20-30 ρmol/L to 200-300 ρmol/L) (Fu *et al*., 2013). In contrast, the same amount of fat or combination of fat and protein results in just about a twofold increase in plasma insulin level relative to the basal level (Fu *et al*., 2013).

Glucose is transported from circulating blood into β-cells predominantly via GLUT1 and GLUT3 in humans and GLUT2 in rodents (Rorsman and Braun, 2013; McCulloch *et al*., 2011). The differences in the predominant glucose transporter in humans and rodents is thought to account for differences in physiological glucose range as well as the detectable glucose concentration that stimulates insulin secretion since these transporters transport glucose into the cells with different K*m* values (1 mM for GLUT1 and GLUT3; 15-20 mM for GLUT2) (Rorsman and Braun, 2013). K*m* values represent the affinity of glucose transporters for glucose. The values are inversely proportional to the degree of affinity of the transporters for glucose molecules (Rorsman and Braun, 2013). In both rodent and human β-cells, electrical activities are influenced significantly by the ATP-sensitive potassium (K_{ATP}) channels. These electrical activities result in elevated intracellular calcium ion concentrations, an important requirement for triggering of exocytosis of insulin-containing granules that are lodged close to the plasma membrane of β-cells.

Glucose-stimulated insulin secretion (GSIS) is thought to follow a biphasic mechanism. The first phase, which last about 10 minutes according to *in vitro* and *in vivo* studies (Krogvold *et al*., 2015; Fan *et al*., 2015) involves a finite release of the readily-releasable pool (RRP) of insulin-containing granules which are located very closely below the plasma membrane. The RRP granules make up 1% of the total insulin granules and they are depleted after repetitive stimulation or as result of reduction in the strength of action potentials during sustained GSIS (Rorsman and Braun, 2013). The second phase of GSIS, which lasts longer (about 60 minutes) than the first phase involves movement/trafficking of reserved pools (RP) of insulin (which are farther from the plasma membrane) to the cellular cortex to be secreted (Gilon *et al*., 2014; Fu *et al*., 2013). The biphasic mechanism of GSIS (Figure 1.2) has been shown to be absent in most transformed β-cell lines used in research (Rorsman and Braun, 2013).

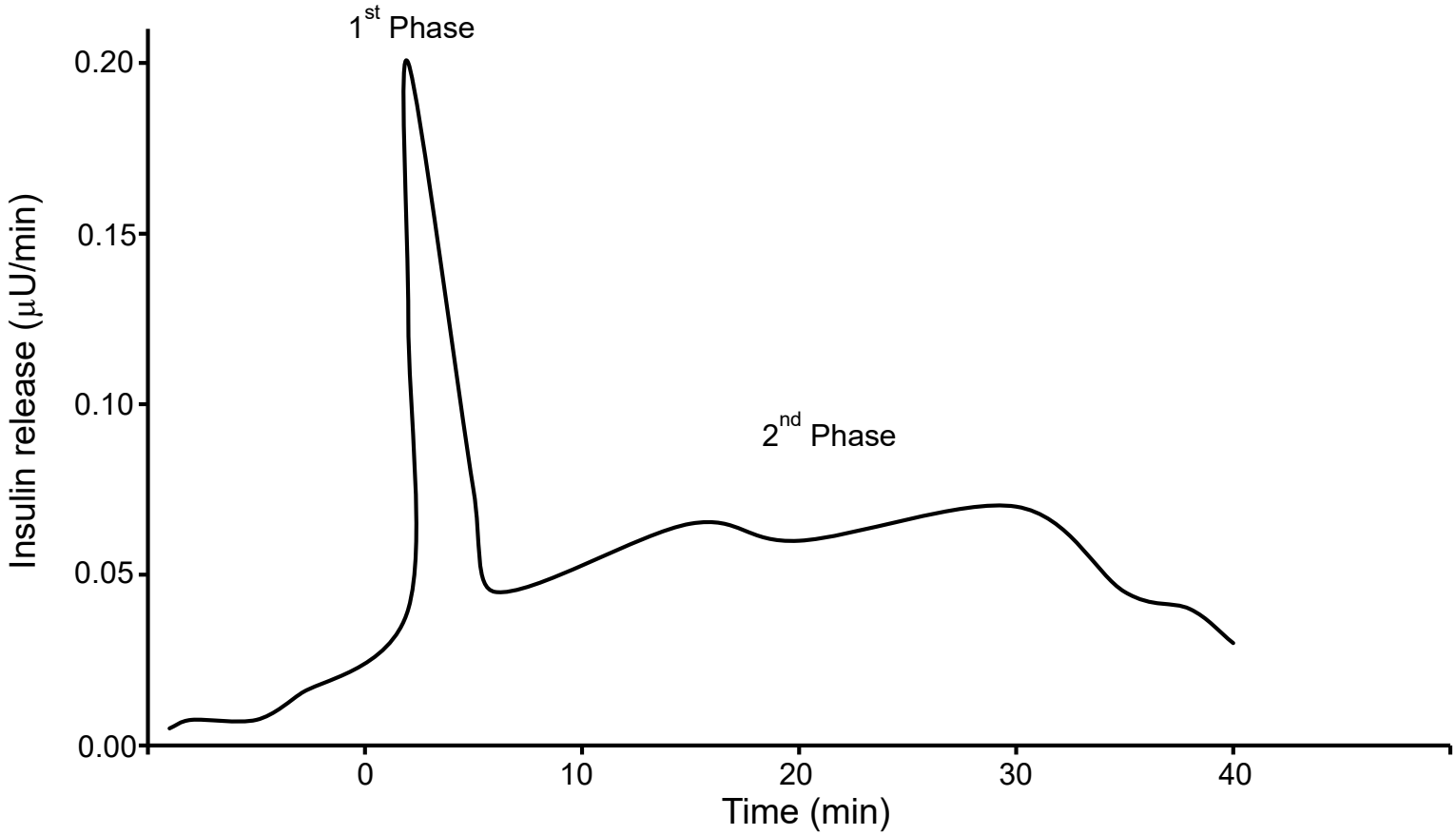

Figure 1.2. Biphasic mechanism of β-cell insulin secretion recorded in isolated normal islets from rats and human. Upon perifusion of stimulatory concentrations (11-15 mM) of glucose, there is an initial rapid burst of insulin release from the readily releasable pool (RRP). This initial release declines after about 10 minutes due to lowered action potential as well as depletion of the RRP. The second phase of secretion involves trafficking of reserved pools of insulin further from the plasma membrane to the cellular cortex to be secreted. This phase is slower, takes longer and involves about 99% of the total insulin content in β-cells. Adapted from Rorsman and Braun, 2013; Henquin *et al.*, 2006.

1.2.4. *Regulation of insulin release by glucose*

After ingestion and absorption of a meal, glucose is transported into β-cells and then phosphorylated by glucokinase to undergo glycolysis. The glycolytic reaction yields pyruvate, which is then oxidised in the mitochondria via the TCA cycle to generate ATP. This mechanism increases the overall ATP and results in an increase in the ATP/ADP ratio in the cell which subsequently causes the closure of the K_{ATP} channels. Closure of these channels results in the opening of voltage-dependent calcium channels (VDCC) and the eventual influx of calcium ions (Ca^{2+}). The increase in Ca^{2+} triggers priming of exocytosis of insulin-containing granules. A recent study indicates that in β-cells of rats, an increase in influx of Ca^{2+} results in activation of adenylyl cyclase 8, which further ensures a sustained exocytosis of releasable insulin granules as well as the priming of reserved pools into readily releasable pools (Dou *et al*., 2015). Moreover, there is another suggested mechanism which triggers insulin secretion. This mechanism is thought to be independent of the K_{ATP} channels and works by enhancing the effects of calcium ions on insulin exocytosis without the influence of an increased concentration of intracellular calcium ions in the cells (Seino *et al*., 2011).

β-cells have several metabolic features that help to prevent excessive insulin secretion; a situation that could lead to hypoglycaemia. One very significant mechanism to avoid excessive insulin secretion is the coupling of glucose metabolism to insulin secretion through ATP levels and insulin vesicle exocytosis. This ensures that insulin secretion remains significantly sensitive to fluctuations in blood glucose levels (Cantley and Ashcroft, 2015). Another recently-discovered mechanism through which β-cells regulate insulin secretion is through control of macroautophagy (Feng *et al*., 2014). Macroautophagy is a form of autophagy that involves the assembly of cellular contents

into a phagophore and its eventual degradation by lysosomes and vacuoles. The degraded cellular contents are released back into the cytoplasm to be recycled. This is an important mechanism employed by most eukaryotic cells to generate energy and maintain their viability in stressful situations such as starvation (Feng *et al*., 2014). A recent study has suggested that macroautophagy is supressed in β-cells during starvation in order to control insulin secretion. In contrast to most mammalian cells, there is suppression of macroautophagy in β-cells in an mTOR-dependent manner during fasting (Goginashvili *et al*., 2015). The suppression of macroautophagy and selective degradation of nascent insulin-secreting granules may be a critical mechanism employed by β-cells to ensure that there is low insulin secretion during starvation in order to avoid hypoglycaemia.

The mechanisms of glucose-stimulated insulin secretion are illustrated in Figure 1.3.

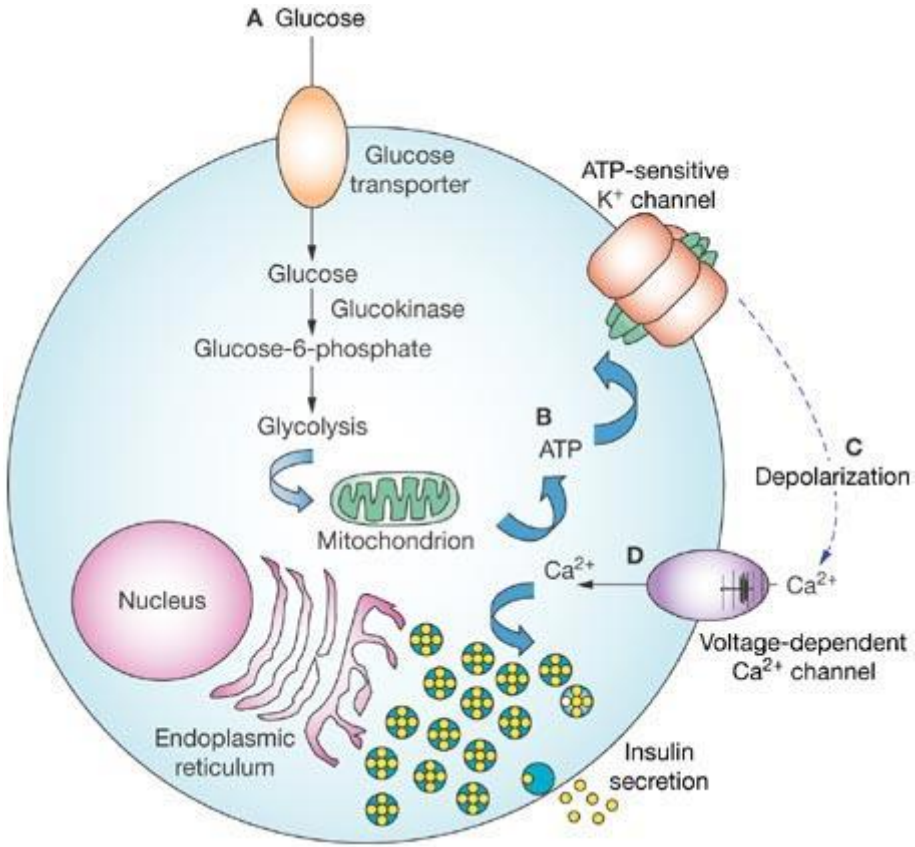

Figure 1.3. Mechanism of glucose-stimulated insulin secretion in human and rodent β-cells: In β-cells, the K_{ATP} channels are open in unstimulated states. This ensures that the resting membrane potential remains around -70 mV. After ingestion of a meal, glucose enters the β-cell via GLUT1 and GLUT3 (in humans) or GLUT2 (in rodents) **(A)** and is phosphorylated before undergoing glycolysis. Pyruvate from glycolysis is then oxidised in the mitochondria to yield ATP **(B)** to cause an increase in the ATP/ADP ratio. This subsequently closes the K_{ATP} channels, causes depolarisation **(C)** which then open the voltage-gated calcium channels **(D)** to increase influx of calcium ions. Increased influx of calcium ions in the cell eventually triggers exocytosis of insulin vesicles. De Leon and Stanley, 2007; Rorsman and Braun, 2013. *Image used with copyright permission from Nature Publishing Group (2016).*

1.2.5. *Physiological actions of insulin*

The physiological actions of insulin are exerted by binding of insulin to a cell surface insulin receptor present on many cells including the liver, muscles and fat cells (Newsholme *et al*., 2014). By binding to these receptors, insulin facilitates uptake of amino acids and glucose into the cells. Insulin also promotes storage of triglycerides in fat cells, suppresses postprandial secretion of glucagon, and promotes synthesis of proteins, glycogen and fat (Yeo and Sawdon, 2013). Insulin as a hormone has also been suggested to act as a neurotrophic agent responsible for enhancing brain function. In a triple-transgenic female mouse model of Alzheimer's disease (3xTg-AD), a high-fat diet induces increased formation of β-amyloid peptide (Aβ) and glucose intolerance (Vandal *et al*., 2014). These high-fat-induced observations were reversed following injection of 3.8 units/Kg of human insulin into these mice. The study showed that the Aβ levels were significantly lowered because insulin caused reduced production and increased clearance of the peptides. These observations underscore the link between neurodegenerative conditions such as Alzheimer's disease and insulin levels/function.

In spite of strict regulation of insulin secretion by β-cells, certain conditions including DM and insulinomas can result in absent, reduced or excessive insulin secretion as well as non-responsiveness of cells to insulin. These situations underlie the pathophysiology of diabetes mellitus, a life-threatening condition which affects millions of individuals worldwide.

In addition to glucagon and insulin, growth hormone from the pituitary gland (Moller and Jorgensen, 2009), epinephrine secreted from the medulla of the adrenal glands (Jensen *et al*., 2011) and thyroxine secreted from the thyroid (Klieverik *et al*., 2009) have all been suggested to contribute to regulation of glucose level in blood.

1.3. Diabetes mellitus

1.3.1. *Definition and epidemiology of diabetes mellitus*

Diabetes mellitus (DM) refers to a group of multifactorial metabolic disorders characterised by persistent hyperglycaemia. The chronic hyperglycaemia is as a result of defective insulin secretion, defect in insulin action or both (Kharroubi and Darwish, 2015). These deficiencies can present with several systemic complications including micro- and macrovascular abnormalities, coma and even death. The disease remains one of the biggest public health challenges in the world, imposing significant financial and emotional costs on sufferers, families and the community in general. According to the 2015 International Diabetes Federation (IDF) Diabetes Atlas, 415 million adults around the world have diabetes and this is expected to rise to 642 million by 2040 (IDF, 2015). From the same IDF report, it was observed that about 5 million people died of diabetes in 2015 and 5-20% of total health expenditure on adults was spent on management of diabetes mellitus and its related complications. Also, countries that have not been generally associated high prevalence of diabetes mellitus have recorded significant increases in prevalence recently. Example, more than 10% of adults in the Middle East now have diabetes whiles about 21 million people in Africa have diabetes with the number estimated to double by 2035. These figures underscore the fast-growing and pandemic nature of diabetes mellitus (IDF, 2015).

1.3.2. *Classification of diabetes mellitus*

Classification of DM remains a controversial subject owing to the increasing heterogeneous nature of the disease. The majority of DM cases fall into two major subdivisions based on pathogenesis and aetiology. T1DM refers to the type caused by total cessation of insulin secretion from the pancreas. T1DM has a multifactorial aetiology and represents 7-12% of all diabetes mellitus cases. T2DM accounts for 87-91% of all cases and is also caused by a combination of several factors particularly obesity and insulin resistance (IDF, 2015). Outside these two major types, other specific types of diabetes mellitus have been recognised and categorised. Maturity onset diabetes of the young (MODY) refers to monogenic forms of the disease which result from genetic defects of β-cells and presents with 'age-onset' diabetes at early age (Leslie *et al*., 2015). MODY accounts for 1-4% of all diabetes mellitus cases. Another form of specific diabetes categorised outside the two main subtypes is gestational diabetes mellitus (GDM). This refers to abnormal levels of blood glucose and glucose intolerance first recognised during pregnancy. GDM is most associated with maternal obesity and affects almost 7% of all pregnancies, resulting in some complications during pregnancy or after birth. It has been suggested that women suffering from GDM have about seven-fold increased risk of developing T2DM as well as some metabolic complications after birth (Bellamy *et al*., 2009; Hod *et al*., 2015). The current classification of diabetes presents with some challenges in terms of management of the disease hence a more effective system of classification is required to accommodate all the challenges and the increasing heterogeneity associated with it.

1.3.3. *Type 1 Diabetes Mellitus*

T1DM is a life-threatening condition which involves the autoimmune destruction of insulin-secreting β-cells of the pancreas. The lack of insulin results in hyperglycaemia together with abnormalities in fat and protein metabolism (Atkinson *et al*., 2014). These metabolic abnormalities contribute to T1DM complications including diabetic ketoacidosis, microvascular complications, neuropathies, coma and death (Rohrer *et al*., 2015; Rewers *et al*,. 2015). The disease is one of the commonest chronic non-communicable conditions and requires life-long insulin administration alongside glucose monitoring and diet modification at significant financial and emotional cost to patients, carers and relatives (Freeborn *et al*., 2013; Balfe *et al*., 2013). T1DM has long been established as a disease of children and young adults, but recent observations of increasing prevalence in adults have raised the question of using age as an important parameter in diagnosis of the condition (Atkinson *et al*., 2014). Though there is a significant variation in incidence and prevalence of T1DM amongst countries (Patterson *et al*., 2014), the number of cases worldwide is increasing especially in children and young adults. It is estimated that about 79,000 children under the age of 14 years around the world develop T1DM each year (Patterson *et al*., 2014).

It is widely accepted that T1DM is a multifactorial autoimmune disease, but the exact cause or trigger of the autoimmune process remains uncertain. This has contributed to the difficulties associated with research into ways of delaying the progression of the disease in high-risk individuals. The current understanding is that the autoimmune process in T1DM results from interaction between genetic predisposition and some environmental factors.

Environmental factors that have been implicated in initiation/development of T1DM include viral infections (enteroviruses, rubella, rotaviruses and cytomegaloviruses) (Krogvold *et al.,* 2015*;* Craig *et al*., 2013), time-onset and duration of breastfeeding (Hall *et al*., 2015; Lund-Blix *et al*., 2015), infant diet regimen (Lamb *et al*., 2015), mode of delivery with Caesarean section being a high risk factor (Puff *et al*., 2015) and levels of vitamin D (Vehik *et al*., 2013). Other environmental factors that have been suggested to increase the risk for T1DM development include maternal lifestyle such as high BMI (Hussen *et al.,* 2015), smoking (Mattsson *et al*., 2015), diet during pregnancy and lactation (Niinisto *et al*., 2014), high birthweight (Cardwell *et al*., 2010a), childhood obesity (Verbeeten *et al*., 2011), maternal age (Cardwell *et al*., 2010b) and order of birth (Cardwell *et al*., 2011).

Though the role of environmental factors as triggers or promoters of T1DM development remain a developing area of research, the current understanding of T1DM aetiology is that genetic predisposition and environmental factors may be independent risk factors for T1DM, but their combined effect increases the risk of developing the disease.

Evidence for an autoimmune process in T1DM has been reported in several studies over a long period of time.

1.3.3a. *Role of genetics in autoimmune process of T1DM*

There is evidence for an association of T1DM with genetic polymorphisms that predispose individuals to an altered immune response. Genome-wide association studies (GWAS) have helped to reveal that polymorphisms in almost fifty genes contribute to the

autoimmune pathogenesis of T1DM (Ehlers, 2016; Mannering *et al*., 2015; Dirice and Kulkarni, 2016).

Polymorphisms at class II HLA gene loci account for about 50% of the overall genetic risk for T1DM (Noble, 2015). The strongest association between risk for initiation of T1DM autoimmune process and HLA is observed in the genotype coded by the DRB1*0401-DQB1*0302 and DRB1*0301-DQB1*0201 loci (Noble, 2015; Silva *et al*., 2016). These polymorphisms are likely to alter the function of antigen presenting cells which may subsequently lead to activation of cytotoxic autoreactive $CD8^+$ T cells and eventual killing of β-cells of the pancreas (Noble, 2015).

Beyond HLA, several genes have been associated with the autoimmune process in T1DM but only few confer relatively high risk for the disease. A nucleotide polymorphism in *PTPN22* is thought to result in T cell hyperresponsiveness, reduced function of Tregs as well as altered antigen presentation all of which can lead to enhanced autoimmune β-cell destruction (Sarmiento *et al*., 2015; Sharp *et al*., 2015). Polymorphisms in *CTLA-4* gene also lead to impaired regulatory T cell (Tregs) function and reduced control of T cell proliferation and function which subsequently increase the likelihood of autoimmune β-cell destruction of cells (de Jong *et al*., 2016; Almasi *et al*., 2015). Also, a polymorphism in *IFIH1* gene impairs response of the innate immune system to viral infections and increases risks for autoimmune process in T1DM (Zurawek *et al*., 2015). This link is interesting considering the long-standing association between T1DM and viral infections. Emerging candidate genes for autoimmune T1DM risk include *HIP14*, *STAT4*, *DLK1*, *CCR5* and *CTSH* (Mannering *et al*., 2015).

A summary of the major genetic polymorphisms associated with the autoimmune process in T1DM is shown in Table 1.1.

Table 1.1 Summary of the major genetic polymorphisms associated with risk for autoimmune process in T1DM. The odds ratio defines the strength of association between polymorphisms in the genes and susceptibility to developing autoimmune T1DM. The higher the odds ratio, the greater the risk of autoimmune process in T1DM.

Gene	Locus	Expression in Human islets	Odds Ratio	Effect of polymorphism	References
HLA	6p21	Yes	Up to 11.4	Altered antigen presentation	Noble, 2015; Silva *et al*., 2015
PTPN22	1p13	Yes	Up to 1.8	T cell hyperresponsiveness, impaired Treg function, altered antigen presentation	Sarmiento *et al*., 2015; Sharp *et al*., 2015
IFIH1	2q24	Yes	Up to 1.2	Impaired response to viral infections	Storling and Brorsson (2013), Zurawek *et al*., 2015
CTLA-4	2q33	No	Up to 1.1	Impaired T-cell regulation impaired Treg function	Jong *et al*., 2016; Almasi *et al*., 2015

1.3.3b. *Antigen targets and autoantibodies in T1DM*

T1DM is thought to be a T cell-mediated disease where autoreactive $CD8^+$ and $CD4^+$ T cells target antigens in β-cells of the pancreas (Mannering *et al*., 2015). Autoantibodies to these β-cell autoantigens have been the most important components of the autoimmune process and they serve as biomarkers and targets of immune therapies for T1DM. This is due to their role in presenting β-cell antigens to cytotoxic T-cells during the autoimmune process (Bonifacio, 2015).

The most-characterised autoantigens in T1DM are insulinoma antigen 2 (IA-2), glutamic acid decarboxylase 65 (GAD65), insulin and zinc transporter 8 (ZnT8) (Morran *et al*., 2015). Studies suggest that combining metabolic investigations with identification of autoantibodies to these four antigens is the best tool to identify β-cell autoimmunity; with about 96% of individuals with β-cell autoimmunity expressing at least one of these four autoantibodies (Bonifacio, 2015; Mannering *et al*., 2015).

Although β-cell antigen targets and their autoantibodies have been explored in clinical and laboratory procedures aimed at delaying T1DM progression, these interventions have not been particularly successful for the following reasons: (i) it is not known if a single β-cell antigen is able to drive the autoimmune process, (ii) it is not clear which of the antigens trigger pathogenic autoimmunity when targeted by autoantibodies (Yu et al., 2012; Bonifacio, 2015), (iii) All the known β-cell antigens are predominantly intracellular (Arvan et al., 2012); hence it is unlikely that they trigger the initial stages of the autoimmune process, (iv) the mechanisms that lead to loss of immune tolerance to these intracellular proteins remain uncertain (Arvan et al., 2012). Thus, an antigen located on the surface of β-cells may be the first targeted the immune system. This could then trigger

an autoimmune process which can result in exposure of intracellular β-cell antigen targets such as IA-2 and GAD65 to the immune cells. These observations underscore the need to probe further for new β-cell-associated antigen targets and autoantibodies that may unlock the mystery surrounding the role of the autoimmune process in the early stages of T1DM.

1.3.4. *Type 2 Diabetes Mellitus (T2DM)*

T2DM is characterised by chronic hyperglycaemia, reduced insulin secretion and impaired insulin action as result of resistance by target cells (adipose, muscle and liver cells) (Cantley and Ashcroft, 2015). T2DM has long been thought to be a disease of adults but accumulating evidence has shown that incidence of the disease is significantly increasing in children and young adults (Tuomi *et al*., 2014). Moreover, results from studies in the United State for instance have reported that there has been a 21% increase in T2DM cases among young adults from 2001 to 2009 (Imperatore *et al*., 2012). This rise in T2DM among the youth is several times higher in China compared to the United States (Li *et al*., 2012). These increasing incidence of T2DM among the young has been attributed partly to corresponding increase in incidence of obesity among individuals in the same age group (Tuomi *et al*., 2014).

Furthermore, the worldwide incidence of T2DM is increasing at an alarming rate. According to the 2015 report of the IDF, 345-370 million people, representing close to 8% of the world's population have T2DM. This is projected to reach about 560 million (almost 9.5% of the world's population) by the year 2035 (IDF, 2015). The increasing incidence is being observed in every geographic region of the world. For instance, almost

12% of China's population has T2DM (Xu *et al*., 2013) while almost 8% of adults in Europe are estimated to be suffering from the disease (Tamayo *et al*., 2014).

1.3.4a. *Causes of T2DM*

Like T1DM, T2DM is thought to be caused by a complex interaction between the environment and predisposing genetic factors. Several studies have helped to establish the role of genetics in T2DM development. An individual stands a 40% increased risk of developing the disease if one parent already has/had it while the risks of having the disease is 70% if both parents have T2DM (Prasad and Groop, 2015). The genetic predisposition to T2DM is further supported by the high prevalence of the disease among certain ethnic groups. For instance, almost 50% of Pima Indians in America have T2DM while less than 10% of Caucasians in Europe are affected (Shaw *et al*., 2010; IDF, 2015). The introduction of genome-wide association studies (GWAS) have contributed significantly to the study of genetic contribution to T2DM development. As of 2014, more than 90 gene loci had been linked to T2DM with the most studied of these variants being Calpain 10, *TCF7L2* (Reynisdottir *et al*., 2013), *PPARG* (Grarup *et al*., 2014), *SLC30A8* (Imamura *et al*., 2012), *HHEX* (Sladek *et al.,* 2007) and *ANKI* (Imamura *et al*., 2012). Most of these gene variants are thought to contribute to the disease development through varied mechanisms including reduction in insulin sensitivity, β-cell destruction, decreased β-cell function, and increased insulin resistance among others (Singh, 2015).

Several environmental factors have also been implicated in the development of the T2DM. The most significant of these factors is obesity and it has been established that the risk of developing T2DM increases considerably among obese individuals (Tuomi *et*

al., 2014). There is evidence to suggest that the global increase in T2DM incidence shows a similar trend and geographic distribution as that of obesity (Cantley and Ashcroft, 2015). Though obesity remains a major risk factor for T2DM, the recent report that obesity is associated with a 50% increase in β-cell mass suggests that the effect of obesity on T2DM may vary from person to person depending on how an individual's system respond these effects (Cantley and Ashcroft, 2015; Saisho *et al*., 2013).

Other environmental factors that have been implicated in increasing the risk for development of T2DM include maternal malnutrition and low protein diet (Tarry-Adkins *et al*., 2010), maternal or infant overnutrition (Lee *et al*., 2013; Black *et al*., 2013), alcoholism (Ramirez *et al*., 2013), maternal smoking (Thiering *et al*., 2011), prenatal psychological stress (Virk *et al*., 2013), gestational diabetes (Bush *et al*., 2013), maternal hormonal levels during pregnancy (Roland *et al*., 2012), early weaning (Lima *et al*., 2011), neonatal monosodium glutamate intake (Roman-Ramos *et al*., 2011), low socio-economic status (Tamayo *et al*., 2010) as well as long duration of night-shift work among women (Vimalananda *et al*., 2015).

1.4. Glutamate Receptors (GluRs)

Glutamate, a non-essential amino acid is the major excitatory neurotransmitter in the CNS involved in mediating several range of neural functions including synaptic plasticity, fast excitatory synaptic transmission, learning and memory, long term potentiation (LTP) as well as neuronal development (Edwards, 2015; Willard and Koochekpour, 2013). The highest concentrations of glutamate in the CNS are mostly present in synaptic vesicles located in nerve terminals of presynaptic neurons from where they are released by exocytosis to bind to glutamate receptors (GluRs) (Zhou and Danbolt, 2014). GluRs are located primarily on the surface of various brain cells including neurons and glial cells (oligodendrocytes and astrocytes) (Parpura and Verkhrastsky, 2013). Due to the characteristic expression of GluRs on neuronal and other brain cells, these receptors can only be activated from the outside by extracellular glutamate (Zhou and Danbolt, 2014). This observation underscores the significant importance that glutamate's release into and uptake from the extracellular fluid (ECF) by glutamate transporters play in activation of GluRs (Vandenberg and Ryan, 2013). Moreover, it has long been established that glutamate as an excitatory neurotransmitter can cause death of neurons and other cells in the brain in a phenomenon termed excitotoxicity. This is a mechanism whereby GluRs are chronically over-activated to cause death of cells via cellular mechanisms including apoptosis and necrosis (Del Rosario *et al*., 2015). To protect the cells from excitotoxicity, glutamate transporters are actively involved in removal of glutamate from ECF. The function of these transporters are particularly important considering that no enzyme is known to degrade glutamate extracellularly (Zhou and Danbolt, 2014). Also, to protect against glutamate-induced excitotoxicity, the brain in general and neuronal cells in

particular are protected from the high glutamate concentration in blood by the blood-brain barrier.

In the CNS, glutamate activates 2 groups of GluRs namely ionotropic (iGluRs) and metabotropic (mGluRs) glutamate receptors. GluR subtypes and their respective subunits are summarised in Figure 1.4 while the mechanism of glutamate signalling and eventual clearance from the synaptic cleft is shown in Figure 1.5.

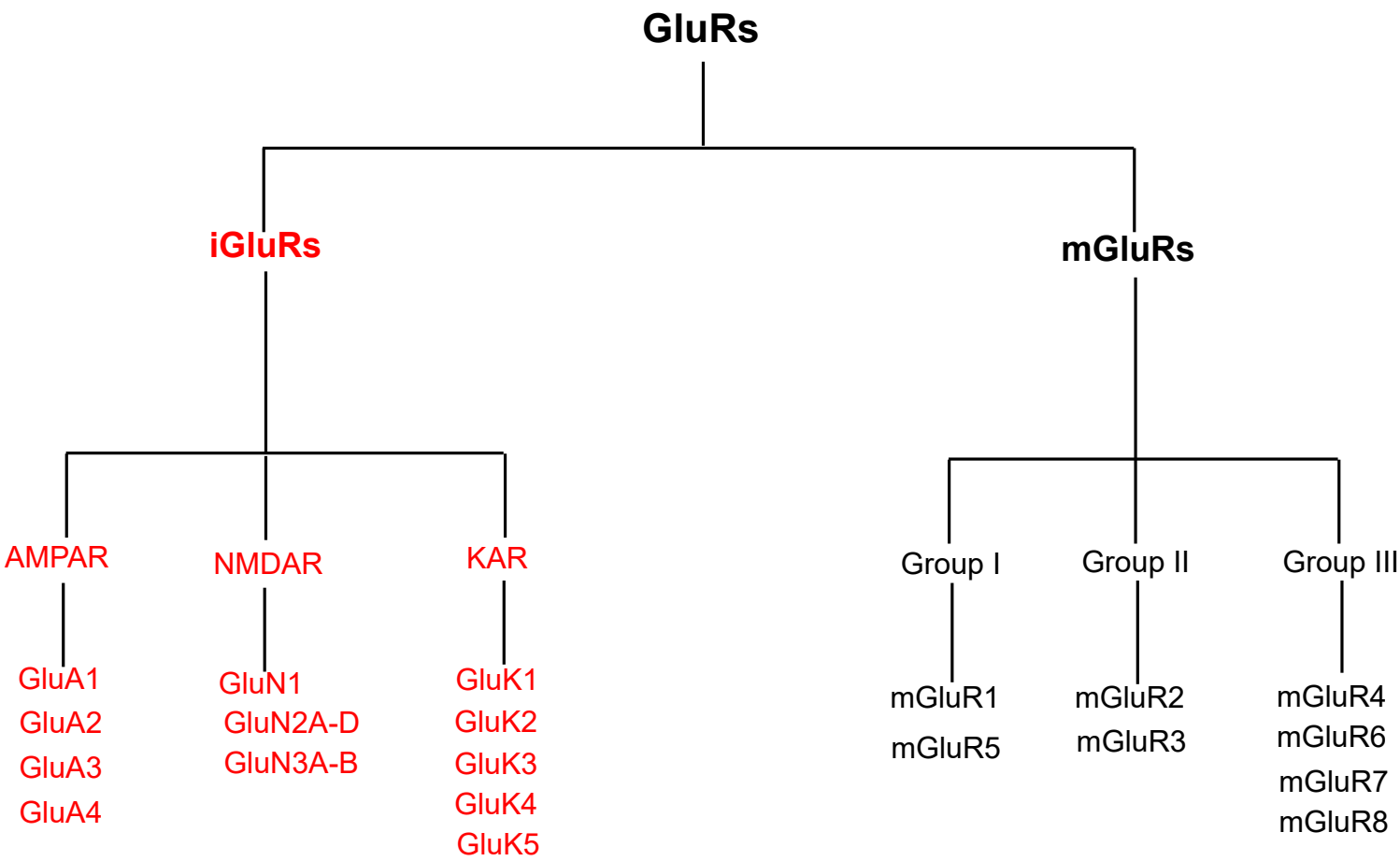

Figure 1.4. Classification of glutamate receptors into groups, subtypes and respective subunits. GluRs are classified into two groups namely ionotropic (iGluRs) and metabotropic (mGluRs) glutamate receptors. The iGluRs are further divided into three main subtypes named after the glutamate analogues that selectively activate these subtypes: AMPA, NMDA and kainate. These three iGluR subtypes are classified into respective subunits based on the genes that encode these subunits. mGluRs are classified into three main groups based on their ligand-binding profile, intracellular signal transduction pathways and sequence homology. The three groups of mGluRs consist of respective isoforms. Traynelis *et al*., 2010; Willard and Koochekpour, 2013; Amalric *et al*., 2015.

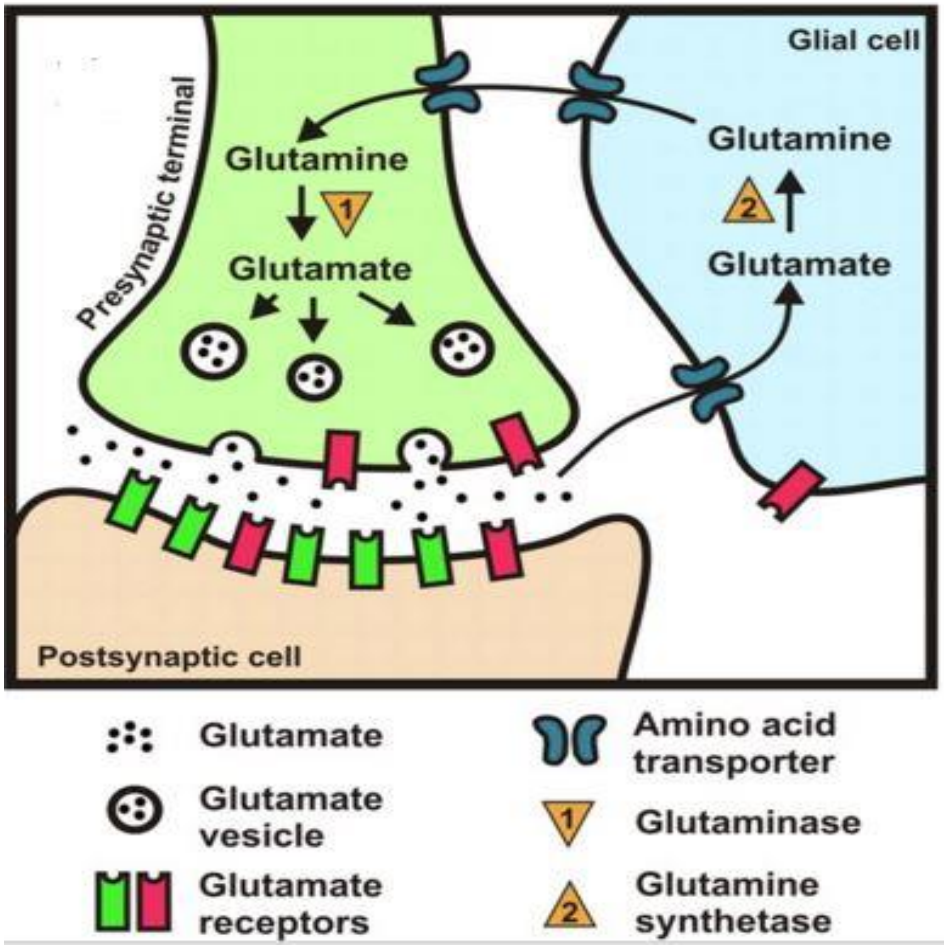

Figure 1.5. Glutamate signalling and recycling between neurons and glial cells. Glutamate is stored in vesicles in presynaptic neuronal cells from where they are released into the synaptic cleft. Release of glutamate from presynaptic neurons into the synaptic cleft is under the modulation of GluRs present on these presynaptic neurons. The released glutamate in the synaptic cleft bind and activate GluRs on postsynaptic neurons to initiate excitatory neurotransmission. After the signalling process excess glutamate is removed from the synaptic cleft by glutamate (amino acid) transporters located on glial cells. The removed glutamate is then converted into glutamine by glutamine synthetase **(1)** and transported back via glutamate transporters into the presynaptic neuronal cell. In the presynaptic neuron, glutamine is converted into glutamate by glutaminase **(2)** and then packaged into vesicles ready to be released into the synaptic cleft. Julio-Pieper *et al*., 2011; Amalric *et al*., 2015. *Image used with copyright permission from American Society for Pharmacology and Experimental Therapeutics (2016).*

1.4.1. *Ionotropic glutamate receptors (iGluRs)*

Molecular cloning has helped to establish that there are three subtypes of iGluRs namely N-methyl-D-aspartate receptors (NMDARs), (S)-2-amino-3-(3-hydroxy-5-methyl-4-isoxazolyl) propionic acid receptors (AMPARs) and kainate receptors KARs. These three subtypes are named after the potent analogues of glutamate that preferentially activate the receptors (Paoletti *et al*., 2013). Structurally, iGluRs are quaternary ligand-gated ion-channel receptors that bind and interact with specific agonists. The ligand-gated ion-channels of iGluRs consists of four domains namely ligand-binding domain (LBD), amino terminal domain (ATD), transmembrane domain (TMD) and an intracellular C-terminal domain (CTD) (Willard and Koochekpour, 2013; Lodge, 2009). Binding of glutamate or an analogue of glutamate to the LBD induces a conformational change in the TMD resulting in influx of cations (sodium, potassium or calcium ions) through the TMD. Stimulation of iGluRs through this mechanism results in significant influx of calcium and firing of an action potential (Traynelis *et al*., 2010). After firing of the action potential, glutamate in the synaptic cleft is removed by glutamate transporters, which are expressed on postsynaptic neuronal and glial cells, to turn off the signal in preparation for a new series of transmission (Willard and Koochekpour, 2013). The basic structure and activation of iGluRs are illustrated in Figure 1.6.

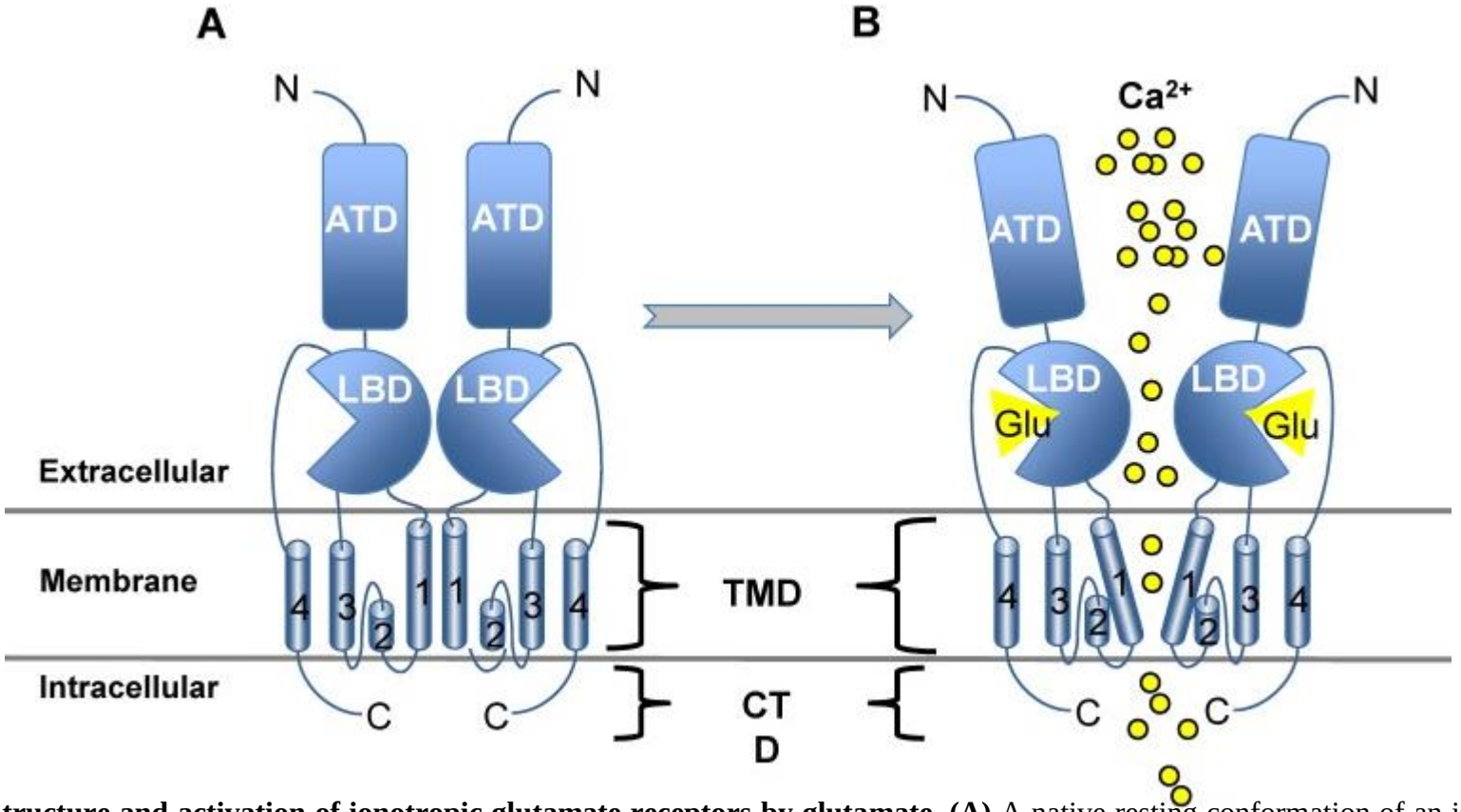

Figure 1.6. Structure and activation of ionotropic glutamate receptors by glutamate. (A) A native resting conformation of an iGluR showing only two instead of four subunits. The receptor consists of an extracellular N-terminal domain (**N**) and a shorter C-terminal domain (**CTD**) which is intracellular. The extracellular amino terminal domain (**ATD**) is followed by an extracellular ligand-binding domain (**(LBD**). The four subunits of a resting iGluR are arranged in such a way that they form a channel pore through the plasma membrane. **(B)** iGluR receptor upon binding of glutamate (**Glu**) induces a conformational change in one of the four transmembrane domain (**TMD**) to allow opening and influx of calcium ions through this transmembrane domain. Willard and Koochekpour, 2013. *Image used with copyright permission from International Journal of Biological Sciences (2016).*

NMDARs are calcium-permeable iGluRs which consist of seven distinct subunits; GluN1, four subunits of GluN2 (GluN2A, GluN2B, GluN2C and GluN2D) which are encoded by four different genes and two units of GluN3 (GluN3A, GluN3B) also encoded by two different genes (Vyklicky *et al*., 2014). For NMDARs to be functional, it must be in the form of a hetero-tetramer containing two GluN2 subunits (or in some cases one GluN2 and one GluN3 subunit) together with two obligatory GluN1 subunits (Paoletti *et al*., 2013). The opening of NMDAR voltage-gated channel requires binding of glutamate (or its analogue) as well as glycine, the co-agonist of NMDARs. Studies have shown that glutamate binds to the GluN2 subunit while glycine binds to the GluN1 subunit of the functional hetero-tetramer (Yang *et al*., 2014). Binding of these agonists open the ion-channels by stabilising a close-cleft conformation whereas binding by antagonists of NMDARs impedes the closure of the cleft and hence prevents the opening of the ion channels. However, recent studies have shown that D-serine is a preferred co-agonist for NMDARs in adult human brain (Mothet *et al*., 2015). NMDARs are thought to be mainly involved in long term potentiation and long term depression of synaptic transmission (Papouin and Oliet, 2014). Dysfunction of NMDARs in the CNS have been linked to several neurological abnormalities including pathological pain, stroke and neurodegenerative diseases (Paoletti *et al*., 2013).

AMPARs are also tetrameric cation-permeable subtypes of iGluRs which are expressed throughout the CNS but more especially at excitatory glutamergic synapses. There are four distinct subunits of AMPAR, namely GluA1, GluA2, GluA3 and GluA4 that are encoded by four distinct genes (Traynelis *et al*., 2010). These subunits are mostly assembled as hetero-tetramers but evidence also suggests that they can be assembled as

homo-tetrameric (Lu *et al*., 2009). When glutamate or its analogue binds to AMPAR, the cation-permeable pores open and allows influx of sodium ions resulting in depolarisation. Calcium ions can also be permitted entry depending on the subunit composition of the AMPAR (GluA2-containing receptors are calcium ion impermeable) (Chater and Goda, 2014). The subunit composition of AMPARs play significant role in determining the functions of the receptors (Monyer and Engelhardt, 2015). AMPARs are primarily involved in mediation of fast excitatory neurotransmission and dysfunction of these receptors have been linked to neurological conditions including progressive memory loss in AD (Tang, 2009).

The third subtype of iGluRs, KARs form the basis of this study hence will be discussed in detail in section 1.5.

1.4.2. *Metabotropic glutamate receptors (mGluRs)*

mGluRs belong to the class C G-protein-coupled receptor superfamily. This C G-protein receptor superfamily also include the receptors for sweet and umami tastes, calcium and $GABA_B$ (Kniazeff *et al*., 2011). mGluRs are made up of three distinct groups that have eight isoforms. The grouping of mGluRs is based on their ligand-binding profile, intracellular signal transduction pathways as well as on the homology of the sequences (Amalric *et al*., 2015). Group I mGluR consists of mGluR1 and mGluR5, group II consists of mGluR2 and mGluR3 while mGluR4, mGluR6, mGluR7 and mGluR8 make up group III (Niswender and Conn, 2010). These receptors are expressed mostly in the basal ganglia where they are responsible for modulation of synaptic transmission as well as neuronal plasticity (Hovelso *et al*., 2011). Structurally, mGluRs consist of a large ligand

(glutamate)-binding region (LBD) made up of a large extracellular N-terminal domain (NTD) and seven α-helical transmembrane domains (7TM) that contain a binding site for synthetic allosteric modulators (Yin and Niswender, 2014; Rondard and Pin, 2015). The most conserved structures or domains of mGluRs are thought to be the sites involved in coupling to the G-protein and the glutamate-binding site (Hovelso *et al*., 2012). The NTD, also called the Venus flytrap domain (VFD), consists of two lobes which upon binding of glutamate or another agonist undergoes a conformational change resulting in closure of these two lobes to initiate activation of the receptor (Yin and Niswender, 2014). The change in conformation of the ligand-binding domain induces rearrangements of a cysteine-rich domain and eventual trigger and activation of the 7TMs.

In the context of downstream signalling, group I mGluRs are coupled to $G_{q/II}$ proteins and activate phospholipase C which results in downstream activation of protein kinase C (PKC) and calcium influx (Niswender and Conn, 2010). On the other hand, group II and group III mGluRs are coupled to $G_{i/0}$ protein which upon activation inhibits adenylyl cyclase and followed by downstream signalling pathways through the activation of potassium ion channels and inhibition of calcium ion channels (Yin and Niswender, 2014).

In the CNS, mGluRs are thought to be primarily involved in modulation of synaptic transmission, neuronal excitability and regulation of neurotransmitter release. Moreover, dysfunction of mGluRs have been linked to several neurological conditions including depression, anxiety disorders, schizophrenia, Parkinson's disease, Alzheimer's disease and epilepsy (Nicoletti *et al*., 2015).

1.5. Kainate Receptors

Among the iGluRs, KARs remain the least studied over the years due to the lack of specific antibodies against KARs as well as inadequate pharmacological tools and transgenic animals to study the properties of this iGluR subtype (Lerma and Marques, 2013). However, there has been considerable research and accumulation of information about the biological and pharmacological properties of KARs since the cloning of GluK1 in 1990 (Contractor *et al*., 2011).

1.5.1. *Subunit classification and receptor combinations of KARs*

Molecular cloning of KAR subunits has shown that these receptors represent a distinct family of iGluRs in terms of structure and function. KARs consists of five distinct subunits namely GluK1, GluK2, GluK3, GluK4 and GluK5 which co-assemble to form functional homomeric or heteromeric receptors. While GluK1-3 can form functional homomeric receptors, GluK4 and GluK5 can only function when in heteromeric combinations with any of GluK1-3 subunits (Crepel and Mulle, 2015). KAR subunits can also be classified based on their affinity for kainate; GluK1-3 have relatively low-affinity for kainate while GluK4 and GluK5 are classified as the high-affinity KAR subunits (Pahl *et al*., 2014). These classifications and properties of KARs indicate that there are considerable limitations in the number of functional KAR combinations since it is necessary that a functional unit of KAR should be a combination of a low-affinity homomeric subunit and a high-affinity obligate heteromeric subunit. Moreover, the low-affinity KAR subunits are also prone to rapid and complete desensitisation upon stimulation with even very low concentrations of glutamate (Fisher and Fisher, 2014).

Also, incorporation of the high-affinity KAR subunits into a functional combination of KARs results in significant changes in the physiological functions and pharmacological properties of recombinant receptors (Fisher and Fisher, 2014). Among these changes include increased affinity for glutamate, enhanced activation by AMPA and other agonists, changes in the concentration-dependence of desensitisation as well as slowing of receptor deactivation (Mott *et al*., 2010; Fisher and Fisher, 2014).

Furthermore, because each of the five KAR subunits has a ligand-binding site, it has been suggested that each subunit is capable of binding to a ligand to initiate and contribute to activation and gating of the receptor channels (Lerma and Marques, 2013). However, other studies suggest that binding of glutamate to the high-affinity subunits within a heteromeric functional receptor combination is sufficient to activate the receptors channel while a higher concentration of glutamate is required to desensitise the receptor combination through binding to the low-affinity GluK2 subunit (Fisher and Mott, 2011). These observations suggest that activation or desensitisation of a KAR subunit combination is considerably dependent on the subunit composition as well as the concentration of ligand. The importance of a high-affinity subunit in KAR combination is further enhanced by the observation that homomeric subunits GluK1 and GluK2 are irreversibly desensitised by dysiherbaine, a high-affinity KAR agonist but GluK2 undergoes a rapid recovery from dysiherbaine-induced desensitisation when co-expressed with GluK5 (Mott *et al*., 2010). Another study also observed that in GluK2/GluK5 heteromeric subunit composition, binding of a ligand to only GluK5 is mandatory and sufficient to induce trafficking of this heteromeric assembly to the plasma/cell membrane (Fisher and Housley, 2013). The study also reported that binding of a ligand to GluK2

only failed to elicit the same response as binding to GluK5. These observations futher support the suggestion that high-affinity KAR subunits play significant roles in regulating the surface expression of heteromeric KARs of which these high-affinity subunits form part.

1.5.2. *Structure of KAR subunits*

The structure of KARs consists of a large extracellular NTD which has two or more component lobes. The extracellular NTD is followed by a single transmembrane domain referred to as M1, a re-entrant or pore-loop known as M2 which penetrates the membrane from its intracellular side between M1 and another transmembrane domain (M3). This is followed by another transmembrane domain (M4) that precedes a cytoplasmic C-terminal domain (Contractor *et al*., 2011; Fisher, 2015). KARs also contain a LBD comprising of two modular lobes (R1 and R2) that are formed from a pre-M1 domain (S1) and the loop formed between M3 and M4 (S2) (Pahl *et al*., 2014).

The subunit topology of KARs is depicted in Figure 1.7.

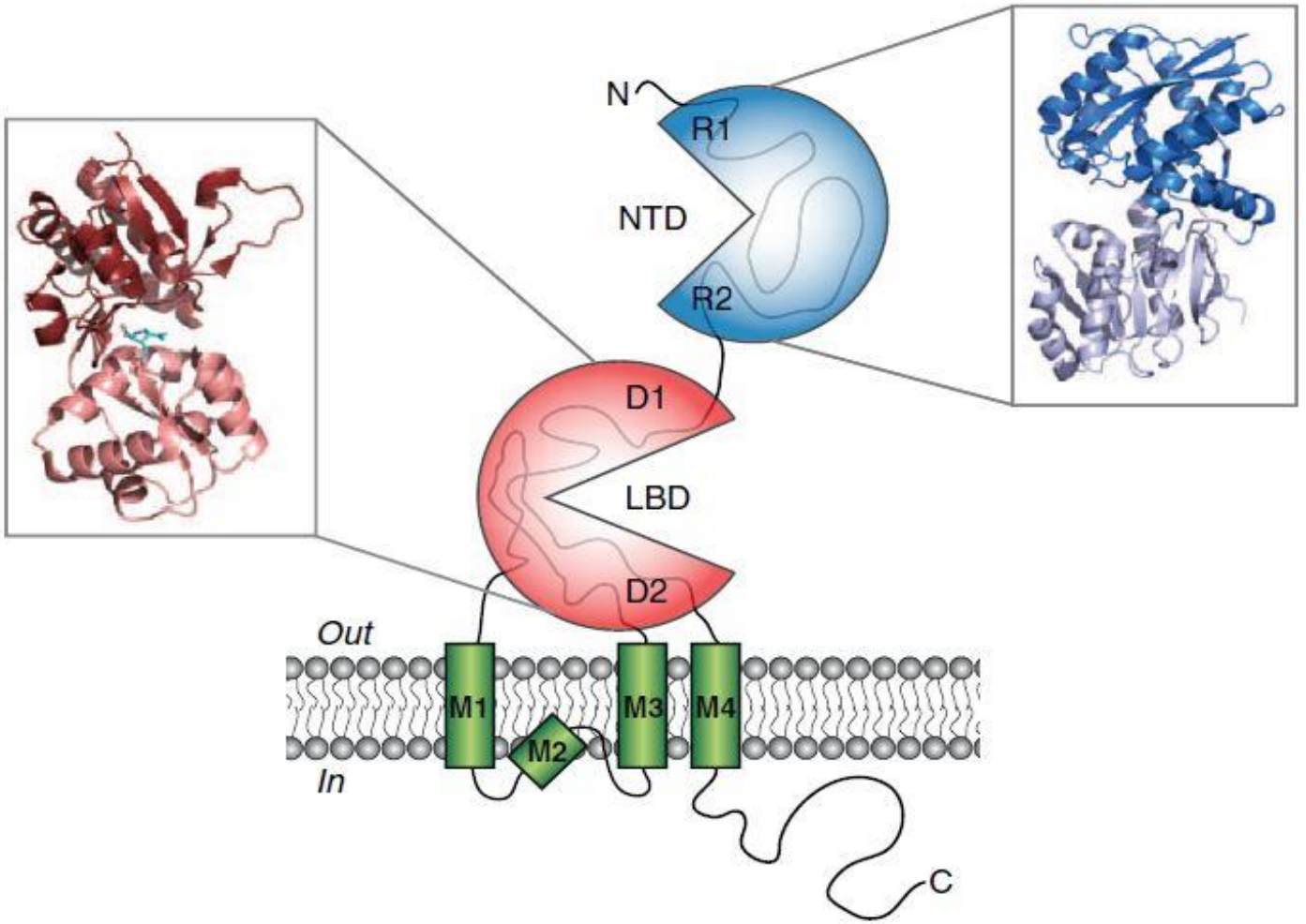

Figure 1.7. KAR subunit topology. A KAR subunit consist of an extracellular large N-terminal domain (which has two component lobes; **R1 and R2**) with its detailed crystal structure shown. The three transmembrane domains (**M1, M3, M4**) and the pore loop (M2) are also depicted followed by the intracellular C-terminal domain. Also shown is the ligand-binding domain (**LBD**) with its two lobes (**D1 and D2**) and detailed crystal structure. Contractor *et al*. (2011). *Image used with copyright permission from Elsevier Limited (2016).*

1.5.3. *KAR subunit diversity*

Previous studies have suggested that there is significant diversity among the KAR subunits in the context of structure. mRNAs that encode for GluK1 and GluK2 subunits are subject to enzymatic editing by RNA deaminase which results in alternate incorporation of an important amino acid in the pore-forming P-loop (the 'Q/R' site) (Carta *et al*., 2014). This insertion of amino acid results in GluK1 and GluK2 having significantly reduced permeability for divalent cations as well as having very low single-channel conductance (Contractor *et al*., 2011; Carta *et al*., 2014). The physiological relevance of these changes however, remain unclear.

KAR subunits GluK1-3 undergo alternative splicing in different components of the receptors. GluK1 undergo alternative splicing within the NTD and CTD which results in two splice variants (GluK1-1 and GluK1-2) in the NTD and four splice variants (GluK1a, GluK1b, GluK1c and GluK1d) in the CTD (Pahl *et al*., 2014). In GluK2, there is alternative splicing within the CTD which results in three GluK2 variants (GluK2a, GluK2b and GluK2c) (Pinheiro and Mulle, 2006; Pahl *et al*., 2014). There is an alternative splicing in the CTD of GluK3 which results in two splice variants; GluK3a and GluK3b (Pahl *et al*., 2014). The KAR subunit diversity as result of alternative splicing as well as mRNA enzymatic editing is shown in Figure 1.8.

Alternative splicing has been suggested to have significant effect on GluK1-3 subunits in areas of cellular trafficking, surface expression as well as how these receptors interact with accessory proteins and intracellular partners (Carta *et al*., 2014; Lerma and Marques, 2013).

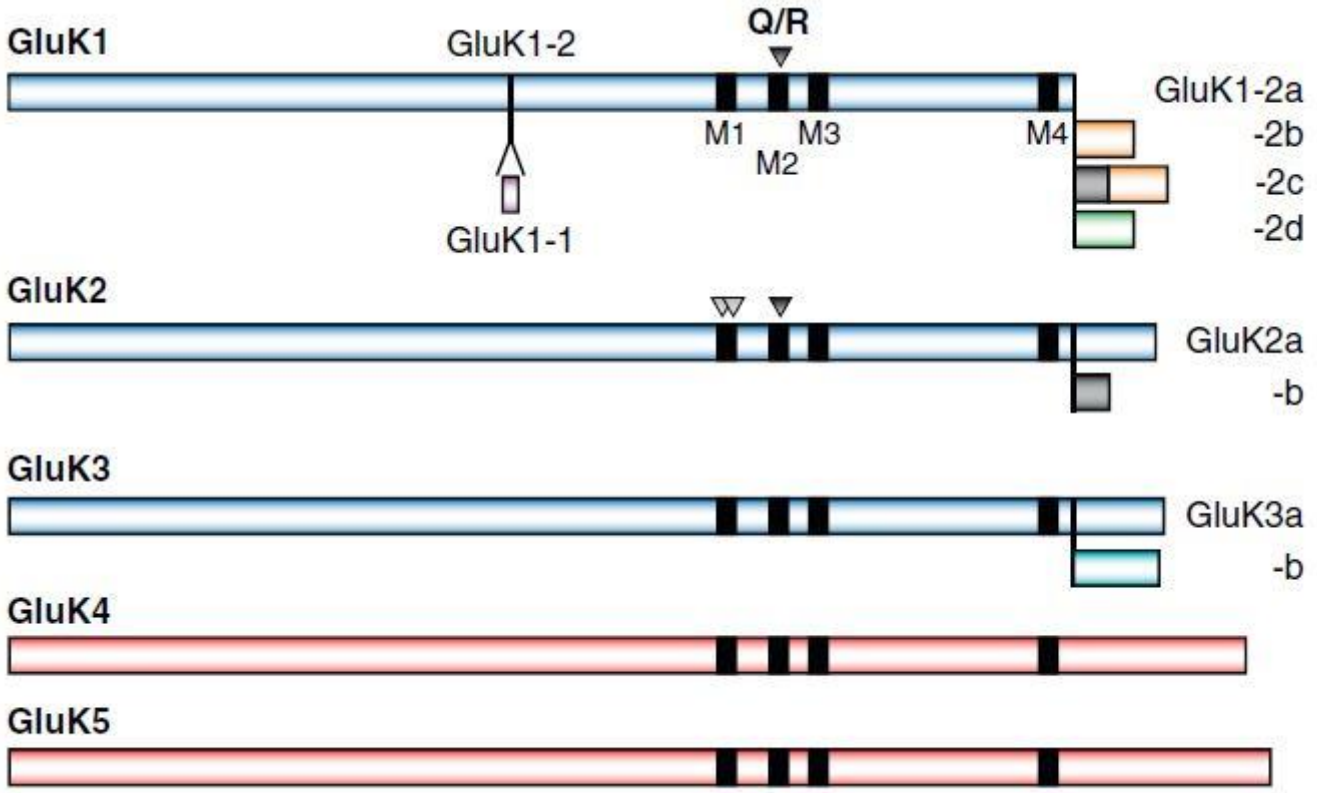

Figure 1.8. KAR subunits and their splice variants. GluK1-3 show significant sequence homology but they differ from GluK4 and GluK5 in the context of sequences as well as affinity for agonists. The black boxes in each subunit represent the four membrane domains (M1, M2, M3 and M4) and the triangles represent positions of RNA editing. Alternative splicing of these subunits leads to splice variants such as GluK2a and GluK2B for the GluK2 KAR subunit. This figure is from Contractor *et al*. 2011. *Image used with copyright permission from Elsevier Limited (2016).*

1.5.4. *Localisation of KAR subunits in the CNS*

Due to inadequate pharmacological tools, transgenic animals and specific antibodies against KAR subunits, most studies regarding the expression of these receptors in the CNS have used *in situ* hybridisation and electrophysiological approaches. These methods however do not provide enough information about the subcellular distribution of KAR subunits (Lerma and Marques, 2013). The most widely-expressed KAR subunit in the CNS is GluK2 and it is significantly expressed in most parts in the brain but particularly at the mossy fiber-CA3 synapse in the hippocampus where they primarily modulate post-synaptic responses (Carta *et al*., 2014). GluK1 expression is however significantly restricted in the adult brain but widely expressed in the developing brain of rodents and humans including the Purkinje cells of the cerebellum as well as in the spinal cord (Fisher, 2014; Perrais *et al*., 2010). It is suggested that the pattern of GluK1 expression in the brain may be related to its function of modulating neuronal maturation in rodents and humans (Carta *et al*., 2014; Fisher and Fisher, 2014). For instance, expression of GluK1 in adult rodents and humans is thought to be primarily in the hippocampal and cortical interneurons where they contribute to the pre- and post-synaptic populations of KARs (Carta *et al*., 2014; Fisher and Fisher, 2014). KAR subunit GluK3 which has not been investigated extensively as other subunits has been shown to be expressed in vast sections of the brain including the dentate gyrus of the hippocampus and also in the neocortex (Perrais *et al*., 2010). In the hippocampus, GluK3 is involved in pre-synaptic functions including modulation of neurotransmitter release. GluK3 modulation of neurotransmitter release is thought to occur in combination with GluK4 (Fisher, 2014). Expression of GluK4 has been observed in the neocortex, Purkinje cells of the cerebellum, CA3

pyramidal neurons as well as in the dentate gyrus (Lerma and Marques, 2013) while GluK5 is widely expressed in several parts of the brain. The heteromeric combination of GluK2 and GluK5 is thought to be the most common KAR unit in the brain (Perrais *et al*., 2010; Fisher, 2015).

The diverse localisation and expression of the various KAR subunits in the CNS may be indicative of specific and distinct roles that each subunit or subunit combination play. These may also explain the diversity of KAR signalling in the CNS.

1.5.5. *Pharmacology of KARs*

Studies into the properties and functions of KARs have not seen much progress compared to the other iGluRs. This is due in part to lack of appropriate and specific pharmacological tools for KAR subunits (Jane *et al*., 2009). The use of pharmacological tools represents an important area in the study of structural and functional diversity of KAR subunits. In addition to glutamate and kainate, several agonists and antagonists of KARs have been discovered or synthesised over the years.

The activities of some of the important KAR agonists and antagonists are is shown in Table 1.2 and Table 1.3 respectively.

Table 1.2. KAR agonist activity (EC_{50} in µM) on recombinant subunit receptors. -: not known or determined; **NE**: no effect. **EC_{50}** refers to the molar concentration of an agonist the results in 50% of the maximum response or effect of the drug. The table is based on data from: Matute, 2011; Jane *et al*., 2009; Pinheiro *et al*., 2013; Artinian *et al*., 2011; Fisher and Mott, 2011; Peret *et al*., 2014; Traynelis *et al*. 2010.

Agonist	GluK1	GluK2	GluK3	GluK1/ GluK2	GluK1/ GluK5	GluK2/ GluK5
Glutamate	47	9	5900	48	19	8
Kainate	4.9	1.1	-	7.4	1.5	0.6
Domoate	0.36	0.07	-	0.19	0.05	0.12
ATPA	0.33	NE	-	0.8	0.38	106
SYM2081	0.18	0.29	-	0.38	0.06	0.34
LY339434	2.5	>100	-	-	-	-
Dysiherbaine	0.0005	0.0013	-	-	-	-
5-Iodowillardiine	0.21	1000	300	0.47	0.06	30

Table 1.3. KAR antagonists and their dissociation constant (in µM) on recombinant subunit receptors. -: not known or determined; **NE**: no effect; K_d: dissociation constant. Dissociation constant is the molar concentration of the drug which occupies 50% of the receptors at equilibrium. The table is based on data from: Matute, 2011; Jane *et al*., 2009; Pinheiro *et al*., 2013; Artinian *et al*., 2011; Fisher and Mott, 2011; Peret *et al*., 2014; Traynelis *et al*. 2010.

Antagonist	GluK1	GluK2	GluK3	GluK1/ GluK2	GluK1/ GluK5	GluK2/ GluK5
UBP310	0.010	NE	0.023	-	0.008	NE
Kynurenate	415	391	-	482	621	NE
CNQX	8	18	-	4	10	72
NBQX	25	21	18	19	26	87
UBP296	0.6	NE	374	0.8	1.0	NE
LY382884	2	NE	NE	4	4	NE
LY377770	0.2	NE	-	0.4	1.0	NE
NS102	6	1.4	-	-	-	-
NS3763	1.6	NE	-	NE	NE	NE

1.5.6. *KAR-interacting proteins*

Studies have shown that properties of KARs including agonist binding, molecular scaffolding, receptor trafficking, surface expression and localisation of KARs depend on interaction between KARs and some proteins (Zhang *et al*., 2014; Fisher, 2015). Though this is a relatively new area in terms of KAR research, the identification of these interacting proteins have contributed considerably to the understanding of KAR physiology as well as provided insights into the differences between native and recombinant KARs. Among the interacting proteins of KAR subunits include PDZ motif-containing proteins (PSD-95, PICK1, GRIP, synthetin, SAP-97, SAP-102), cytoskeleton proteins (cadherins, β-catenin, Velis), BTB/Kelch proteins (actinfilin), calcium/calmodulin-dependent serine protein kinases (CASK), phosphatases (calcineurin), CUB proteins (Neto 1, Neto 2) and other proteins (calmodulin, contactin, SNAP25) (Pahl *et al*., 2014; Fisher, 2015). The key KAR-interacting proteins are summarised in Table 1.5.

Table 1.4. KAR-interacting and auxiliary proteins.

Interacting protein	Interacting domain	Interacting KAR subunit	Role	References
Neto 1	CUB2, RKK	GluK1/Gluk2/GluK3/GluK5	Trafficking, gating, rectification	Sheng *et al*., 2015; Fisher, 2015; Howe, 2015
Neto 2	CUB2, RKK	GluK1/Gluk2/GluK3/GluK5	Trafficking, ion channel function	Sheng *et al*., 2015; Fisher, 2015; Howe, 2015; Rutkowska-Wlodarczyk *et al*., 2015
SNAP-25	-	GluK5	Trafficking	Pahl *et al*., 2014
PSD95	PDZ1, SH3	GluK1/GluK2/GluK5	Clustering, desensitisation	Pahl *et al*., 2014
PICK1	PDZ	GluK1/GluK2/GluK5	Trafficking	Pahl *et al*., 2014
Cadherin	-	GluK2	Localisation, trafficking	Lerma and Marques, 2013
Parkin	-	GluK2	Gating	Maraschi *et al*., 2014
GRIP	PDZ4, PDZ5	GluK1/GluK2	Trafficking	Pahl *et al*., 2014
4.1N	-	GluK1/GluK2	Trafficking	Lerma and Marques, 2013

1.5.6a. *PDZ motif-containing interacting proteins of KARs*

Through transient interactions with KAR subunits, some PDZ domain-containing proteins regulate and promote several functions and properties of KARs. Binding PSD-95 and SAP-102 to the C-terminal of GluK2 enhances the recovery of GluK2 homomeric and GluK2/GluK5 heteromeric assembly from desensitisation and also promotes the clustering of KARs (Suzuki and Kamiya, 2015; Pahl *et al*., 2014). Also, SAP-97 protein interacts with GluK2 to promote KAR clustering. Promotion of KAR clustering is also observed when SAP-102 interacts with GluK2/GluK5 heteromeric assembly (Lerma and Marques, 2013; Pahl *et al*., 2014). Another PDZ domain-containing protein, PICK1 interacts with GluK1 and GluK2 subunits to promote KAR membrane anchoring and trafficking (Rutkowska-Wlodarczyk *et al*., 2015; Pahl *et al*., 2014).

1.5.6b. *Cytoskeleton interacting proteins of KARs*

Cytoskeleton interacting proteins include cadherins, β-catenin and catenin. They have been shown to interact with GluK2 to enhance localisation and stability of KARs at synaptic junctions. The 4.1N scaffolding proteins interact with GluK2 and GluK1 to promote stability, receptor trafficking as well as endocytosis of KARs (Rutkowska-Wlodarczyk *et al*., 2015; Copits and Swanson, 2013). Also, interaction between profilin II and GluK2 has been observed to promote KAR trafficking (Mondin *et al*., 2010).

1.5.6c. *CUB domain-mediated interactions with KARs*

Recently, Neto 1 and Neto 2 proteins have been identified as auxiliary or accessory proteins of KAR subunits. This is because Neto 1 and Neto 2 fulfil the four criteria for classification of iGluR auxiliary proteins (Fisher, 2015). First, Neto 1 and Neto 2 do not constitute an integral part of the structure or pathway of KARs. Second, Neto 1 and Neto 2 have a stable interaction with KARs for most or the entire duration subsequent to the receptor's assembly in the ER. The third criteria is that Neo 1 and Neto 2 significantly modulate or influence several components of KAR pharmacology, trafficking and channel properties. Fourth, co-assembly of the KARs with Neto 1 or Neto 2 is thought to be required for effective function of the receptors *in vivo* (Copits and Swanson, 2012; Yan and Tomita, 2012; Molnar *et al*., 2013). These underscore the significance of these transmembrane proteins for effective function of post-synaptic KAR subunits in particular.

Structurally, Neto proteins carry two extracellularly-located CUB domains (Complement C1r/C1s, Uegf, Bmp1) followed by an extracellular juxtamembrane LDLa (low-lipoprotein receptor class A) and an intracellular C-terminal domain (Griffith and Swanson, 2015). Studies suggest that regulation of KAR subunit function by Neto 1 and Neto 2 proteins is via mediation of the LDLa domain while interactions between KARs and Neto 1 and Neto 2 proteins are modulated primarily through the second CUB domain (Fisher, 2015; Pahl *et al*., 2014). However, other Neto 1- or Neto 2-induced effects on KARs including rectification characteristics are not thought to be mediated by CUB or LDLa domains but instead by three positively charged RKK residues in the transmembrane domains of Neto 1 and Neto 2 (Fisher and Mott, 2013). While Neto 1 has

a class I PDZ domain, Neto 2 has a class II PDZ ligand at their respective C-terminals (Pahl *et al*., 2014).

In the CNS, Neto 1 is expressed predominantly in the CA3 region of the hippocampus while Neto 2 is abundantly expressed in the cerebellar granule cells and cortical neurons of the brain (Fisher, 2015; Tomita and Castillo, 2012). These proteins have also been shown to be expressed in the retina of rodents (Pahl *et al*., 2014).

Neto 1 and Neto 2 subunits were initially thought to be auxiliary proteins of NMDAR subunits in the CNS (Ng *et al*., 2009) but recent observations do not support this suggestion (Molnar *et al*., 2013). However, accumulating evidence points to a strong interaction between these proteins and KARs that leads to significant modulation of function of these receptors.

Studies have suggested an important role for Neto 1 and Neto 2 in regulation of KAR surface expression. In hippocampal neurons, co-expression of Neto 2 and GluK1 enhances the surface expression and synaptic co-localisation of the latter (Sheng *et al*., 2015; Copits *et al*., 2011). Moreover, in the PSD of cerebellum from Neto 2 knockout mice, there is reduced expression of GluK2. In other studies, expression of Neto 2 in the plasma membrane was enhanced by co-expression or interaction with GluK2 in oocytes of *Xenopus* which is also supported by significantly reduced expression of Neto 2 in the plasma membrane of cerebella from GluK2 knockout mice (Sheng *et al*., 2015; Zhang *et al*., 2009). The effect of Neto 2 on KAR subunit expression is further supported by evidence that Neto 2 promotes stabilisation of GluK2 at the synapse by promoting interaction of GluK2 with the scaffolding protein, GRIP (Rutkowska-Wlodarczyk *et al*., 2015; Tang *et al*., 2012).

The effect of Neto 1 on surface expression of KAR subunits has also been reported. Neto 1 knockout mice have been shown to have significantly reduced expression of GluK2 and GluK5 in the PSD of hippocampal neurons. However, the overall expression of GluK2 and GluK5 in the hippocampus remained unchanged (Sheng *et al*., 2015; Tang *et al*., 2012). GluK2/GluK3 in mossy-fiber-CA3 of the hippocampus has also been shown to be significantly decreased in Neto 1 knockout mice (Wyeth *et al*., 2014) though other studies reported of no change in expression of GluK2/GluK3 or GluK5 in Neto 1 knockout mice (Sheng *et al*., 2015; Straub *et al*., 2011a). The effect of Neto 1 and Neto 2 on KAR subunit expression may however not be entirely due to the interactions between KARs and Neto proteins. Possible factors leading to this reduced expression may include the genetic profile or background of the knockout mice.

Furthermore, interactions between KAR subunits and Neto 1 or Neto 2 proteins result in significant changes in gating pharmacology of KARs. When Neto 1 and Neto 2 are co-expressed with recombinant KAR subunits (GluK1, GluK2 and GluK2/GluK5) receptors, these receptors undergo significant changes in how they recover from desensitisation and their rates of deactivation (Fisher, 2015). These observations may however, be dependent on the type of Neto subunit. Co-expression of Neto 2 with GluK1 or GluK2 homomers slows onset of desensitisation and subsequent recovery of these subunits from desensitisation (Griffith and Swanson, 2015; Straub *et al*., 2011b; Zhang *et al*., 2009). In contrast, co-expression of KAR subunits (GluK1, GluK2 and GluK2/GluK5) with Neto 1 accelerates the onset of desensitisation and subsequent recovery from desensitisation of these KAR subunits (Copits *et al*., 2011; Fisher and Mott, 2013; Howe, 2015).

Also, interactions between Neto proteins and KARs leads to enhanced affinity of KARs for glutamate and kainate. Silencing of Neto 1 and Neto 2 in the hippocampus does not terminate the excitatory post-synaptic current (EPSC) of kainate but reduces the affinity of CA3 neurons for kainate (Howe, 2015; Tang *et al*., 2011). This observation is supported by recent report that GluK1 forms functional homomeric channels whose sensitivity to glutamate increases in the presence of Neto 1 and Neto 2 in transiently-transfected HEK293T cells (Fisher, 2015). Moreover, in Neto 1 knockout mice, there is alteration in synaptic KAR output characterised by fast mossy fiber $EPSC_{KA}$ decay kinetics (Straub *et al*., 2011a; Tang *et al*., 2011). This was observed only in post-synaptic but not in pre-synaptic KARs and was not present in Neto 2 knockout mice (Straub *et al*., 2011b; Tang *et al*., 2011).

Taken together, the roles of Neto 1 and Neto 2 proteins in expression, physiology and diversity of native KAR subunits cannot be understated and could become potential drug targets for certain conditions in which KARs are implicated. However, several questions remain unanswered about interactions of Neto 1 and Neto 2 proteins with KAR subunits. First, the mechanism by which kainate synaptic responses are kept at a minimal compared to the responses of AMPAR and NMDAR even though Neto 1 and Neto 2 enhance the affinity of KARs for kainate/glutamate remain unexplored. Secondly, the structural basis on which Neto proteins and KARs interact remains unclear while the role of Neto proteins in metabotropic signalling of KARs also remain unknown. The number of Neto subunits which are required in formation of a single receptor complex is unclear.

1.5.7. *Metabotropic signalling of KARs*

KARs represent a unique subtype of iGluRs because some functions of KARs in the CNS have can be mediated through an unconventional non-canonical (metabotropic) signalling involving G-proteins and second messengers. This metabotropic signalling of KARs is particularly involved in the regulation of neurotransmitter release from pre-synaptic neurons (Gonzalez-Gonzalez and Henley, 2013; Crepel and Mulle, 2015). At the post-synaptic terminal, mechanisms such as recycling and surface expression of KARs as well as modulation of neuronal excitability have been shown to involve metabotropic signalling (Crepel and Mulle, 2015). Co-localisation of KAR subunits (GluK4 and GluK5) with group I mGluR subunits has been reported in rat hippocampus and in cultured rat cortex (Rojas *et al*., 2013). In these tissues, activation of group I mGluRs enhanced KAR-induced calcium signals. The potentiation of KARs by group I mGluRs was observed only in heteromeric GluK2/GluK5 or GluK2/GluK4 subunit assembly but not in homomeric receptor combinations. The group I mGluR-potentiation of KARs was observed to involve PKC and calcium ion mobilisation (Rojas *et al*., 2013). Other studies have shown that KAR subunits and some mGluR subtypes exhibit interchangeable roles under certain circumstances. For instance, both KARs (GluK1) and mGluRs (mGluR1 and mGluR5) are able to induce mossy fiber LTP in rat hippocampus and this role is interchangeable since activation of one of these receptors alone was sufficient to induce mossy fiber LTP *in vivo* (Wallis *et al*., 2015). Studies suggest that the most dominant KAR subunits which interact with G-proteins to induce non-canonical signalling are GluK1 and GluK5 (Salmen *et al*., 2012; Rutkowska-Wlodarczyk *et al*., 2015).

Moreover, G_0 is thought to be the dominant G-protein that mediates the metabotropic effects of KAR subunits (Lerma and Marques, 2013; Rutkowska-Wlodarczyk *et al*., 2015) although G_i has also been shown to play important roles in this signalling especially in KAR-induced inhibition of adenylate cyclase and cAMP reduction (Gelsomino *et al*., 2013).

However, due to the consensus that KARs do not possess conventional motifs in their C-terminals, it is considerably unlikely that this metabotropic signalling of KARs occur through the direct coupling of the receptors to G-proteins (Contractor *et al*., 2011). This raises the possibility that some auxiliary proteins of KARs may be involved in the KAR-G-protein signalling complex. A recent study using proteomic analysis has shown that already-established KAR-interacting proteins including β-catenin, synapsin II, $G_{\alpha 0}$, Rab3a, BASP1 interact with GluK1 in its metabotropic signalling action (Rutkowska-Wlodarczyk *et al*., 2015). An overview of the putative effects of mGluRs and non-canonical signalling on KAR function is shown in Figure 1.9.

In spite of ongoing research into non-canonical signalling of KARs and the influence of metabotropic receptors on potentiation of KAR subunit function, several questions remain unanswered. The molecular mechanisms involved in activation of G-proteins by KARs as well as what determines the mode (conventional ionotropic versus metabotropic) of KARs at any point remain unclear. These issues however, has not overshadowed the unique signalling characteristics of KARs and the potential of KARs as an important target for development of therapies directed at both iGluRs and mGluRs signalling mechanisms.

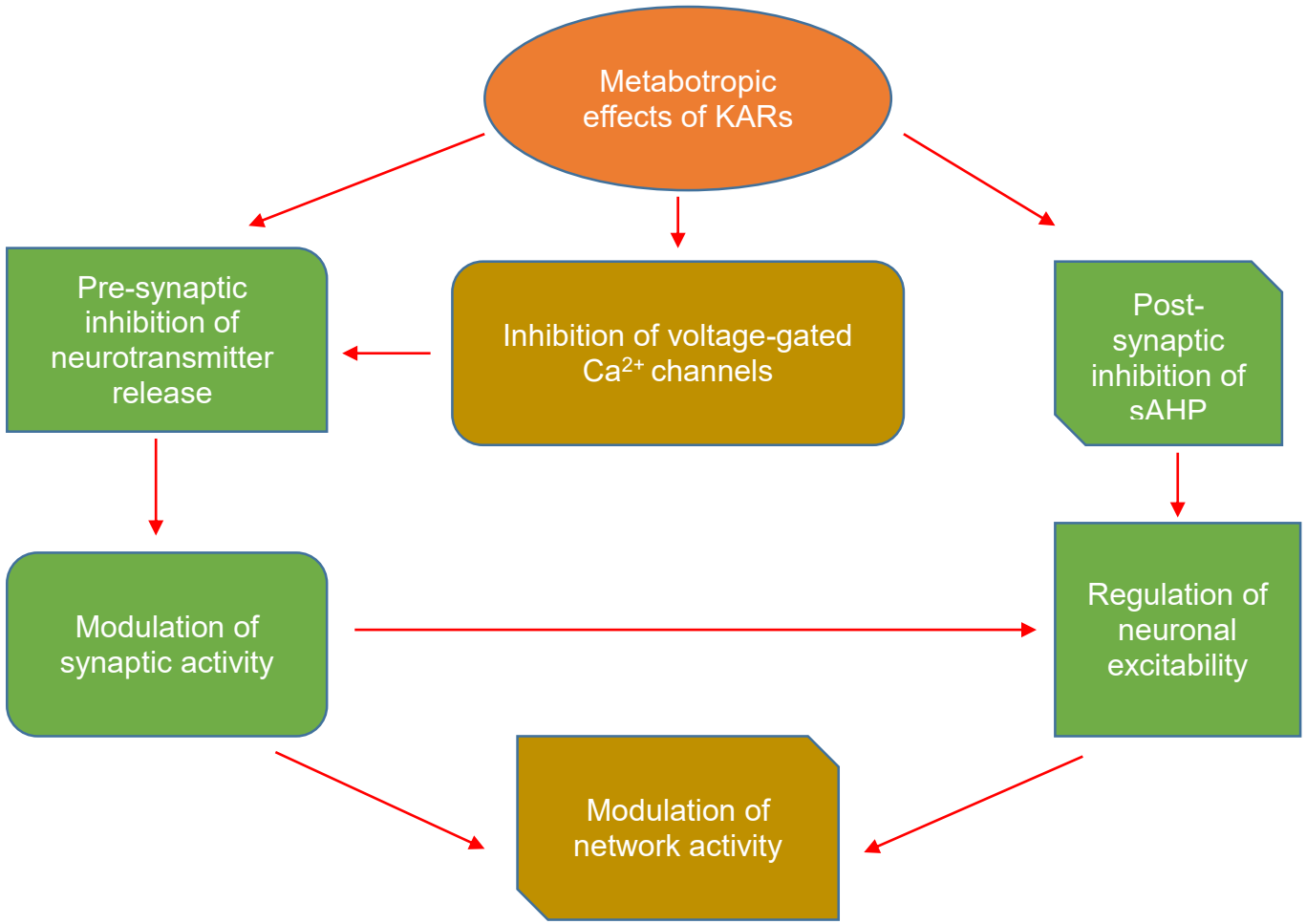

Figure 1.9. Summary of the metabotropic effects of KARs in CNS function: At pre-synaptic terminals. KARs modulate the release of both GABA and glutamate in a bidirectional manner using metabotropic signalling which leads to modulation of synaptic activity and subsequently modulation of network activities. The regulation of neurotransmitter release by pre-synaptic KARs may also be in part to the inhibition of voltage-gated Ca^{2+} channels. This KAR-induced inhibition of Ca^{2+} channels is via interaction of KARs with G-proteins and PKC. Using metabotropic mechanism, post-synaptic KARs induce inhibition of slow after-hyperpolarization currents (sAHP) which subsequently regulates neuronal excitability. Adapted from Crepe and Mulle, 2015; Wallis *et al*., 2015; Rodrigues and Lerma, 2012.

1.6. Roles of KARs in the CNS

KARs have been linked to several roles in the CNS many of which are dependent on their distribution/expression as well as subunit combinations. Among the major roles of KARs in the CNS include modulation of synaptic transmission and network excitability, brain development and synaptic plasticity. Most of the functions of KARs have become evident due to the recent development of several selective pharmacological tools for KARs as well as the generation of KAR-knockout rodents. The functions of KARs in the CNS can be grouped into two main part; pre-synaptic functions and post-synaptic functions.

1.6.1. *Pre-synaptic roles of KARs*

Accumulating evidences support a pre-synaptic role of KARs in the CNS. An early study into this hypothesis indicated that activation of KARs by pharmacological agonists resulted in enhanced modulation of glutamate release from the synaptosomes via a Ca^{2+}-dependent mechanism (Chittajallu *et al*., 1996). Currently, it is thought that KARs modulate release of glutamate and GABA at excitatory and inhibitory synapses respectively (Lerma and Marques, 2013). As discussed previously, GluK2 subunits co-assemble with GluK3 at the pre-synaptic neurons to regulate neurotransmitter release (Fisher, 2014). Though it was initially thought that pre-synaptic KARs were involved in depressing neurotransmitter release, emerging reports point to a biphasic modulatory effect at some of the glutamatergic synapses. At these synapses, low concentrations of kainate was observed to result in significant increase in KAR-induced release of glutamate whereas a high concentration of kainate resulted in depressed glutamate release (Lyon *et al*., 2011). The mechanism behind this biphasic mechanism of neurotransmitter

release at the glutamatergic synapse remains largely unexplored. The biphasic mechanism is thought to be occur only when KARs are activated by exogenous agonist since activation of KARs by endogenous glutamate almost always leads to facilitation of neurotransmitter release (Contractor *et al*., 2011). Recent studies have linked KAR-induced modulation of glutamate release from the synaptosome of rats to the intrasynaptosomal Ca^{2+} stores as well as to the activation/inhibition of calmodulin (Sihra and Rodriguez-Moreno, 2013; Andrade-Talavera *et al*., 2012) indicating a conventional ionotropic mechanism for this modulation. KAR-induced depression of glutamate release from pre-synaptic neurons has however been linked to a non-canonical (metabotropic) mechanism by KARs. This observation is supported by studies which have shown that KAR-induced depression of glutamate release is negatively affected by application of pertussis toxin (PTX); a potent inhibitor of $G_{i/0}$ (Sihra and Rodriguez-Moreno, 2013; Negrete-Diaz *et al*., 2006).

In the context of GABA release by KARs, earlier studies suggested that activation of KARs at the GABAergic synapses resulted in reduced GABA release (Rodriguez-Moreno *et al*., 1997). This has been supported by current studies which have shown that activation of GluK1-containing KARs results in depressed release of GABA from the hippocampus (Bonfardin *et al*., 2010; Caiati *et al*., 2011). These inhibitory effects on GABA release by KARs is thought to be via a G-protein-dependent mechanism (Lerma and Marques, 2013).

In summary, KAR subunits are present on pre-synaptic terminals where they play an important role in regulating release of inhibitory and excitatory neurotransmitters into the synaptic cleft for subsequent binding and downstream signalling. In addition to

modulation of neurotransmitter release, KAR subunits at the presynapse have been shown to contribute to the development and maintenance of synaptic connectivity and maturation. GluK1 remains the most significant subunit involved in development of the brain (Lerma and Marques, 2013).

1.6.2. *Post-synaptic roles of KARs*

At post-synaptic terminals, activation of KARs by glutamate have been observed to mediate excitatory neurotransmission and synaptic plasticity (Sihra *et al*., 2013). Studies have shown that activation of post-synaptic KARs by glutamate results in small-amplitude EPSCs characterised by slow activation and deactivation compared to the currents induced AMPAR activation (Lerma and Marques, 2013). These EPSCs, unlike those of AMPARs and NMDARs are localised only to a select subset of neurons (Lerma and Marques, 2013). This characteristically slow kinetics of post-synaptic KARs are thought to enhance the capabilities of information transfer integration of KARs; a mechanism which is not significant in other iGluRs (Pinheiro *et al*., 2013). In terms of subunit composition, GluK2, GluK4 and GluK5 constitute the majority of post-synaptic KARs at mossy fiber to CA3 pyramidal cell synapses (Fernandes *et al*., 2009). These postsynaptic KAR subunits are also involved in regulation of slow Ca^{2+} and K^{+} currents. The varied roles of KAR subunits contribute to the balance that exist between excitation and inhibition of neuronal networks with subsequent effects on cognition as well as contributing to established forms of short and long-term plasticity.

1.7. Putative roles of KARs in CNS-related diseases

Kainate is a potent neurotoxin and a neural excitant which when injected into the brain of rodents elicit persistent convulsion and neurotoxicity that mimic the classical symptomatic episodes of temporal lobe epilepsy (TLE) in human (Vincent and Mulle, 2009). In addition to inducing seizures, injection of kainate leads to neurodegeneration (Vincent and Mulle, 2009). In the CNS, neurodegeneration is considered to be one of the important pathogenic mechanisms underlying acute and chronic neurodegenerative conditions such as TLE, Alzheimer's disease, Parkinson's disease and Huntington's disease (Mohd Sairazi *et al*., 2015). The major mechanism underlying neurodegeneration is excitotoxicity; a consequence of prolonged excitation or activation of excitatory GluRs. Excitotoxicity-induced death of neuronal cells is thought to be mediated mainly through increased influx of Ca^{2+} with subsequent programmed-cell death and apoptosis (Mohd Sairazi *et al*., 2015).

Seizures induced in rodents after injection of kainate results mainly from over-activation of KARs by kainate though few studies have implicated endogenous glutamate in induction of epileptic seizures (Crepel and Mulle, 2015; Matute, 2011). Due to the potent neurotoxic and excitatory action of glutamate and its analogues including kainate, KARs have been linked to pathogenesis of several neurological conditions including epilepsy, mood disorders, mental retardation, chronic pain, migraine, autism and Huntington's.

1.7.1. *Putative roles of KARs in epilepsy*

Epilepsy refers to the neurological disorder that involves prolonged and synchronised neuronal discharges leading to occurrence of spontaneous or chronic seizures (Crepel and Mulle, 2015). Several studies support a probable role of KARs in the pathogenesis of epilepsy. The most significant of these putative roles involve the contribution of KARs to the excitatory/inhibitory imbalances; the classical feature of epilepsy (Lerma and Marques, 2013). Intra-amygdaloid administration of kainate into adult rats have been shown to result in persistent seizures and neuronal damage that mimics details of human TLE (Crepel, 2013). The most cited KAR subunits in epilepsy studies are GluK1 and GluK2. Studies have suggested that GluK2 is highly expressed in hippocampal CA3; a region of the brain that is highly excitable and strongly linked to TLE (Crepel and Mulle, 2015; Matute, 2011). Also, knockout of GluK2 in mice results in reduced vulnerability of these mice to kainate-induced seizures (Peret *et al*., 2014; Crepel, 2013). In addition, in both *in vitro* and *in vivo* models of TLE, GluK2/GluK5 receptor antagonist UBP310 significantly reduced seizure-like activities induced by kainate (Peret *et al*., 2014) which suggests a role for GluK2/GluK5 heteromeric combination in generating recurrent seizures in chronic epilepsy and also provides evidence that activation of KARs by endogenous agonists plays a role in eliciting epileptic seizures. However, injection of considerably high concentrations of kainate into GluK2 knockout mice induced the same epileptic characteristics observed in wild type mice (Matute, 2011) which confirms the possible role of other KAR subunits in development of kainate-induced epileptic seizures. Moreover, high kainate concentration can also activate other iGluRs implicated in generation of epileptic seizures including AMPARs.

Furthermore, inhibition of GluK1 has been shown to prevent epileptic activities in certain areas of the hippocampus (Crepel and Mulle, 2015; Smolders *et al*., 2002) and one of the most successful anti-epileptic medications in clinical use; topiramate appears to exert its anti-epileptic actions in part through inhibition of GluK1 (Fritsch *et al*., 2014; Jane *et al*., 2009). Use of tissues from human TLE patients has shown that there is significant upregulation of GluK1 expression in the hippocampus (Li *et al*., 2010) which may be indicative of a role for KARs in rearrangement of neural circuits in these patients (Lerma and Marques, 2013).

Other KAR subunits have also been linked to epilepsy. For instance, in addition to GluK1 and GluK2, expression of GluK4 and GluK5 was significantly upregulated in hippocampal astrocytes of rats after induction of status epilepticus (Vargas *et al*., 2013). Altogether, there is accumulating evidence to suggest a significant role for KAR subunits in pathogenesis of epilepsy.

1.7.2. *Putative roles of KARs in psychiatric disorders*

KARs have been linked to the pathogenesis of several psychiatric conditions including schizophrenia, autism, major depression, bipolar disease and obsessive-compulsive disorder (OCD). In patients suffering from schizophrenia, there is decreased in expression of GluK1, GluK2 and GluK3 subunits in the orbitofrontal cortex (Garey *et al*., 2006) whiles several polymorphic variants of GluK2 have been reported in patients suffering from autism, OCD and schizophrenia (Bowie, 2008). Also, genetic variants of GluK3 have been observed to be present in patients suffering from major depression, bipolar disorder and schizophrenia (Matute, 2011). However, there was no evidence of change in

quantitative expression of KAR subunit mRNA or protein in brain samples of patients diagnosed with schizophrenia (Matute, 2011). A single nucleotide polymorphism in the *Grik4* gene is thought to give protection from bipolar disorders (Sklar *et al*., 2011) while *Grik4* knockout mice develop schizophrenia and learning deficits (Lowry *et al*., 2013). These contrasting observations indicate different roles and mechanisms for KAR subunits in psychiatric disorders. Also, *Grik2* and *Grik4* genes have been implicated in the pathogenesis of autism. Mice with significantly high expression of *Grik4* in the brain displayed symptoms and behaviours consistent with autism spectrum disorders (Aller *et al*., 2015; Freitag, 2007).

Though this is still an active area of research, there are significant evidences to suggest putative roles for KAR subunits in psychiatric disorders.

1.7.3. *Putative roles of KARs in mental retardation*

A single sequence change in the *Grik2* gene has been linked to cognitive impairment and mental retardation arising from defective glutamatergic signalling (Lerma and Maques, 2013). This observation is corroborated by a report that GluK2-deficient rodents display significant delay in maturation of important areas of the brain including hippocampus which is responsible for higher brain function (Lanore *et al*., 2012). This study however, did not report of the long-lasting effects of this delayed maturation in the animals hence it is debatable to relate delayed maturation of certain brain parts to cognitive impairment or mental retardation in adult life.

1.7.4. *Putative roles of KARs in Huntington's disease*

Prolonged activation of KARs leads to excitotoxicity which subsequently leads to neurodegeneration; one of the most noted mechanisms underlying Huntington's (Mohd Sairazi *et al*., 2015). Though early studies suggested a link between age of onset of Huntington's and polymorphisms in *Grik2* (Rubinsztein *et al*., 1997), later studies involving larger sample of patients with Huntington's did not observe such linkage (Lee *et al*., 2012). Moreover, 3-nitropropionic acid, a common drug used to induce Huntington-like symptoms in rodents did not induce these expected symptoms in GluK2 knockout mice (Diguet *et al*., 2004). These studies therefore indicate an unlikely direct mechanism of KAR subunits in pathogenesis of Huntington's. However, the probable contribution of KAR subunits might arise from excitotoxicity-induced neurodegeneration subsequent to prolonged activation of these receptors by endogenous glutamate.

1.8. GluRs as autoantibody targets in neurological diseases

Subtypes of GluRs have been implicated as targets for autoantibodies in a number of autoimmune neurological conditions including Rasmussen's encephalitis and epilepsy (Levite, 2014). Analysis of the levels and effects of autoantibodies in the CNS suggests that autoantibodies against GluRs represent the commonest, most potent and most dangerous type of autoantibodies involved in pathological processes in the CNS (Levite, 2014). The most commonly identified GluR subtype that serve as antigen targets for autoantibodies are AMPARs and NMDARs whiles few studies also suggest mGluRs as autoantigens.

1.8.1. *AMPARs as antigen targets in autoimmune CNS disorders*

Autoantibodies to AMPARs have been linked to Rasmussen's encephalitis, anti-AMPAR-encephalitis and some focal epilepsies (Gleichman *et al*., 2014; Levite, 2014; Hoftberger *et al*., 2015). All these conditions present with varying degrees of seizures and the importance of AMPARs as autoantigens in these conditions is supported by the observation that almost 30% of all patients suffering from epilepsy have autoantibodies against GluA3 AMPAR subunit in their sera or CSF (Hoftberger *et al*., 2015).

Rasmussen's encephalitis is a rare childhood inflammatory neurological disorder characterised by mild dementia or cognitive decline, frequent severe drug-resistant seizures, hemiparesis and encephalitis (Nibber *et al*., 2016). There is no conclusive detail on the aetiology of Rasmussen's encephalitis but previous and emerging evidences point to the role of autoantibodies to GluA3B and GluA2 in pathogenesis of the conditions (Nibber *et al*., 2016). Though autoantibodies to these AMPARs are not present in all

Rasmussen's encephalitis patients, there is a temporary or long-lasting improvement in symptoms subsequent to plasma exchange or removal of GluA3B antibodies from serum of Rasmussen's encephalitis patients (Varadkar *et al*., 2014; Golberg-Stern *et al*., 2014). These antibodies are however not restricted or specific for Rasmussen's encephalitis since they are also present in other forms of epilepsy (Levite, 2014) and sera from GluA3B- or GluA2-positive Rasmussen's encephalitis patients did not recognise singly-GluA2- or GluA3-transfected HEK293 cells (Nibber *et al*., 2016).

Quite recently, analysis of sera and CSF of ten patients with limbic encephalitis revealed that these patients had autoantibodies against GluA1 and GluA2 subunits (Lai *et* al., 2009; Hoftberger *et al*., 2015). Limbic encephalitis is an autoimmune inflammatory condition characterised by seizures, emotional and behavioural disturbances as well as defects in short-term memory (Fauser *et al*., 2015; Lai *et al*., 2009). Application of purified IgG from anti-GluA1- and GluA2-positive LE patients to cultured hippocampal neuronal cells showed a dose-dependent decrease in amplitude and frequency of $mEPSC_{AMPAR}$ (Gleichman *et al*., 2014) implying a role of these autoantibodies is alterations or disruption in AMPAR signalling in the CNS.

1.8.2. *NMDARs as antigen targets in autoimmune CNS disorders*

Anti-NMDARs have been linked to autoimmune conditions such as systemic lupus erythematosus (SLE) and anti-NMDAR encephalitis. The effect these antibodies on survival and function of neurons in these conditions have also been reported (Levite, 2014).

Anti-NMDAR encephalitis is a very severe but treatable disorder with about 4% mortality rate and was first described in 2007 in patients with ovarian teratomas. It is characterised by memory deficits, seizures, reduced consciousness, hypoventilation and psychiatric symptoms (Dalmau *et al*., 2007; Dalmau *et al*., 2011; Barry *et al*., 2015). Detection of GluN1 antibodies in serum or CSF correlates with severity and prognosis of the condition and also represents the gold-standard diagnostic feature (Dalmau *et al*., 2007; Dalmau *et al*., 2011). Moreover, there is significant intrathecal synthesis of anti-GluN1 antibodies in patients and there has not been a single case of the condition in which antibodies were present in serum but not in CSF (Pillai *et al*., 2015; Varma and Sapra, 2015). These observations indicate that there is a very potent, active and ongoing immune process against GluN1 subunits in anti-NMDAR encephalitis.

Furthermore, autoantibodies to GluN2A and GluN2B have been detected in serum and CSF of about 30% of patients suffering from SLE and the antibody titre correlates positively with cognitive and psychiatric impairments associated with the disease (Levite, 2014). Injection of these autoantibodies into mice have been shown to activate NMDARs and cause excitotoxicity-mediated death of hippocampal neurons (Lauvsnes *et al*., 2013).

1.8.3. *mGluRs as antigen targets in autoimmune CNS disorders*

Autoantibodies against mGluR1 have been detected in serum and CSF of patients with paraneoplastic cerebellar ataxia (PCA), an autoimmune condition associated with ovarian, lung and breast cancers and Hodgkin's Lymphoma. Some of the patients showed intrathecal synthesis of anti-mGluR1 (Levite, 2014). Moreover, purified antibodies from CSF and serum of PCA patients have been shown to bind strongly and impair basal

actions of Purkinje cells in brain slices and cultured mouse Purkinje cells of both human and mice (Levite, 2014). Autoantibodies against mGluR5 have been detected in CSF and serum of some individuals suffering from Hodgkin's lymphoma-associated limbic encephalitis (Ophelia syndrome). Sera from these patients were observed to bind and react with isolated hippocampal rat neurons *in vitro* (Mat *et al*., 2013; Levite, 2014).

Taken together, some GluR subtypes serve as important autoantigen targets in a considerable number of autoimmune neurological conditions and some receptor subunits have been targeted in treatment and management of these conditions.

Up to date, there has not been any studies suggesting KARs as potential antigen targets in autoimmune neurological conditions.

A summary of some of the common autoimmune neurological disorders in which GluRs have been suggested as antigen targets is shown in Table 1.5.

Table 1.5. Summary of autoimmune neurological disorders in which GluRs have been suggested as autoantibody targets including GluR targets, methods of antibody identification, response of patients to immunotherapies directed against the respective GluR subunit as well as the type of sample for investigation.

Neurological disorder	GluR subunit	Sample	Methodology	Immunotherapy response	Reference
Rasmussen's encephalitis	GluA2, GluA3	Serum, CSF	Radioimmunoassay Immunohistochemistry	Yes	Nibber *et al*., 2015 Rogers *et al*., 1994
Anti-AMPAR-encephalitis	GluA1, GluA2	Serum, CSF	Immunoblotting ELISA	Yes, with frequent relapses	Gleichman *et al*., 2014 Lai *et al*., 2009
anti-NMDA receptor encephalitis	GluN1	Serum, CSF	Immunohistochemistry Immunocytochemistry	Yes	Barry *et al*., 2015 Dalmau *et al*., 2008
Systemic lupus erythematosus	GluN2A, GluN2B	Serum, CSF	ELISA Immunofluorescence	Yes	Steup-Beekman *et al*., 2007 Lauvsnes *et al*., 2014
Paraneoplastic cerebellar ataxia	mGluR1	Serum, CSF	Immunohistochemistry	Poor	Smitt *et al*., 2000 Marignier *et al*., 2010
Ophelia syndrome	mGluR5	Serum, CSF	Immunohistochemistry Immunoprecipitation	Unknown	Mat *et al*., 2013 Lancaster *et al*., 2011

1.9. GluRs outside the CNS

1.9.1. *NMDARs, AMPARs and mGluRs in non-neuronal tissues*

Outside of the CNS, mRNAs and proteins of GluR subunits have been shown to be present in cells of the pancreas, skin, heart, adrenal gland, platelets and lymphocytes (Davalli *et al*., 2012). Several studies have proposed roles for GluRs in cells and tissues outside of the CNS. NMDARs have been shown to be present in several components of human renal system including glomeruli, podocytes, medulla and collecting ducts (Dryer, 2015). In these cells, activation, dysfunction or polymorphisms in NMDARs have been linked to alterations in several components of renal function including proximal reabsorption and glomerular filtration (Anderson *et al.,* 2011; Dryer, 2015). Within the circulatory system, mRNA and protein of GluRs including KARs (GluK1 and GluK2) (Sun *et al*., 2009), NMDARs (GluN1, GluN2A, GluN2D and GluN3A) (Kalev-Zylinska *et al*., 2014) and AMPARs (Morrell *et al*., 2008) are expressed in human platelets. Activation of these iGluRs induce platelet activation and aggregation while polymorphisms in KAR subunits are thought to be associated with altered human platelet functions including defective activation and aggregation (Sun *et al*., 2009). Cultured mouse macrophages express AMPARs and activation of these receptors plays an important role in inflammation via stimulation of release of tumour-necrosis factor (TNF)-α in macrophages as well as generation of reactive oxygen species (ROS) (Cheng *et al*., 2015). GluK4, GluN1 and mGluR2 subunits are expressed in human tendon tissues where they regulate the resolution of pain in several pathological conditions associated with the tendons including human rotator cuff tendinopathy (Dean *et al*., 2015). Also, group III mGluRs are expressed in the GIT of human (Julio-Pieper *et al*., 2013) and in

components of rat male reproductive (Marciniak *et al*., 2014). In human GIT, group III mGluRs are thought to be involved in regulation of intestinal motility, microbiota composition and intestinal fluid secretion (Julio-Pieper *et al*., 2013) whiles they are involved in erection, ejaculation mechanisms and formation /maturation of spermatozoa in rats (Marciniak *et al*., 2014). Furthermore, GluA2, GluA3 and particularly mGluRs have been detected in human adrenocortical tissues and have been shown to significantly regulate synthesis of steroid hormones from cholesterol (Felizola *et* al., 2014). mGluRs within the taste buds have also been suggested to contribute to savoury or delicious taste (umami) (Choudhuri *et al*., 2015; Kurihara *et al*., 2015; Yasumatsu *et al*., 2015).

1.9.2. *KAR subunits outside the CNS*

Outside the CNS, not much is known about the expression and role of KARs. mRNAs and proteins of GluK2, GluK3, GluK4 and GluK5 have been shown to be present on primary B-cells where activation of these receptors increases proliferation and synthesis of IgG and IgE as well as enhances the promotion of IgE-mediated allergic lung inflammation (Sturgill *et al*., 2011). These actions have been shown to be mediated through KAR-induced increase in expression and activity of a cell surface protein called ADAM10 that cleaves the IgE receptor CD23 (Sturgill *et al*., 2011; Weskamp *et al*., 2006).

In cultured immature and mature calvarial osteoblasts of rats, GluK4 and GluK5 mRNA are expressed together with GluA1 (Hinoi *et al*., 2002) though the exact role or function of these KAR subunits were not reported.

A study using immunohistochemical techniques has shown expression of GluK5 in cartilage and synovial cells together with significantly high amounts of glutamate in human patients suffering from osteoarthritis and rheumatoid arthritis. In these patients, a single intra-articular injection of the KAR antagonist; NBQX significantly reduced inflammation, swelling, cartilage degradation and pain (Bonnet *et al*., 2015). These observations indicate a possible role of GluK5 in bone pathology and a potential for the use of KAR antagonists in management of complications associated with joint pathologies such as arthritis.

Other non-neuronal tissues which have been reported to express some KAR subunits include adrenal gland where they stimulate release of cathecolamines (Gonzalez *et al*,. 1998), pituitary gland where they facilitate secretion of growth hormones and gonadotropin (Niimi *et al*., 1994; Zanisi *et al*., 1994), pineal gland (Sato *et al*., 1993) and heart (Wang *et al*., 2007).

1.9.3. *GluRs in pancreatic endocrine cells*

Studies with rodent and human tissues have shown that both ionotropic and metabotropic GluRs are present in the endocrine pancreas and are able to modulate important functions *in vitro* and *in vivo* (Wu et al., 2012; Marquard *et al*., 2015; Gheni *et al*., 2014). Subunit mRNA and protein of kainate, AMPA, NMDA and mGlu receptors have been shown to be expressed in primary islets of Langerhans, cultured α-cells and β-cells, as well as in sorted β-cells and α-cells of human, rat and mouse. The expression of GluR subunits in pancreatic endocrine cells of mouse, rat and human are summarised in Table 1.6, 1.7, 1.8.

Table 1.6. Review of GluR subtype mRNAs and proteins in pancreatic endocrine cells of mouse.

	mRNA and protein of GluR subtypes and subunits			
Pancreatic endocrine cells	**GluN**	**GluA**	**GluK**	**mGluR**
MIN6 clonal β-cells	**mRNA:** 1, 2C-D (Molnar *et* al., 1995; Gonoi *et* al., 1994) **Protein:** 1 (Molnar *et* al., 1995)	1, 2, 3, 4 (Molnar *et* al., 1995; Gonoi *et* al., 1994; Wu *et al*., 2012) 2 (Wu *et al*., 2012)	2, 4, 5 (Kutlu *et al*., 2009; Gonoi *et* al., 1994) 5 (Molnar *et* al., 1995)	2, 3, 5, 8 (Storto *et al*., 2006; Brice *et al*., 2002) 2, 3, 5 (Storto *et al*., 2006; Brice *et al*., 2002)
Mouse α-cells	**mRNA:** 1, 2A-D, 3A-B (Kutlu *et al*., 2009)	2, 3, 4 (Benner *et al*, 2014)		
Mouse β-cells	**mRNA:** 1, 2A-D, 3A-B (Kutlu *et al*., 2009)	1, 2, 3, 4 (Benner *et al*, 2014; Wu *et al*., 2012)	1, 2, 4, 5 (Kutlu *et al*., 2009)	
Mouse islets	**mRNA:** 1, 2A, 2C-D (Inagaki *et al*., 1995) **Protein:** 1 (Molnar *et* al., 1995)	2, 3 (Kutlu *et al*., 2009)	4 (Kutlu *et al*., 2009)	3, 4, 5, 8 (Brice *et al*., 2002) 2, 3, 4, 5 (Brice *et al*., 2002)

Table 1.7. Review of GluR subtype mRNAs and proteins in pancreatic endocrine cells of rat.

	mRNA and protein of GluR subtypes and subunits			
Pancreatic endocrine cells	**GluN**	**GluA**	**GluK**	**mGluR**
INS-1 clonal β-cells (rat)	**mRNA:** 1, 2A-D, 3A-B (Kutlu *et al*., 2009)	1, 2, 3, 4 (Kutlu *et al*., 2009)	3, 4, 5 (Kutlu *et al*., 2009)	
RINm5F clonal β-cells (rat)	**mRNA:** 1, 2D (Molnar *et* al., 1995) **Protein:** 1 (Molnar *et* al., 1995)	2 (Inagaki *et al*., 1995)	5 (Inagaki *et al*., 1995) 5 (Molnar *et* al., 1995)	3,5,8 (Brice *et al*., 2002)
Rat α-cells	**mRNA:** 1, 2A-D, 3A-B (Benner *et al*, 2014; Bramswig *et al*., 2013; Dorrel *et al*., 2011)	1, 2, 3, 4 (Kutlu *et al*., 2009)	1, 2, 3, 4, 5 (ref a, h, i, l)	
Rat β-cells	**mRNA:** 1, 2A-D, 3A-B (Kutlu *et al*., 2009; Inagaki *et al*., 1995)	1, 2, 3, 4 (Kutlu *et al*., 2009)	1, 2, 3, 4, 5 (Kutlu *et al*., 2009; Bramswig *et al*., 2013; Nica *et* al., 2013; Dorrel *et al*., 2011)	1, 2, 4, 7 (Uhlen *et al*., 2015) 1, 2, 4, 7 (f)
Rat islets	**mRNA:** 1, 2A-D, 3A-B (Kutlu *et al*., 2009; Eizirik *et al*, 2012; Uhlen *et al*., 2015) **Protein:** 1 (Molnar *et* al., 1995)	3 (Inagaki *et al*., 1995)	5 (Inagaki *et al*., 1995) 5 (Molnar *et* al., 1995)	1, 2, 3, 4, 5, 7, 8 (Brice *et al*., 2002) 2,3,5 (Brice *et al*., 2002)

Table 1.8. Review of GluR subtype mRNAs and proteins in pancreatic endocrine cells of human.

	mRNA and protein of GluR subtypes and subunits			
Pancreatic endocrine cells	**GluN**	**GluA**	**GluK**	**mGluR**
Human α-cells	**mRNA:** 1, 2C-D, 3A-B (Benner *et al*, 2014)	1, 2, 3, 4 (Bramswig *et al*., 2013; Cabrera *et* al., 2008; Dorrel *et al*., 2011)	2, 4, 5 (Benner *et al*, 2014)	
Human β-cells	**mRNA:**	1, 2, 3, 4 (Bramswig *et al*., 2013; Cabrera *et* al., 2008; Dorrel *et al*., 2011)	3, 5 (Kutlu *et al*., 2009)	
Human islets	**mRNA:** 1, 2C-D, 3A-B (Benner *et al*, 2014)	1, 2, 3, 4 (Kutlu *et al*., 2009; Eizirik *et al*, 2012)	1, 2, 3, 4, 5 (Eizirik *et al*, 2012; Uhlen *et al*., 2015; Benner *et al*, 2014)	3,5 (Brice *et al*., 2002)

The most important physiological function of pancreatic β-cells is synthesis and secretion of insulin to regulate blood glucose concentration. Studies have shown that activation or inhibition of GluR subunits in β-cells or islets of Langerhans can significantly alter GSIS from these cells. Of particular emphasis is the observation that some of these β-cell GluRs are able to induce or enhance GSIS is a manner similar to the effect of stimulatory glucose concentrations (Rorsman and Braun, 2013; Marquard *et al*., 2015).

In a recent study, inhibition of β-cell NMDARs in both mouse and human islets using dextromethorphan resulted in significant increase in $[Ca^{2+}]_c$ and GSIS in these cells as well as enhanced viability of the islets (Marquard *et al*., 2015). Results from the study also suggested that dextromethorphan-induced inhibition of NMDARs enhanced glucose tolerance and also resulted in increased serum insulin concentrations in human subjects. This was the first conclusive report on the effect of NMDARs in rodent and human β-cells and islets. Another study has recently reported similar observations where activation of NMDARs in cultured BRIN-BD11 β-cells significantly reduced GSIS but the NMDAR antagonist did not have any effect on GSIS in the cells (Patterson *et al*., 2015). Previous studies (Gonoi *et al*., 1994; Inagaki *et al*., 1995) have however reported conflicting observations where activation of NMDARs by NMDA resulted in increased $[Ca^{2+}]_i$ as well as enhanced GSIS in clonal β-cells and isolated pancreatic islets. Also, activation of β-cell NMDARs did not result in any change in GSIS or $[Ca^{2+}]_i$ (Bertrand *et al*.,1992) whereas another study reported of an increase in GSIS upon NMDAR activation but this increase was not significant compared to the baseline insulin secretion (Molnar *et al*. 1995). These observations indicate an important role of β-cell NMDARs in the regulation and control of insulin secretion.

AMPARs are also present in pancreatic β-cells and their activation by agonists enhances GSIS and increases $[Ca^{2+}]_i$. Using isolated rat pancreas (Bertrand *et al.*,1992) and cultured MIN6 β-cells (Gonoi *et al.*,1994), a significant increase in GSIS subsequent to activation of AMPAR by AMPA was observed. These observations have been corroborated by a recent study in mouse β-cells (Wu *et al.*, 2012). The study observed that activation of GluA2 by glutamate resulted in increased cytosolic $[Ca^{2+}]$ as well as enhanced GSIS in the presence of stimulatory (16 mM) glucose. However, these effects of AMPAR activation on GSIS were absent in the presence of 5 mM glucose hence raising an interesting possibility that the actions of AMPARs in β-cells may be glucose-dependent. Another study observed an increase in $[Ca^{2+}]_i$ in single β-cells in the presence of high glucose concentration subsequent to the initial exposure to AMPA but this effect was absent in the second application of AMPA (Inagaki *et al.*, 1995). This can be explained in the context of the agonist depolarising the cells after the initial application hence the second application did not have significant response.

Furthermore, the effect of mGluR activation on the function of β-cells appears to depend significantly on the group of mGluRs that are activated in the cells. This follows observations from studies which have shown that activation of group II and group III mGluRs significantly decrease the plasma insulin concentration in rats (Babic *et al.*, 2012). In contrast, activation of group I mGluRs have been shown to enhance GSIS and increase $[Ca^{2+}]_i$ in both clonal β-cells and mouse islets (Storto *et al.*, 2006). Moreover, the type of mGluR group activated in β-cells may also play an important role in determining the concentration of glucose required for the activated mGluRs to modulate insulin secretion and calcium influx. Agonists of group I mGluRs activate these receptors to

induce an increase in GSIS at 3 and 10 mM glucose while agonists of group II mGluRs stimulate GSIS at both low (3 Mm) and high (25 mM) glucose concentrations. Group III mGluRs however, stimulate GSIS at 10-25 mM glucose (Brice *et al*., 2002).

1.9.4. *KAR subunits in pancreatic endocrine cells*

Subunit mRNA and protein of KARs have been detected in pancreatic endocrine cells including clonal cells, isolated α-cells and β-cells as well as in primary islets of rodents as summarised in Tables 1.6, 1.7 and 1.8.

Functional studies have reported that application of kainate results in increased $[Ca^{2+}]_i$ and enhanced GSIS in rat pancreas (Bertrand *et al*., 1992), isolated single β-cells of rats (Inagaki *et al*., 1995) as well as in cultured MIN6 β-cells (Gonoi *et al*., 1994) although these effects were observed subsequent to application of varying kainate concentrations and also in the presence of different glucose concentrations. Other studies however, did not observe any significant increase in GSIS in rat islets of Langerhans after application of kainate at stimulatory (8.3-16.7 mM) and non-stimulatory (3.3 mM) glucose concentrations (Molnar *et al*., 1995). These contrasting results raise the possibility that the effect of kainate on β-cell GSIS may be dependent on series of factors including species and cell type.

Furthermore, no single study has characterised the molecular organisation of KARs and their auxiliary proteins neither has any study reported of putative role for KAR dysfunction in pancreatic endocrine cell function or the development of any pancreatic-related conditions such as diabetes mellitus.

1.10. Potential role of glutamate and GluRs in diabetes mellitus

1.10.1. *Potential role of glutamate in diabetes mellitus development and progression*

The link between diabetes and glutamate is not clearly defined but several studies have reported of similar effects of glutamate on neuronal cells and pancreatic β-cells. First, studies have shown that β-cells and neurons share many common features including cell surface receptors, (Del Rosario *et al*., 2015; Marquard *et al*., 2015), transporters (Di Cairano *et al*., 2011; Cheng *et al*., 2015; Hanson *et al*., 2015), cell adhesion molecules, genes and proteins that are involved in transmission of signals between cells (Selway *et al*., 2012; Otter and Lammert, 2016). Second, glutamate is released together with glucagon by α-cells (Cho *et al*., 2010) of the pancreas which implies that concentration of this neurotransmitter in islets is partly dependent on the hormonal activities in the pancreas. This suggestion is however disputed by another study which reported that glutamate is not co-secreted with glucagon from α-cells but is rather released through glutamate transporters located in α-cells (Feldman *et al*., 2011). Inhibition of these transporters in rat results in increased intracellular concentration of glutamate and eventual increase in GSIS from β-cells (Feldmann *et al*., 2011). Another indirect link between glutamate and diabetes stems from reports which shows that children who later progressed to T1DM had significantly high concentration of glutamate in blood compared to children who remained non-diabetic (Oresic *et al*., 2008). Also, in obese mouse and rat models of T2DM, dietary supplementation with monosodium glutamate (MSG) resulted in reduced β-cell mass (Boonnate *et al*., 2015), insulin resistance (Nagata *et al*., 2006), high fasting blood glucose levels and subsequently T2DM (Sasaki *et al*., 2009). Though this observation may not necessarily be linked to diabetes mellitus, it is possible that hyperglutamataemia could result in excessive activation of GluRs on β-cells with subsequent cell death via apoptosis and necrosis. Hyperglutamataemia may also alter the

activity of GAD65, one of the main β-cell antigen targets in autoimmune T1DM. Though increased activity of GAD is likely to enhance conversion of glutamate to GABA to reduce glutamate levels (Guerriero *et al*., 2015), change in activity of this enzyme in β-cells may also make it prone to autoimmune attack. Moreover, a study has shown that chronic exposure to glutamate is able to induce a relatively high increase in insulin secretion from human islets than induction with high concentration of glucose (Di Caraino *et al*., 2011). Further evidence from the study suggests that β-cells, not α-cells are vulnerable to chronic exposure to glutamate and large population of these cells undergo apoptosis. The prevalent mechanism of glutamate-induced β-cell death is via oxidative stress-induced cytotoxicity (Guemez-Gamboa *et al*., 2011).

Other studies have however reported of an inverse relationship between the concentration of monosodium glutamate (MSG) in blood and the risk of hyperglycaemia (Shi *et al*., 2013). This study was conducted among an adult population in China over a period of twenty years. These observations underscore the importance of glutamate in β-cell function.

Furthermore, studies have suggested that glutamate acts as a positive signal for insulin secretion from pancreatic β-cells. In one study, it was observed that cytosolic glutamate from the malate-aspartate shuttle serve as the positive link between cAMP action in incretin-induced insulin secretion and elevated glucose concentration in β-cells (Gheni *et al*., 2014). Also, glutamate is generated from glucose in the mitochondria of β-cells through a number of cycles. Uptake of this glutamate by insulin-containing granules results in enhanced secretion of insulin, particularly the second phase of insulin secretion (Carobbio *et al*., 2009). These studies, coupled with the observation that elevated glucose in rat clonal INS-1 β-cells and isolated human pancreatic islets increases the concentration

of glutamate followed by enhanced insulin secretion (Carobbio *et al*., 2009) underscore the importance of glutamate in insulin secretion from pancreatic β-cells.

Though no study is yet to record a direct link between glutamate levels or action and diabetes mellitus, accumulating evidences strongly indicate that glutamate is a significant molecule in the function, proliferation, viability and survival of pancreatic endocrine cells including β-cells.

1.10.2. *Potential role of glutamate receptors in diabetes mellitus development and progression*

To date, no study has shown a direct causal effect of GluRs in diabetes mellitus but several studies have suggested a role of GluRs in pancreatic endocrine function and dysfunction. First, inhibition of NMDARs in pancreatic β-cells and islets of mouse and human have been shown to induce significant increase in glucose-stimulated insulin secretion as well as enhanced proliferation and viability of these cells (Marquard *et al*., 2015). Also, according to the study, inhibition of NMDARs with dextromethorphan greatly enhanced glucose tolerance, improved glucose control, improved β-cell mass, enhanced insulin content in islets and also increased the effect of exendin-4 (anti-diabetic drug) on inducing glucose-stimulated insulin secretion in T2DM patients. This study represents a significant contribution to understanding how GluRs influence β-cell function and dysfunction.

Second, diabetes mellitus has been linked to significant cognitive impairment in both rodent and humans (Mayeda *et al*., 2015). This cognitive impairment is attributed in part to alterations in the expression of both iGluRs and mGluRs in the brain (Anu *et al*., 2010; Viswaprakash *et al*., 2015). Though these do not give a direct causal relationship between diabetes and GluRs, the observation that insulin treatment of streptozotocin-induced T1DM rats restores cognitive impairments by correcting AMPAR dysfunction suggests a significant mutual relationship between the function of GluRs and diabetes mellitus.

Moreover, GPRC5B, an orphan receptor of the group C family of GPCRs is highly expressed and play important roles in human islets of Langerhans (Amisten *et al*., 2013). Dysregulation of GPRC5B in intact human and mice islets results in significant increase in basal and glucose-stimulated insulin secretion as well as enhanced positive effect of glutamate on insulin secretion (Soni *et al*., 2013). Also, GPRC5B mRNA and protein have been shown to be significantly higher in islets form T2DM patients compared to healthy controls. Though not directly classified under GluRs, GPRC5B shares lots of similar properties with mGluRs and hence their function and role in β-cell function is of significant interest in understanding the possible role of GluRs in diabetes mellitus (Soni *et al*., 2013).

T1DM has also been linked to excitotoxicity-induced epileptic conditions. There appear to be a higher prevalence of epilepsy in children and adolescents with T1DM compared to non-T1DM controls (McCorry *et* al., 2006; Schober *et al*., 2012). Other studies have found similar prevalence of epilepsy in T1DM and controls (O'Connell *et al*., 2008). However, the observation that T1DM patients who also have epilepsy are twice as likely to develop both mild and severe diabetic ketoacidosis (Schober *et al*., 2012) gives a fairly strong indication of how GluRs affect development and progression of diabetes mellitus. The possibility that T1DM also affect development of epilepsy cannot be ruled out. These suggestions are enforced further by observations that GAD autoantibodies play a major role in both acute and chronic epilepsy (Liimatainen and Peltola, 2012) considering that autoantibodies to this enzyme are implicated in T1DM. Another interesting observation about GluRs and T1DM is how drugs which are prescribed for management of T1DM have similar effect on epilepsy and vice versa. Interestingly, antidiabetic drugs such as exenatide (Tsunekawa *et al*., 2007) and glitazones (Cunha *et al*., 2009) which are known to preserve β-cell integrity and survival also possess neuroprotective properties, while the

anti-epileptic drug topiramate which attenuates glutamate-induced excitotoxicity also have antidiabetic properties and preserve β-cell survival and function (Davalli *et al*., 2012; Toplak *et al*., 2007; Angehagen *et al*., 2003).

Even though these observations provide circumstantial evidence to implicate glutamate and GluRs in triggering or progression of diabetes mellitus, they provide very good insight into the possibility that glutamate and GluRs may be involved in both β-cell function and death. They also provide a good foundation for investigating GluR expression and function in α-cells, β-cells and islets. The observation that all the well-established autoantigens in T1DM are involved in the secretory pathway in β-cells (Arvan *et al*., 2012) enforces the quest to explore the possible role of GluRs as a possible T1DM autoantigen.

1.11. Aims and objectives of the study

Based on existing data, not much is known about KARs outside the CNS. The aim of this study is to investigate the presence and role of KAR subunits in pancreatic endocrine function and in the pathogenesis of T1DM.

The first part will investigate the molecular composition and function of KARs in pancreatic endocrine cells as well as the role of these receptors in the viability of pancreatic endocrine cells.

The second part of the study will investigate the presence of autoantibodies against GluR subunits in sera of newly-diagnosed T1DM patients. This will help to assess the potential role of KARs in the development of T1DM.

Chapter Two

Kainate Receptors in Pancreatic Endocrine Cells

2.1. Introduction

The presence of some KAR subunit mRNA and protein in pancreatic endocrine cells has been investigated (Chapter one, section 1.10 and Tables 1.5-1.7). However, no study has conclusively characterised the molecular organisation of these receptors in pancreatic endocrine cells in general and β-cells in particular. Moreover, the only KAR subunit protein which has been identified in rodent β-cell lines or islets of Langerhans is GluK5 (Molnar *et al*, 1995). Since this subunit (GluK5) can only form heteromeric combinations with any of GluK1-3 subunits (Crepel and Mulle, 2015), existing data are not sufficient to explain how these receptors assemble or function in pancreatic endocrine cells. Also, the presence of KAR-interacting or auxiliary mRNA and protein in these cells remains unexplored. In addition, the specific role of KAR subunits and their interacting/auxiliary proteins in modulating the functions and survival of pancreatic endocrine cells remain uncertain.

Because of the emerging role of KARs in the CNS and their unique dual signalling properties, these receptors represent potential targets for therapeutic agents for several neurological conditions. Also, since NMDARs have recently been reported to modulate β-cell function and contribute directly to glucose tolerance in both rodent and human diabetic patients (Marquard *et al*., 2015), it is likely that the other iGluRs including KARs modulate specific functions of the endocrine pancreas and may also represent important factors in dysfunction of these cells. Thus, this current study investigates the molecular characterisation, organisation and function of KAR subunits in pancreatic endocrine cells. This would be a significant contribution to understanding the function of KARs in non-neuronal cells and also provides a good foundation for understanding the role of these

receptor subunits and their ligands in modulation of pancreatic β-cell function, survival and the development of T1DM.

2.2. Aims

This section of the study aims to establish the molecular composition and function of KAR subunits in pancreatic endocrine cells and how these receptors affect the survival of pancreatic endocrine cells.

The specific objectives of this section were:

1) To investigate the presence of KAR subunit mRNA and protein in mouse clonal MIN6 β-cells, rat clonal INS-1 β-cells and mouse clonal α-TC16 α-cells and in rat primary islets of Langerhans
2) To investigate the presence of Neto 1 and Neto 2 mRNA and protein in clonal MIN6 and INS-1 β-cells and α-TC cells and in rat primary islets of Langerhans
3) To analyse the effect of varying concentrations of glutamate and kainate on $[Ca^{2+}]_i$ in clonal MIN6 β-cells.
4) To investigate the effect of kainate on glucose-stimulated insulin secretion (GSIS) in MIN6 and INS-1 β-cells.
5) To investigate the effect of chronic exposure to glutamate, kainate and dihydrokainic acid on viability of INS-1 and MIN6 β-cells and α-TC cells.

2.3. Materials and Method

2.3.1. *Materials*

Details of materials are supplied in Appendix 1.

2.3.2. *Cell culture*

Mouse insulinoma pancreatic β-cell line (MIN6) was cultured in DMEM cell culture medium supplemented with 15% (v/v) foetal calf serum (FCS), 100 U/ml penicillin, 0.1 mg/ml streptomycin, 2 mM L-glutamine and 0.05 mM β-mercaptoethanol (Diraison *et al.,* 2011; Brozzi *et al*., 2012). Mouse adenoma α-TC1 clone 6 (α-TC) pancreatic α-cells were cultured in RPMI-1640 cell culture medium supplemented with 10% (v/v) FCS, 100 U/ml penicillin, 0.1 mg/ml streptomycin, 2 mM L-glutamine, 0.05 mM β-mercaptoethanol and 11.0 mM glucose (Piro *et al*., 2014). Rat insulinoma pancreatic β-cell line (INS-1) was cultured in RPMI-1640 medium supplemented with 10% (v/v) FCS, 100 U/ml penicillin, 0.1 mg/ml streptomycin, 2 mM L-glutamine, 0.05 mM β-mercaptoethanol, 10 mM HEPES, 1 mM sodium pyruvate and 11.1 mM glucose (Pepaj *et al*., 2014). Human neuroblastoma cell line (SH-SY5Y) was cultured in Advanced DMEM supplemented with 10% (v/v) FCS, 2 mM L-glutamine, 100 U/ml penicillin, 0.1 mg/ml streptomycin and 1X RPMI-1640 amino acids solution (Zheng *et al*., 2014). Human embryonic kidney (HEK)293 cells were cultured in DMEM supplemented with 10% (v/v) FBS, 100 U/ml penicillin, 0.1 mg/ml streptomycin, 2 mM L-glutamine and 0.05 mM β-mercaptoethanol (Copik *et al*., 2015). Cells were maintained at 37°C in 95% humidified atmosphere and 5% CO_2. The culture medium was replaced every 48 hours and cells were passaged every 4 days (Diraison *et al.,* 2011). Cells between passage numbers 18-38 (MIN6, α-TC and INS-1), 20-30 (HEK293) and 6-14 (SH-SY5Y) were used for experiments (Cheng *et al*., 2012; Copik *et al*., 2015).

2.3.3. *Isolation of total RNA from cell lines and tissues*

MIN6, INS-1, HEK293 and α-TC cells at about 80% confluency were detached from the culture flask by incubating with 3 ml of 0.25 M sterile trypsin-EDTA at 37ºC for 5 minutes. Cells were transferred into sterile 15 mL conical tubes and centrifuged at 900 x g for 5 minutes. The supernatant was discarded and 3 mL of TRIzol® reagent was added to the cell pellet. For islets of Langerhans and brain/liver tissue, 3 mL of TRIzol® was added to 300 individual islets or 300 mg brain/liver. The TRIzol® reagent-cell/tissue mixture was incubated for 10 minutes at room temperature (RT) and then 600 µL of chloroform was added, mixed and incubated for 5 minutes. The mixture was centrifuged at 14,000 x g for 15 minutes. The top and middle layers were retained for RNA isolation and protein extraction, respectively. The top layer was incubated with 1.5 mL of isopropanol for 10 minutes at RT and centrifuged at 12,000 x g for 10 minutes. The supernatant was discarded and the pellet was incubated with 900 µL of 75% (v/v) ethanol for 5 minutes at RT. The mixture was centrifuged at 7,500 x g for 5 minutes and the supernatant was discarded after which the pellets were air-dried for 5 minutes and re-suspended in 30 µL of diethylpyrocarbonate (DEPC)-treated water (Rio *et al*., 2010). The concentration and purity of the RNA was determined using a NanoDrop-1000 spectrophotometer (Thermo Scientific, Leicestershire, UK). The ratio of absorbance at 260 nm to 280 nm was used to assess the purity of RNA and samples with ratio above 1.80 were used to avoid sample contamination with DNA and protein (Eldh *et al*., 2012).

2.3.4. *Protein extraction from TRIzol®-treated tissue samples*

The middle layer retained from the RNA isolation (section 2.3.3) was incubated with 300 µL of absolute ethanol for 3 minutes at RT and centrifuged at 3,000 x g for 5 minutes. The supernatant was transferred into a new tube and incubated with 1.5 mL of absolute (v/v) isopropanol for 10 minutes at RT. The mixture was then centrifuged at 12,000 x g

for 15 minutes and the resulting pellets were washed three times by incubating with 2 mL of 0.3 M guanidine hydrochloride for 20 minutes and centrifuged at 7,500 x g. The pellets were then incubated with 2 mL absolute ethanol for 20 minutes and then centrifuged at 7,500 x g for 5 minutes. The pellets were resuspended in 50 µL of 1% (w/v) sodium dodecyl sulfate (SDS) and centrifuged at 10,000 x g. The supernatant (protein) was retained and quantified by Bradford assay using Coomassie Brilliant Blue (Sigma, UK). The extracted proteins were then used for gel electrophoresis and immunoblotting (Likhite and Warawdekar, 2011).

2.3.5. *Preparation of membrane lysate from MIN6, α-TC, INS-1 and HEK293 cells*

The culture medium was removed and the cells were rinsed twice with 1X PBS (137 mM NaCl, 2.7 mM KCl, 4.3 mM Na_2HPO_4, 1.47 mM KH_2PO_4, pH 7.4) and incubated with 250 µL of RIPA buffer (150 mM NaCl, 0.5% (w/v) sodium deoxycholate, 0.1% (w/v) SDS, 25 mM Tris, pH 7.5, 0.1 mM EDTA, 1% (v/v) Triton-X), 1X protease inhibitor cocktail (2 mM 4-(2-aminoethyl) benzenesulfonyl fluoride hydrochloride, 1 mM phosphoramidon disodium salt, 130 mM bestatin hydrochloride, 14 mM N-(trans-epoxysuccinyl)-L-leucine 4-guanidinobutylamide, 1 mM leupeptin, 0.2 mM aprotinin, 10 mM pepstatin A), 1 mM sodium orthovanadate and 1 mM PMSF) at 4^{o}C for 15 minutes with occasional agitation. The cells were scraped off the culture flask and transferred into 1.5 mL Eppendorf tubes and then passed through a 1 mL syringe attached to a 25 x 1 inch (0.5 x 25 mm) needle 20-25 times. The mixture was incubated at 4^{o}C with gentle rotation for 40 minutes and centrifuged at 15000 x g for 15 minutes at 4^{o}C. The supernatant (protein) was collected, quantified and used immediately or stored at -80^{o}C (Diraison *et al.,* 2011).

2.3.6. *Bradford Assay for protein quantification*

Bradford assay was set up in a 96-well plate with 1 µg/µL standard bovine serum albumin (BSA) as shown in Table 2.1. Triplicates of 1:5 and 1:10 dilutions of each test protein sample were prepared in separate wells of the plate. All dilutions were made with de-ionised water and each well contained 5 µl dilutions of BSA standard or test proteins.

Table 2.1. Concentration of BSA standard in each well of the 96-well plate

Rows	A_{1-3}	B_{1-3}	C_{1-3}	D_{1-3}	E_{1-3}	F_{1-3}	G_{1-3}
BSA (µg/µL)	0.0	0.2	0.4	0.6	0.8	1.0	1.2

To each well, 200 µL of 0.6 M Coomassie Brilliant Blue dye was added and optical density at 610 nm was measured with Fluostar Optima plate reader (BMG Labtech, Aylesbury, UK). A standard curve of concentration against absorbance for BSA was generated using the following equation: $y = mx + c$, (where y: optical density, m: gradient of the curve, x: concentration and c: y intercept). The optical density of the test samples was inserted into the equation to determine the concentration (x) of protein (Luther *et al*., 2005).

2.3.7. *Reverse transcription and PCR*

Total RNA was revere-transcribed at 45ºC for 30 minutes in 20 µL of reaction mixture containing 3 µg RNA, 0.5 mM of dNTP, 2.5 µM of oligo $(dT)_{18}$ primers, 1X reverse transcriptase buffer (50 mM Tris-HCl, pH 8.6, 40 mM KCl, 1 mM MnSO4, 1 mM dithiothreitol, 0.5 mM [methyl-3H] thymidine 5'-triphosphate), 0.5 U/µL RNase inhibitor and 10 U/µL reverse transcriptase. The reaction was terminated at 85ºC for 5 minutes and cooled on ice (Balkowiec-Iskra *et al*., 2011; Luyt *et al*., 2007).

Primers specific for KAR, Neto 1 and Neto 2 subunits were designed using the NCBI Primer-Blast design tool (http://www.ncbi.nlm.nih.gov/tools/primer-blast/). To optimise PCR conditions for the primers, rat and mouse brain cDNA were subjected to gradient PCR using annealing temperatures between 50ºC and 65ºC. The PCR reaction mixture containing 3 µg cDNA, 2 mM dNTP mix, 1X PCR buffer (200 mM Tris-HCl, pH 8.4, 500 mM KCl), 0.8 mM of each primer, 2.0 mM $MgCl_2$ and 0.1 U/µL BIOTAQ™ DNA polymerase was used with PCR conditions of 95ºC for 5 minutes, followed by 34 cycles (except in experiments in which linear phase was determined) at 95ºC for 30 seconds, annealing temperature of 50ºC-65ºC for 30 seconds and then 72ºC for 30 seconds. The last cycle was followed by a final extension step at 72ºC for 10 minutes in a VWR Thermal Cycler (Biorad, Hertfordshire, UK) (Varadi *et al*., 1996; Rajatileka *et al*., 2013). The selected PCR conditions for the primers are detailed in Tables 2.2-2.4. Using these conditions, cDNA of MIN6, α-TC, INS-1, islets of Langerhans and brain were used for PCR.

The housekeeping β-actin gene has been shown to be expressed in all cells including MIN6 (Gao *et al*., 2015), α-TC (Klein *et al*., 2013), INS-1 and rodent islets of Langerhans (Skrzypski *et al*., 2015). Thus primers specific for mouse and rat β-actin were used as control to test the quality and integrity of templates.

KAR subunit transcripts have been detected in brain tissues of mice, rats and humans (Sihra and Rodriguez-Moreno, 2013). Thus, cDNA templates synthesised from rat and mouse brain tissues were used as a positive control for the different stages of PCR.

The PCR products were separated on 2% (w/v) agarose gels containing 0.4 µg ethidium bromide in 1X TAE buffer (40 mM Tris-acetate, 1 mM EDTA, pH 8.3) and the bands were visualised using the Syngene gel imaging and analysis system (Cambridge, UK).

For negative control, RNA taken through cDNA synthesis in the absence of reverse transcriptase enzyme was used as template for each set of primers. In addition, PCR was ran for each primer pair in the absence of template.

The PCR products were purified using the Wizard® SV Gel and PCR Clean-Up System. The separated DNA bands were excised from the gel and transferred into pre-weighed 1.5 ml eppendorf tubes. Membrane binding solution (MBS) was added to the excised gel at ratio of 10 µL MBS to 10 mg of excised gel. The mixture was incubated at 65^{o}C for 10 minutes to dissolve the gel in the MBS, transferred into a minicolumn-collection tube system and centrifuged at 12,000 x g for 1 minute. The DNA in the column was washed by adding 700 µL of membrane wash solution to the column followed by centrifugation at 12,000 x g for 5 minutes. Elution of DNA from the column into new DNase-free tube was performed by adding 40 µL of nuclease-free water followed by centrifugation at 12,000 x g for 1 minute (Uil *et al*., 2011; Rajatileka *et al*., 2013; Luyt *et al*., 2007). The purified PCR products were sequenced (Eurofins MWG, Ebersberg, Germany).

Three independent experiments using cDNA templates from different RNA preparations were carried out.

Table 2.2. Primer sequences and PCR conditions for the amplification of the various mouse KAR subunits. The primers were based on mRNA sequences accessed from the NCBI GenBank database (http://www.ncbi.nlm.nih.gov/genbank/).

Gene	Forward primer (5'-3')	Reverse primer (5'-3')	Size(bp)	Annealing temperature (°C)	$MgCl_2$ (mM)
GluK 1 (NM_010348)	TCAGACTCGCTGGAAACACC (Position: 949-968)	TGCTTCAGTTGTCATCACGC (Position: 1519-1500)	571	60	2.0
GluK 2 (NM_001111268)	GACTTCTCTTCCCTCAGCCG (Position: 867-886)	CAGAGCAGCATCAGTCGTCA (Position: 1379-1360)	513	55	2.0
GluK 3 (NM_001081097)	GGTTCCGCATACTCAACGTG (Position: 842-861)	ATGCAGTAGCCCTCAAACCG (Position: 1400-1381)	559	60	2.0
GluK 4 (NM_175481)	ATCCGGGATGACAAGACAGC (Position: 819-838)	CAATGTGGCCGGTAAGACCT (Position: 1290-1271)	472	60	2.0
GluK 5 (NM_008168)	TGATGCCAATGCGTCCATCT (Position: 1028-1047)	TACCACACCCCTATCTCACG (Position: 1555-1536)	528	55	2.0
β-actin (NM_007393.5)	CATCCTGCGTCTGGACCTG (Position: 600-619)	TTCCATACCCAAGAAGGAAGGC (Position: 887-865)	289	56	2.0

Table 2.3. Primer sequences and PCR conditions for the amplification of the various rat KAR subunits. The primers were based on mRNA sequences accessed from the NCBI GenBank database (http://www.ncbi.nlm.nih.gov/genbank/).

Gene	Forward primer (5'-3')	Reverse primer (5'-3')	Size(bp)	Annealing temperature (°C)	$MgCl_2$ (mM)
GluK 1 (NM_001111117)	GGAAGGAACTGAAAAGATTGGG (Position: 1376-1397)	CCATTGGGCTTCCGGTAAAG (Position: 1825-1806)	450	56	2.0
GluK 2 (NM_019309)	CTTGACGTGGAGCCCTACAG (Position: 1070-1089)	CGGTTCTTCCAAAATGGTGGT (Position: 1606-1586)	537	56	2.0
GluK 3 (NM_181373)	CCGAGGTCCTAATGTCACCG (Position: 1397-1416)	AGGGCTGAATCTGGCAATGA (Position: 1895-1876)	499	56	2.0
GluK 4 (NM_012572)	CCACCATCCTGGAAAACCCA (Position: 1338-1357)	CCAGGTTGGCTGTGTACGAT (Position: 1997-1978)	660	56	2.0
GluK 5 (NM_031508)	GGACTTCCCCATCCTGCATC (Position: 1045-1064)	CCACACCCCTATCTCACGGT (Position: 1477-1458)	433	59	2.0
β-actin (NM_031144.3)	CATCCTGCGTCTGGACCTG (Position: 599-618)	TTCCATACCCAAGAAGGAAGGC (Position: 888-866)	289	56	2.0

Table 2.4. Primer sequences and PCR conditions for the amplification Neto 1 and Neto 2. The primers were based on mRNA sequences accessed from the NCBI GenBank database (http://www.ncbi.nlm.nih.gov/genbank/). Human Neto 1 and Neto 2 primers were used to investigate presence of Neto 1 and Neto 2 in the cell lines and tissues whiles mouse and rat Neto 1 and Neto 2 were used for the semi-quantitative analysis.

Gene	Forward primer (5'-3')	Reverse primer (5'-3')	Size(bp)	Annealing temperature (°C)	$MgCl_2$ (mM)
Human Neto 1 (NM_001201465)	CACCAGTGGGACTGTCATTG [Positions: human (1304-1323); mice and rats (1951-1970)].	TCTGCCACATCTGCAAAGTC [(Positions: human (1525-1505); mice (2166-2146) and rats (2167-2147)].	216	50.2	2.0
Human Neto 2 (NM_001201477)	TTTGCTTCGCCAAATTATCC [(Positions: human (582-601); mice (309-329) and rats (168-188)].	TTAATGGAGGGCTTTTCACG [(Positions: human (801-782); mice (529-509) and rats (388-368)].	220	50.2	2.0
Mouse Neto1 (NM_144946)	TTGAAACCATTGCCAGCGTG	AACCTGCTGTTACGGCTACC	344	50.2	2.0
Mouse Neto2 (NM_001081324)	TTTTGGAAGCTGCTCCTCGT	CCAGAGAGCTCAAACTGGCA	304	50.2	2.0
Rat Neto1 (NM_001107371)	TCTTTGCTGATGGGGAGCTG	TTGCCTTCACAGGGAGGTTC	475	50.2	2.0
Rat Neto2 (NM_001107417)	TGCCGGTTTGATCACTTGGA	GTACAGGGAGGCTCCACAAAG	596	50.2	2.0

2.3.8. *Semi-quantitative analysis KAR subunits, Neto 1 and Neto 2 mRNA in pancreatic endocrine cells.*

To determine the optimum number of PCR cycles required for the amplification of KAR subunits, Neto 1 and Neto 2 to be within the linear phase, mouse brain cDNA was subjected to PCR with specific primers for β-actin, KAR (GluK2, GluK5), Neto 1 and Neto 2 with conditions described in section 2.3.7 and PCR cycles of 15, 20, 25, 30 and 35. PCR products were separated on 2% (w/v) agarose gels and visualised using Syngene gel imaging and analysis system. The tagged image format (TIF) file of the gel images were loaded on to ImageJ image processing software (Maryland, USA) and the image background was subtracted. The 'Rectangle Area Selection Tool' of the software was selected to draw a rectangle around the first band of interest to create an area that will be operated on separately from the rest of the image. The mean intensity of the selected band was measured using the software. The rectangle was then moved to other bands to measure the mean intensity of these bands. A profile plot representing the relative density of the contents of the rectangle over each lane was plotted the area under the plots represented the amount of signal in the band (pixel volume). A curve of pixel volume against PCR cycle number was plotted for each primer and used to establish the linear phase of the reaction (Luyt *et al*., 2007; Varadi *et al*., 1996). The cycle numbers for PCR were narrowed down to intervals of 2 for primers which had curves with no distinct linear regions. Curves for each of the primers were used to select PCR cycle numbers at which amplification of the target mRNA is in linear phase.

Pancreatic β- (MIN6 and INS-1) and α-cells (α-TC) and mouse brain cDNA were used in PCR with the selected number of PCR cycles for the GluK2, GluK5, Neto 1, Neto 2 and β-actin primers. The PCR products were separated on 2% agarose gels and visualised. ImageJ was used to determine the pixel volumes. Pixel volume of GluK2 was divided with that of β-actin and the obtained ratio from each experiment was averaged to give the

relative amount of GluK2 mRNA in the cells. The same procedure was carried out for GluK5, Neto 1 and Neto 2 to determine their relative amounts.

Three independent experiments each carried out in duplicate were performed and bar charts representing the means ± standard error of means (SEM) from the three experiments were plotted. One-way *ANOVA* analysis was used to compare mean relative amounts of KAR (GluK2, GluK5), Neto 1 and Neto 2 mRNA between β- (MIN6 and INS-1) and α-cells (α-TC).

2.3.9. *Immunoblotting*

Membrane lysate prepared from cell lines (10-60 μg) or brain tissue (5 μg) was added to equal volume of 2X loading buffer (0.0625 M Tris-HCl; pH 6.8, 1% (v/v) SDS, 10% (w/v) bromophenol blue), heated for 5 minutes at 95^{o}C and proteins separated by electrophoresis on 4% SDS PAGE stacking (4% acrylamide (v/v); 0.5M Tris, pH 6.8; 0.1% (v/v) SDS; 0.1% (w/v) TEMED; 0.1% (w/v) APS) and 10% SDS PAGE resolving (10% (v/v) acrylamide, 1.5 M Tris, pH 8.8, 0.1% (w/v) SDS, 0.1% (v/v) TEMED, 0.1% (w/v) APS) gel in a Bio-Rad Protean II electrophoresis tank (Bio-Rad, Hertfordshire, UK) at 120 V for 35 minutes in SDS running buffer (0.025M Tris, 0.192 M Glycine and 0.1% (w/v) SDS) (Whitehead *et al*., 2013; Luyt *et al*., 2007). Proteins were transferred on to a polyvinyl difluoride (PVDF) membrane using Trans-Blot SD Semi-Dry Transfer Cell system (Biorad, Hertfordshire, UK) with discontinuous anode (40 mM CAPS, 60 mM Tris, 15% (v/v) methanol) and cathode (40 mM CAPS, 60 mM Tris, 0.1% (w/v) SDS) buffer solutions for 35 minutes at 25V. The membrane was washed twice in 1X TBS-T (50 mM Tris-HCl, pH 7.4, 150 mM NaCl, 0.1% (v/v) Tween) for 5 minutes each, then blocked in 5% (w/v) non-fat milk for 1 hour and incubated overnight at 4^{o}C with primary antibodies as shown in Table 2.5. The membrane was then washed six times in TBS-T for 5 minutes each and incubated at RT for 45 minutes with horseradish peroxidase

(HRP)-linked anti-mouse or anti-rabbit secondary antibody (dilution 1:4000) in 5% (w/v) non-fat milk. After incubation, the membrane was washed six times in TBS-T for 5 minutes each and incubated with 2 mL of HRP substrate for 1 minute. Detection of immunopositive bands was performed by incubating the membrane with HRP substrate (Millipore, Hertfordshire, UK) for 1 minute followed by visualisation with Syngene gel imaging and analysis system (Syngene, Cambridge, UK). The β-actin content of each sample was assessed to confirm that comparable amount of membrane lysates was loaded (Storto *et al*., 2006; Whitehead *et al*., 2013; Diraison *et al*., 2010).

2.3.10. *Semi-quantitative analysis of immunoblot bands*

Immunoblot images acquired with the Syngene gel imaging system were analysed using ImageJ image processing software as described in section 2.3.8 to determine the pixel volume of immunopositive bands for KAR subunits (GluK2/3, GluK5), Neto 1, Neto 2 and β-actin.

Pixel volume of KAR subunits (GluK2/3, GluK5), Neto 1 and Neto 2 was divided with that of β-actin and the obtained ratio from each experiment was averaged to give the relative amount of KAR subunits (GluK2, GluK5), Neto 1 and Neto 2 protein (Luyt *et al*., 2007; Wicht *et al*., 1999).

Three independent experiments were performed and bar charts representing the means ± standard error of means (SEM) from the three experiments were plotted. One-way *ANOVA* was used to compare mean relative amounts of KAR (GluK2/3, GluK5), Neto 1 and Neto 2 protein between β- (MIN6 and INS-1) and α-cells (α-TC).

Table 2.5. Primary antibody dilutions used for the investigation of GluK protein in pancreatic endocrine cells

Antibody	Dilution (in 5% milk)	Species
Anti-GluR6/7 (Millipore; 04-921)	1:2000	Rabbit
Anti-KA2 (GluK 5) (Millipore; 06-315)	1:1000	Rabbit
Anti-Neto1 (Tomita, Yale) (Straub et al., 2011)	1:1000	Rabbit
Anti-Neto-2 (Tomita, Yale)	1:1000	Rabbit
Anti-β actin (CST; #3700)	1:3000	Mouse
Anti-pan-AMPAR (Molnar, Bristol) (Cathala et al., 2005)	1:500	Rabbit

2.3.11. *Measurement of intracellular calcium concentration $[Ca^{2+}]_i$ in MIN6 pancreatic β-cells*

Sterile-filtered 0.01% (v/v) poly-l-lysine (PLL) solution in water was used to coat 13 mm coverslips by adding 100 µL of PLL to each coverslip and incubating for 5 minutes at RT. The coverslips were rinsed with sterile deionised water and dried at RT for 2 hours before use. MIN6 β-cells were seeded at a density of 1.0×10^5 onto PLL-treated coverslips in a 12-well cell culture plate and incubated at 37ºC, 5% CO_2 in 25 mM-containing DMEM (section 2.3.2) for 24 hours after which the medium was replaced with fresh complete DMEM containing 3 mM and incubated for further 24 hours. The media was removed and cells were rinsed with pre-warmed (37ºC) Hanks' balanced salt solution (HBSS) (135 mM NaCl, 5 mM KCl, 10 mM HEPES, 1 mM $MgCl_2$, 2 mM $CaCl_2$, pH 7.3) supplemented with 3 mM glucose. FURA-2AM calcium dye solution was prepared to a concentration of 4 µM in 3 mM glucose-supplemented HBSS buffer. Cells were loaded with FURA-2AM calcium dye by incubating the cells with the dye for 90 minutes at 37ºC in the dark. The dye was washed off with HBSS and cells kept away from light for 15 minutes at RT for de-esterification of FURA-2AM before imaging. All drugs used in the experiment were diluted in HBSS buffer supplemented with either 3 mM or 30 mM glucose and were kept at room temperature during the experiment. The cells were then transferred onto a perifusion chamber and mounted on the stage of a Zeiss Axiovert 200 inverted microscope (Oberkochen, Germany). The cells were perifused with HBSS buffer with or without drugs at constant flow rate of 3 mL/min with 1-minute delay in-between flows. This delay was corrected on the image traces. To test the responsiveness of the cells and sensitivity of the system, cell membranes were depolarised by application of 15 mM KCl after every round of experiment.

The cells were illuminated by excitation with a dual ultraviolet light source at 340 nm and 380 nm. A dichroic mirror transmitted the emitted fluorescence from the cells through a

460 nm filter and images were captured with a high-sensitivity cooled Nikon charge-coupled device (CCD) camera (Nikon, Surrey, UK).

The background reading was subtracted from the region of interest (ROI) and the ratio channel of the intensity readings was measured using the 'ratio' tool of the Volocity Image Analysis software (PerkinElmer, Cambridgeshire, UK). The mean intensity ratio was measured by drawing a square around the whole field of ROI (containing 30-50 cells) and then using the 'analysis' tool of the software to acquire the raw data for mean intensity ratio for each time point (Tarasov *et al*., 2013; Varadi and Rutter, 2002; Varadi *et al*., 2004).

The time-lapse intensity ratio data was imported into Excel data analysis suite (Microsoft, Berkshire, UK) and the mean of 3-4 independent experiments was determined for each timepoint and then used to generate scatter plots of fluorescence ratio against time. The change in fluorescence ratio which represents the change in $[Ca^{2+}]_i$ was determined by dividing the fluorescence ratio induced by a drug with the fluorescence ratio of the first four minutes of the experiment where no drug was applied to cells. The ratio obtained from each experiment was averaged and bar charts representing the mean change in fluorescence ratio ± SEM were plotted using Excel. Means of change in fluorescence ratio were compared statistically using Student's *t*-test, one-way or two-way *ANOVA.*

The different drugs and incubation times used in the experiment are shown in Figure 2.1.

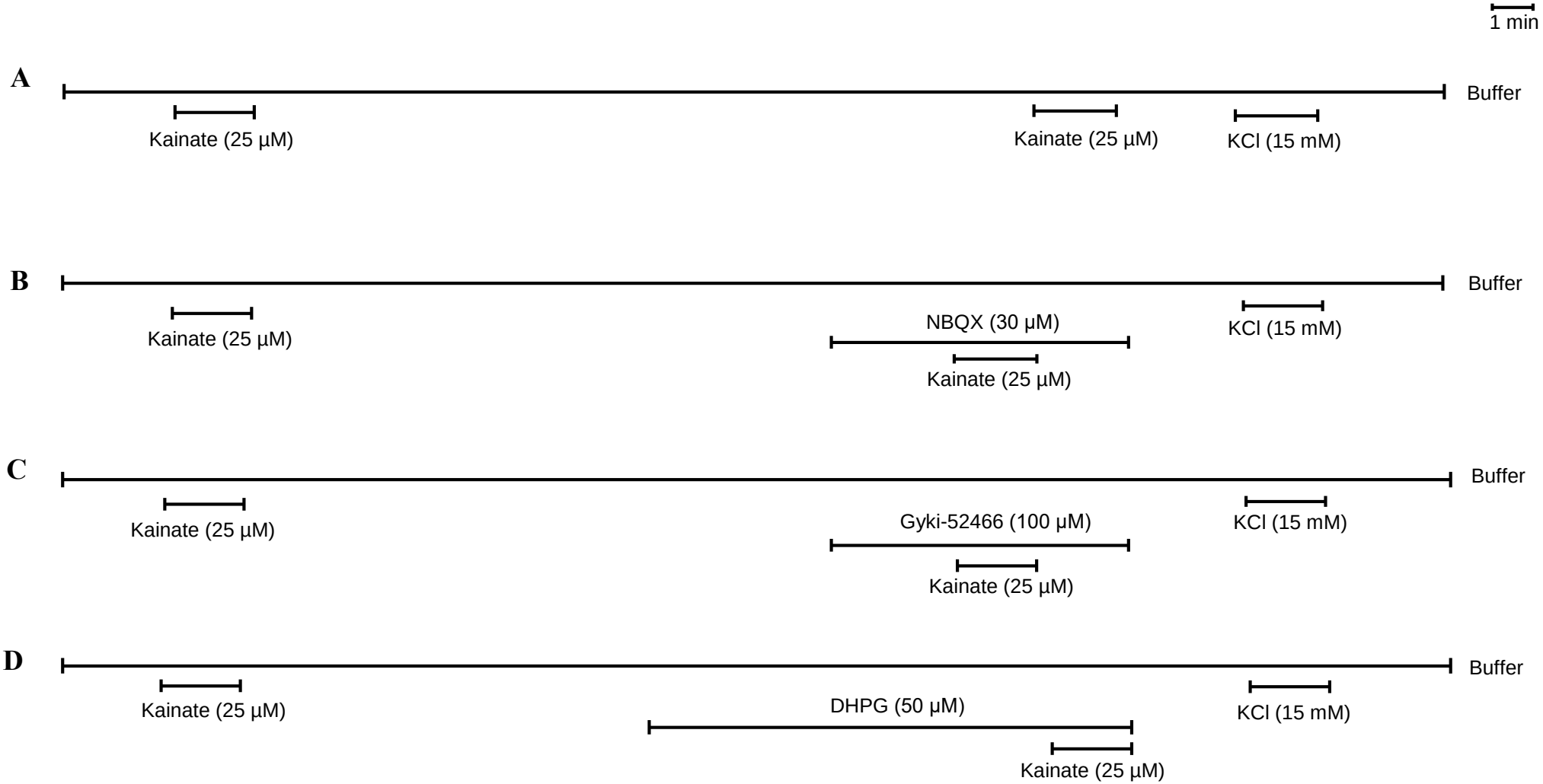

Figure 2.1. Summary of drugs and perifusion times used in calcium imaging of MIN6 β-cells. Experiments were performed with drugs dissolved in HBSS buffer containing 3 mM or 30 mM glucose. Drugs: kainate (KAR agonist), 2,3-dihydroxy-6-nitro-7-sulfamoyl-benzo[f]quinoxaline-2,3-dione (NBQX: AMPAR/KAR antagonist); Gyki-hydrochloride (Gyki-52466: NMDAR/AMPAR antagonist); (*S*)-3,5-dihydroxyphenylglycine (DHPG: group I mGluR agonist); potassium chloride (KCl: depolarises cell membrane).

2.3.12. *Measurement of cell viability using 3-[4,5-dimethylthiazol-2-yl]-2,5 diphenyl tetrazolium bromide (MTT) assay*

The MTT assay is based on conversion of the yellow MTT solution to dark-blue insoluble formazan crystals by mitochondrial dehydrogenase present in living cells (Wang *et al*., 2010). The optical density of dissolved crystals at 550 nm is directly proportional to the amount of mitochondrial dehydrogenase in the cells.

Pancreatic β- (INS-1) and α-cells (α-TC) and neuroblastoma cells (SH-SY5Y) were seeded at densities of 2 x 10^4 onto 96-well plates for 24 hours under culture conditions described in section 2.2.3. The media was replaced with fresh media containing different concentrations of glutamate, kainate, NBQX, DHK, Triton X-100 and ethanol as described in Figure 2.2. For kainate/NBQX treatment, cells were cells pre-incubated with 0.025-0.1 mM NBQX for 12 hours followed by incubation with 0.1 mM-0.5 kainate for 60 hours. For glutamate/DHK, cells were treated with DHK for 12 hours followed by incubation with media containing 0.5 mM glutamate for 60 hours. Cells used as controls were cultured in growth media only.

To test the specificity of the MTT assay, cultured INS-1, α-TC and SH-SY5Y cells were incubated with 40% ethanol or 2% triton X-100 for 72 hours. These concentrations of ethanol and triton X-100 have been shown to be lethal to cultured cells resulting in no formation of formazan crystals when these cells are incubated with MTT. Thus, these conditions were used as negative controls (Phonnok *et al*., 2010). SH-SY5Y cells were used as positive control for kainate- and glutamate-induced changes in cell viability (Zhu *et al*., 2016; Cannarsa *et al*., 2008).

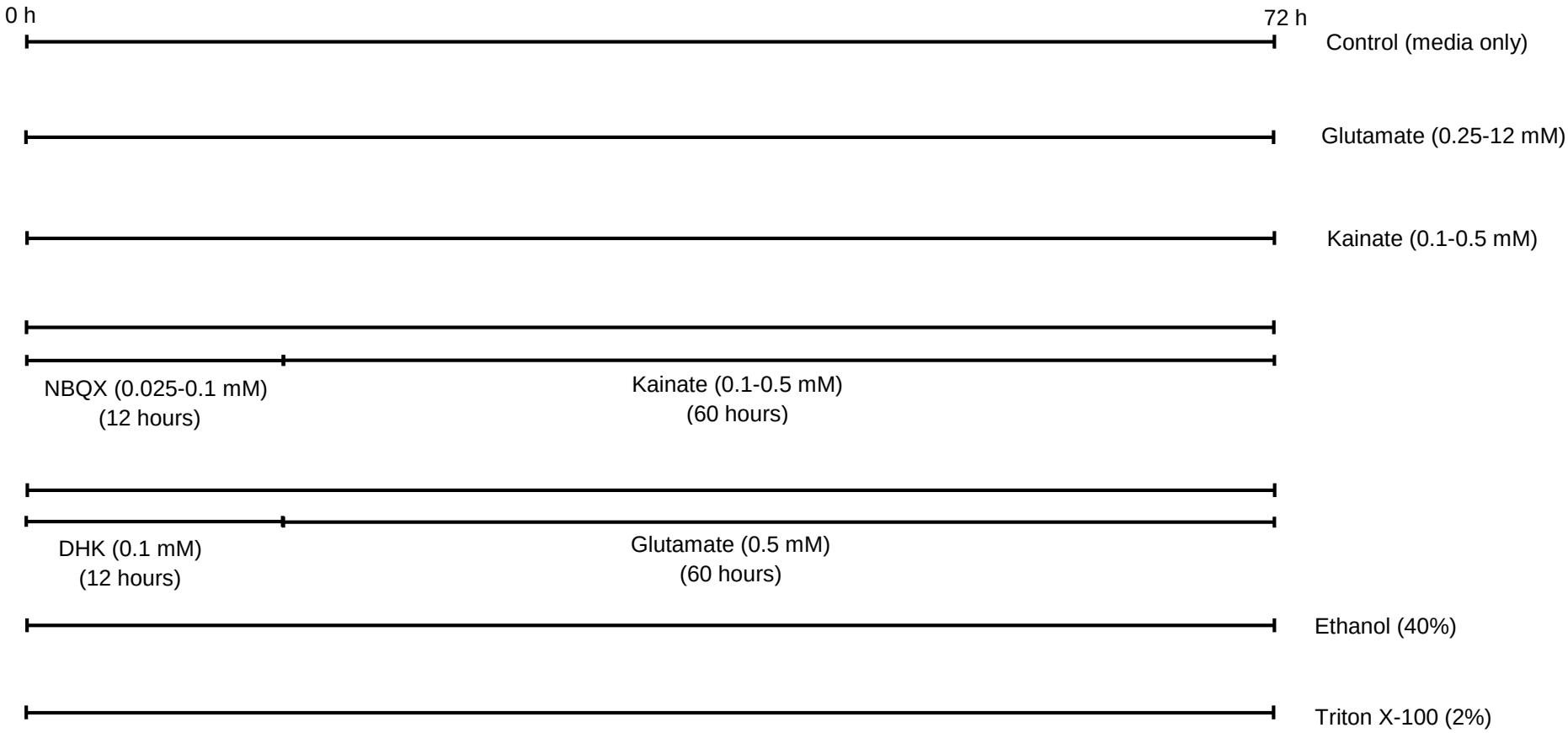

Figure 2.2. Summary of treatment procedure for cell viability analysis in INS-1, α-TC and SH-SY5Y cells. Cells were seeded in 96-well culture plates for 24 hours. The media was replaced with fresh media containing different combinations of drugs and incubated for 72 hours.

After treatment, 20 µL of 1 mg/mL MTT solution (prepared in phenol- and serum-free media) was added to each well and incubated for 2 hours in 37°C in 95% humidified atmosphere and 5% CO_2. The media was removed from the cells and 100 µL of DMSO was added to each well. Cells were incubated at 37°C on an orbital shaker (100 rpm) for 30 minutes to dissolve the formazan crystal precipitates completely and optical density of the solution was measured at 550 nm (Maioli *et al*., 2009; Di Cairano *et al*., 2011). Experiments were carried out in triplicates and mean optical density of each treatment was expressed as percentage of the mean optical density of non-treated controls.

Bar charts representing mean cell viability ± SEM of 3-6 experiments were plotted using Excel data analysis suite (Microsoft, Berkshire, UK) and comparisons in mean cell viability were performed using one-way *ANOVA* (Minitab, Pennsylvania, USA) or Student's *t*-test.

2.3.13. *Measurement of insulin release using ELISA*

Pancreatic β-cells (MIN6 and INS-1) were seeded at densities of 2 X 10^5 in 12-well cell culture plates for 24 hours in growth media (25 mM for MIN6 and 11.1 mM for INS-1) as discussed in section 2.2.3. The growth media was replaced with fresh media containing 3 mM glucose for 24 hours. The media was removed and cells were rinsed three times with pre-warmed (37ºC) PBS. Cells were then incubated in 0.5 mL pre-warmed (37ºC) Krebs Ringer buffer (120 mM NaCl, 24 mM $NaHCO_3$, 4.8 mM KCl, 2.5 mM $CaCl_2.6H_2O$, 1.2 mM $MgCl_2.6H_2O$ and 0.1% (w/v) radioimmunoassay grade BSA freshly gassed with 95% O_2 for 10 minutes, pH 7.5) containing 3 mM glucose at 37°C in a water bath for 1 hour. The buffer was replaced with 0.5 mL fresh Krebs Ringer buffer containing different glutamate receptor agonists and antagonists in the presence of 3 mM or 30 mM glucose as described in Figure 2.3.

Experiments were conducted in triplicates and repeated a minimum of three times.

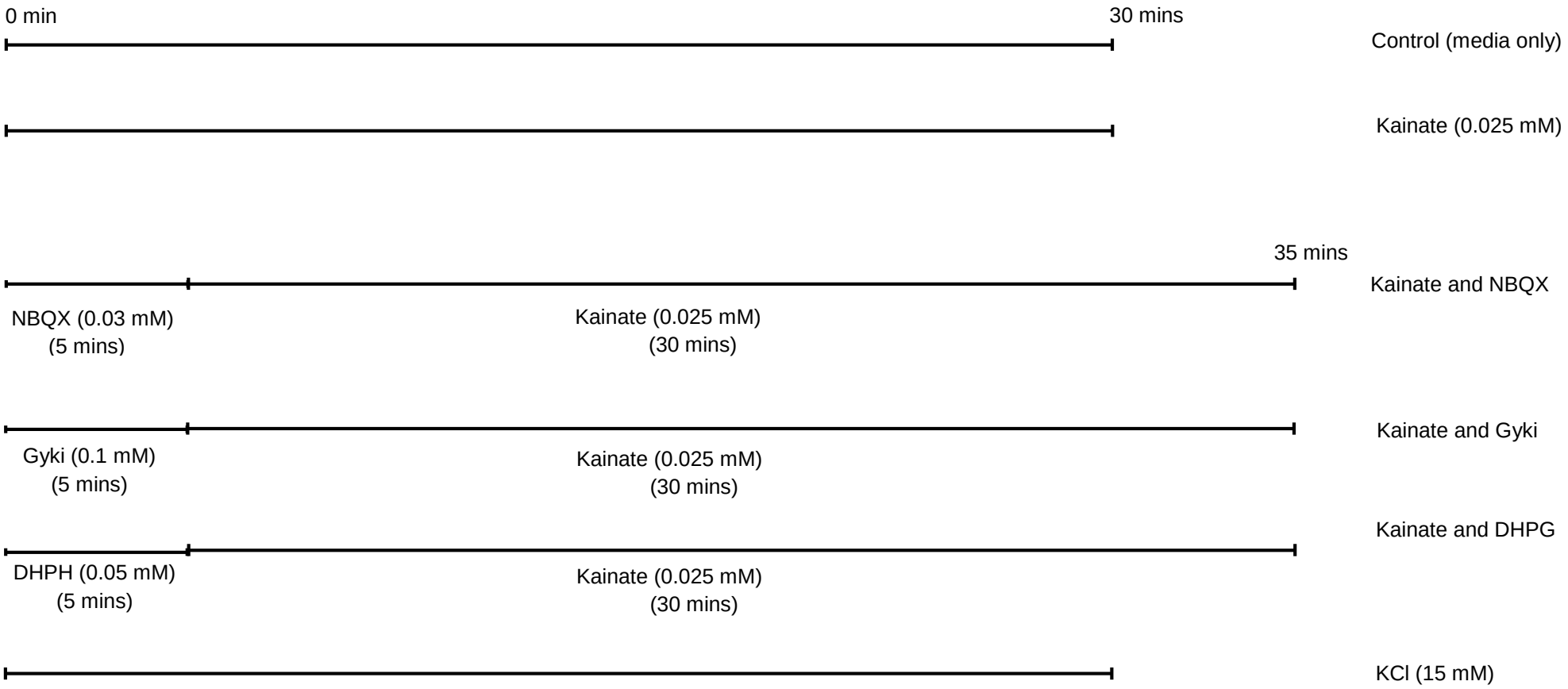

Figure 2.3. Summary of experimental procedure for measurement of insulin secretion in MIN6 and INS-1 β-cells. Cells were seeded in 12-well plates for 24 hours in growth media containing 25 mM for MIN6 and 11 mM for INS-1. The media was replaced with fresh media containing 3 mM glucose for MIN6 and INS-1 for 24 hours. The media was removed and cells were incubated with different combinations of drugs.

After incubation, the supernatant was removed and centrifuged at 700 x g to remove dead cells and debris. The supernatant, which contains secreted insulin, were stored at -20°C for insulin assay. 100 µL of lysis buffer (75% (v/v) ethanol, 23.5% (v/v) deionised water, 1.5% (v/v) HCl) supplemented with 1X (v/v) protease inhibitor cocktail (Roche complete mini EDTA-free) was added to the cells and incubated for 5 minutes at 4°C. The cells were scrapped from the wells and transferred into eppendorf tubes on ice. Another 100 µL of lysis buffer was added to the wells to remove residual cells and transferred into eppendorf tubes. The mixture was passed through a GS 351 (21g x 1.5 inches; 0.8 x 40mm) needle attached to a syringe for about 20-25 times to break down the cells. The lysate was centrifuged at 900 x g for 5 minutes at 4°C and the supernatant, which contains the retained insulin, were stored at -20°C for insulin assay.

The insulin ELISA assay was carried out following the Mercodia Mouse or Rat Insulin ELISA instructions. MIN6 samples were diluted 1:15 for secreted insulin and 1:3000 for retained insulin while INS-1 samples were diluted 1:2 for secreted insulin and 1:20 for retained insulin.

To prepare standard curves for the Mercodia mouse and rat insulin ELISA assays, 10 µL of standard calibrators (0, 0.2, 0.5, 1.5, 3.0 and 6.5 µg/µL for mouse and 0, 0.15, 0.4, 1.0, 3.0 and 5.5 µg/µL for rat) and 100 µL enzyme conjugate were added to coated ELISA wells and incubated at room temperature for 2 hours on an ELISA plate shaker. The reaction mixture was discarded and the wells were rinsed four times with wash buffer solution after which 200 µL of TMB substrate solution was added to the wells and incubated at room temperature for 15 minutes away from light. The reaction was then stopped by adding 50 µL of stop solution for 10 seconds and optical density measured at 450 nm using Fluostar Optima plate reader (BMG Labtech, Aylesbury, UK). The test samples were analysed using the same protocol as for the standards.

A calibration curve of optical density against concentration of the standard calibrators was plotted using the following: $y = mx + c$, (where y- optical density, m- gradient of the curve, x- concentration and c- y intercept).

Secreted insulin was expressed as a percentage of total insulin (secreted + retained) and the proportion obtained from each experiment averaged.

Bar charts representing mean insulin secretion (% of total insulin content) ± SEM of five experiments were plotted using Excel data analysis suite (Microsoft, Berkshire, UK) and means were compared using one-way or two-way *ANOVA* (Minitab, Pennsylvania, USA) or Student's *t*-test.

2.3.14. *Statistical analysis*

Data are presented as means ± SEM/SD of at least three independent experiments with number of replicates stated in respective experiments. Statistical comparisons were performed by one-tailed Student's *t*-test using Microsoft Excel, one-way or two-way *ANOVA* using Minitab data analysis software. Differences between means were considered statistically significant if the *p* value was less than 0.05.

2.4. Results

2.4.1. KAR subunits in pancreatic endocrine cells

To establish the molecular composition of KAR subunits in pancreatic endocrine cells, reverse transcription PCR and immunoblotting were used to investigate the presence of pore forming GluK1-5 subunits and auxiliary Neto1 and Neto 2 subunit mRNAs and proteins, respectively. The relative amounts of KAR subunit mRNA and protein in pancreatic endocrine cells were also determined.

2.4.1a. *KAR subunit transcripts are expressed in pancreatic α- and β-cells lines and rat islet of Langerhans*

To establish the molecular composition of KAR subunits in pancreatic endocrine cells, total RNA from MIN6 (mouse), INS-1 (rat), α-TC (mouse) cell lines and rat islets of Langerhans were reverse-transcribed and the cDNA was subjected to PCR. The primer sequences, annealing temperatures, PCR product sizes and Mg^{2+} concentration are shown in Tables 2.2-2.4.

MIN6, INS-1 and α-TC cells expressed GluK2, GluK3, GluK4 and GluK5 KAR subunits (Figures 2.4 and 2.5) while all five (GluK1-5) pore forming KAR subunits were expressed in rat islets of Langerhans (Figure 2.5). These observations indicate that cultured pancreatic endocrine cells lack GluK1 subunit-containing KARs.

As expected, all five KAR subunits were detected in both mouse and rat brain (Figures 2.4 and 2.5). The housekeeping β-actin gene was also detected in all samples tested (Figures 2.4-2.6). These results confirmed the integrity of cDNA templates and also indicated that each step of the sample preparation and PCR worked appropriately.

The sizes of PCR products of KAR subunits corresponded to those predicted by the primer design software. There were no PCR products in the negative controls, which

consisted of all reagents in the absence of cDNA templates. All PCR products were confirmed by sequencing (Appendix 1).

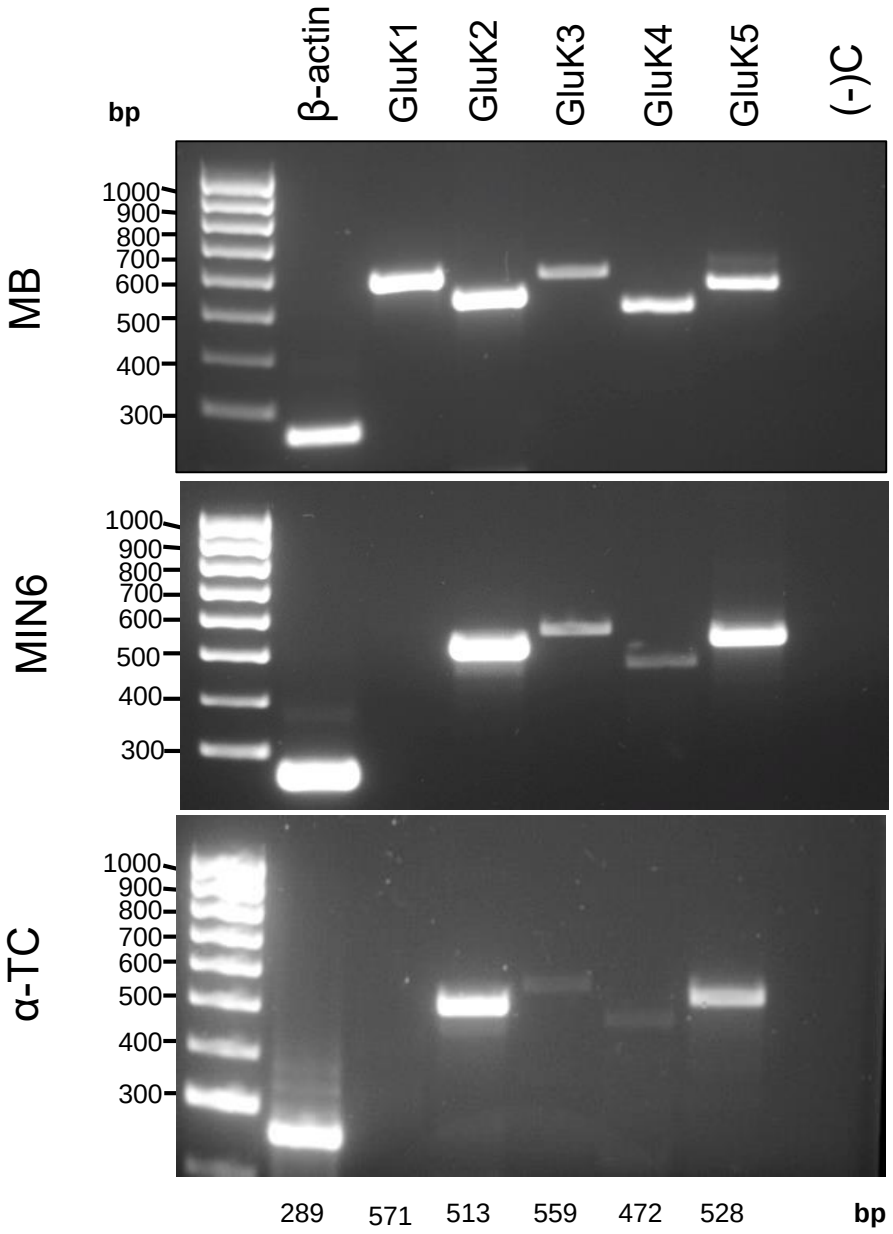

Figure 2.4. KAR subunit transcripts are expressed in cultured mouse pancreatic β- and α-cells. Mouse KAR subunit-specific primers were used to detect mRNAs for GluK1-5 in MIN6 and α-TC cells. Mouse brain (MB) was used as positive control. Negative controls were PCR without template ((-) C). Sizes of the products are indicated at the bottom of the panel. PCR bands were purified and verified by sequencing. Figure is representative of three separate experiments performed using cells at different passages.

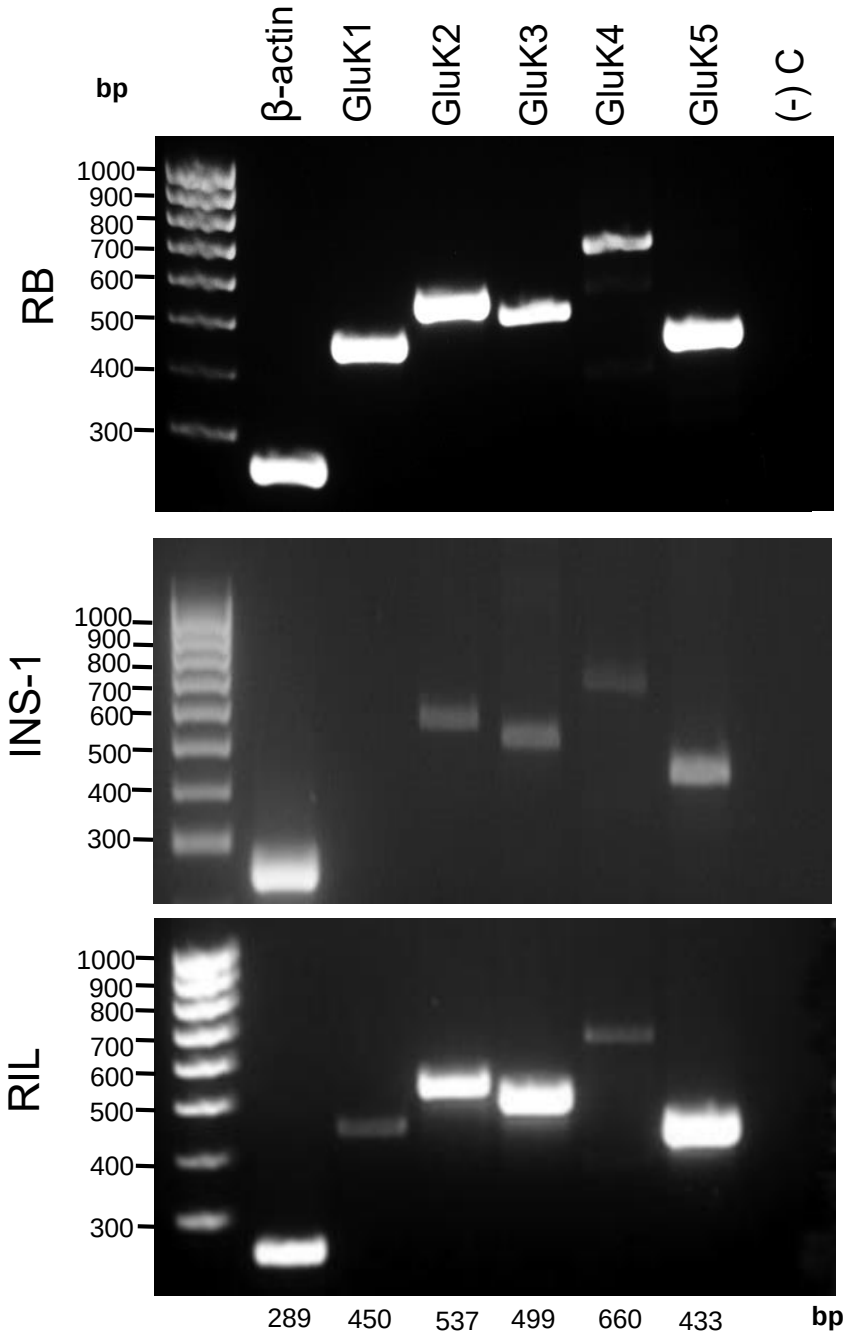

Figure 2.5. KAR subunit transcripts are expressed in cultured rat pancreatic β-cells and primary islets of Langerhans. Rat KAR subunit-specific primers were used to detect GluK1-5 in INS-1 β-cells and rat primary islets of Langerhans (RIL). Rat brain (RB) was used a positive control. Sizes of PCR products are indicated at the bottom of the panel. Figure is representative of three separate experiments performed using cells at different passages.

Previous studies have shown that KAR subunits are not expressed in mouse (Gonoi *et al*., 1994) or rat liver (Chew *et al*., 2001). Mouse and rat liver cDNA were used in PCR using KAR subunit primers. β-actin was amplified from rat liver cDNA template. mRNAs of KAR subunits were not present in mouse or rat liver tissue (Figure 2.6). This observation confirms the specificity of the KAR primers.

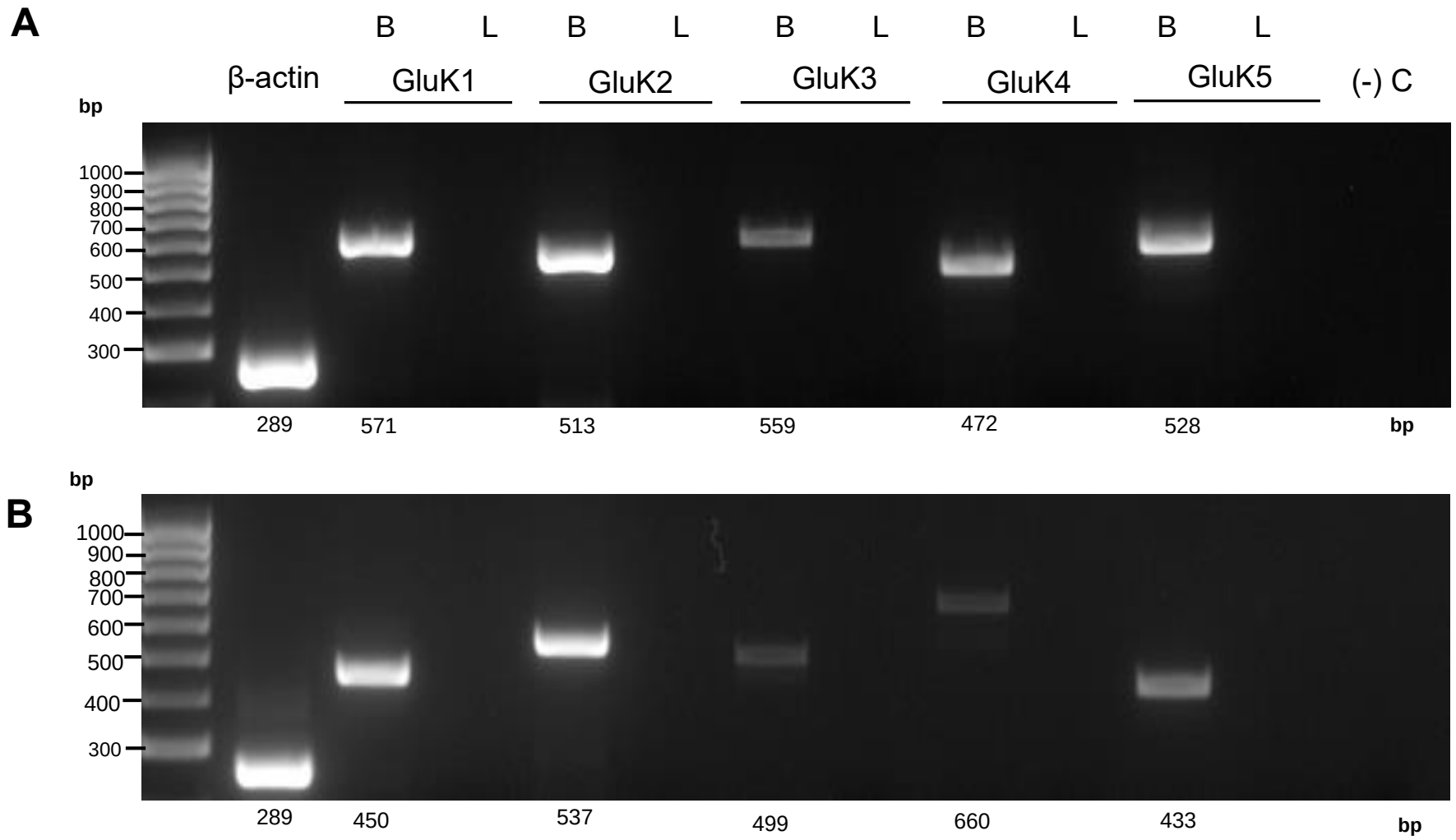

Figure 2.6. **KAR subunit transcripts are not expressed in the liver.** KAR subunit specific primers were used to investigate expression of KAR subunits in mouse (A) or rat (B) liver**.** cDNA from mouse and rat brain were used in the reaction as positive control whiles negative controls were PCR without template ((-) C). β-actin was amplified from rat liver cDNA template. Sizes of the products are indicated at the bottom of the panel. B: brain; L: liver. Figure is representative of three separate experiments.

2.4.1b. *Semi-quantitative analysis of KAR subunit mRNA expression in pancreatic α- and β-cell lines*

To investigate whether there are differences in KAR subunit mRNA expression between pancreatic α- and β-cells, amounts of GluK2 and GluK5 mRNAs normalised to β-actin in MIN6 and α-TC cells were determined. The optimum number of cycles of PCR required for the amplification of KAR subunit mRNA to be within the linear phase was determined using PCR cycle numbers of 15, 20, 25, 30 and 35 (Section 2.3.8). Pixel volume was plotted against PCR cycle number for GluK2, GluK5 and β-actin to select cycles within the linear phase of the reaction (Figure 2.7).

Based on the initial curves obtained, the PCR cycle analysis was repeated for GluK2 (26, 28, 30 cycles) and GluK5 (28, 30, 32) to select the optimum number of PCR cycles for these primers (Figure 2.8).

The densitometry analysis and PCR curves indicated that the PCR reaction was linear at 29 cycles for GluK2, 31 cycles for GluK5 and 20 cycles for β-actin.

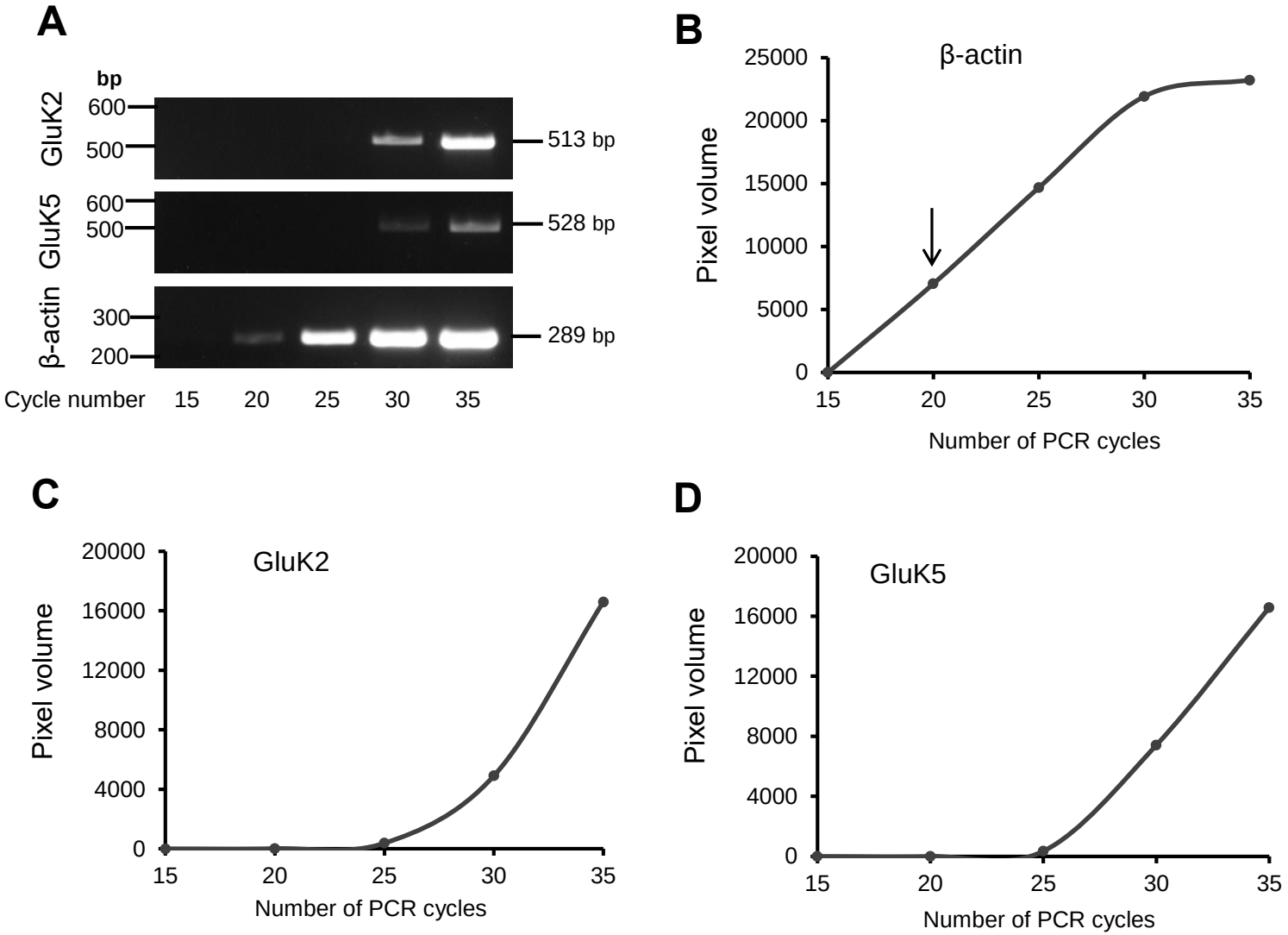

Figure 2.7. **Determination of the linear phase of GluK2 and GluK5 amplification.** Mouse brain cDNA was subjected to PCR using primers specific for β-actin, GluK2 and GluK5. PCR products were separated and visualised (A) and the pixel volume of the bands were measured using ImageJ. Pixel volume was plotted against PCR cycle number for β-actin (B), GluK2 (C) and GluK5 (D) and then PCR cycle numbers (20 for β-actin) was selected from the linear regions of the curve. One experiment was performed.

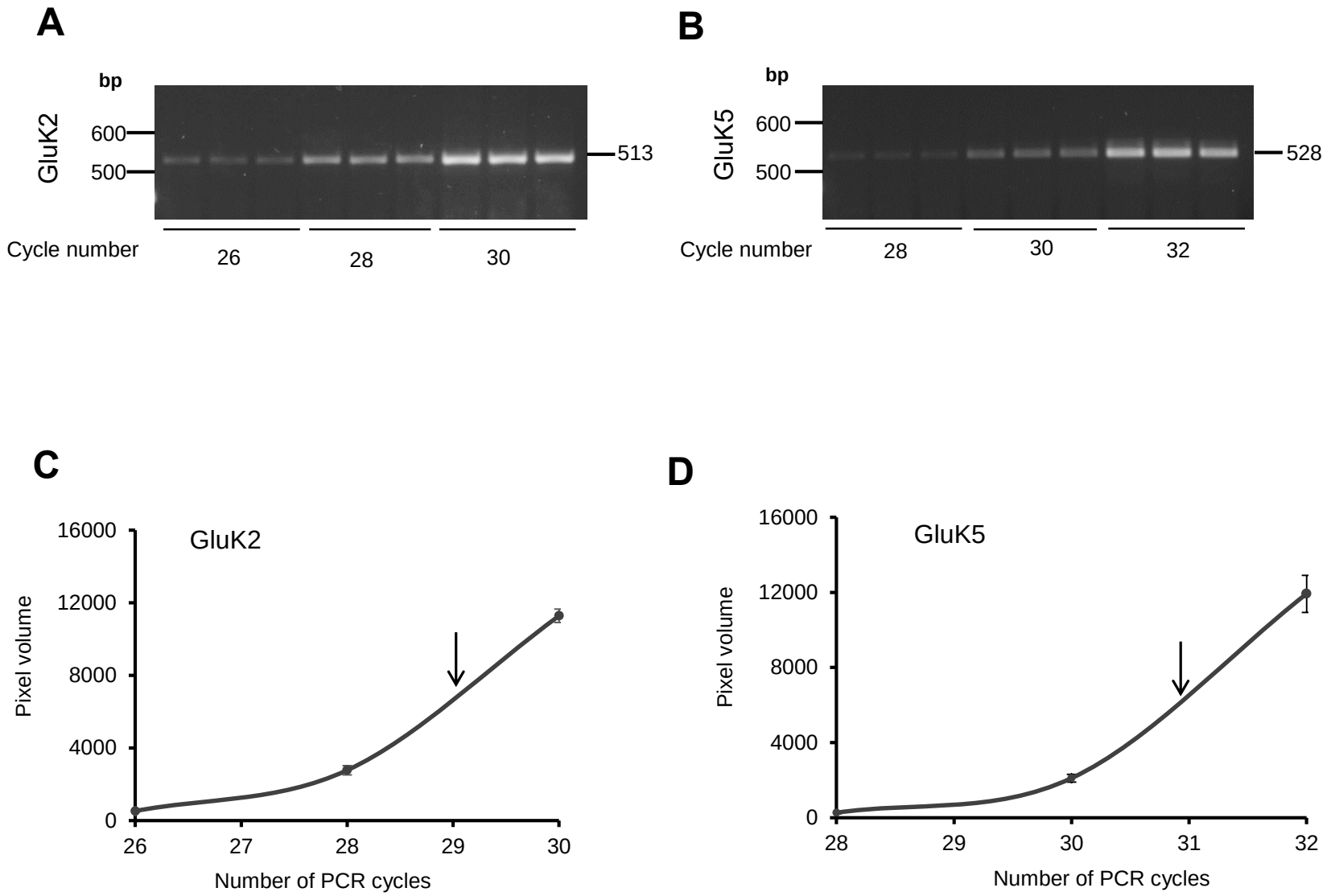

Figure 2.8. **Determination of the linear phase of the PCR for GluK2 and GluK5 amplification.** Mouse brain cDNA was used as templates for PCR using primers specific for GluK2 (cycles 26, 28, 30) and GluK5 (cycles 28, 30, 32). PCR products were separated and visualised (A and B) and the pixel volume of the bands were measured using ImageJ. Pixel volume was plotted against PCR cycle number for GluK2 (C) and GluK5 (D) and then PCR cycle numbers (29 for GluK2 and 31 for GluK5) were selected from the linear regions of each of the curves. Graphs represents means ± SD from one experiment performed in triplicate.

PCR using the selected number of cycles was performed and pixel volume of GluK2 was divided with that of β-actin and the obtained ratio from each experiment was averaged. The same procedure was used to determine the amount of GluK5 in islet cell lines and brain tissue. The obtained values were compared between the various samples using Student's *t*-test analysis (Figure 2.9).

There was no significant difference in expression of GluK2 or GluK5 subunit mRNAs between MIN6 β-cells and α-TC cells. Expression of GluK2 mRNA in the brain was significantly higher compared to MIN6 and α-TC whiles there was no significant difference in expression of GluK5 in the brain compared to MIN6 β-cells and α-TC cells (Figure 2.9).

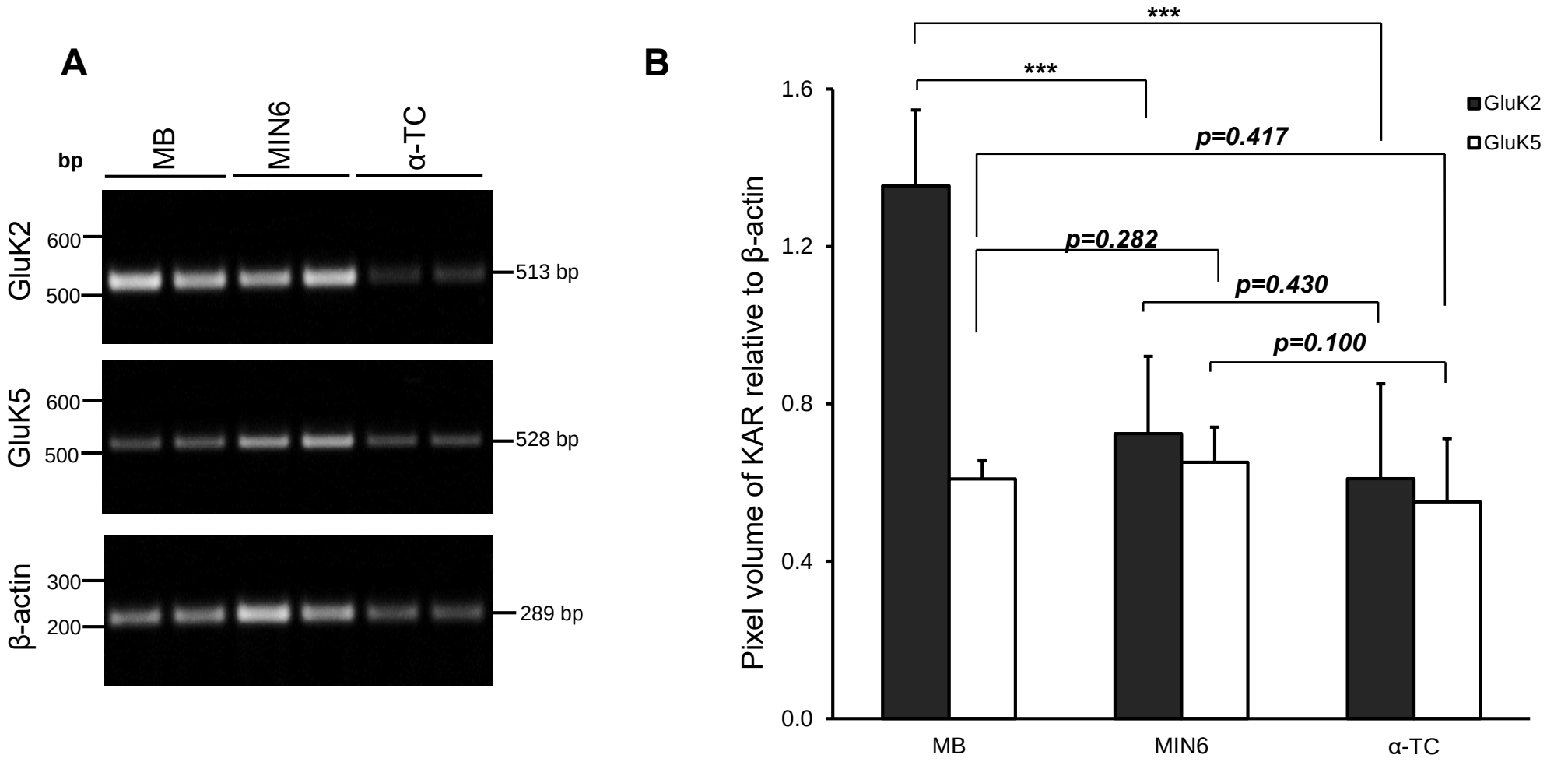

Figure 2.9. **Expression of GluK2 and GluK5 mRNA in MIN6 β-cells is not significantly different from α-TC cells.** PCR products were separated on agarose gel and visualised (A). Pixel volume were measured for each PCR band using ImageJ and normalised to β-actin. The mean relative amounts of mRNA in the cells were compared using Student's *t*-test (B). Bar chart represents means ± SEM from three separate experiments each performed in duplicate. ***p*<0.05; ****p*<0.01; *****p*<0.001.**

2.4.1c. *KAR subunit proteins are present in pancreatic α- and β-cell lines.*

The presence of KAR proteins in MIN6 and INS-1 β-cells and α-TC cells was investigated using antibodies specific for GluK2/3 and GluK5 subunits (section 2.3.9). Immunoblotting of KAR subunit proteins showed that both GluK2/3 and GluK5 are present in MIN6, α-TC and INS-1 pancreatic endocrine cells (Figure 2.10). As expected, GluK2/3 and GluK5 receptor protein were also present in the positive control, mouse brain.

The relative amounts of KAR protein in MIN6, INS-1 and α-TC was determined by measuring the pixel volume of KAR immunopositive bands using the ImageJ software. The pixel volume of KAR bands were normalised to pixel volume of β-actin internal standards (section 2.3.10).

Statistical analysis using Student's *t*-test showed that there was no significant difference in KAR subunit protein (GluK2/3 and GluK5) levels between β-cells (MIN6, INS-1) and the α-cells (α-TC) (Figure 2.11).

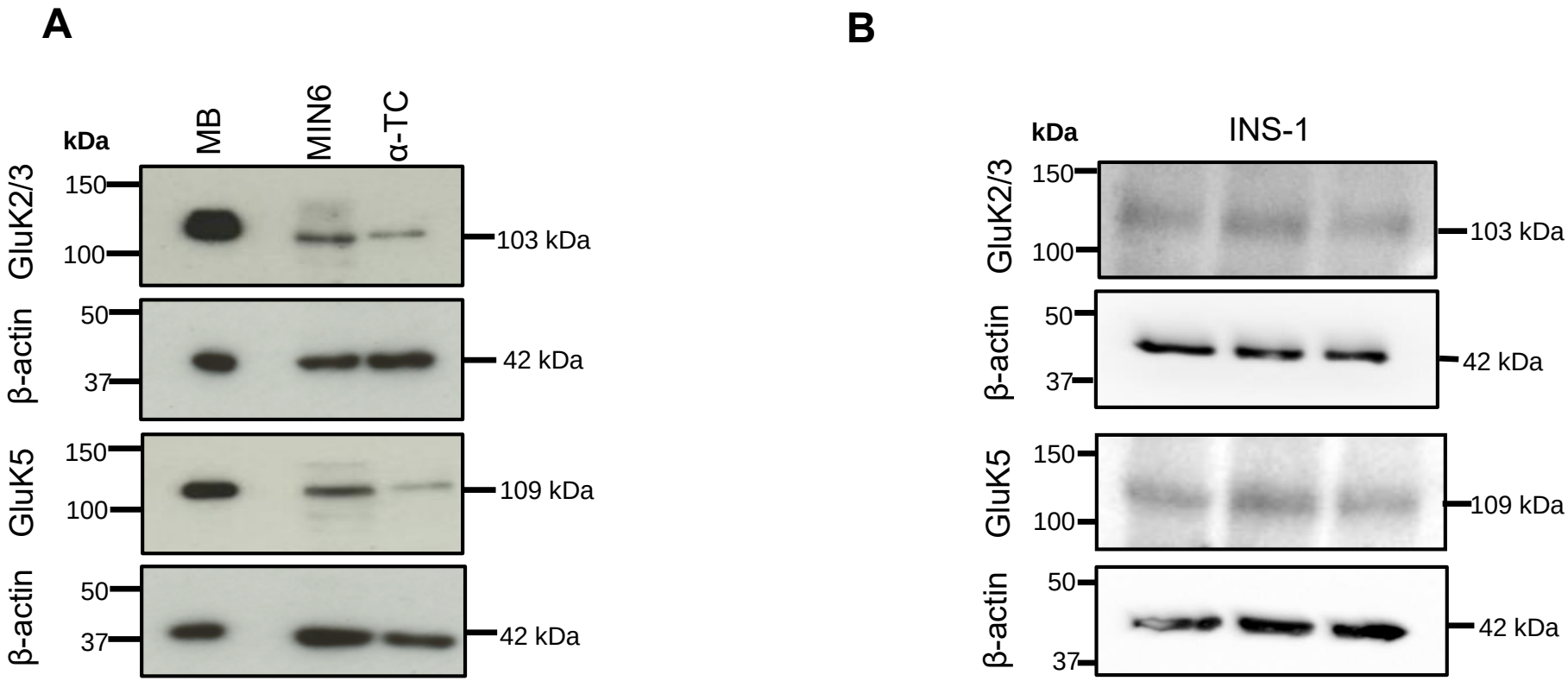

Figure 2.10. **Investigation of KAR subunit proteins in pancreatic endocrine cell lines.** The presence of GluK2/3 and GluK5 proteins in mouse brain, MIN6 and α-TC (A) and INS-1 (B) was detected on immunoblots by subunit-specific antibodies. Figure (A) is representative of three independent experiments using cells at different passages. Each lane in Figure (B) represents protein lysate prepared from cells at different passages.

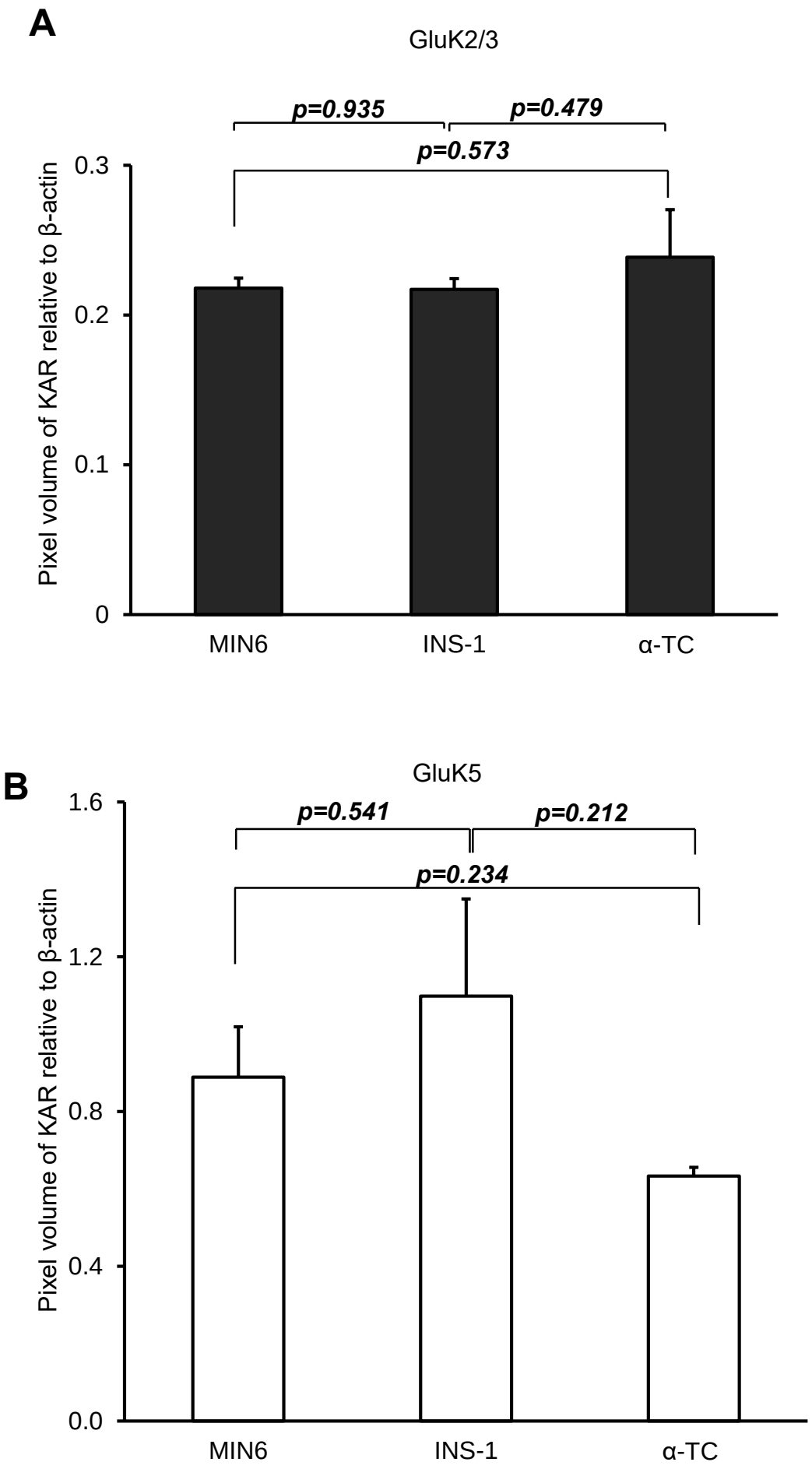

Figure 2.11. A**nalysis of relative amounts of KAR subunit protein in MIN6 and INS-1 β-cells and α-TC cells.** Immunoblotting with specific antibodies against GluK2/3 (A) and GluK5 (B) were used to detect the proteins and the pixel volume of the bands was measured using ImageJ software. Pixel volume of the bands were normalised to their corresponding β-actin. Results represent means ± SEM from three separate experiments. ***p<0.05; **p<0.01; ***p<0.001.

2.4.2. Investigation of KAR auxiliary subunits in pancreatic endocrine cells

2.4.2a. *Neto 1 and Neto 2 subunit mRNA are expressed in pancreatic α- and β-cells and in rat islet of Langerhans*

Neto 1 and Neto 2 are transmembrane auxiliary subunits of KARs therefore they are of significant importance for the function of pre- and post-synaptic KARs (Chapter one, section 1.5). The expression of Neto 1 and Neto 2 mRNAs in pancreatic endocrine cells was investigated using specific primers in PCR. Rat brain cDNA was used as positive control since Neto 1 and Neto 2 are expressed in rat brain (Tomita and Castillo, 2012). Neto 1 and Neto 2 mRNAs were shown to be expressed in MIN6 and INS-1 β-cells, α-TC cells and in rat islets of Langerhans (Figure 2.12). As expected, both were present in the positive control, rat brain.

In addition to setting up PCR reactions without templates, cDNA from rat liver was used to test for specificity of Neto 1 and Neto 2 primers. Transcript of Neto 1 was present in rat liver but Neto 2 was not detected. cDNA from liver was used to determine whether the liver can be used as a reliable template for negative control of Neto 1 and Neto 2 PCR. Data from the EMBL Expression Atlas (https://www.ebi.ac.uk/gxa/home) and T1DBase (https://www.t1dbase.org/page/Welcome/display) show that detectable levels of Neto 1 and Neto 2 subunit mRNA are present in rat liver. Thus, the liver is not a reliable source of template for negative control of PCR for Neto 1 and Neto 2 mRNA.

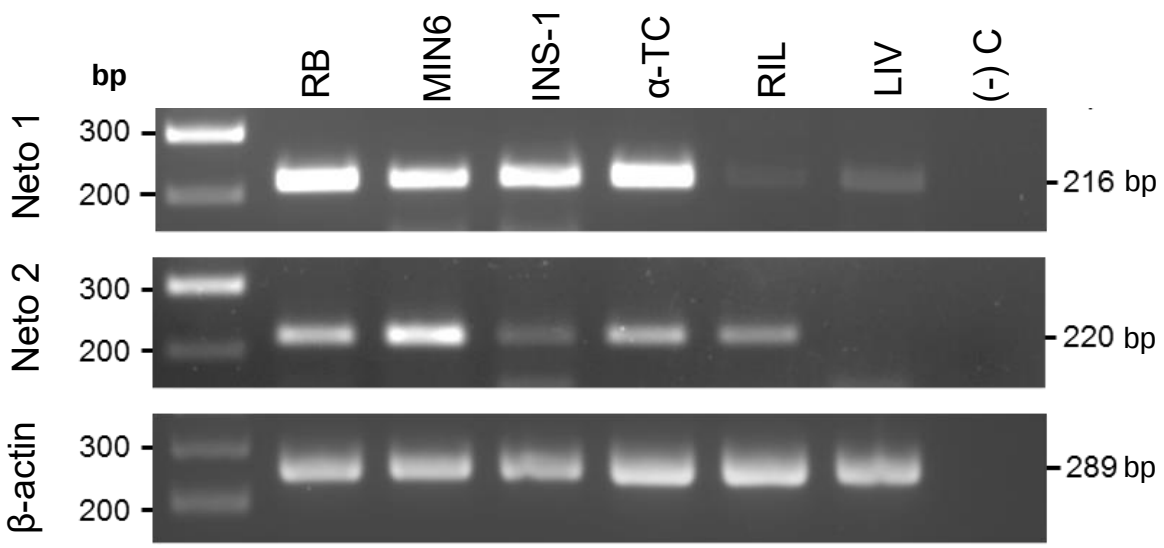

Figure 2.12. Neto 1 and Neto 2 mRNA are expressed in pancreatic α- and β-cells and rat islet of Langerhans. The presence of Neto 1 and Neto 2 mRNAs was determined using specific primers in PCR. Negative controls were PCR reaction without template ((-) C). RB: rat brain, RIL: rat islets of Langerhans, LIV: rat liver.

2.4.2b. *Semi-quantitative analysis of Neto 1 and Neto 2 mRNA expression in cultured pancreatic α- and β-cells.*

To investigate whether there is a difference in Neto 1 and Neto 2 subunit mRNA expression between α- and β-cells, the linear phase of the PCR for Neto 1 and Neto 2 were determined using 15, 20, 25, 30 and 35 cycles for PCR (section 2.3.8). The pixel volume was plotted against number of PCR cycles to select cycles within the linear phase of the reaction (Figure 2.13). The plots indicated that the PCR reaction was linear at 30 cycles for Neto 1 and 28 cycles for Neto 2, cycles used for β-actin was as described in section 2.4.1, Figure 2.7. The selected cycles were used for PCR with MIN6, α-TC and mouse brain cDNA templates and pixel volume of Neto 1 was divided with that of β-actin and the obtained ratio from each experiment was averaged. The same procedure was used to determine the amount Neto 2 in the cell lines and brain tissue. The obtained values were compared between the various samples using Student's *t*-test analysis (Figure 2.14). Neto 1 mRNA expression was significantly higher in α-cells than in β-cells. In contrast, Neto 2 mRNA was higher in β-cells than in α-cells. Both Neto 1 and Neto 2 expression was significantly higher in brain tissue compared to either endocrine cells (Figure 2.14).

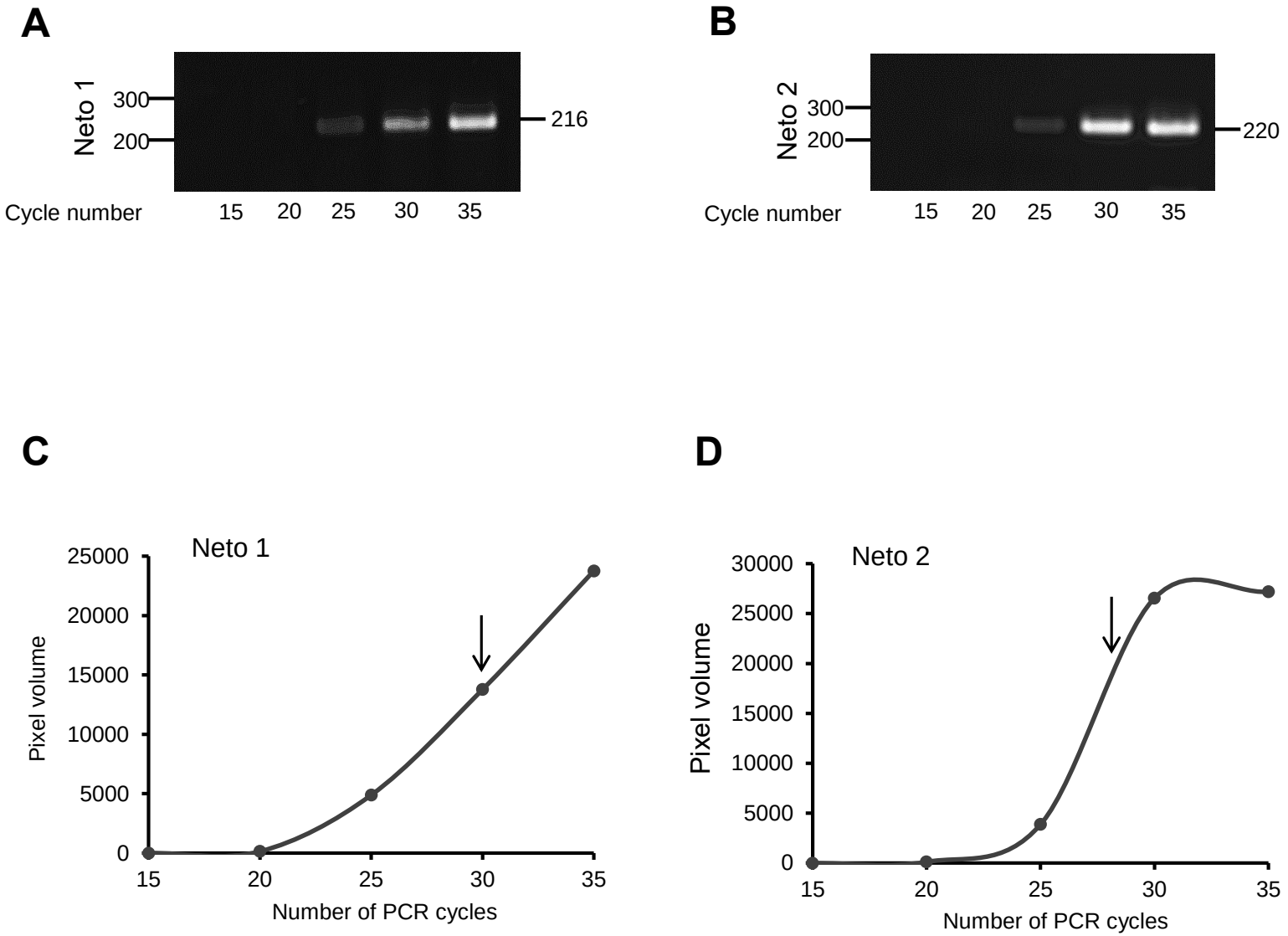

Figure 2.13. Determination of the linear phase of Neto 1 and Neto 2 PCR. Mouse brain cDNA was used as templates for PCR using primers specific for Neto 1 and Neto 2. PCR products were separated and visualised (A and B) and the pixel volume of the bands were measured using ImageJ. Pixel volume was plotted against PCR cycle number for Neto 1 (C) and Neto 2 (D) and then PCR cycle numbers (30 for Neto 1 and 28 for Neto 2) were selected from the linear regions of each of the curves. One experiment was performed.

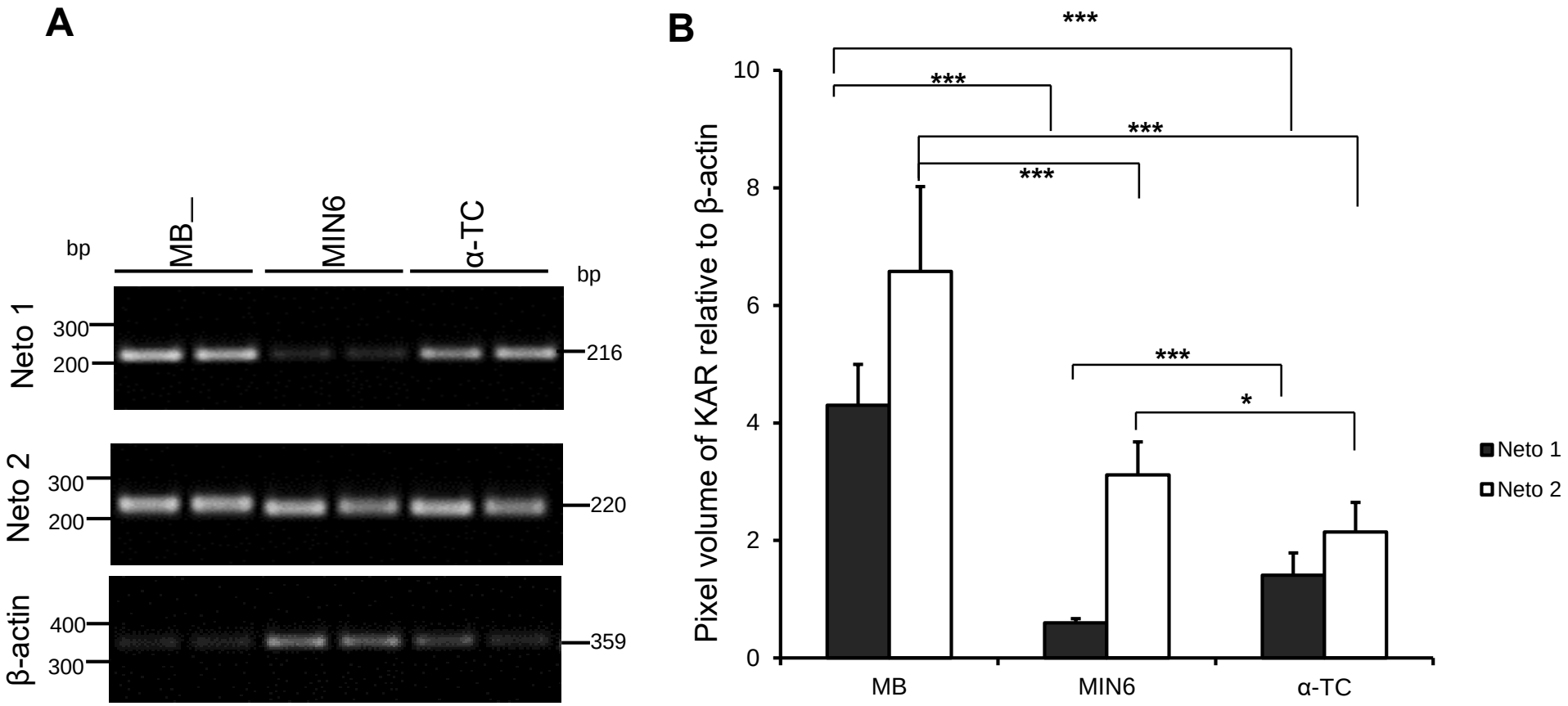

Figure 2.14. Semi-quantitative analysis of Neto 1 and Neto 2 mRNA expression in MIN6 β-cells and α-TC cells. PCR products were separated on agarose gel and visualised (A). Pixel volume were measured for each PCR band using ImageJ and normalised to β-actin. The mean relative amounts of mRNA in the cells were compared using Student's *t*-test analysis (B). Bar chart represents means ± SEM from three separate experiments each performed in duplicate. ***p*<0.05; ****p*<0.01; *****p*<0.001.**

2.4.2c. *Neto 1 and Neto 2 subunit protein are present in pancreatic α- and β-cell lines.*

To investigate the presence of Neto 1 and Neto 2 protein in pancreatic endocrine cells, antibodies against these proteins were used in immunoblotting (section 2.3.9).

Immunoblotting showed that Neto 1 and Neto 2 proteins are present in MIN6 and INS-1 β-cells and α-TC cells (Figure 2.15). This indicates that KAR subunits proteins are present in pancreatic endocrine cells together with their auxiliary proteins. As expected, Neto 1 and Neto 2 proteins were present in mouse brain.

The relative amounts of Neto 1 and Neto 2 protein in MIN6 and INS-1 β-cells and α-TC cells were determined by measuring the pixel volumes of Neto 1 and Neto 2 immunopositive bands (section 2.3.10). The pixel volume of Neto 1 and Neto 2 were normalised to β-actin internal standards.

In agreement with the mRNA, the relative amount of Neto 1 protein in α-TC cells was found to be significantly higher than in MIN6 and INS-1 β-cells. In contrast, the relative amounts of Neto 2 proteins in MIN6 and INS-1 β-cells were significantly higher than in α-TC cells (Figure 2.16).

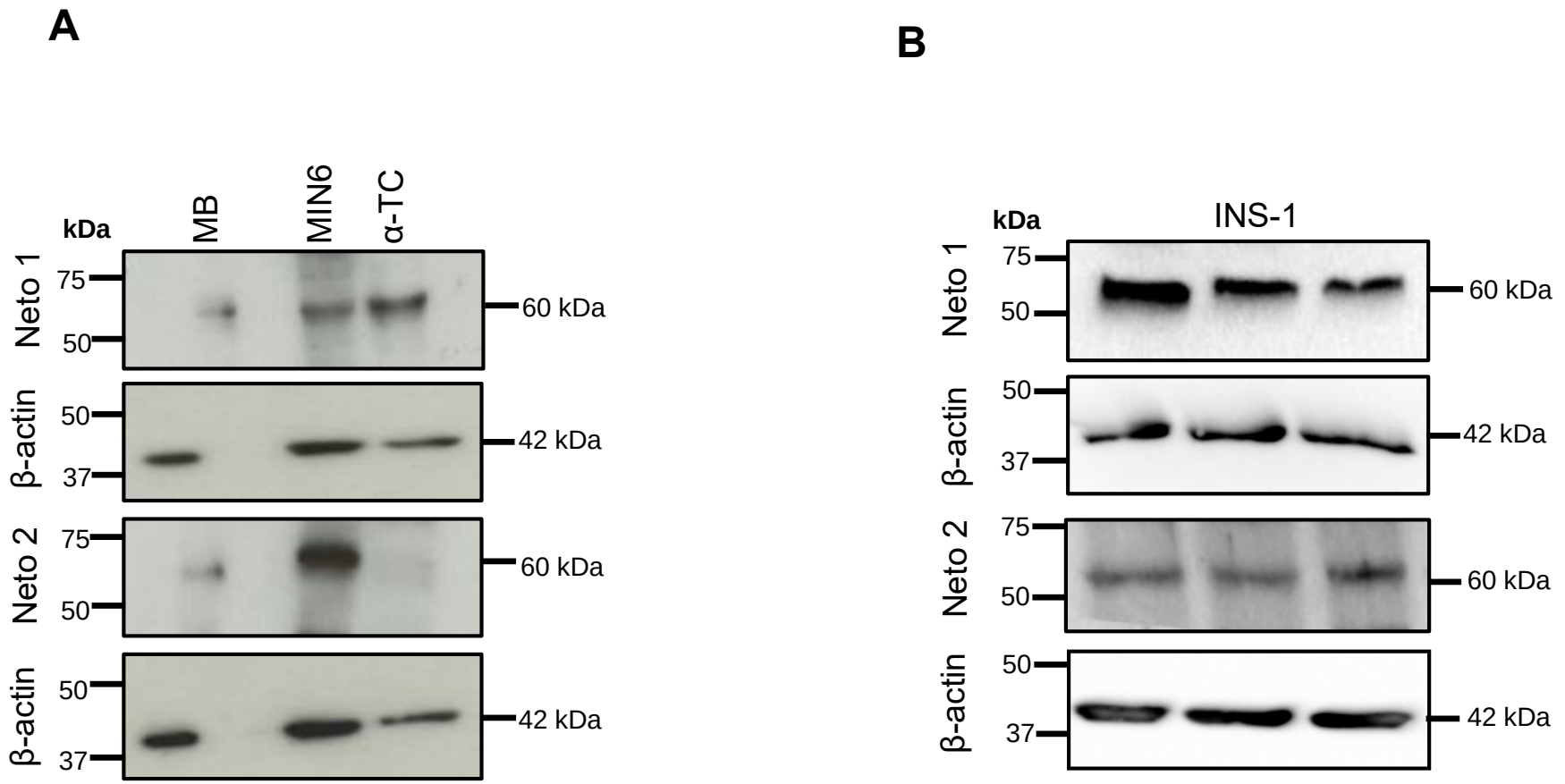

Figure 2.15. Neto 1 and Neto 2 proteins are present in pancreatic endocrine cells. The presence of Neto 1 and Neto 2 protein in MIN6**,** α-TC (A) and INS-1 cells (B) was detected on immunoblots by subunit-specific antibodies. Figure (A) is representative of three independent experiments using cells at different passages. Each lane in Figure (B) represents protein lysate prepared from cells at different passages.

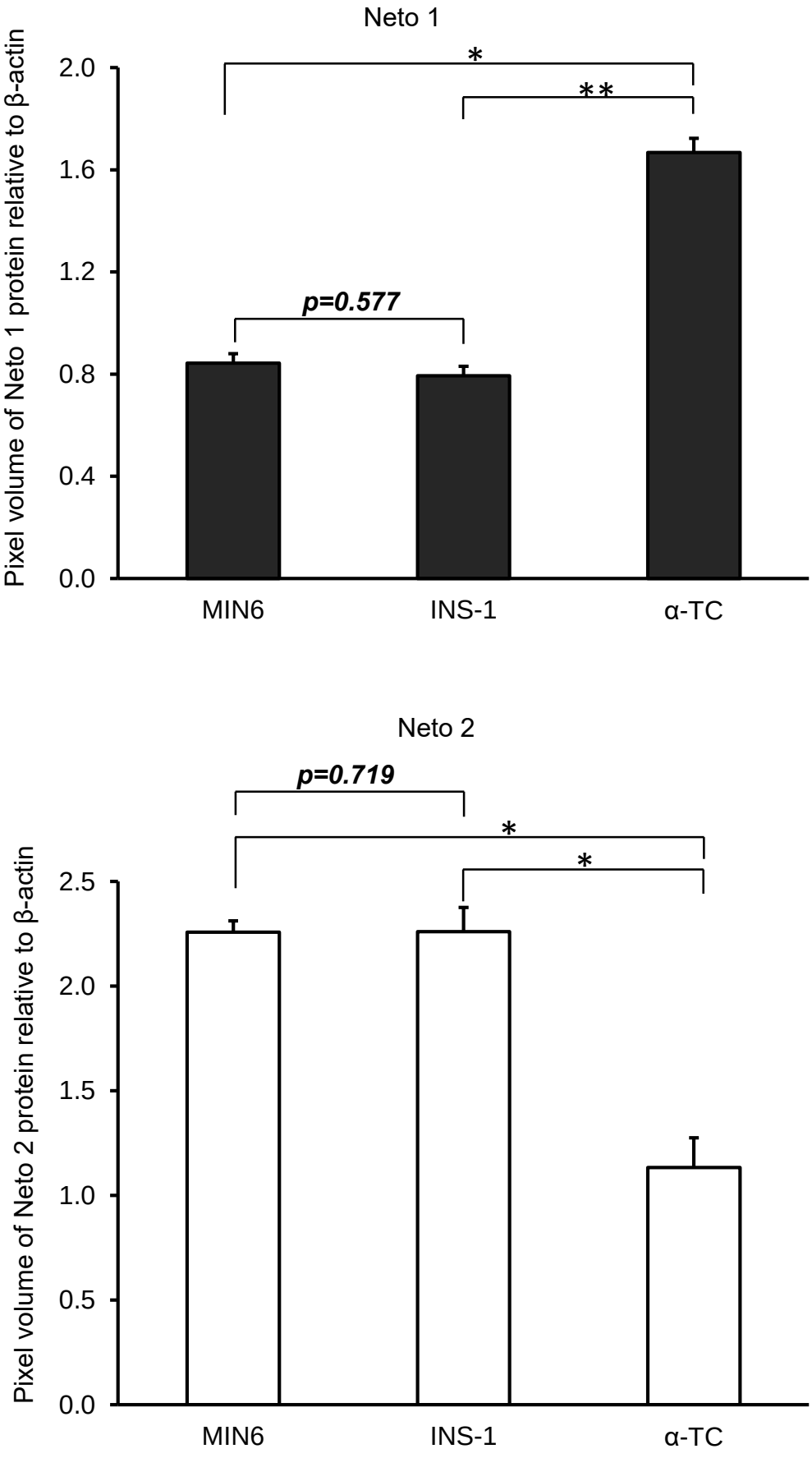

Figure 2.16. Analysis of relative amounts of Neto 1 and Neto 2 protein in MIN6 and INS-1 β-cells and α-TC cells. Immunoblotting with specific antibodies against Neto 1 **(A)** and Neto 2 **(B)** were used to detect the proteins and the pixel volumes of the bands were measured using ImageJ software. Pixel volume of the bands were normalised to their corresponding β-actin immunoreactivities. Results represent means ± SEM from three separate experiments. ***p*<0.05; ****p*<0.01; *****p*<0.001.**

2.4.3. Measurement of changes in intracellular calcium ion concentration $[Ca^{2+}]_i$ in cultured MIN6 pancreatic β-cells.

KAR subunits are present in pancreatic α- and β-cells and islets of Langerhans together with Neto 1 and Neto 2 auxiliary subunits (Sections 2.4.1-2.4.2). These observations suggest that functional KARs could assemble in α- and β-cells of the pancreas.

The main function of β-cells is secretion of insulin to regulate blood glucose (Rorsman and Braun, 2013) and studies have shown that exocytosis of insulin granules from β-cells is primarily dependent on the intracellular calcium concentration ($[Ca^{2+}]_i$) (Pedersen *et al*., 2011; Hou *et al*., 2009). Thus, the role of KARs in the regulation of $[Ca^{2+}]_i$ in MIN6 β-cells was investigated.

2.4.3a. *Kainate induces transient changes in $[Ca^{2+}]_i$ in MIN6 β-cells.*

MIN6 β-cells cultured in low (3 mM) glucose and loaded with FURA-2AM calcium was perifused with 25 μM kainate prepared in HBSS solution containing either 3 mM or 30 mM glucose. The mean fluorescence intensity ratio which represents changes in $[Ca^{2+}]_i$ was measured and analysed using Volocity Image Analysis software (section 2.3.11). A plot of fluorescence ratio against time after application of kainate is shown in Figure 2.17 and bar charts representing the mean change in fluorescence ratio ± SEM are shown in Figure 2.18. Two-way *ANOVA* was used to determine if there is significant evidence for interaction between concentration of glucose and first/second stimulation.

Activation of KARs in MIN6 β-cells with 25 μM kainate induced an increase in $[Ca^{2+}]_i$ relative to the baseline measurements at both stimulatory (30 mM) and non-stimulatory (3 mM) glucose concentrations. These changes in $[Ca^{2+}]_i$ were observed subsequent to both first and second applications of kainate (Figure 2.17).

Two-way *ANOVA* showed that mean increase in $[Ca^{2+}]_i$ induced by kainate was significantly higher in the presence of 30 mM glucose compared to 3 mM glucose. In the presence of 3 mM or 30 mM glucose, the mean increase in $[Ca^{2+}]_i$ induced by the first kainate perifusion was not significantly different from the second application (Figure 2.18). The two-way *ANOVA* showed that there was no significant evidence for a glucose concentration*stimulation interaction effect on the mean increase in $[Ca^{2+}]_i$ induced by kainate (p=0.557).

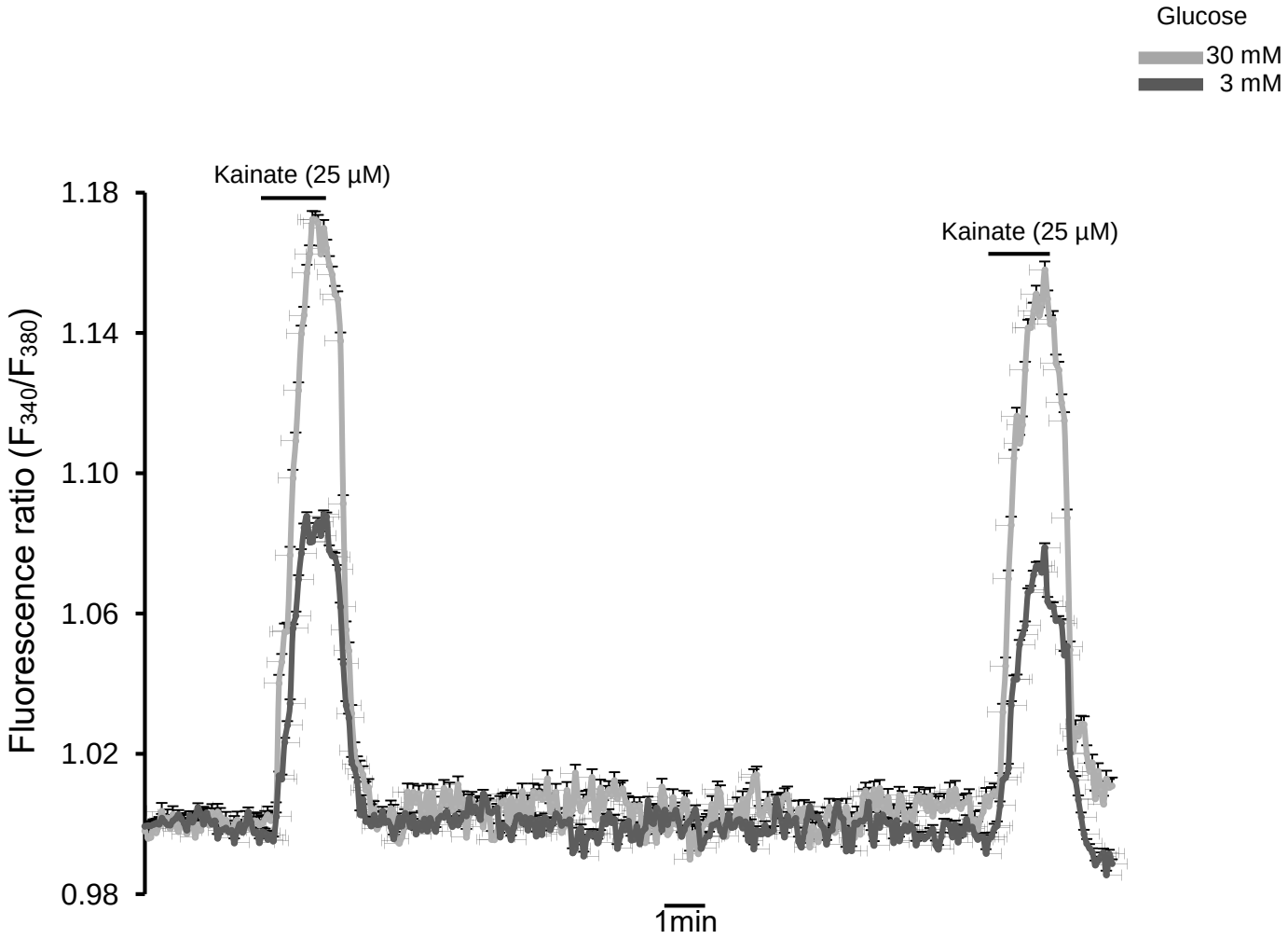

Figure 2.17. Kainate induces transient changes in $[Ca^{2+}]_i$ in MIN6 β-cells. MIN6 β-cells were perifused with 25 µM kainate and fluorescence ratios were measured in 30-50 cells and normalised to ratios obtained during the first three minutes of recording under basal conditions. Results represent mean ± SEM of four independent experiments.

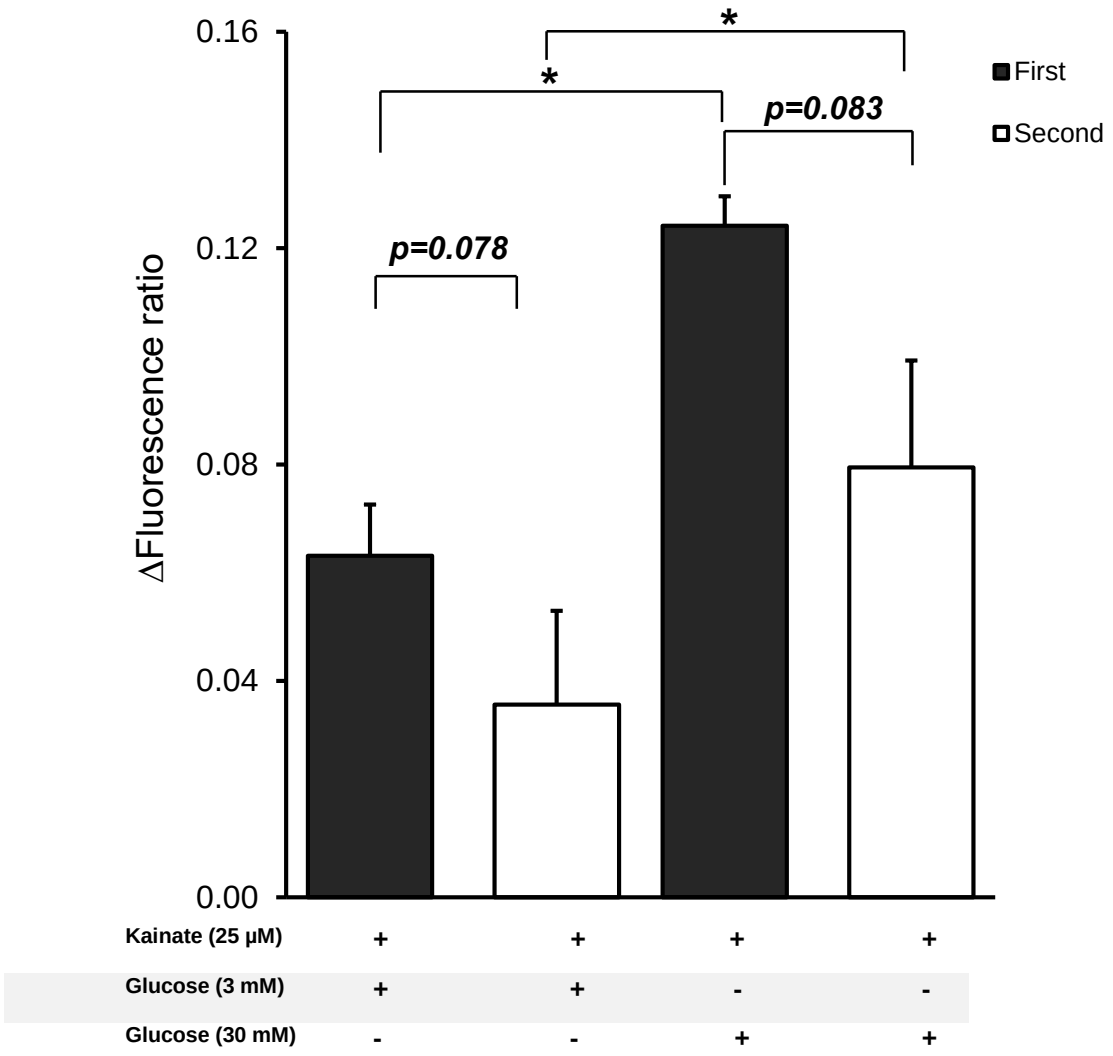

Figure 2.18. Kainate induces transient changes in $[Ca^{2+}]_i$ in the presence of 3 mM and 30 mM glucose in MIN6 β-cells in. Means were compared using two-way *ANOVA.* Results are presented as mean ± SEM of four separate experiments. ***p*<0.05; ****p*<0.01; *****p*<0.001.**

2.4.3b. *Kainate-induced change in $[Ca^{2+}]_i$ is not affected by the inactivation of AMPA and NMDA receptors.*

AMPARs and KARs have been shown to possess some similar characteristics including their response to agonists at specific concentrations (Rogawski, 2011). Moreover, both NMDA and AMPA receptors are expressed in pancreatic β-cells (Molnar *et al*., 1995; Gonoi *et al*., 1994). Thus, the observed kainate-induced change in $[Ca^{2+}]_i$ could be due to AMPAR or NMDAR activation. To investigate this hypothesis, changes in $[Ca^{2+}]_i$ in MIN6 β-cells subsequent to application of kainate in the presence of Gyki-52466; a competitive inhibitor of NMDA and AMPA receptors was monitored using FURA-2AM calcium dye (section 2.3.11).

Application of 25 µM kainate only or after pre-incubation of the cells with 100 µM Gyki-52466 resulted in changes in $[Ca^{2+}]_i$ (Figure 2.19). The mean increase in $[Ca^{2+}]_i$ normalised to the baseline was significantly higher in the presence of 30 mM glucose than 3 mM glucose indicating a significant evidence for glucose concentration on the mean increase in $[Ca^{2+}]_i$ induced by kainate (p<0.001). This was observed subsequent to application of kainate only or kainate after pre-incubation with Gyki-52466 (Figure 2.20). In addition, the increase in $[Ca^{2+}]_i$ induced by 25µM kainate only was not statistically different from the increase in $[Ca^{2+}]_i$ induced by 25µM kainate in the presence of 100 µM Gyki-52466. This was observed at both glucose concentrations and thus indicates that there is no significant evidence for Gyki-52466 on the mean increase in $[Ca^{2+}]_i$ induced by kainate (p=0.285) (Figure 2.20).

The two-way *ANOVA* also indicated that there was no significant evidence for a glucose concentration*stimulation interaction effect on the mean increase in $[Ca^{2+}]_i$ induced by kainate (p=0.590).

These results indicate that the observed change in $[Ca^{2+}]_i$ subsequent to application of kainate was due to activation of KARs and that inhibition of NMDA and AMPA receptors had no significant effect on this change.

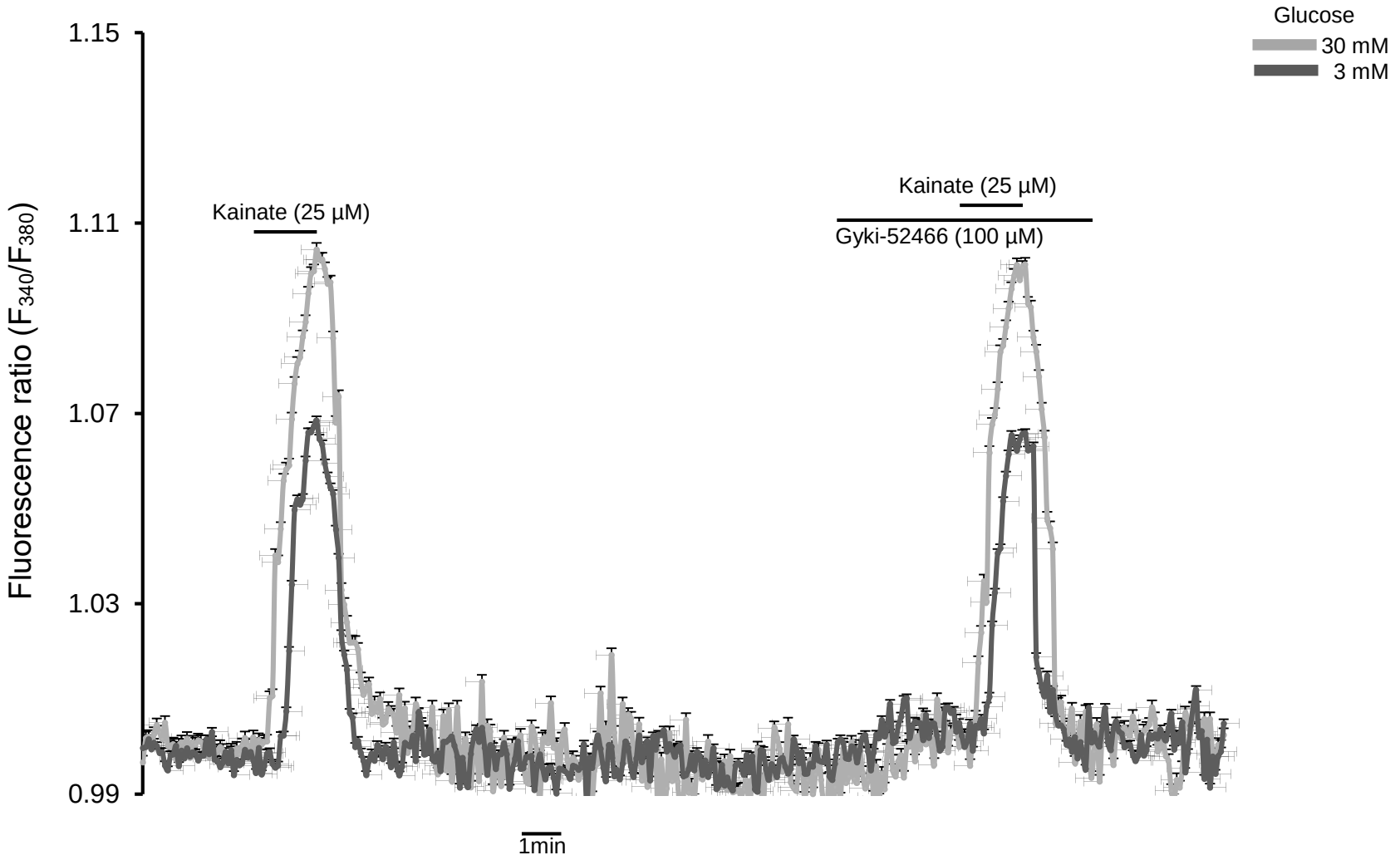

Figure 2.19. Kainate-induced $[Ca^{2+}]_i$ change is not blocked by competitive inhibitor of AMPA/NMDA receptor, Gyki-52466. MIN6 β-cells were perifused with 25 µM kainate or kainate after pre-incubation with 100 µM Gyki-52466 and fluorescence ratios were measured in 30-50 cells and normalised to ratios obtained during the first three minutes of recording under basal conditions. Results represent mean ± SEM of four independent experiments.

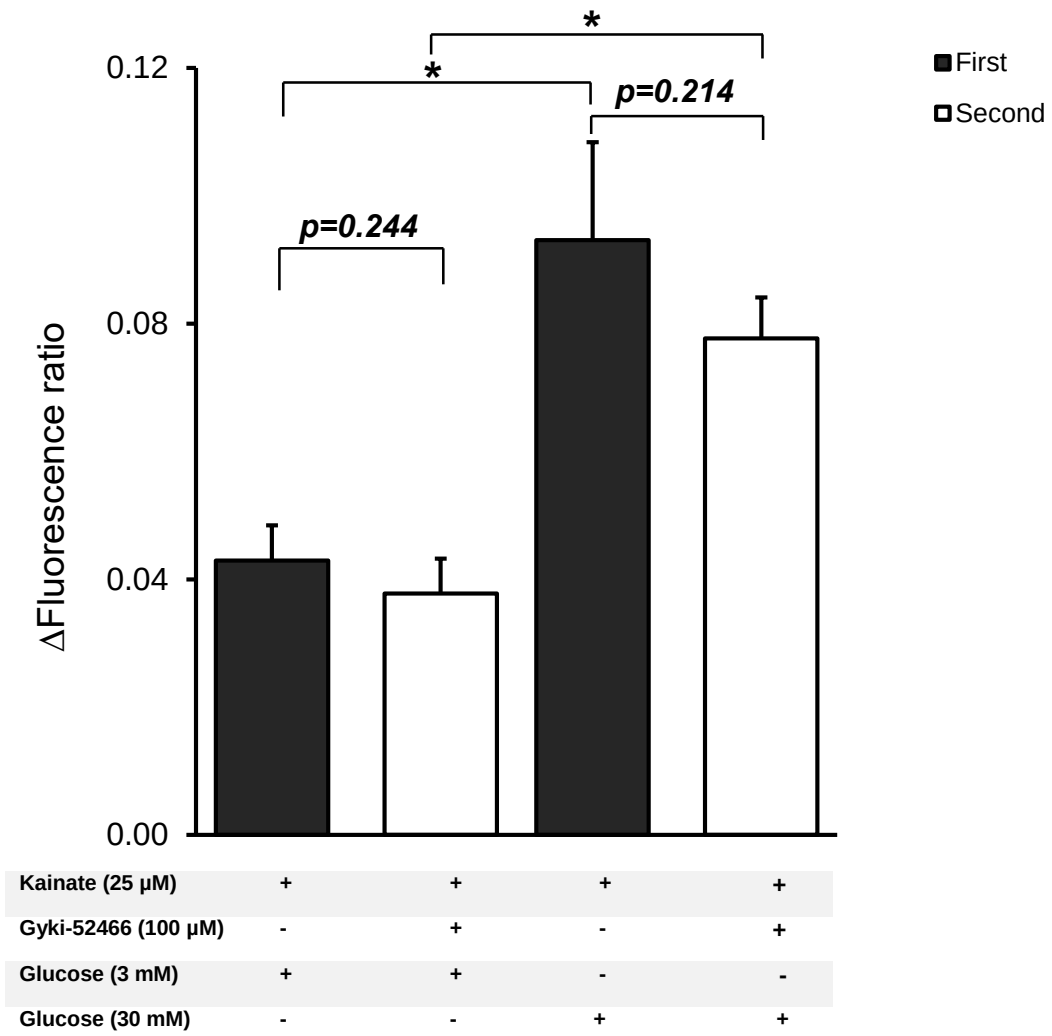

Figure 2.20. Bar graph representing the maximal variation in the fluorescence ratio induced by kainate or kainate in the presence of AMPA/NMDA receptor antagonist Gyki-52466. Means were compared using two-way *ANOVA*. Results represent mean ± SEM for four independent experiments. ***p*<0.05; ****p*<0.01; *****p*<0.001.**

2.4.3c. *Kainate-induced change in $[Ca^{2+}]_i$ is specifically blocked by the KAR/AMPA receptor antagonist NBQX.*

NBQX has been shown to inhibit homomeric GluK1, GluK2, GluK3 as well as heteromeric combination of GluK2 and GluK5 (Matute, 2011; Jane *et al*., 2009) (Chapter one, section 1.5.5). Thus, to further confirm the effect of kainate on $[Ca^{2+}]_i$ in MIN6 β-cells, cells were perifused with 25 µM kainate only or kainate after pre-incubation with 30 µM of a competitive AMPAR/KAR antagonist; NBQX,

Application of kainate induced changes in $[Ca^{2+}]_i$ in the presence of 3 mM or 30 mM glucose compared to the baseline measurements. In contrast, application of kainate subsequent to pre-incubation with NBQX in the presence of 3 mm or 30 mM glucose induced a minimal change in $[Ca^{2+}]_i$ in MIN6 β-cells relative to baseline measurements (Figure 2.21). The mean increase in $[Ca^{2+}]_i$ induced by kainate only and normalised to baseline measurements was significantly higher in the presence of 30 mM glucose compared to 3 mM glucose indicating that there is significant evidence for glucose concentration on the mean increase in $[Ca^{2+}]_i$ induced by kainate ($p<0.04$). The increase in $[Ca^{2+}]_i$ induced by kainate only and normalised to baseline measurements was significantly higher than the change induced by kainate subsequent to pre-incubation with NBQX at both glucose concentrations (Figure 2.22). The two-way *ANOVA* indicates that there is significant evidence for kainate inhibitor (NBQX) on the mean increase in $[Ca^{2+}]_i$ induced by kainate ($p<0.001$). The analysis also indicates that there is significant evidence for a glucose concentration*inhibitor interaction effect on the mean increase in $[Ca^{2+}]_i$ induced by kainate ($p=0.031$).

These results suggest that the observed increase in $[Ca^{2+}]_i$ were due to activation of KARs and that inhibition of these receptors by NBQX attenuated the observed effect.

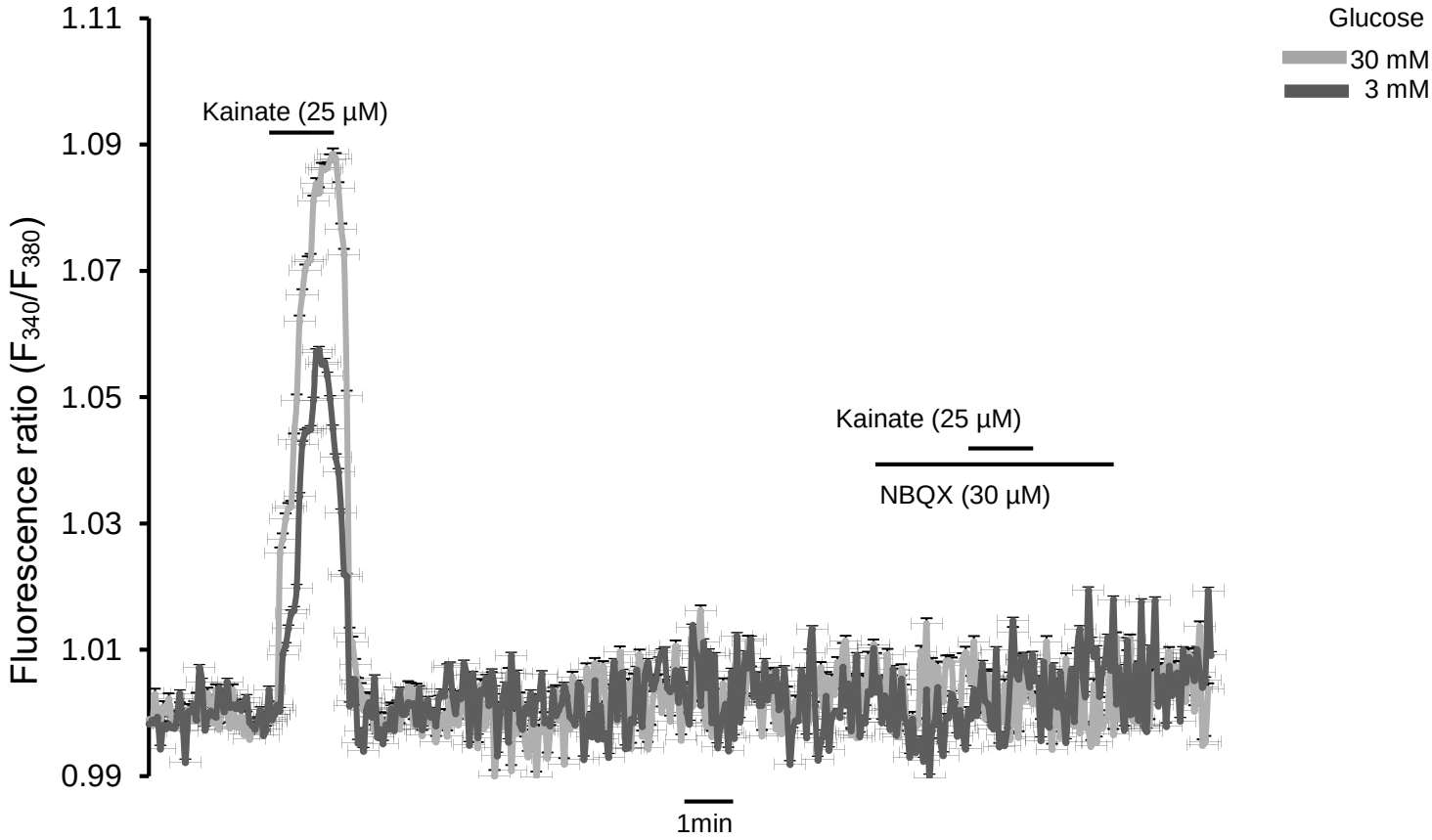

Figure 2.21. Kainate-induced changes in $[Ca^{2+}]_i$ are blocked by KAR/AMPA receptor antagonist NBQX. MIN6 β-cells were perifused with 25 µM kainate or kainate after pre-incubation with 30 µM NBQX and fluorescence ratios were measured in 30-50 cells and normalised to ratios obtained during the first three minutes of recording under basal conditions. Results represent mean ± SEM of three independent experiments.

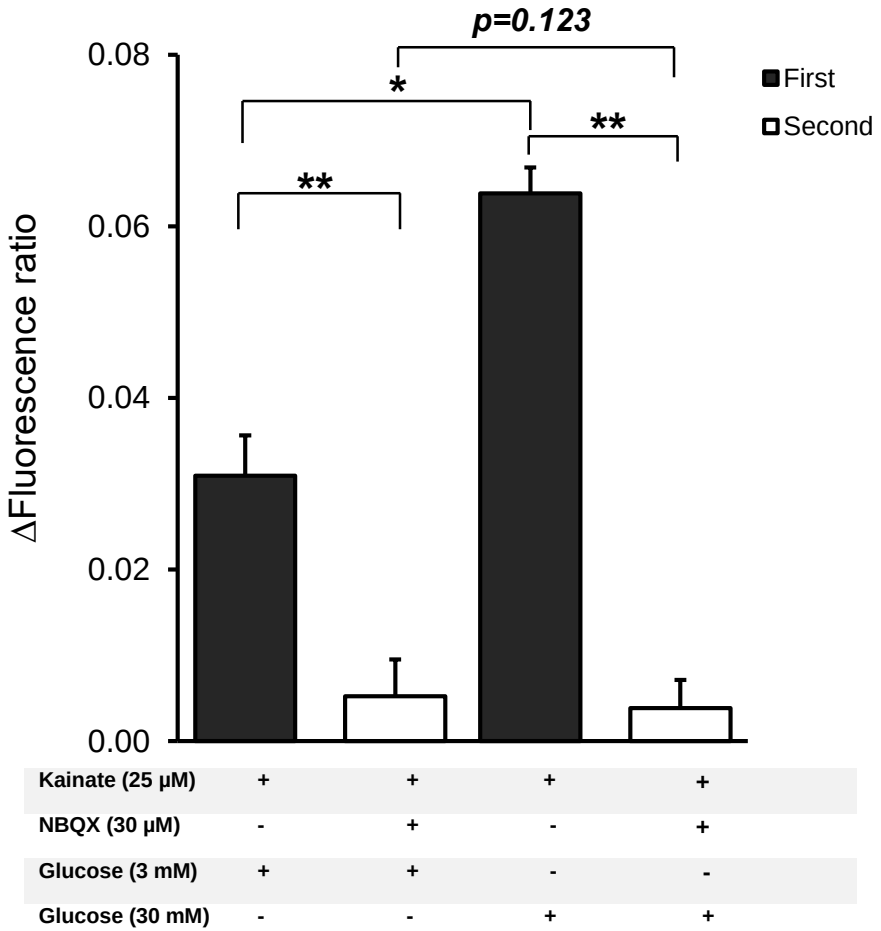

Figure 2.22. Bar graph representing the maximal variation in the fluorescence ratio induced by kainate or kainate in the presence of KAR/AMPA receptor antagonist NBQX. Means were compared using two-way *ANOVA*. Results represent mean ± SEM for three independent experiments. ***p*<0.05; ****p*<0.01; *****p*<0.001. *p*<0.05; ***p*<0.01; ****p*<0.001.

2.4.3d. *Kainate-induced change in $[Ca^{2+}]_i$ is potentiated by the selective group I mGlu receptor agonist DHPG.*

KARs represent a unique subtype of iGluRs because some of the functions of KARs in the CNS are mediated through an unconventional non-canonical (metabotropic) signalling involving G-proteins and second messengers and activation of group I mGluRs also potentiates KAR signalling and action (Rutkowska-Wlodarczyk *et al*., 2015) (section 1.5.8). To investigate this possibility with respect to changes in $[Ca^{2+}]_i$, MIN6 β-cells were perifused with 25 µM kainate only or kainate after pre-incubation with 50 µM of a selective group I mGlu receptor agonist, DHPG.

Application of kainate only or kainate subsequent to pre-incubation of the cells with DHPG induced changes in $[Ca^{2+}]_i$ in the presence of 3 mM or 30 mM glucose compared to the baseline measurements (Figure 2.23). In the presence of 30 mM glucose, incubation of the cells with DHPG induced minor changes in $[Ca^{2+}]_i$ relative to baseline measurements (Figure 2.23).

The mean increase in $[Ca^{2+}]_i$ induced by kainate only and normalised to baseline measurements was significantly higher in the presence of 30 mM glucose compared to 3 mM glucose indicating that there is significant evidence for glucose concentration effect on the mean increase in $[Ca^{2+}]_i$ induced by kainate ($p<0.001$). Perifusion of the cells with kainate after pre-incubation with DHPG (normalised to DHPG only) induced significantly higher increase in $[Ca^{2+}]_i$ compared to increase in $[Ca^{2+}]_i$ induced by application of kainate (normalised to baseline measurements). This was observed at both glucose concentrations (Figure 2.24). The two-way *ANOVA* indicates that there is significant evidence for group I mGlu receptor agonist (DHPG) on the mean increase in $[Ca^{2+}]_i$ induced by kainate ($p<0.002$). The analysis also indicates that there is no

significant evidence for a glucose concentration*DHPG effect on the mean increase in $[Ca^{2+}]_i$ induced by kainate (p=0.190).

These observations indicate that activation of group I mGluRs by DHPG in β-cells potentiates the kainate-induced increase in $[Ca^{2+}]_i$.

The responsive of the cells and sensitivity of the calcium imaging system was tested by application of 15 mM KCl after each experiment. This concentration of KCl has been shown to depolarise cell membranes to cause influx of Ca^{2+} (Andersson *et al*., 2015). Application of 15 mM KCl resulted in increased $[Ca^{2+}]_i$ in MIN6 β-cells which indicates that the cells were responsive during the experiment (Figure 2.25).

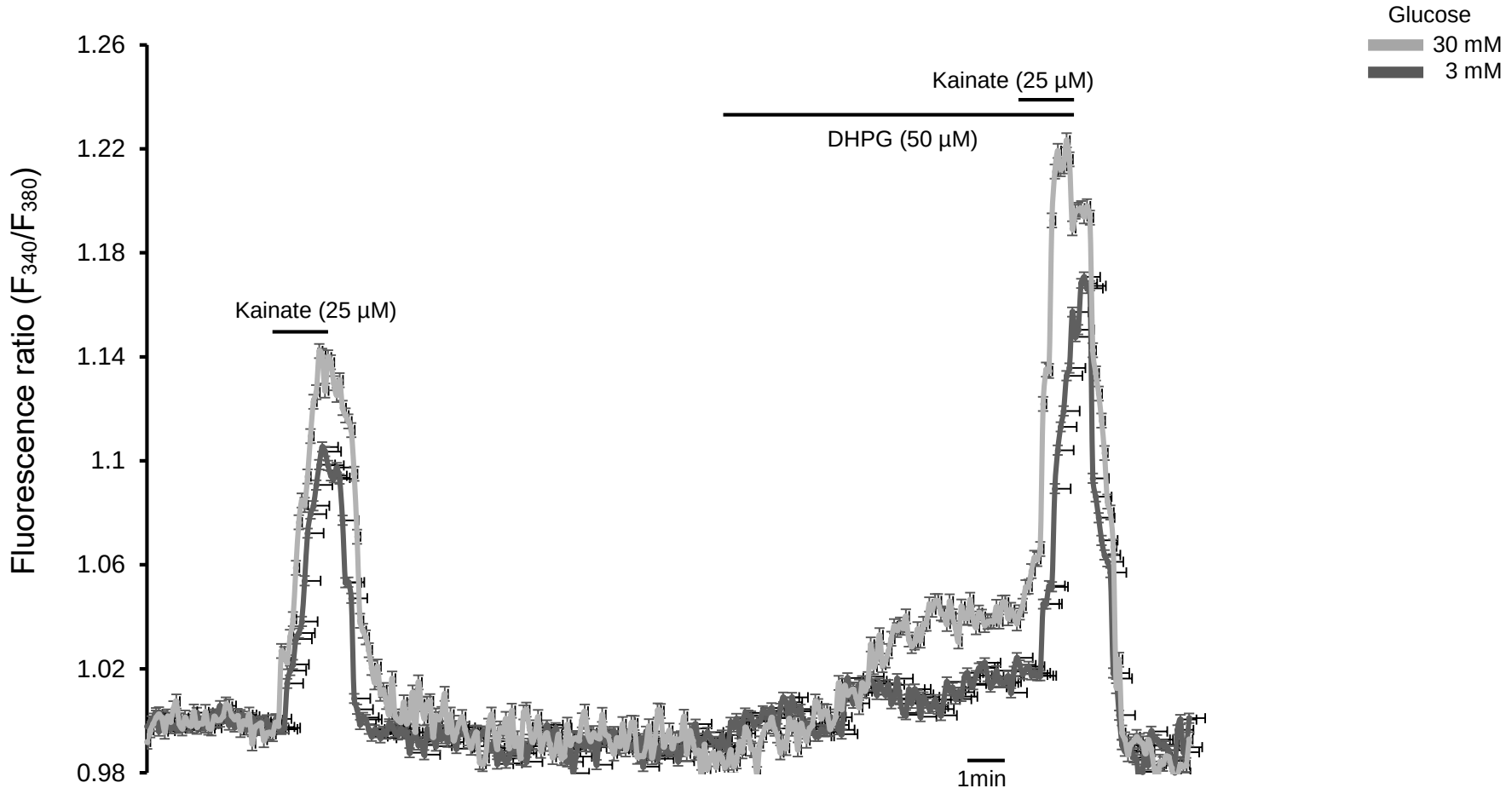

Figure 2.23. Kainate-induced change in $[Ca^{2+}]_i$ is potentiated by mGluR I receptor agonist DHPG. MIN6 β-cells were perifused with 25 µM kainate or kainate after pre-incubation with 50 µM DHPG and fluorescence ratios were measured in 30-50 cells and normalised to ratios obtained during the first three minutes of recording under basal conditions. Results represent mean ± SEM of three independent experiments.

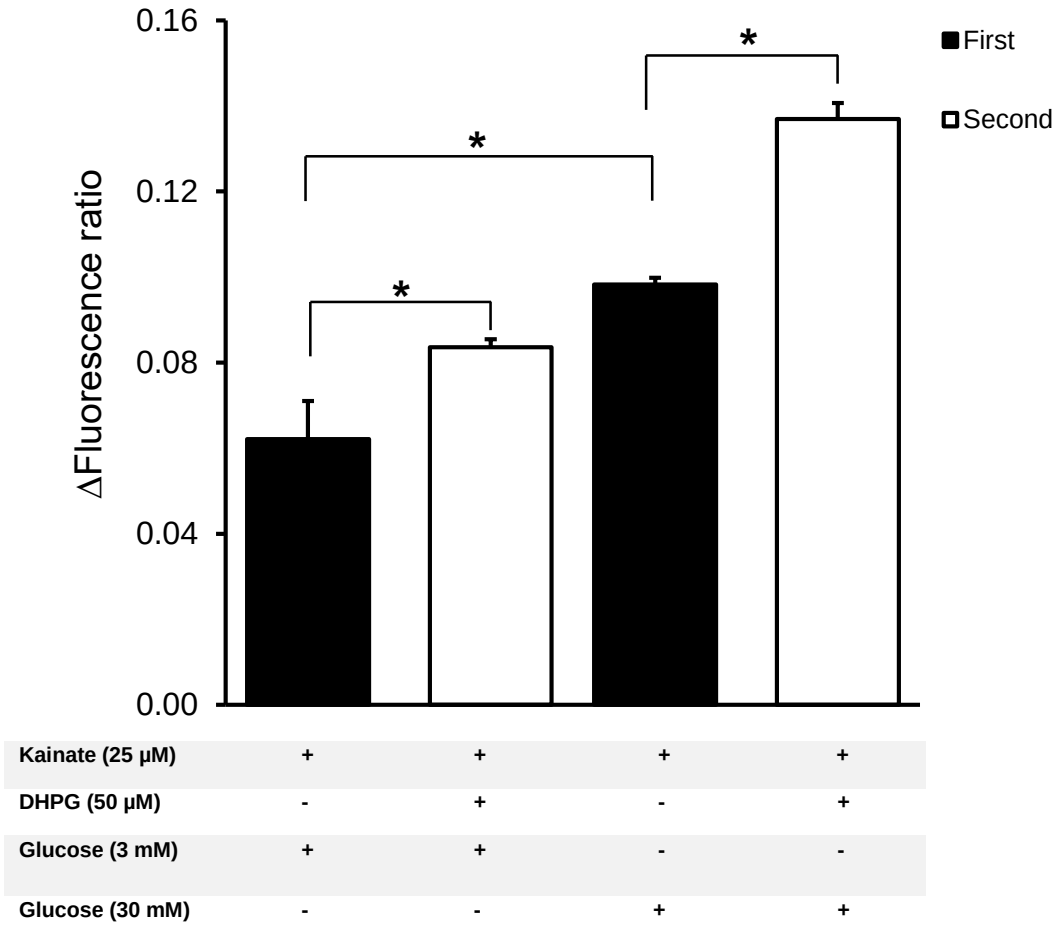

Figure 2.24. Bar graph representing the maximal variation in the fluorescence ratio induced by kainate or kainate in the presence of group I mGlu receptor agonist, **DHPG.** Means were compared using two-way *ANOVA*. Results represent mean ± SEM for three independent experiments. ***p*<0.05; ****p*<0.01; *****p*<0.001. *p*<0.05; ***p*<0.01; ****p*<0.001.

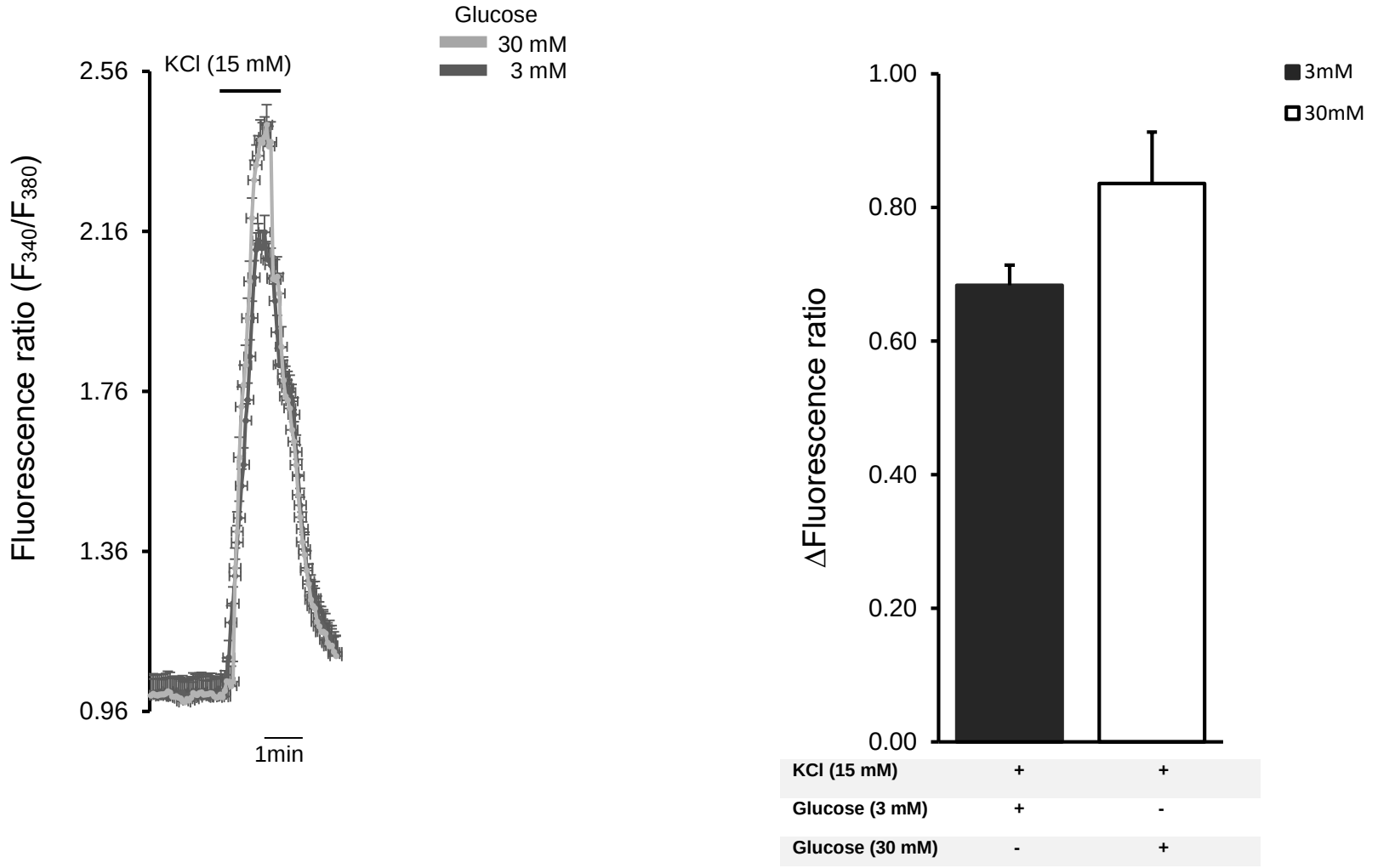

Figure 2.25. **KCl-induced increase in $[Ca^{2+}]_i$ in MIN6 β-cells.** MIN6 β-cells were perifused with 15 mM KCl and fluorescence ratios were measured in 30-50 cells and normalised to ratios obtained during the first three minutes of recording under basal conditions (A). Bar graph representing the maximal variation in the fluorescence ratio induced by KCl (B). Results represent mean ± SEM of three independent experiments.

2.4.4. Investigation of the effect of KAR activation on insulin secretion in cultured MIN6 and INS-1 pancreatic β-cells

The main function of pancreatic β-cells is insulin secretion (section 1.2). In these cells, secretion of insulin is primarily controlled by concentration of glucose but other nutrients including lipids and amino acids also modulate insulin release (Dou *et al*., 2015). Results from the calcium imaging studies (section 2.4.3) suggest that activation of KAR subunits by kainate increases $[Ca^{2+}]_i$ in β-cells. Based on these observations; we tested the effect of kainate on insulin secretion from pancreatic β-cells was investigated.

To investigate insulin secretion subsequent to KAR activation, MIN6 (mouse) and INS-1 (rat) pancreatic β-cells were seeded and incubated with KAR agonists (kainate) and antagonists (NBQX), NMDAR/AMPAR antagonist (Gyki-52466) and group 1 mGluR agonist (DHPG) described in section 2.3.13 and Figure 2.3.

A calibration curve was plotted for the Mercodia mouse and rat insulin ELISA assay (Diagenics, Milton Keynes, UK) and used to determine the amount of insulin secreted from the cells (section 2.3.13). Secreted insulin from MIN6 and INS-1 β-cells was calculated as a percentage of total insulin which includes the secreted and retained insulin. Insulin secretion was measured in both rat and mouse cell lines to ensure that the observed effect is not species-specific. Plots of optical density of the insulin standards against their concentration for mouse and rat ELISA assays are shown in Figures 2.26 and 2.27 respectively.

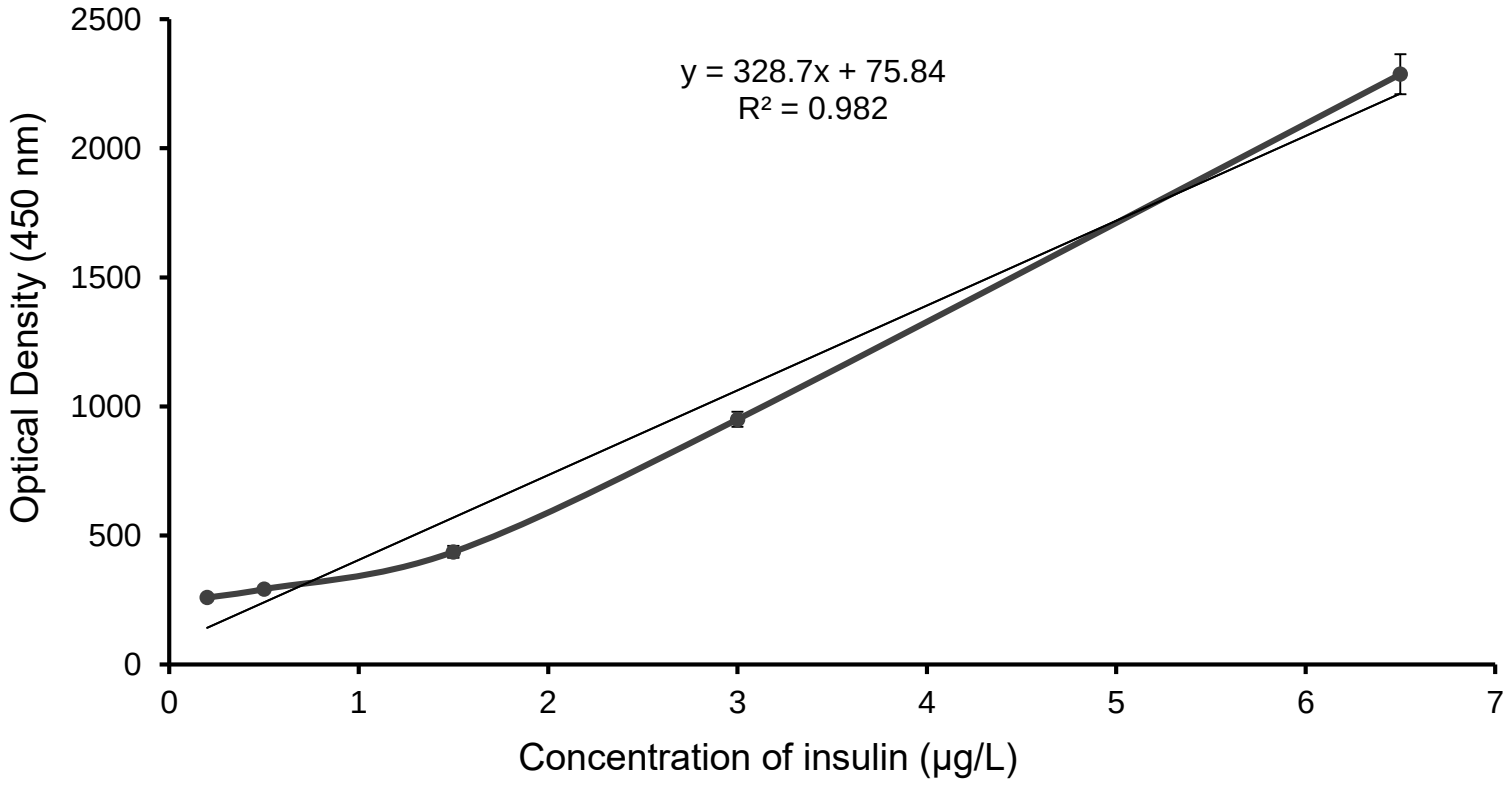

Figure 2.26. Calibration curve of Mercodia mouse insulin ELISA assay. The equation of the standard curve was derived and used to estimate the concentration of insulin in the test samples. Results represent means ± SD from a single experiment performed in triplicate.

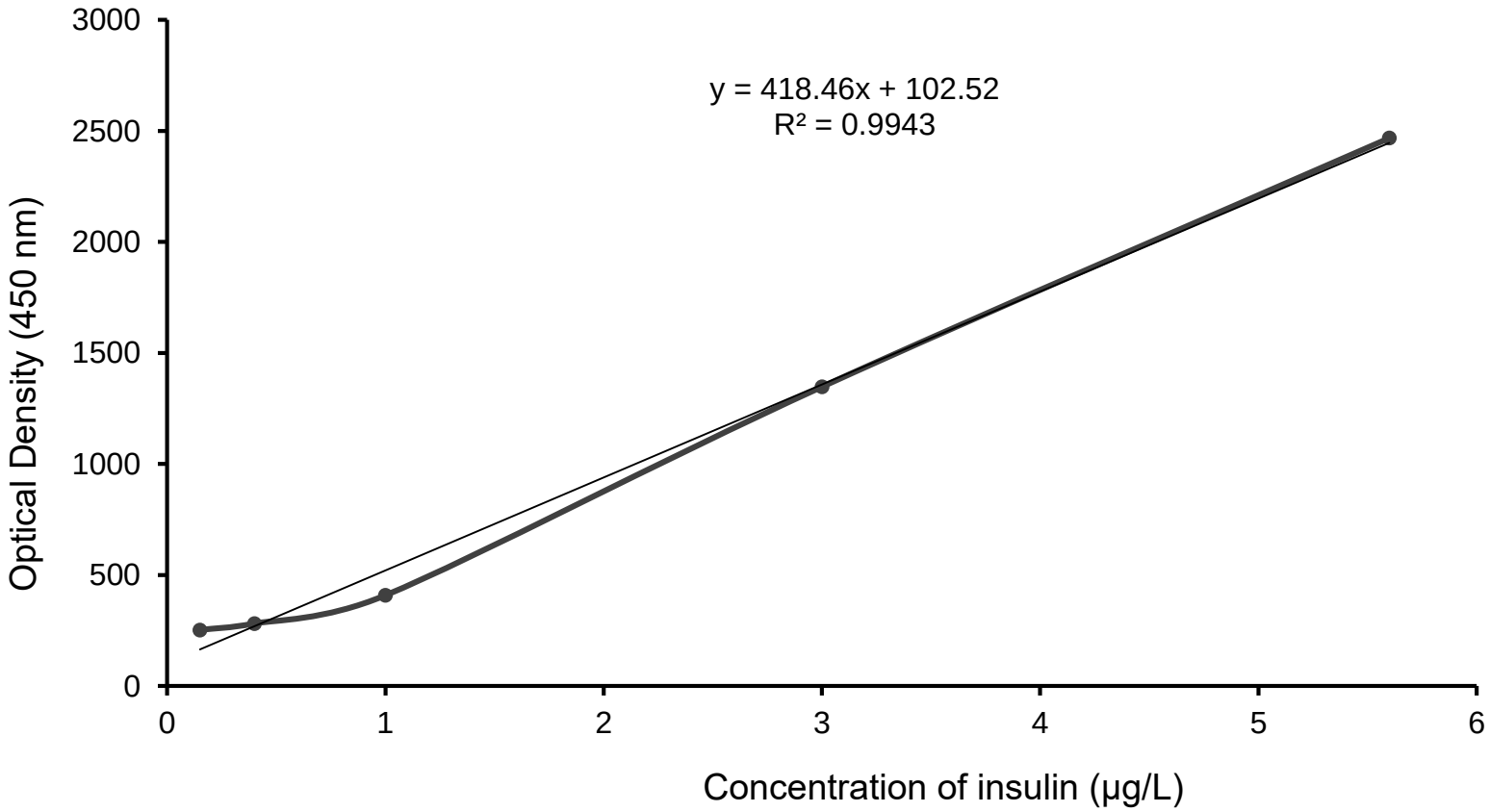

Figure 2.27. Calibration curve of Mercodia rat insulin ELISA assay. The equation of the standard curve was derived and used to estimate the concentration of insulin in the test samples. Results represent a single experiment performed.

2.4.4a. *Activation of KARs by kainate potentiates glucose-stimulated insulin secretion (GSIS) from MIN6 and INS-1 β-cells.*

To determine the effect of KAR activation on GSIS, MIN6 and INS-1 β-cells were incubated with KAR agonists and antagonists as described in section 2.3.13.

In both MIN6 and INS-1 β-cells, 25 µM kainate increased significantly the amount of insulin released from the cells compared to controls. This significant increase in insulin secretion was observed in the presence 3 mM or 30 mM glucose (Figures 2.28-2.31).

Insulin secretion induced by incubation of MIN6 and INS-1 β-cells with kainate subsequent to pre-incubation with 30 µM NBQX (selective and competitive AMPA and kainate receptor antagonist) was significantly lower compared to insulin secretion induced by kainate only.

In both MIN6 and INS-1 cells, insulin secretion induced by kainate in the presence of a competitive inhibitor of NMDA and AMPA receptors, Gyki-52466 was not statistically different from the amount of insulin induced by kainate only.

In the presence of group 1 mGluR agonist, DHPG insulin secretion induced by kainate in MIN6 or INS-1 cells was not statistically different from the amount of insulin induced by kainate only.

Incubating the cells with 15 mM KCl caused significant increase in insulin secretion from both MIN6 and INS-1 β-cells (Figures 2.28-2.31). The aim of incubating the cells with KCl was to test the responsiveness of the cells and the sensitivity of the assay since KCl has been shown to induce significant increase in GSIS in β-cell lines (Andersson *et al*., 2015).

Kainate-induced increase in insulin secretion from both MIN6 and INS-1 β-cells was shown to be dependent on the concentration of glucose. In both cell lines, kainate-induced

increase insulin secretion was significantly higher in the presence of 30 mM compared to 3 mM glucose (Figure 2.32).

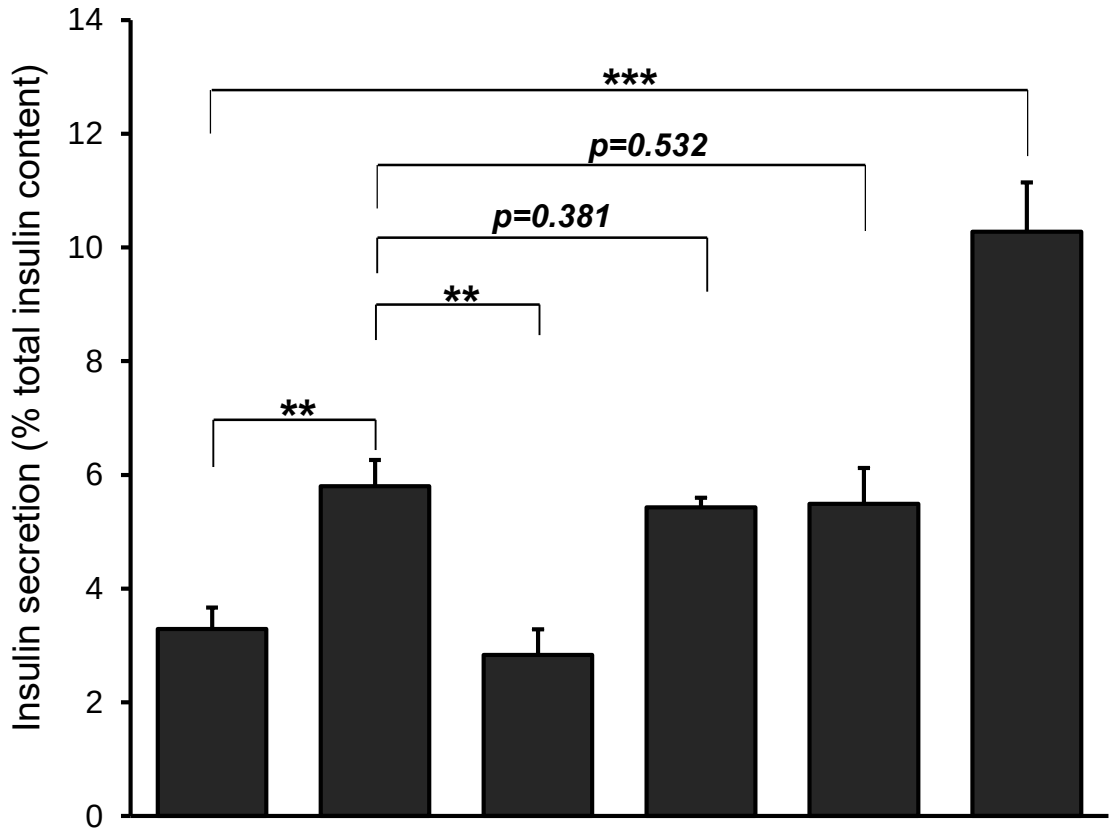

Kainate (25 µM)	-	+	+	+	+	-
NBQX (30 µM)	-	-	+	-	-	-
GYKI (100 µM)	-	-	-	+	-	-
DHPG (50 µM)	-	-	-	-	+	-
KCl (15 mM)	-	-	-	-	-	+
Glucose (3 mM)	+	+	+	+	+	+

Figure 2.28. Activation of KARs potentiates insulin secretion from MIN6 mouse pancreatic β-cells in the presence of 3 mM glucose. Means were compared using Student's *t*-test analysis. Results are presented as means ± SEM from five separate experiments. ******p*<0.05; *******p*<0.01; ********p*<0.001.

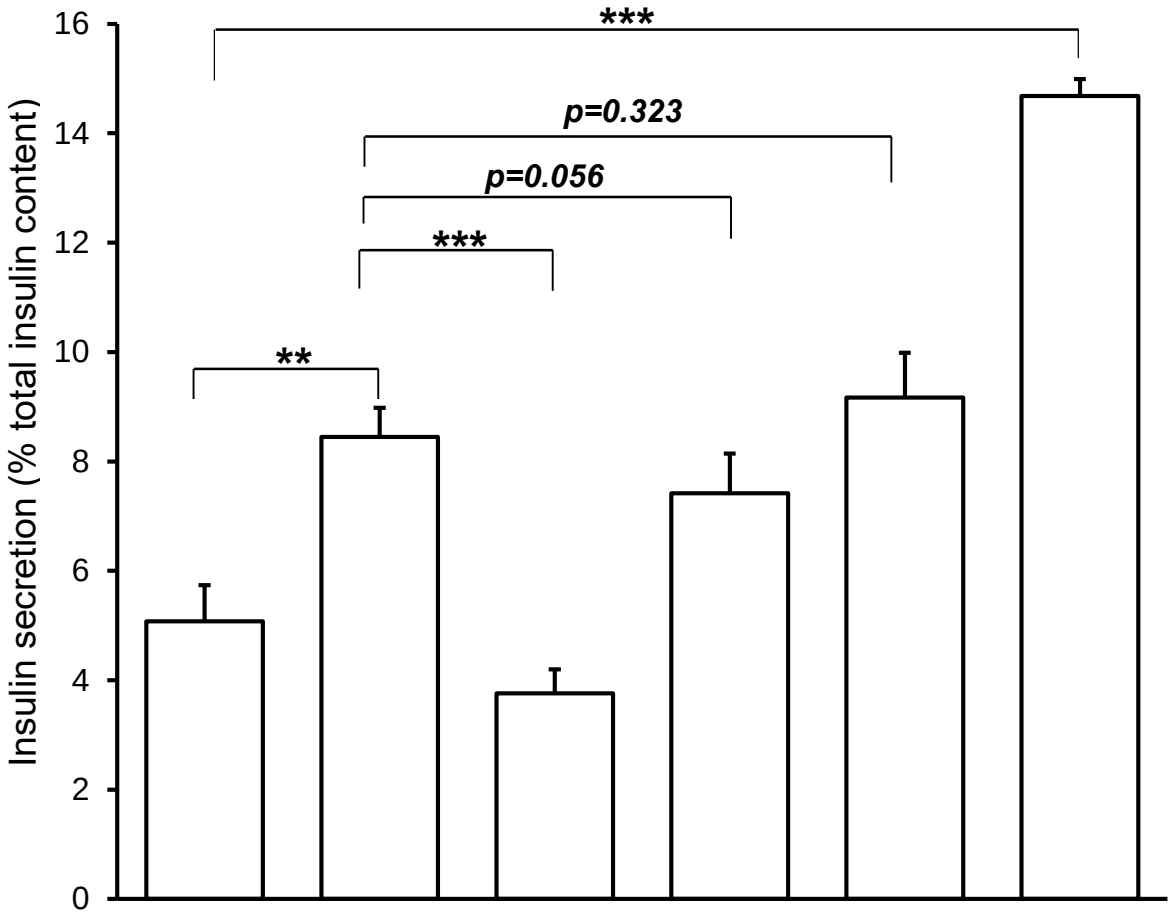

Kainate (25 μM)	-	+	+	+	+	-
NBQX (30 μM)	-	-	+	-	-	-
GYKI (100 μM)	-	-	-	+	-	-
DHPG (50 μM)	-	-	-	-	+	-
KCl (15 mM)	-	-	-	-	-	+
Glucose (30 mM)	+	+	+	+	+	+

Figure 2.29. KAR activation potentiates insulin secretion from MIN6 mouse pancreatic β-cells in the presence of 30 mM glucose. Student's *t*-test was used to compare means. Results are presented as means ± SEM from five separate experiments. ******p*<0.05; *******p*<0.01; ********p*<0.001.

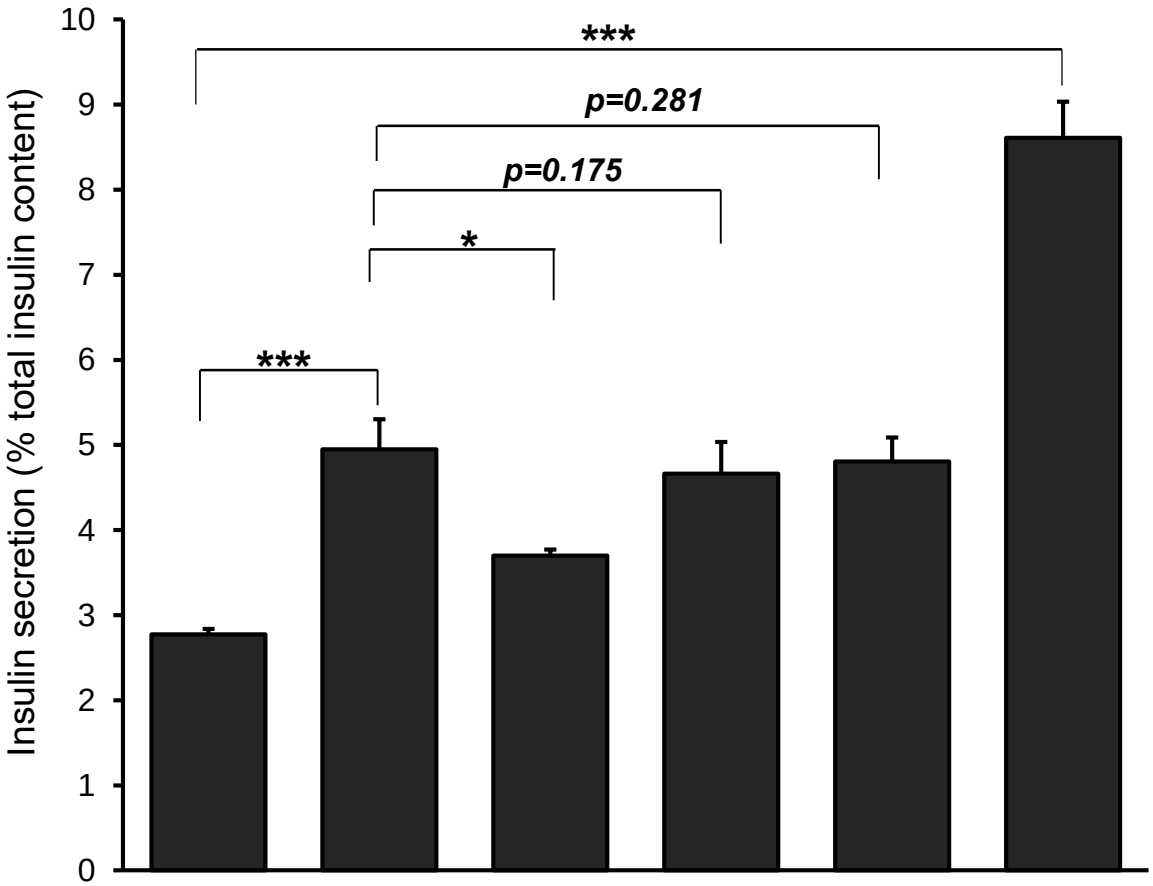

Kainate (25 µM)	-	+	+	+	+	-
NBQX (30 µM)	-	-	+	-	-	-
GYKI (100 µM)	-	-	-	+	-	-
DHPG (50 µM)	-	-	-	-	+	-
KCl (15 mM)	-	-	-	-	-	+
Glucose (3 mM)	+	+	+	+	+	+

Figure 2.30. Activation of KARs potentiates insulin secretion from INS-1 rat pancreatic β-cells in the presence of 3 mM glucose. Means were compared using Student's *t*-test analysis. Results are presented as means ± SEM from five separate experiments. ***p*<0.05; ****p*<0.01; *****p*<0.001.**

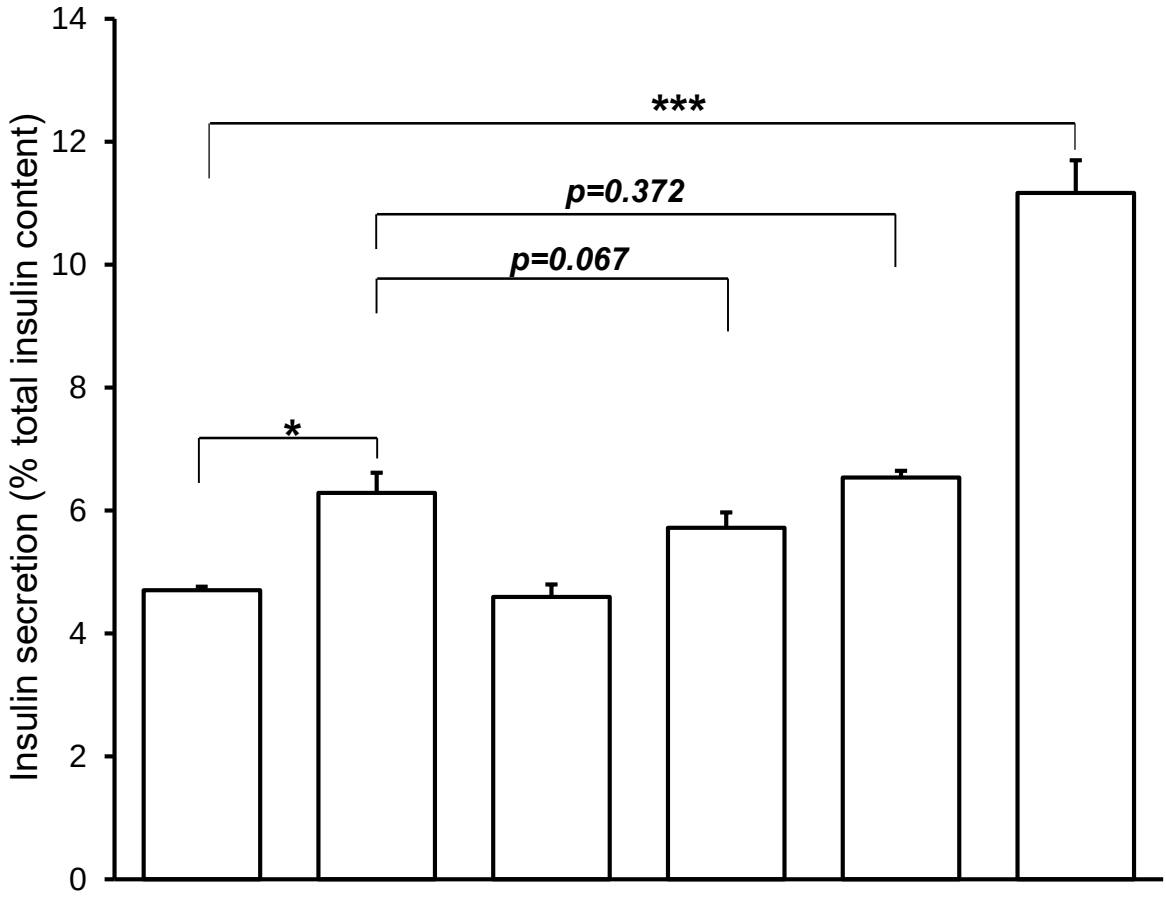

Kainate (25 μM)	-	+	+	+	+	-
NBQX (30 μM)	-	-	+	-	-	-
GYKI (100 μM)	-	-	-	+	-	-
DHPG (50 μM)	-	-	-	-	+	-
KCl (15 mM)	-	-	-	-	-	+
Glucose (30 mM)	+	+	+	+	+	+

Figure 2.31. Activation of KARs potentiates insulin secretion from INS-1 rat pancreatic β-cells in the presence of 30 mM glucose. Means were compared using Student's *t*-test analysis. Results are presented as means ± SEM from five separate experiments. ***p*<0.05; ****p*<0.01; *****p*<0.001.**

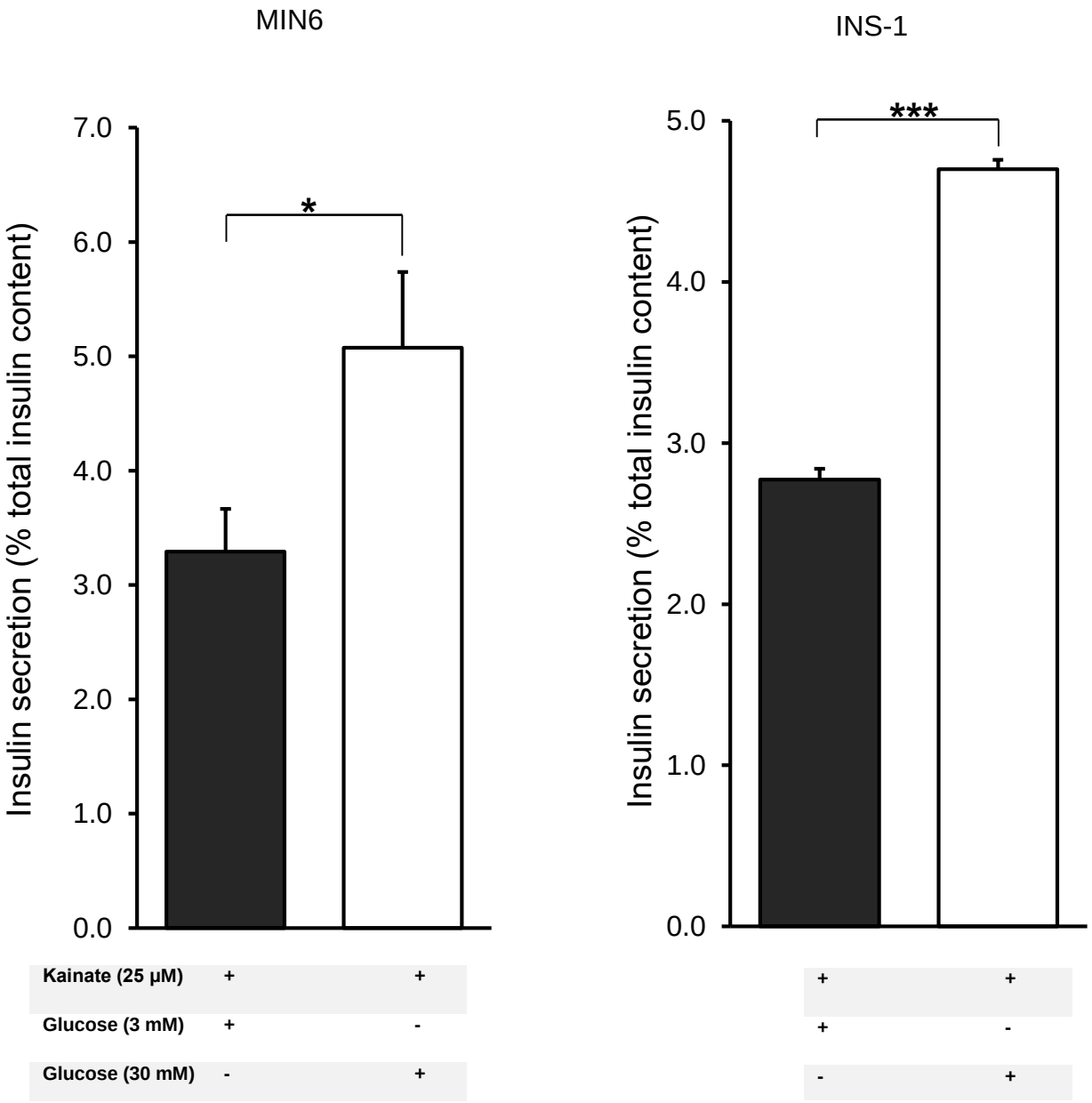

Figure 2.32. Kainate-induced insulin secretion from MIN6 and INS-1 β-cells is dependent on glucose concentration. Means were compared using Student's *t*-test analysis. Results are presented as means ± SEM from five separate experiments. ***p*<0.05; ****p*<0.01; *****p*<0.001.

2.4.5. Effect of prolonged exposure to glutamate and kainate on the viability of pancreatic α-cells and β-cells.

Extensive research has shown that cells of the CNS are vulnerable to chronic activation of iGluR subtypes. Prolonged exposure to kainate and glutamate has been shown to cause excitotoxicity in primary neurons, oligodendrocytes, astrocytes as well as in mice (Dong *et* al., 2012; Domin *et* al., 2010).

Since KAR subunit mRNA and protein have been shown to be present in pancreatic endocrine cells (section 2.4.1), the effect of prolonged exposure of β-cells and α-cells to glutamate and kainate was investigated.

2.4.5a. *Prolonged exposure to glutamate and kainate results in significant reduction in viability of cultured pancreatic α-cells and β-cells.*

Change in cell viability subsequent to chronic exposure of cells to kainate and glutamate was investigated using the MTT assay. This assay has been used extensively to study the viability of cultured cells in several areas of research including endocrinology and neuroscience (Di Cairano *et al*., 2011; Zhu *et al*., 2016). Cultured INS-1 β-cells and α-TC cells were incubated with different concentrations of kainate and glutamate for 72 hours (section 2.3.12). As control INS-1, α-TC and SH-SY5Y cells were cultured under the same conditions in the absence of glutamate or kainate. Viability of the cells after treatment was determined by MTT assay (section 2.3.12).

Similar to other neuronal cells, viability of SH-SY5Y cells have been shown to reduce significantly subsequent to prolonged exposure to kainate and glutamate (Zhu *et al*., 2016; Cannarsa *et al*., 2008) hence this cell line was used as a positive control for kainate- and glutamate-induced changes in cell viability.

Chronic exposure of α-TC and INS-1 cells to 0.25-12.0 mM glutamate or 0.1-0.5 mM kainate resulted in significantly reduced cell viability relative to controls (Figure 2.33). As expected, there was significant reduction in viability of SH-SY5Y cells after exposure to glutamate or kainate (Figure 2.33). Glutamate- and kainate-induced reduction in viability of INS-1 cells was dose-dependent (Figure 2.34).

Moreover, as expected, viability of INS-1, α-TC and SH-SY5Y cells after incubation with 40% ethanol or 2% triton X-100 was reduced to less than 2% of control (Figure 2.34). These observations suggest that similar to cells of the central nervous system, both α-cells and β-cells of the pancreas are vulnerable to prolonged exposure to glutamate and kainate and show significant reduction in viability.

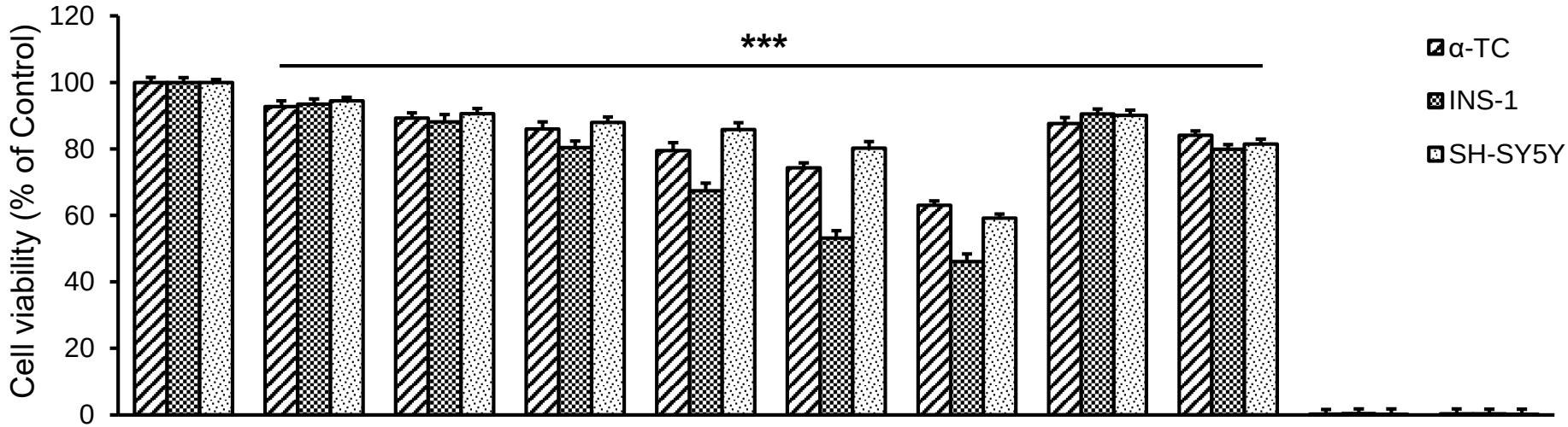

Glutamate (0.25 mM)	-	+	-	-	-	-	-	-	-	-	-
Glutamate (0.5 mM)	-	-	+	-	-	-	-	-	-	-	-
Glutamate (1.0 mM)	-	-	-	+	-	-	-	-	-	-	-
Glutamate (2.5 mM)	-	-	-	-	+	-	-	-	-	-	-
Glutamate (5.0 mM)	-	-	-	-	-	+	-	-	-	-	-
Glutamate (12.0 mM)	-	-	-	-	-	-	+	-	-	-	-
Kainate (0.1 mM)	-	-	-	-	-	-	-	+	-	-	-
Kainate (0.5 mM)	-	-	-	-	-	-	-	-	+	-	-
40% Ethanol	-	-	-	-	-	-	-	-	-	+	-
2% Triton X	-	-	-	-	-	-	-	-	-	-	+

Figure 2.33. Prolonged exposure to glutamate and kainate results in reduced viability of pancreatic α-cells and β-cells. INS-1 β-cells and α-TC cells were cultured in the presence of varying concentrations of glutamate and kainate and then cell viability was measured using MTT assay. Viability was determined by expressing the optical density of treated cells as percentage of controls. Means were compared using Student's *t*-test analysis. Results are presented as means ± SEM from four separate experiments each performed in triplicate. ***p*<0.05; ****p*<0.01; *****p*<0.001.**

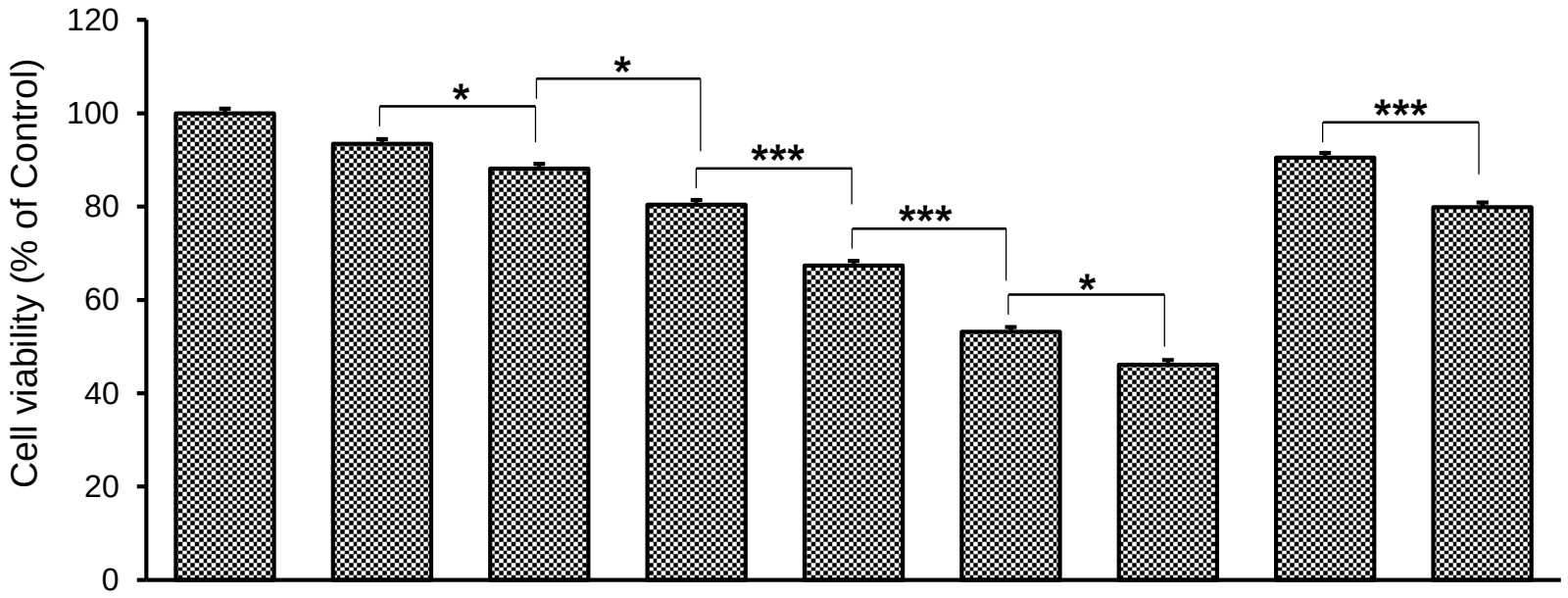

Glutamate (0.25 mM)	-	+	-	-	-	-	-	-	-
Glutamate (0.5 mM)	-	-	+	-	-	-	-	-	-
Glutamate (1.0 mM)	-	-	-	+	-	-	-	-	-
Glutamate (2.5 mM)	-	-	-	-	+	-	-	-	-
Glutamate (5.0 mM)	-	-	-	-	-	+	-	-	-
Glutamate (12.0 mM)	-	-	-	-	-	-	+	-	-
Kainate (0.1 mM)	-	-	-	-	-	-	-	+	-
Kainate (0.5 mM)	-	-	-	-	-	-	-	-	+

Figure 2.34. Reduction in cell viability of INS-1 β-cells after exposure to glutamate and kainate is concentration-dependent. INS-1 β-cells was cultured in the presence of varying concentrations of glutamate and kainate and then cell viability was measured using MTT assay. Viability was determined by expressing the optical density of treated cells as percentage of controls. Means were compared using Student's *t*-test analysis. Results are presented as means ± SEM from four separate experiments each performed in triplicate. ***p*<0.05; ****p*<0.01; *****p*<0.001.**

2.4.5b. *KAR antagonists reduces the effect of kainate on the viability of pancreatic α-cells and β-cells*

To determine whether kainate-induced reduction in cell viability involves KAR activation, INS-1 β-cells and α-TC cells were exposed to kainate after pre-incubation of the cells with NBQX (selective and competitive AMPA and kainate receptor antagonist). Viability of the cells was then measured (section 2.3.12).

Prolonged exposure to 0.1 or 0.5 mM kainate significantly reduced the viability of α-TC cells and INS-1 β-cells. INS-1 and α-TC cells exposed to kainate alone showed significantly reduced viability compared to cells which were pre-incubated with 0.025 mM or 0.1 mM NBQX prior to kainate (Figure 2.35).

As expected, there was significant reduction in cell viability of SH-SY5Y neuronal cells after chronic exposure to 0.1-0.5 mM kainate and this effect was blocked by NBQX (Figure 2.35).

These observations suggest that the reduced cell viability is linked to prolonged KAR activation.

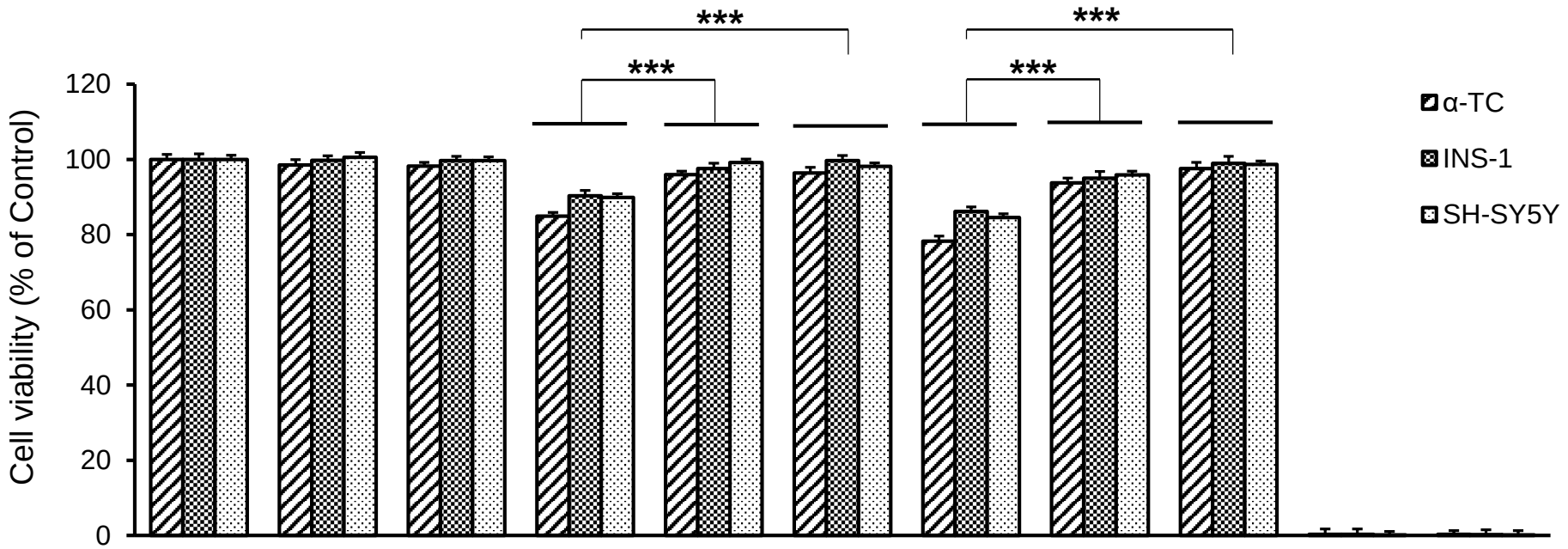

NBQX (0.025 mM)	-	+	-	-	+	-	-	+	-	-	-
NBQX (0.1 mM)	-	-	+	-	-	+	-	-	+	-	-
Kainate (0.1 mM)	-	-	-	+	+	+	-	-	-	-	-
Kainate (0.5 mM)	-	-	-	-	-	-	+	+	+	-	-
40% Ethanol	-	-	-	-	-	-	-	-	-	+	-
2% Triton X	-	-	-	-	-	-	-	-	-	-	+

Figure 2.35 NBQX improves survival of pancreatic α-cells and β-cells following prolonged exposure to kainate. Cultured INS-1 β-cells and α-TC cells were pre-incubated with NBQX (0.025 and 0.1 mM) followed by chronic exposure to kainate (0.1 and 0.5 mM). Means were compared using Student's *t*-test analysis. Results are presented as means ± SEM from four separate experiments each performed in triplicate. ***p*<0.05; ****p*<0.01; *****p*<0.001.**

2.4.5c. *Dihydrokainic acid (DHK) enhances the effect of glutamate on pancreatic α-cell and β-cell viability.*

Studies have shown that the concentration of extracellular glutamate is kept at physiological levels by high affinity glutamate transporters including the glial glutamate transporter 1 (GLT 1) (Di Cairano *et al*., 2011). Dihydrokainic acid (DHK) is a potent selective inhibitor of GLT 1. Inhibition of GLT1 by DHK prevents the uptake of glutamate by cells (Di Cairano *et al*., 2011).

To investigate if inhibition of glutamate transporters affects pancreatic cell viability, cultured MIN6, INS-1, α-TC cells were pre-incubated with DHK (0.1 mM) followed by prolonged exposure to glutamate (0.5 mM). Viability of the cells was determined and compared to viability of cells which have been exposed to glutamate only (section 2.3.12). There was no significant change in viability of MIN6 β-cells after chronic exposure to 0.5 mM glutamate. In contrast, INS-1 and α-TC cells showed reduced viability subsequent to incubation with glutamate (Figures 2.36-2.37). Exposure of MIN6, INS-1 and α-TC cells to glutamate in the presence of DHK resulted in significantly reduced cell viability compared to cells which were exposed to glutamate only (Figures 2.36-2.37).

As expected, exposure of SH-SY5Y cells to glutamate after pre-incubation with DHK resulted in significant reduction in viability compared to cells exposed to glutamate without prior incubation with DHK (Figure 2.37).

These observations suggest an important role of GLT 1 in the regulation of the extracellular concentration of glutamate and viability in pancreatic endocrine cells.

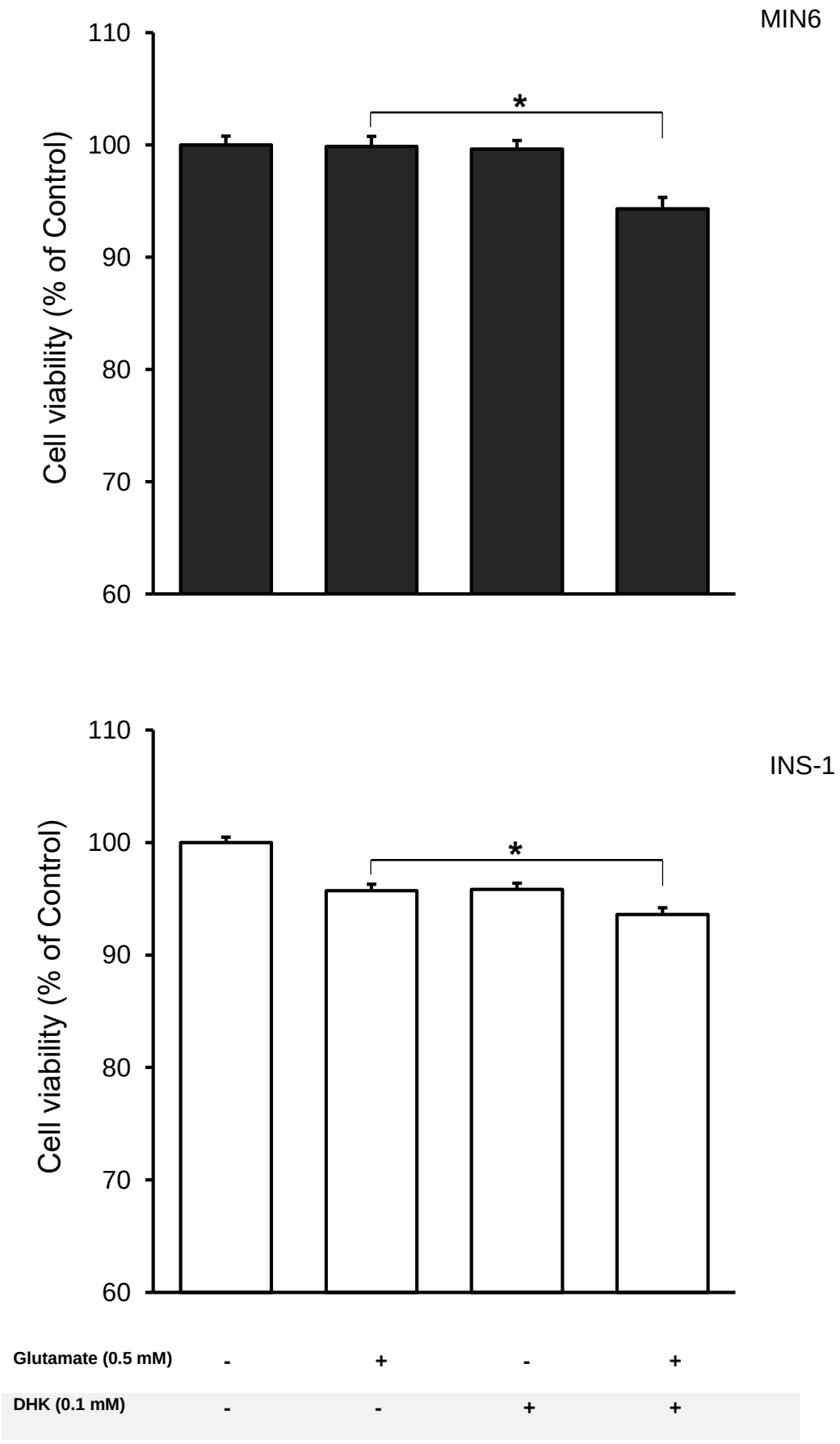

Figure 2.36. Dihydrokainic acid (DHK) enhances the effect of glutamate exposure on the viability of pancreatic β-cells. Means were compared using Student's *t*-test analysis. Results are presented as means ± SEM from four separate experiments each performed in triplicate. ***p<0.05; **p<0.01; ***p<0.001.**

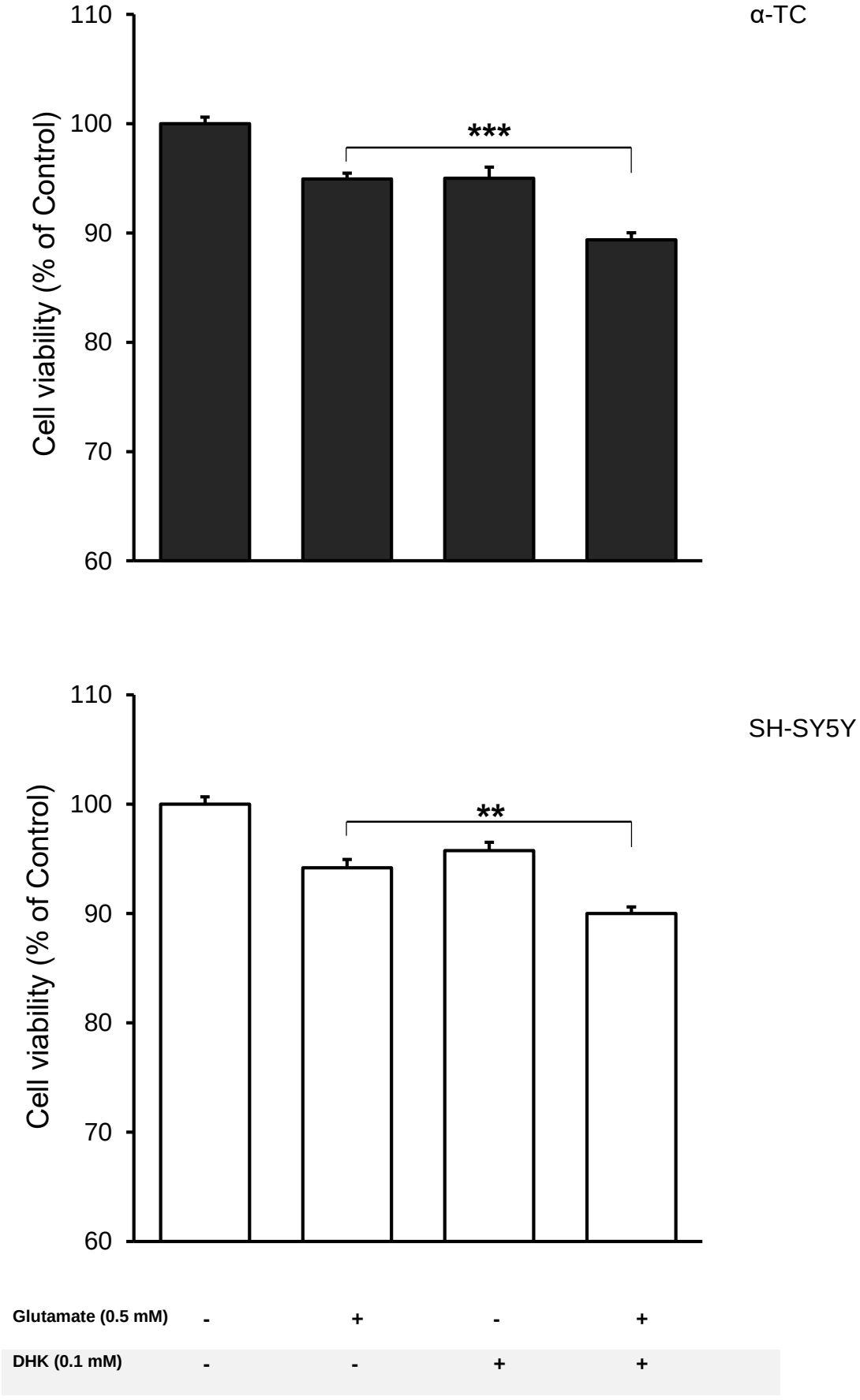

Figure 2.37. Dihydrokainic acid (DHK) enhances the effect of glutamate exposure on the viability of pancreatic α-cells and neuronal cells. Means were compared using Student's *t*-test analysis. Results are presented as means ± SEM from four separate experiments each performed in triplicate. ***p*<0.05; ****p*<0.01; *****p*<0.001.**

2.5. Summary of results

The aim of this chapter was to investigate the molecular composition and function of KAR subunits in pancreatic endocrine cells. The following is a summary of the results:

- GluK2-5 subunit mRNAs are expressed in both α- and β-cells of the pancreas whiles GluK1-5 are expressed in pancreatic islets of Langerhans.
- GluK2/3 and GluK5 subunit proteins are present in both α- and β-cells of the pancreas. There is no statistical differences in expression of GluK2/3 and GluK5 in α- and β-cells.
- Auxiliary Neto 1 and Neto 2 mRNAs and proteins are present in α- and β-cells and islets of Langerhans of the pancreas. There is preferential expression of Neto 1 in α-cells and Neto 2 in β-cells
- KAR stimulation with kainate increased both $[Ca^{2+}]_i$ and GSIS secretion in pancreatic β-cells. These effects were attenuated by KAR antagonist (NBQX) but not AMPAR/NMDAR antagonist (Gyki-52466).
- Group I mGluR agonist (DHPG) potentiated the effect of KAR stimulation on $[Ca^{2+}]_i$ but had no significant effect on kainate-induced increase in GSIS from β-cells.
- Prolonged exposure to kainate or glutamate significantly reduced the viability of both α- and β-cells. The effect of kainate on viability of α- and β-cells was significantly reduced by KAR antagonist (NBQX).
- DHK, an inhibitor of glutamate transporter 1 potentiated the effect of glutamate on the viability of both α- and β-cells.

2.6. Discussion

Relatively little is known about the molecular composition and function of KARs in the CNS compared to other GluRs. The emergence of pharmacological tools, antibodies and transgenic animals created exciting opportunities for the investigation of KARs. However, even less is known about native KARs and their interacting partners outside the CNS. Up to now, relatively few studies have reported the expression of KARs in pancreatic endocrine cells (Molnar *et al*., 1995; Gonoi *et al*., 1994; Kutlu *et al*., 2009; Inagaki *et al*., 1995). The only KAR subunit protein which has been identified in pancreatic endocrine cells in previous studies is GluK5 (Molnar *et al*., 1995). Considering that GluK5 can only function when expressed in heteromeric combinations with GluK1-3 subunits (Crepel and Mulle, 2015), it was important to investigate systematically the molecular composition and role of KARs in pancreatic endocrine cells.

2.6.1. *Functional KAR subunits are present in pancreatic endocrine cells*

In this study, mRNA and protein of all five KAR subunits was investigated in MIN6 mouse β-cells, INS-1 rat β-cells, α-TC mouse cells and primary rat islets of Langerhans. Investigations using both mouse and rat tissues were to ensure that the presence of these KAR subunits in pancreatic endocrine cells was consistent in different species. Identification and characterisation of all the KAR subunits in pancreatic endocrine cells could lead to further investigations into the potential role, function and effect of these receptors in the endocrine pancreas.

2.6.1a. *mRNAs and proteins of functional KARs are present in pancreatic β-cells*

In this study, four KAR subunit transcripts (GluK2, GluK3, GluK4 and GluK5) were identified in mouse MIN6 and rat INS-1 β-cells (Figures 2.4 and 2.5). Only mRNA of GluK5 has previously been identified in MIN6 β-cells using reverse-transcriptase PCR (Gonoi *et al*., 1994). Other studies have shown that KAR agonists have significant effect on insulin secretion, membrane potential and influx of calcium in MIN6 and other β-cell lines (Molnar *et al*, 1995; Inagaki *et al*, 1994; Gonoi *et al*., 1994). These observations indicate that functional KARs could be present in β-cells but the specific subunit composition of KARs in β-cells remains unknown. Thus, identification of GluK2-5 subunit mRNA in MIN6 β-cells in this current study indicates that functional homomeric and heteromeric KAR channels could assemble in β-cells. The current study is the first to identify these four KAR subunit mRNAs in INS-1 β-cells using the RT-PCR technique. A study using microarray and MPSS analysis identified GluK2 in MIN6 β-cells, GluK4 and GluK5 in INS-1 β-cells (Kutlu *et al*., 2009).

Results from this current study support previous studies and provide further information to suggest that mRNA of heteromeric and homomeric KAR channels are expressed in β-cells of both mouse and rat.

At protein level, GluK2/3 and GluK5 were identified in MIN6 and INS-1 β-cells using immunoblotting (Figure 2.10). Previous studies using immunoblotting identified only GluK5 protein in MIN6 mouse and RINm5F rat β-cell lines (Molnar *et al*., 1995) but GluK5 does not form a functional homomeric channel. Thus this current study supports findings from the previous study (Molnar *et al*., 1995) of the presence of heteromeric GluK5 in β-cells and also provide new evidence for the presence of GluK2/3 in β-cell lines. Identification of these subunit proteins indicates that both low-affinity homomeric

and high affinity obligate heteromeric functional KAR channels could assemble in β-cells of the pancreas.

2.6.1b. *mRNAs and proteins of functional KARs are present in pancreatic α-cells*

In mouse pancreatic α-TC cells, mRNA transcripts of low-affinity homomeric (GluK2, GluK3) and high-affinity obligate heteromeric (GluK4, GluK5) KAR subunits were identified (Figure 2.4). In isolated primary human α-cells, mRNA of GluK2 has been identified (Cabrera *et al*., 2008). Thus, results from this current study indicate that KAR subunits which can form homomeric or heteromeric channels are present in pancreatic *α-cells*. At protein level, GluK2/3 and GluK5 proteins were identified in α-TC cells. This is the first study to identify KAR subunit proteins in α-cells.

It has been shown in previous studies that under low glucose conditions, glutamate is released from α-cells of the pancreas and subsequently bind and activate AMPAR and KAR subunits present on α-cells. This leads to increased release of glucagon from α-cells (Cabrera *et al*., 2008). Thus, identification of functional KAR subunits in α-cells of the pancreas provides evidence to support the role of KARs in modulating glucagon secretion from the α-cells. Studies have also shown that glutamate is co-secreted with glucagon from α-cells or released via glutamate transporters located in α-cells (Cho *et al*, 2010; Feldmann *et al*., 2011). Thus, in addition to enhancing glucagon secretion, KAR subunits in α-cells of the pancreas may modulate glutamate release from α-cells to regulate the concentration of extracellular glutamate in the islets of Langerhans.

2.6.1c. *mRNAs and proteins of functional KARs are present in rat islets of Langerhans*

In rat islets of Langerhans, all five KAR subunit mRNA were detected (Figure 2.5). This is the first study to show that all five KAR subunits of KARs are expressed in rat islets of Langerhans. Previous investigations using reverse-transcriptase PCR identified only GluK5 mRNA in rat pancreatic islets of Langerhans (Inagaki *et al*., 1995).

Identification of GluK1 mRNA in islets of Langerhans but not in β- or α-cells suggests that other cells within the islets of Langerhans (δ-cells, PP cells or ghrelin-producing cells) express mRNA of GluK1.

KAR subunit mRNAs were not found in mouse or rat liver tissue (Figure 2.6). This observation is in agreement with previous studies (Gonoi *et al*., 1994; Chew *et al*., 2001) and shows that in addition to setting up template negative PCR reactions, liver tissue could be used as a reliable template for PCR negative control and also to test primers specific for KAR subunits.

2.6.1d. *KAR subunits show equal or similar expression in β-cells and α-cells of the pancreas*

The relative amounts of KAR subunit mRNA and protein in MIN6 β-cells and α-TC cells was investigated by a semi-quantitative reverse-transcription PCR and semi-quantitative immunoblotting (Section 2.3.8). Semi-quantitative analysis of immunopositive bands has been used in several studies to determine the relative amounts of proteins in cells and tissues (Luyt *et al*., 2007). This method is relatively less cumbersome and is a very feasible option when time is of essence in a study. A number of techniques are available for quantitative analysis of mRNAs in cells. Real-time PCR and competitive PCR give relatively accurate quantification of mRNA expression. However, competitive PCR requires a large volume of starting cDNA as template and also requires an internal

competitor DNA fragment that must contain sequences for which the primers intended for the mRNA of interest can amplify (Marone *et al*., 2001). On the other hand, there are several technical challenges with real-time PCR including normalisation and the use of reference (housekeeping) genes (Bustin and Nolan, 2004). Furthermore, both techniques are costly and time-consuming thus they were not feasible options at the time. Semi-quantitative analysis represents a feasible and relatively simple method for investigating levels of receptor mRNAs and proteins in cells and tissue samples. In the semi-quantitative reverse-transcription method, one of the most significant factors for consideration is the selection of appropriate number of PCR cycles at which the amplification of the transcripts is in a linear phase whiles at the same time, the amplified product can be visualised on agarose gel and quantified. This method has been shown to generate reliable semi-quantitative information when all the appropriate procedures and controls are set up (Marone *et al*., 2001).

In this study, the relative amounts of GluK2 and GluK5 mRNA in MIN6 β-cells were not significantly different from the amount of these KAR subunits in α-TC cells (Figure 2.9). However, the amount of GluK2 mRNA in brain tissue was significantly higher than in MIN6 and α-TC cells indicating a preferential expression of this subunit for the brain relative to α- and β-cells. There was no significant differences between the amount of GluK5 mRNA in brain and the endocrine cells (MIN6 and α-TC cells) (Figure 2.9) which could indicate that KAR subunits may have different expression profiles in the CNS and pancreatic endocrine cells. Furthermore, there was no significant difference in the relative amounts of GluK2/3 and GluK5 proteins between β-cells (MIN6, INS-1) and α-cells (α-TC) of the pancreas which (Figure 2.11) which confirms the mRNA results. The observation that the relative amounts of GluK2/3 and GluK5 proteins in mouse (MIN6) β-cells was not significantly different from rat (INS-1) β-cells (Figure 2.11) suggests that

relative levels of KAR subunit proteins in β-cells could be independent of species. No study has analysed or reported of the relative amounts of mRNA and proteins of KAR subunits in α- and β-cells of the pancreas. The semi-quantitative analyses in this study was carried out using cells that were cultured under their conventional conditions without treatments with any drug, thus the relative amounts of KARs could not be affected by any external agent or condition. The results suggest an equal or similar expression of these KAR subunits in β-cells and α-cells of the pancreas. The results also suggest equal or similar expression of GluK5 in brain and endocrine cells (β-cells and α-cells) whiles the amount GluK2 in the brain is significantly higher than in endocrine cells (β-cells and α-cells).

2.6.2. *Neto 1 and Neto 2 subunits in pancreatic endocrine cells*

The role of Neto 1 and Neto 2 subunits in modulating KAR subunit expression and receptor properties in the CNS is a subject of several studies but there is very little information about these KAR auxiliary subunits outside the CNS (Fisher, 2015; Copits and Swanson, 2012; Griffith and Swanson, 2015; Sheng *et al*., 2015; Rutkowska-Wlodarczyk *et al*., 2015) (Chapter one, Section 1.5.6).

2.6.2a. *mRNAs and proteins of Neto 1 and Neto 2 are present in pancreatic endocrine cells*

In this study, mRNA of Neto 1 and Neto 2 were identified in β-cell (MIN6, INS-1) and α-cell (α-TC) lines and also in rat islets of Langerhans (Figure 2.12). This is the first study to detect both Neto 1 and Neto 2 in α-, β-cells and the islets of Langerhans in two different species. A previous study used massively parallel signature sequencing (MPSS) and microarray for quantitative mRNA expression profiling of Neto 1 and Neto 2 in pancreatic endocrine cells (Kutlu *et al*., 2009). The study reported that transcripts of Neto 1 are present in MIN6 β-cells but not in INS-1 β-cells or α-TC cells (Kutlu *et al*., 2009). The study also reported the expression of Neto 2 transcript in MIN6 β-cells, but in contrast to the current study, Neto 2 was not detected in rat islets of Langerhans (Kutlu *et al*., 2009). This conflicting findings may be due to the different methods used in these two studies as well as the method for the isolation of islets of Langerhans.

Neto 1 and Neto 2 proteins were detected in β-cells (MIN6, INS-1) and α-cells (α-TC) of the pancreas (Figure 2.15). This is the first study to report of the presence of Neto 1 and Neto 2 subunit proteins in pancreatic α- and β-cell lines.

The presence of both mRNA and protein of Neto 1 and Neto 2 in pancreatic endocrine cells suggests that these auxiliary proteins could have modulatory or regulatory effects

on KARs in the endocrine pancreas. In the CNS, Neto 1 and Neto 2 modulates the function and properties of KARs (Sheng *et al*., 2015; Fisher, 2015). Thus, expression of Neto 1 and Neto 2 in α-, β-cells and islets of Langerhans suggests that mechanisms by which Neto 1 and Neto 2 regulate KARs in the CNS may also be present in pancreatic endocrine cells.

2.6.2b. *There are differences in relative amounts of Neto 1 and Neto 2 in β-cells and α-cells of the pancreas.*

Semi-quantitative analysis showed that the amount of Neto 1 mRNA and protein are significantly higher in α-TC cells than in MIN6 β-cells (Figure 2.14). On the other hand, levels of Neto 2 mRNA and protein are significantly higher in MIN6 β-cells than α-TC cells (Figure 2.14). These observations reveal a preferential expression of Neto 1 in α-cells and Neto 2 in β-cells.

Though both Neto 1 and Neto 2 are present, the preferential expression of Neto 1 mRNA and protein in α-cells is suggestive that Neto 1 interacts predominantly with KARs in α-cells to influence characteristics including modulation of slow kinetics of KARs. The modulation of slow kinetics of KARs by Neto 1 has been reported in neurons (Copits *et al*., 2011; Fisher and Mott). Increased levels of Neto 2 mRNA and protein in β-cells indicates that Neto 2-related properties of KARs including agonist binding, membrane surface expression and synaptic co-localisation may be predominant in β-cells. These effects of Neto 2 on KARs have been reported in hippocampal neurons of the CNS (Sheng *et al*., 2015; Copits *et al*., 2011; Wyeth *et al*., 2014).

Moreover, interactions of Neto 1 and Neto 2 with KARs results in enhanced affinity of KARs for glutamate and kainate (Howe, 2015; Tang *et al*., 2011). Thus, the presence Neto 1 and Neto 2 in both α- and β-cells of the pancreas indicates that the KARs in these

cells may likely have an increased affinity for glutamate and kainate. The preferential expression of Neto 1 for α-cells and Neto 2 for β-cells could result in KAR functions and properties being different between α-cells and β-cells of the pancreas. For instance, preferential expression of Neto 2 in β-cells could result in β-cell KARs having a higher affinity for glutamate compared to KARs on α-cells.

In conclusion, mRNAs and proteins of KAR subunits are present in α- and β-cells and islets of Langerhans. This indicates that functional low-affinity homomeric and high-affinity heteromeric functional KARs could assemble in these pancreatic endocrine cells. There was no significant difference in KAR subunit mRNA or protein between β- and α-cells of the pancreas. In addition, Neto 1 and Neto 2 auxiliary subunits of KARs are present in α- and β-cells and islets of Langerhans. While Neto 1 shows relatively higher expression in α-cells, Neto 2 expression is higher in β-cells.

These results suggest that properties of KARs in pancreatic endocrine cells could be modulated by Neto 1 and Neto 2 to control release of intracellular glutamate as well as binding to and controlling the concentration of extracellular glutamate. The preferential expression of Neto 1 and Neto 2 in α- and β-cells could also result in KAR functions and properties being different between these cells.

2.6.3. *Effect of KAR activation on intracellular calcium concentrations in pancreatic β-cells* $[Ca^{2+}]_{i.}$

It has been established in this study that functional units of KARs together with their auxiliary proteins are present in pancreatic α-, β-cells and islets of Langerhans (Sections

2.4.1 and 2.4.2). To understand the functions of KAR subunits in β-cells, it was important to study the effect of KAR agonists on changes in intracellular calcium concentration $[Ca^{2+}]_i$ in MIN6 β-cells.

A number of studies have shown that several calcium channels are present in rat, mouse and human β-cells, with the most common being the L- and P/Q types (Rorsman and Braun, 2013; Pratt *et al*., 2016; Xie *et al*., 2016). Though the concentration of cytosolic calcium ions ($[Ca^{2+}]_c$) has been shown to contribute to insulin secretion from pancreatic β-cells (Marquard *et al*., 2015), majority of studies have established that exocytosis of insulin granules and other molecules from β-cells of the pancreas is primarily dependent on $[Ca^{2+}]_i$ (Rorsman and Braun, 2013; Christensen *et al*, 2015; Thorn *et al*., 2016; Dou *et al*., 2015). Thus, it was important to establish the effect of β-cell KAR activation on the changes in $[Ca^{2+}]_i$.

2.6.3a. *Kainate induces transient increase in $[Ca^{2+}]_i$ in MIN6 pancreatic β-cells.*

In the presence of 3 mM or 30 mM glucose, activation of β-cell KARs with 25 μM kainate induced an increase in $[Ca^{2+}]_i$ which was significantly higher than the basal measurements (Figures 2.17-2.18). This observation is consistent with reports from previous studies albeit different concentrations of kainate were used in the previous studies. In one study, there was a dose-dependent transient increase in $[Ca^{2+}]_i$ in MIN6 β-cells subsequent to perifusion with 0.01-1 mM kainate in the presence of 3.3 mM glucose (Gonoi *et al*., 1994). Another study reported of transient increase in $[Ca^{2+}]_i$ in isolated rat β-cells after application of 0.1 and 0.5 mM kainate in the presence of 8.3 mM glucose (Inagaki *et al*., 1995). However, 0.1-1.0 mM kainate used in these previous studies could potentially activate AMPARs in addition to KARs. Thus, the increase in $[Ca^{2+}]_i$ subsequent to 25 μM kainate in this current study has addressed the questions surrounding which or what

receptors are activated in β-cells by kainate to induce increase in $[Ca^{2+}]_{i.}$ Washing out kainate after the initial application resulted in decrease in $[Ca^{2+}]_i$ to basal levels (Figure 2.17). A second application of kainate to the cells resulted in increased $[Ca^{2+}]_i$ similar to the increase observed after the first exposure. Reduction in $[Ca^{2+}]_i$ after washing out kainate could be the result of reduction in membrane potential as shown in previous studies (Gonoi *et al*., 1994).

Results from this study thus indicate that similar to observations in the CNS, kainate induces a transient increase in $[Ca^{2+}]_i$ in pancreatic β-cells. This may be a significant mechanism underlying potentiation of GSIS from β-cells by glutamate.

Two mechanisms may account for the kainate-induced increase in $[Ca^{2+}]_i$ in β-cells. First, variants of GluK2 and GluK3 subunits in the CNS have been shown to be Ca^{2+}-permeable (Perrais *et al*., 2010; Sakha *et al*., 2016) hence KAR-induced increase in $[Ca^{2+}]_i$ in MIN6 β-cells may be the result of direct permeation of Ca^{2+} through these receptor channels when they are activated.

Second, increase in $[Ca^{2+}]_i$ in MIN6 β-cells could be via activation of voltage-dependent Ca^{2+} channels as a result of the depolarising effect of kainate. The first mechanism could involve the direct opening of the voltage-dependent Ca^{2+} channels (VDCCs) subsequent to kainate-induced depolarisation of the plasma membrane of pancreatic β-cells. The second mechanism could involve kainate-induced inhibition of K_{ATP} channels which will lead to increased Ca^{2+} influx (Otter and Lammert, 2016). One of the key mechanisms that induces inhibition of K_{ATP} channels in pancreatic β-cells involves increase in cyclic GMP (cGMP) levels (Wu *et al*., 2012). Thus, the increase in $[Ca^{2+}]_i$ subsequent to application of kainate in this study could be via a kainate-induced increase in cGMP levels in the cells leading to inhibition of K_{ATP} to induce $[Ca^{2+}]_i$. Studies have shown that application of kainate or glutamate results in a dose-dependent increase in cGMP levels in rat cerebellar

tissue (Briley *et al*., 1979; Oh and McCaslin, 1996) and isolated mouse pancreatic β-cells (Wu *et al*., 2012). Activation of AMPAR, one of the iGluR subtypes have also been shown to increase the concentration of cGMP and subsequent increase in $[Ca^{2+}]_i$ (Wu *et al*., 2012).

The kainate-induced increase in $[Ca^{2+}]_i$ was shown to be significantly higher in the presence of 30 mM glucose compared to 3 mM glucose (Figure 2.18). This is suggestive that the effect of kainate on $[Ca^{2+}]_i$ is dependent in part on the concentration of glucose. Several studies have shown that in pancreatic β-cells and in islets of both rodent and human, glucose metabolism leads to increased concentration of intracellular glutamate (Otter and Lammert, 2016; Maechler and Wollheim, 1999). In another study, glutamate was the only amino acid out of twelve to increase upon glucose stimulation (Maechler and Wollheim, 1999). Thus, cells exposed to high concentration (30 mM) of glucose will have a higher concentration of intracellular glutamate compared to cells exposed to low glucose (3 mM). Glutamate generated as result of glucose metabolism in β-cells is imported into insulin-containing vesicles via vesicular glutamate transporter (VGLUT)1 and VGLUT3 (Otter and Lammert, 2016; Gheni *et al*., 2014) and then exported out of the secretory granules to the outside of the cell via excitatory amino acid transporter 2 (EAAT2) (Gammelsaeter *et al*., 2011). Transport of glutamate to the outside of the cells could lead to increased extracellular concentration of glutamate which could make more glutamate available to bind GluRs including KARs on β-cells to initiate depolarisation and eventual influx of calcium.

2.6.3b. *Kainate-induced increase in $[Ca^{2+}]_i$ is attenuated by NBQX but not Gyki-52466*

In previous studies, 100 µM of kainate activated both kainate and AMPA receptors in neurons while lower concentrations (10-30 µM) preferentially activated KARs (Muller *et* al., 2003; Lee *et* al., 2004; Palacios-Filardo and Lerma, 2014). Though 25 µM of kainate

was used in this current study, it was important to block AMPARs to establish that the increase in $[Ca^{2+}]_i$ was induced by activation of KARs. Gyki-52466 is a selective non-competitive antagonist of AMPA (IC_{50}: 10-20 µM), kainate (IC_{50}: 450 µM) and NMDA (IC_{50}: 50 µM) receptors (Rogawski *et al*., 2013; Donevan and Rogawski, 1993). The IC_{50} value represents the concentration of an inhibitor where the response (or binding) to an agonist is reduced by half (Matute, 2011; Donevan and Rogawski, 1993). Thus, based on these $IC_{50,}$ 100 µM of Gyki-52466 will inhibit AMPA and NMDA receptors but not KARs. In the presence of 3 mM or 30 mM glucose, pre-incubation of the cells with 100 µM Gyki-52466 did not affect the kainate-induced increase in $[Ca^{2+}]_i$ (Figures 2.19-2.20). This observation indicates that in this current study, kainate bound to β-cell KARs but not AMPAR/NMDAR to elicit a transient increase in $[Ca^{2+}]_i$.

Furthermore, incubation of the cells with 30 µM NBQX prior to application of kainate resulted in significantly reduced influx of Ca^{2+} (Figures 2.21-2.22). Studies have shown that 10-100 µM NBQX inhibits both native and recombinant kainate and AMPA receptors in clonal cell lines, isolated neurons, brain slices and rodents (Matute, 2011; Jane *et al*., 2009; Dohare *et al*., 2016; Park *et al*., 2015). This study is the first to report of β-cell KAR inhibition by NBQX. The results indicate that inhibition of β-cell KARs results in reduction or attenuation of mechanisms which trigger kainate-induced increase in $[Ca^{2+}]_i$.

2.6.3c. *Kainate-induced change in $[Ca^{2+}]_i$ is potentiated by the selective group I mGlu receptor agonist DHPG.*

In the presence of 3 mM or 30 mM glucose, incubation of MIN6 β-cells with DHPG prior to application of kainate induced an increase in $[Ca^{2+}]_i$ which was significantly higher than the increase observed when only kainate was applied (Figures 2.23-2.24). This is the first study to report of KAR potentiation by group I mGluR activation in pancreatic β-

cells. Isoforms of mGluRs including group I mGluRs (mGluR1 and mGluR5) have been shown to be present in MIN6 and other β-cell lines as well as in isolated β-cells and islets of rodent and human (Brice *et al*., 2002; Storto *et al*., 2006) (Chapter one, tables 1.6-1.8). Potentiation of kainate-induced increase in $[Ca^{2+}]_i$ in MIN6 β-cells by DHPG is in agreement with a previous study (Cho *et al*., 2003; Rojas *et al*., 2013). In these studies, co-application of amino-3-(3-hydroxy-5-tert-butylisoxazol-4-yl) propanoic acid (ATPA); a KAR agonist and DHPG resulted in significant increase in $[Ca^{2+}]_i$. This increase in $[Ca^{2+}]_i$ was significantly higher than the increase induced by ATPA alone. Furthermore, co-localisation of KAR subunits (GluK4 and GluK5) with group I mGluR has been reported in rat hippocampus and in cultured rat cortex (Rojas *et al*., 2013). In the study, activation of group I mGluRs with 50 μM DHPG enhanced KAR-induced calcium signals. The potentiation of KARs by group I mGluRs was observed only in heteromeric GluK2/GluK5 or GluK2/GluK4 subunit assembly but not in homomeric receptor combinations (Rojas *et al*, 2013).

The potentiation of β-cell KARs group 1 mGluRs may be via a number of mechanisms. The first mechanism could be via an mGluR-mediated increase in protein kinase C (PKC). Previous studies have shown that mGluR-mediated enhancement of KAR signalling in neurons is attenuated by the inhibition of PKC (Cho *et al*., 2003; Rojas *et al*., 2013) while modulation of KAR signalling by PKC has also been reported in previous studies (Cho *et al*., 2003; Melyan *et al*., 2002). PKC has been shown to induce phosphorylation of key residues in the C-terminal domain of KARs which leads to enhanced response of KAR subunits to agonists including glutamate and kainate (Cho *et al*., 2003; Rojas *et al*., 2013). In conclusion, kainate binds to and activate β-cell KARs to cause transient increase in $[Ca^{2+}]_i$ which was significantly higher in the presence of stimulatory glucose concentrations compared to non-stimulatory concentrations. The transient increase in

$[Ca^{2+}]_i$ could be due to direct permeation of Ca^{2+} through calcium-permeable KAR channels or through activation of voltage-dependent calcium channels. The transient increase in $[Ca^{2+}]_i$ is attenuated by NBQX but not Gyki-52466 thus one of the effect of kainate on $[Ca^{2+}]_i$ is through activation of KARs. Furthermore, activation of group I mGluRs potentiated the kainate-induced transient increase in $[Ca^{2+}]_i$.

These observations indicate that similar to mechanisms in cells of the CNS, kainate binds to β-cell KARs with resultant increase in $[Ca^{2+}]_i$. Exocytosis of insulin granules from β-cells is primarily dependent on the intracellular calcium concentration ($[Ca^{2+}]_i$) (Pedersen *et al*., 2011; Hou *et al*., 2009). Thus, the observations that activation of β-cell KARs results in increased $[Ca^{2+}]_i$ indicate that these receptors play significant roles in modulating one of the most important processes and mechanisms of the pancreatic β-cell; calcium influx.

2.6.4. *Kainate potentiates glucose-stimulated insulin secretion in MIN6 and INS-1 pancreatic β-cells*

The effect of kainate on insulin secretion from β-cells was investigated in MIN6 mouse and INS-1 rat clonal β-cells. In both MIN6 and INS-1 β-cells, kainate enhanced glucose-stimulated insulin secretion in the presence of 3 mM or 30 mM glucose. Insulin secretion induced by kainate in the presence of 3 mM or 30 mM glucose was significantly higher than insulin secretion induced by glucose only (Figures 2.28-2.31). Previous studies have investigated GSIS in MIN6 and INS-1 β-cells in the presence of glucose concentrations

ranging from 3 mM to 28 mM (Reinhardt *et al*., 2016; Suzuki *et al*., 2015; Nakatsu *et al*., 2015) and both MIN6 and INS-1 β-cells are cultured in high glucose medium (25 Mm for MIN6 and 11.1 for INS-1) (Suzuki *et al*., 2015; Reinhardt *et al*., 2016). Thus, the concentrations of glucose used in investigation of how kainate modulate GSIS in this current study is within the range used by previous studies and also fall into the physiological glucose concentrations in which these cells are cultured. The kainate-induced increase in GSIS is consistent with a previous study (Gonoi *et al*., 1994). However, in this previous study (Gonoi *et al*., 1994), 0.5 mM of kainate was used to stimulate GSIS. The use of 0.5 mM kainate to induce GSIS has a limitation because kainate concentrations of 0.1 mM and above have been shown to activate both kainate and AMPA receptors in neurons (Muller *et* al., 2003; Lee *et* al., 2004). The use of 0.025 mM in this current study is consistent with previous studies where 0.01-0.05 mM kainate has been shown to preferentially activate KARs and not AMPAR (Lee *et* al., 2004; Palacios-Filardo and Lerma, 2014). Furthermore, kainate (0.01-1 mM) has been shown to enhance insulin secretion from isolated rat islets of Langerhans in the presence of 8.3 mM glucose in one study (Inagaki *et al*., 1995). 0.5 mM kainate did not stimulate insulin secretion from isolated rat islets of Langerhans in the presence of 3.3-16.7 mM glucose in another study (Molnar *et al*., 1995). Thus, in addition to using concentrations of kainate which could potentially activate AMPARS, previous studies have produced conflicting results about the effect of kainate on GSIS from pancreatic endocrine cells. Results from the current study has thus addressed the limitations in the previous studies by using kainate concentrations that preferentially activates KARs to study how KARs potentiate insulin secretion. The current study has also highlighted a novel observation of how kainate could enhance GSIS at both stimulatory and non-stimulatory glucose concentrations and thus there is the need to consider the effect of kainate on GSIS when

substances or medications which can potentially activate KARs are being prescribed or used.

It has been established that exocytosis of insulin-containing secretory granules from β-cells is principally dependent on the influx of Ca^{2+} (Rorsman and Braun, 2013; Cantley and Ashcroft, 2015; Otter and Lammert, 2016). As shown in section 2.4.3, kainate increases the $[Ca^{2+}]_i$ in β-cells hence the observed increase in insulin secretion is likely to be the result of increased influx of Ca^{2+}. Increased $[Ca^{2+}]_i$ in β-cells has been shown to increase the docking of insulin-containing secretory granules and also stimulate exocytosis of these granules (Wu *et al*., 2012). This may be one of the mechanisms of kainate-induced increase in insulin secretion from pancreatic β-cells.

In both MIN6 and INS-1 β-cells, there was no increase in insulin secretion when the cells were incubated with NBQX (selective and competitive KAR antagonist) prior to kainate incubation. Incubation of the cells with Gyki-52466 (highly selective, non-competitive antagonist of AMPAR/NMDAR) prior to kainate incubation resulted in increased GSIS which was statistically not different from insulin secretion observed after incubation with kainate alone. These observations indicate that the observed kainate-induced increase in GSIS is as a result of activation of β-cell KARs.

In the presence of 3 mM or 30 mM glucose, incubation of MIN6 or INS-1 β-cells with DHPG prior to kainate incubation resulted in enhanced GSIS which was not statistically different from insulin secretion observed after incubation with kainate alone. DHPG has been shown to cause significant increase in insulin secretion from MIN6 at glucose concentrations of 3-10 mM but not in the presence of higher glucose (25 mM) concentration (Brice *et al*., 2002). As discussed previously (Chapter one, section 1.5.7) and shown in this study (section 2.6.3c), DHPG activates group I mGluRs which subsequently potentiates KAR signalling including increased influx of Ca^{2+}. Thus, the

observation that there is no statistical difference between insulin secretions induced by kainate alone or kainate after pre-incubation with DHPG may be due to the biphasic nature of insulin secretion from β-cells. DHPG potentiates kainate-induced increase in $[Ca^{2+}]_i$ which could only result in increased docking of insulin-containing secretory granules to the plasma membrane but not exocytosis of these granules.

2.6.5. *Effect of prolonged exposure to glutamate and kainate on the viability of pancreatic α-cells and β-cells.*

Change in cell viability after chronic exposure to kainate and glutamate was investigated using the MTT assay. Similar to other neuronal cells, prolonged exposure to kainate (10-50 µM) and glutamate (10-40 mM) significantly reduces viability of SH-SY5Y cells (Zhu *et al*., 2016; Cannarsa *et al*., 2008). Thus, this cell line was used as a positive control for kainate- and glutamate-induced changes in cell viability.

2.6.5a. *Prolonged exposure to glutamate and kainate causes reduced viability of cultured pancreatic α-cells and β-cells.*

Exposure to 0.1-0.5 mM of kainate resulted in significant reduction in viability of both α- (α-TC) and β- (INS-1) cells (Figure 2.33). Kainate is a potent neurotoxin which has been shown to be about thirty times more potent as a neurotoxin than glutamate (Zhang and Zhu, 2011). This is the first study to report of kainate-induced reduction in viability of β- and α-cell of the pancreas. This is also the first study to show that kainate-induced reduction in viability of β-cells is dose-dependent (Figure 2.34). Thus, similar to observations in neuronal cell lines (Cannarsa *et al*., 2008), kainate induced a dose-dependent reduction in viability of INS-1 β-cells.

Exposure of INS-1 β-cells and α-TC cells to glutamate (0.25-12.0 mM) and kainate (0.1-0.5 mM) for 72 hours resulted in significant reduction in viability of the cells (Figure 2.33). The observation that glutamate induces significant reduction in α-TC cells is in contrast to a previous study which reported that incubation of α-TC with 0.1-5 mM glutamate for 120 hours did not cause any significant reduction in α-TC cells (Di Cairano *et al*., 2011). This observed differences regarding the effect of glutamate on viability of α-TC cells may be due to a number of technical factors. First, in the previous study (Di

Cairano *et al*., 2011), 8 x 10^3 cells were seeded compared to 2 x 10^4 cells in this current study. Also, the culture medium for the current study contained 2 mM L-glutamine while the previous study used media containing 0.1 mM glutamic acid supplemented with 0.7 mM L-glutamine. The observed glutamate-induced reduction in viability of cultured β-cells is in agreement with a previous study in which 0.1-5 mM glutamate caused significant reduction in viability of mouse βTC3 (Di Cairano *et al*., 2011). This indicates that glutamate-induced reduction in viability of pancreatic β-cells is not cell line-specific. Glutamate- and kainate-induced reduction in α- and β-cell viability could likely be the result of excitotoxicity. Studies have shown that cells of the endocrine pancreas including α- and β-cells are exposed to 50-100 µM glutamate concentration which can increase to about 500 µM after ingestion of glutamate-rich diet (Hawkins, 2009; Otter and Lammert, 2016; Graham *et al*., 2000). Both neuronal and pancreatic β-cells have been shown to keep extracellular glutamate at physiologically low concentrations to prevent excessive or chronic activation of GluRs (Di Cairano *et al*., 2011; Robinson and Jackson, 2016). One of the most significant mechanisms of excitotoxicity involves increased influx of Ca^{2+}. Calcium overload in cells triggers excitotoxic cascades including ER stress, mitochondrial dysfunction, depletion of ATP, activation of Ca^{2+}-dependent enzymes (including nitric oxide synthase), generation of free radicals, oxidative stress and other mechanisms that lead to apoptosis and autophagy (Mohd Sairazi *et al*., 2015). Moreover, increased Ca^{2+} influx leading to apoptosis and autophagy has been shown to be the underlying mechanism of glutamate-induced β-cell death (Di Cairano *et al*., 2011). Administration of kainate has been shown to increase $[Ca^{2+}]_i$ in β-cells (Figures 2.17-2.18) whiles glutamate has been shown to activate α-cells to induce an increase in $[Ca^{2+}]_i$ (Cabrera *et al*., 2008). Thus, the observed glutamate- and kainate-induced reduction in viability of α- and β-cells may the as a result of increased $[Ca^{2+}]_i$. Moreover, kainate- or

glutamate-induced death or dysfunction of α-cells in the islets of Langerhans could result in increased release of glutamate from the cell into the ECF (Davalli *et al*., 2012). This may increase the amount of glutamate available to bind to KARs on β-cells to cause sustained activation and eventual cell death. Increased concentration of plasma glucagon has been reported in T1DM and T2DM subjects indicating α-cell hypersecretion (Muller *et al*., 1973; Dunning *et al*., 2007). Since glucagon is co-secreted with glutamate (Cho *et al*, 2010; Feldmann *et al*., 2011), it can be inferred that glutamate levels may be high in diabetes. If this happens, the excess glutamate could further contribute to destruction of both α- and β-cells leading to exacerbation of the condition.

Furthermore, excitotoxic-induced death of pancreatic β-cells may be a mechanism to remove 'overexcited' cells whose continuous signalling may result in excessive insulin secretion and eventual hypoglycaemia.

2.6.5b. *KAR antagonists reduces the effect of kainate on the viability of pancreatic α-cells and β-cells*

Pre-incubation of INS-1 β-cells and α-TC cells with NBQX (selective and competitive AMPA and kainate receptor antagonist) prior to chronic exposure to kainate resulted in significantly improved viability of the cells (Figure 2.35). This is the first study to report of protective properties of KAR antagonists in pancreatic endocrine cells. NBQX has been shown to protect neurons and other cells of the CNS from kainate-induced toxicity *in vitro* (Twele *et al*., 2015). *In vivo* studies have also shown that NBQX protects mice from seizure-induced excitotoxic cell death (Schauwecker, 2010; Twele *et al*., 2015). The protective effect of α- and β-cells by NBQX may be via mechanisms including reduction in $[Ca^{2+}]_i$. This is supported by results from this study, which has shown that application of NBQX attenuates the effect of kainate on $[Ca^{2+}]_i$ (Figures 2.21-2.22). Moreover,

another KAR antagonist, CNQX has been shown to attenuate glutamate-induced increase in $[Ca^{2+}]_i$ in βTC3 in previous studies (Di Cairano *et al*., 2011). Attenuation of kainate-induced increase in $[Ca^{2+}]_i$ by CNQX has also been reported in isolated human islets of Langerhans (Cabrera *et al*., 2008). Thus, reduction in $[Ca^{2+}]_i$ may be the primary mechanism by which KAR antagonists protect α- and β-cells from kainate-induced cell death. Protection of β-cells and α-cells from kainate-induced excitotoxicity by KAR antagonists may explain why anti-epileptic drugs such as topiramate which attenuates glutamate-induced excitotoxicity also have antidiabetic properties and preserve β-cell survival and function (Davalli *et al*., 2012; Toplak *et al*., 2007; Angehagen *et al*., 2003).

2.6.5c. *Dihydrokainic acid (DHK) enhances the effect of chronic exposure of glutamate on pancreatic α-cell and β-cell viability.*

Exposure of mouse MIN6 β-cells to glutamate did not cause significant reduction in cell viability (Figure 2.36). This is in agreement with a previous study which showed that chronic exposure to glutamate had no significant effect on the viability of MIN6 β-cells (Morley *et al*., 2000). In another study, it was observed that glutamate cause significant reduction in viability of mouse βTC3 β-cells (Di Cairano *et al*., 2011). The reasons for discrepancy between the effect of glutamate on these two mouse β-cell lines remains unclear and needs further investigations but it could be due to differences in mechanisms by which these cells regulate glutamate concentrations or could also be due to presence or absence of certain proteins or channels in these cells. Application of glutamate in the presence of DHK; a selective inhibitor of glial glutamate transporter-1 (GLT 1) resulted in significantly reduced cell viability compared to application of glutamate alone. This was observed in MIN6 and INS-1 β-cells and α-TC cells (Figures 2.36-2.37). This is the first study to show that DHK potentiates glutamate-induced reduction in viability of

pancreatic α-cells. Potentiation of glutamate-induced β-cell death agrees with reports from a previous study which observed that DHK increased extracellular concentration of glutamate and potentiated glutamate-induced cell death in mouse βTC3 and human β-cells (Di Cairano *et al*., 2011).

Extracellular concentration of glutamate in the CNS is kept at physiological levels by glutamate transporters located on plasma membrane of neuronal and astroglial cells (Omote *et al*., 2016; Raiteri and Raiteri, 2015). In the endocrine pancreas, studies have shown that variants of the glial glutamate transporter-1 (GLT 1) are expressed on plasma membrane of INS-1 and β-TC3 β-cell lines as well as in isolated mouse and human α- and β-cells (Di Cairano *et al*., 2011; Meabon *et al*., 2012). Thus, it can be inferred that application of DHK inhibited GLT 1 on the plasma membrane which resulted in inability of the cells to undertake clearance of extracellular glutamate. This subsequently led to increased glutamate concentration and chronic activation of the KARs resulting in excitotoxicity.

2.7. Conclusion

The primary aim of this part of the study was to establish the molecular characterisation of KAR subunits and their auxiliary proteins in pancreatic endocrine cells. The study also aimed to establish the effect of these KAR subunits on the function and viability of pancreatic α- and β-cells. RT-PCR and immunoblotting confirmed the presence of functional KAR subunits that can form homomeric or heteromeric units. In addition, Neto 1 and Neto 2 auxiliary proteins of KARs were also present in cultured α- and β-cells as well as in rat islets of Langerhans.

Fura-2AM imaging of cultured MIN6 β-cells showed that activation of KARs with kainate increased that intracellular calcium concentration and potentiated glucose-stimulated insulin secretion at both non-stimulatory and stimulatory glucose concentrations. This effect of kainate was blocked by the KAR antagonist but not by an AMPAR/NMDAR antagonist. Furthermore, prolonged exposure of kainate and glutamate reduced the viability of both cultured α- and β-cells of the pancreas. KAR antagonist showed significant protection of cultured α- and β-cells from kainate-induced cell death.

These results indicate that functional KAR subunits are important components of pancreatic endocrine cells and their activation or inhibition has several implications on the function of survival of these cells.

The proposed mechanisms of KAR subunit functions and their role in survival of pancreatic endocrine cells is illustrated in figure 2.38.

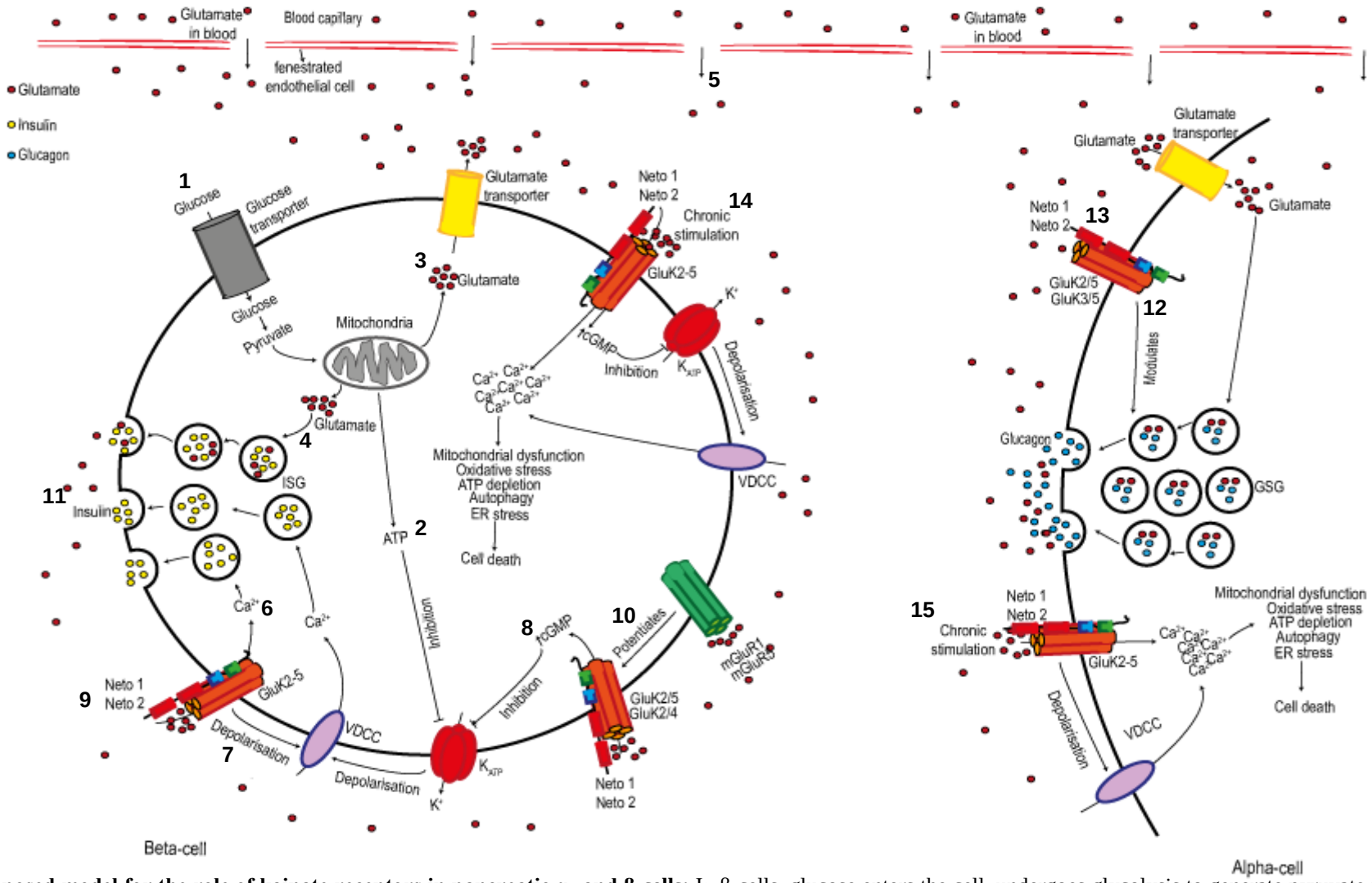

Figure 2.38. Proposed model for the role of kainate receptors in pancreatic α- and β-cells: In β-cells, glucose enters the cell, undergoes glycolysis to generate pyruvate which is oxidised in the mitochondria to yield ATP and glutamate **(1)**. Increased ATP inhibits the ATP-sensitive potassium channel (K_{ATP}) channels leading to opening of voltage-dependent calcium channel (VDCC) and Ca^{2+} influx **(2)**. Glutamate from glucose metabolism leaves the cell via glutamate transporter **(3)** or enters insulin-containing secretory granules (ISG) to potentiate release of insulin **(4)**. Glutamate from circulation passes through the fenestrated endothelium of the islet vasculature **(5)** to bind to KARs on β-cells leading to increased influx of Ca^{2+} via three mechanisms: direct permeation through Ca^{2+}-permeable GluK2 and GluK3 subunits **(6)**; direct opening of VDCC by depolarising effect of GluK2/5 **(7)**; KAR (GluK2/5; GluK2/4)-induced increase in cGMP levels which leads to inhibition of K_{ATP} channels and subsequent opening of VDCC **(8)**. Neto 1 and Neto 2 modulates binding of glutamate **(9)** and the depolarising effect of KARs is enhanced by group I mGluRs (mGluR1, mGluR5) **(10)**. KAR-induced influx of Ca^{2+} potentiates GSIS **(11)**. In α-cells, extracellular glutamate binds and activates KARs (GluK2/5, GluK3/5). Activated KARs regulates the co-secretion of glutamate with glucagon from glucagon-containing secretory granules (GSG) **(12)**. This mechanism may be modulated by Neto 1 and Neto 2 **(13)**. Prolonged activation of α- and β-cell KARs (GluK2-5) leads to increased Ca^{2+} influx and cell death via mechanisms including mitochondrial dysfunction, ER stress and oxidative stress **(14) (15)**.

Chapter Three

Role of GluRs in autoimmune T1DM

3.1. Introduction

There is no report of a direct link between GluR antigens and the autoimmune process in T1DM but circumstantial evidences exist that suggest that further investigation into this link is justified. First, the prevalence of T1DM among autoimmune epilepsy patients is double the prevalence in the general population (Keezer *et al*., 2015). This prevalence was also more than double that of T2DM among these epilepsy patients. Moreover, significantly high titres of anti-GAD antibodies have been reported in serum of children suffering from refractory epilepsy and autoimmune limbic encephalitis (Abd El-Aziz and El-Serogy, 2013; Blanc *et al,* 2009). These observations indicate the existence of autoantibodies against both GluRs and islet autoantigen in the same condition, suggesting a possible linkage between these receptors and T1DM autoimmune process. These suggestions are enforced further by observations that GAD autoantibodies play a major role in both acute and chronic epilepsy (Liimatainen et al., 2012) considering that autoantibodies to this enzyme are implicated in T1DM. Interestingly, antidiabetic drugs such as exenatide (Tsunekawa et al., 2007) and glitazones (Cunha et al., 2009) which are known to preserve β-cell integrity and survival also possess neuroprotective properties, while the anti-epileptic drug topiramate which attenuates glutamate-induced excitotoxicity also have antidiabetic properties and preserve β-cell survival and function (Davalli et al., 2012).

Even though all these observations are circumstantial, they provide significant insights into the possibility that GluRs may be involved in both β-cell function and death. Investigating the presence of antibodies against GluR subunits in serum of T1DM patients

is a novel study which will contribute significantly to the search for the exact trigger or cause of the autoimmune process in T1DM. All the well-established autoantibodies in T1DM are targeted against intracellular antigens involved in secretory pathways (Arvan *et al*., 2012) which implies that an extracellular or transmembrane antigen may be the first target of the autoimmune process resulting in the release of these intracellular proteins. Since GluRs are transmembrane proteins, identification of autoantibodies against GluR antigens in serum of T1DM patients will provide a good foundation to investigate the possibility of these autoantibodies in the initiation or trigger of the autoimmune process in T1DM.

3.2. Aims

The aim of this chapter is to investigate the presence of autoantibodies against GluR subunits in serum of newly-diagnosed T1DM patients.

Specific objectives for this chapter include:

1) Isolation of GluR-rich synaptosomal plasma membrane (SPM) fraction from whole rat brain.
2) Optimisation of an ELISA for detection of GluRs in SPM fractions using commercial GluR antibodies, T1DM and non-diabetic control serum samples.
3) Analysis and selection of T1DM sera which react against SPM proteins in ELISA for further analysis.
4) Immunoblotting of SPM proteins using commercial GluR antibodies, T1DM and non-diabetic control serum samples.
5) Transient overexpression of specific GluR subunits in HEK293 cells
6) Optimisation of immunoblotting technique for detecting antibodies against GluR subunits in sera of T1DM patients.

3.3. Materials and Method

3.3.1. *Materials*

Details of materials are supplied in Appendix 1.

3.3.2. *Preparation of synaptosomal plasma membrane (SPM)*

All procedures were carried out at 4^{o}C using pre-cooled reagents and buffers. Ten volumes (1:10 ratio of buffer to volume of brain tissue) of HEPES-buffered sucrose solution (4 mM HEPES pH 7.4, 0.32 M sucrose) containing 0.1 mM PMSF and 1 mM sodium orthovanadate was added to one volume of rat brain and then the brain homogenised using a Potter-Elvehjem tissue grinder (Thermo-Fisher Scientific, Paisley, UK). The homogenate was centrifuged at 1000 x g at 4^{o}C to yield a nuclear fraction pellet (P1). The supernatant (S1) was transferred into a fresh tube and centrifuged at 10,000 x g for 15 minutes to produce a crude synaptosomal pellet (P2). The resulting supernatant (S2) was discarded and the P2 pellet was resuspended in 10 volumes of HEPES-buffered sucrose and centrifuged at 10,000 x g for 15 minutes to yield a washed crude synaptosomal fraction (P2^{I}). The P2^{I} pellet was lysed by resuspending in 10 mL of ice-cold deionised water containing 1X protease inhibitor, 0.1 mM PMSF and 1 mM sodium orthovanadate and then passing the suspension through a 1 mL syringe attached to a 25 x 1 inch (0.5 x 25 mm) needle 20-25 times. The solution was quickly adjusted to 4 mM HEPES using 1 M HEPES (pH 7.4) stock solution and mixed constantly for 30 minutes in cold room (4^{o}C) to ensure complete lysis. The lysate was then centrifuged at 25,000 x g for 20 minutes to yield a lysed synaptosomal membrane fraction (P3). The P3 pellet was resuspended in 2-5 mL of HEPES-buffered sucrose solution. Using a Pasteur pipette, the resuspended membrane was layered onto a discontinuous sucrose gradient (0.8 M, 1.0 M and 1.2 M from top to bottom of the tube (supplemented with 0.1 mM PMSF and 1

mM sodium orthovanadate) from top to bottom respectively in an ultraclear tube. The gradient was centrifuged at 150,000 x g for 2 hours in a swinging bucket rotor and the synaptic plasma membrane in the layer between 1.0 M and 1.2 M sucrose was recovered by carefully puncturing the tube with a needle and withdrawing the layer with a syringe. The concentration of sucrose in the recovered fraction was diluted to 0.32 M by adding 2.5 volumes of 4 mM HEPES pH 7.4 and then centrifuged at 150,000 x g for 30 minutes. The pellet, P5 was resuspended in 1-2 mL ice-cold HEPES buffer (50 mM pH 7.4, 2 mM EDTA, 0.1 mM PMSF and 1 mM sodium orthovanadate) (Hahn *et al*., 2009; Carlin *et al*., 1980; Cho *et al*., 1992; Dosemeci *et al*., 2006; Molnar *et al*., 1994). Figure 3.1 summarises the procedure.

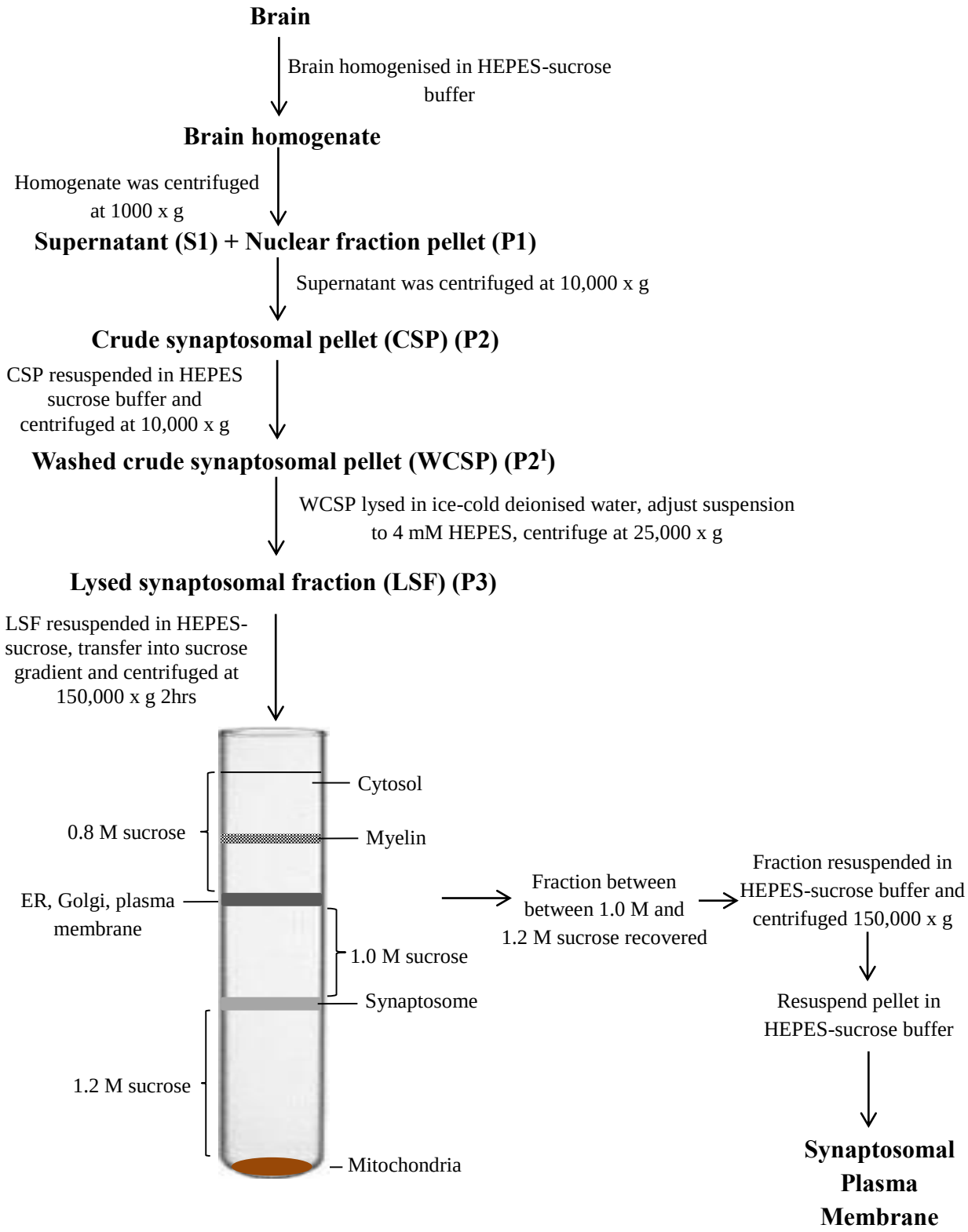

Figure 3.1. Summary of experimental procedure for preparation of synaptosomal plasma membrane fraction. **ER**: Endoplasmic reticulum; **Golgi**: Golgi apparatus

3.3.3. *Optimisation of amount of antigen required for immobilisation*

Rat SPM fraction was diluted to concentrations of 0.25 µg, 0.5 µg, 1.0 µg, 2.0 µg and 4 µg per 100 µL in coating buffer (13 mM Na_2CO_3, 35 mM $NaHCO_3$, pH: 9.6) and then 100 µL transferred into Nunc-Immuno™ MicroWell™ 96-well ELISA plates. The plates were sealed with sealing films and incubated at 4°C overnight on plate shaker at 500 rpm. The plates were inverted to remove unbound solution and then rinsed three times 5 minutes each on a plate shaker using PBS-T washing buffer (1X PBS with 0.05% (v/v) Tween-20). After each wash, the plates were inverted and blotted firmly on paper towel to remove residual buffer (Miura *et al*., 2008; Chiodo *et al*., 2013; Molnar *et al*., 1994). After rinsing, the wells were blocked with 200 µL of 5% (w/v) BSA diluted in washing buffer for 1 hour at room temperature on plate shaker (500 rpm). The blocking solution was removed and the wells were rinsed with PBS-T and blotted by inverting the plates and tapping firmly on paper towel to remove residual liquid from the wells. 200 µL of anti-GluK2/3, anti-GluK5 and anti-pan-AMPAR diluted to 1:1000 in 1% (w/v) BSA were added to designated wells in the SPM-coated plates and sealed. The plates were then incubated for 2 hours at room temperature on a plate shaker (500rpm). Controls were set by adding 200 µL of 1% (w/v) BSA to designated coated wells. After incubation, the plates were inverted to remove unbound antibody and then the wells were rinsed three times using 400 µL of PBS-T washing buffer. HRP-conjugated anti-rabbit IgG secondary antibody diluted to 1:5000 in 1% BSA was added to the wells and incubated at room temperature for 1 hour on a plate shaker at 500 rpm. Coated wells incubated with anti-rabbit only were also set up as controls. The antibody solution was disposed of and the wells were rinsed and blotted three times. After the last wash, 100 µL of enhanced K-blue TMB substrate was added to the wells and the plate was shaken at 500 rpm until a blue colour developed. The reaction was immediately stopped by adding 100 µL of 1 M HCl

solution and optical density was read at 450 nm using the Megallan Infinite® F50 microplate reader (Tecan, Mannedorf, Switzerland) within 20 minutes of adding the HCl solution. A bar chart representing mean ± SEM of optical density (450 nm) against concentration of SPM for three independent experiments was plotted using Excel. Statistical comparisons were performed using one-way *ANOVA* and differences between means were considered statistically significant if the *p* value was less than 0.05.

The amount of bound SPM protein was measured using the BCA protein quantification assay as follows: triplicates of 10 µL BSA standards of concentrations 0-1000 µg/mL were prepared in wells of the 96-well plate after which 200 µL of BCA working reagent (50:1; BCA reagent: copper (II) sulphate solution) was added to each of the BSA standards. To the immobilised SPM protein, 210 µL of the working reagent was added followed by incubation at 60^0C for 20 minutes. Absorbance at 492 nm was read with Megallan plate reader (Tecan, Reading, UK). A BSA standard curve of absorbance against concentration was plotted and used to determine the concentrations of the immobilised SPM proteins (da Luz *et al*., 2015).

Based on the measurement of bound protein and the optical density of the reaction between the coated antigen and antibody, 3 µg/100 µL was selected as the optimal concentration of SPM for coating the plates for ELISA.

3.3.4. *Testing for the presence of autoantibodies to GluRs subunits in sera of T1DM patients and aged-matched non-diabetic control subjects.*

3.3.4a. *Details of T1DM patients and control subjects*

Serum samples from forty newly-diagnosed T1DM patients and forty age-matched non-diabetic healthy individuals were collected at the University Hospital of Wales (Wales, UK). Tables 3.1-3.2 show details of the T1DM patients and non-diabetic controls.

Table 3.1. Details and sample codes of newly-diagnosed T1DM patients and healthy non-diabetic controls

T1DM patients			Non-diabetic healthy controls		
Sample ID	**Gender**	**Age**	**Sample ID**	**Gender**	**Age**
ND603	F	39	***1***	F	39
ND604	M	38	***2***	M	38
ND605	M	44	***3***	M	44
ND607	F	40	***4***	F	40
ND609	F	47	***5***	F	47
ND614	F	29	***6***	F	29
ND615	F	37	***7***	F	37
ND637	F	45	***8***	F	45
ND638	F	43	***9***	F	43
ND650	M	46	***10***	M	46
ND662	F	48	***11***	F	48
ND674	M	47	***12***	M	47
ND675	F	38	***13***	F	38
ND490	M	46	***14***	M	46
ND488	F	29	***15***	F	29
ND450	M	50	***16***	M	50
ND419	F	50	***17***	F	50
ND517	M	40	***18***	M	40
ND522	F	42	***19***	F	42
ND530	M	29	***20***	M	29

Table 3.2. Details and sample codes of newly-diagnosed T1DM patients and healthy non-diabetic controls

T1DM patients			Non-diabetic healthy controls		
Sample ID	**Gender**	**Age**	**Sample ID**	**Gender**	**Age**
ND534	M	35	***21***	M	35
ND548	F	30	***22***	F	30
ND568	M	48	***23***	M	48
ND398	M	47	***24***	M	47
ND358	F	42	***25***	F	42
ND397	M	48	***26***	M	48
ND557	M	43	***27***	M	43
ND456	M	39	***28***	M	39
ND455	M	45	***29***	M	45
ND365	F	52	***30***	F	52
ND667	M	44	***31***	M	44
ND512	F	46	***32***	F	46
ND596	F	42	***33***	F	42
ND494	F	47	***34***	F	47
ND507	M	51	***35***	M	51
ND480	M	50	***36***	M	50
ND533	M	42	***37***	M	42
ND609	F	47	***38***	F	47
ND366	F	47	***39***	F	47
ND541	M	50	***40***	M	50

3.3.4b. *Testing for the presence of antibodies to GluR-enriched SPM proteins in sera of T1DM control patients.*

Nunc-Immuno™ MicroWell™ 96-well ELISA plates were coated overnight at 4^{o}C with 3 µg/100 mL SPM fraction, washed and then blocked with 5% (w/v) BSA as described in section 3.3.3. Serum samples from T1DM patients, control patients and commercially-acquired delipidated (free of cholesterol, triglycerides and most other lipids) human serum (TCS Biosciences, Buckingham, UK) were diluted to 1:1000 in 1% (w/v) BSA and added to the SPM-coated wells. The plates were sealed and incubated at room temperature for 2 hours on a shaker (500 rpm). The wells were rinsed three times and 200 µL of 1:10,000 HRP-conjugated anti-rabbit IgG secondary antibody was added to the wells and incubated at room temperature for 1 hour on a plate shaker (500 rpm). The wells were rinsed, blotted and 100 µL of K-blue solution was added followed by 50 µL HCl as described in section 3.3.3. The optical density was determined at 450 nm and a bar chart representing mean ± SEM optical density from three independent experiments was plotted. Samples with mean optical density higher than mean optical density of the delipidated serum were selected to be used for reaction against SPM fractions in immunoblotting.

3.3.5. *Visualisation of the SPM proteins recognised by autoantibodies in serum of T1DM patients and non-diabetic controls*

Synaptosomal plasma membrane fraction (20 µg) was added to equal volume of 2X loading buffer (0.0625 M Tris-HCl, pH 6.8, 1% (w/v) SDS, 10% (v/v) bromophenol blue) and subjected to polyacrylamide gel electrophoresis followed by transfer onto a PVDF membrane (Chapter two, Section 2.3.9). The membrane was incubated with ponceau red

for 5 minutes at RT and then the stain was rinsed off with distilled water and TBS-T. This enhanced visualisation of the protein bands and enabled cutting the membranes into individual strips each containing a lane of separated SPM fraction. The membrane was then rinsed in TBS-T (50 mM Tris-HCl; pH: 7.4, 150 mM NaCl, 0.1% Tween) until the stained protein bands disappeared. The membranes were blocked in 5% milk for 1 hour and incubated overnight at 4^{o}C with human T1DM or control sera (1 in 1000 diluted in 5% milk), delipidated commercial human serum (1 in 1000), anti-GluK2/3 (1 in 3000) and anti-GluK5 (1 in 3000). The membrane was washed six times in TBS-T for 5 minutes each and incubated with 1:10,000 dilution of HRP-conjugated anti-human IgG secondary antibody for 45 minutes followed by washing the membrane six times in TBS-T for 5 minutes each. The membrane was then incubated with 2 mL of HRP substrate for 1 minute. Detection of immunopositive bands was performed using the enhanced chemiluminescence detection system and Syngene gel imaging and analysis system (Syngene, Cambridge, UK). (Storto *et al*., 2006; Whitehead *et al*., 2013; Diraison *et al*., 2010).

3.3.6. *Transient transfection of HEK293 cells with plasmids encoding GluR subunits*

HEK293 cells were seeded onto 10 cm^2 cell culture-treated dishes at density of 3 x 10^6 cells/10 mL and cultured in DMEM (Chapter two, Section 2.3.2).

Cells were transfected with plasmids encoding kainate (GluK2, GluK5), AMPA (GluA1) and NMDA (GluN1, GluN2A, GluN2B) receptors. These constructs were provided courtesy of Professor Elek Molnar (University of Bristol, UK). The transfection mixture was prepared by adding 7 µg of plasmid to 500 µL of Opti-MEM® I reduced serum media. The transfection reagent was prepared by adding polyethylenimine (PEI) (three and half times the volume of plasmid DNA required) to 500 µL of Opti-MEM® I. Both mixtures

were briefly vortexed and the transfection reagent mixture was added to the plamid-Opti-MEM mixture and incubated at room temperature for 20 minutes. The mixture was then added to the cultured HEK293 cells and incubated under cell culture conditions for 48-72 hours (Tom *et al*., 2008; Longo *et al*., 2013; Varadi and Rutter, 2002).

Protein lysate was prepared using RIPA extraction method and quantified using Bradford assay (Chapter two, sections 2.3.5-2.3.6).

3.3.7. *Visualisation of overexpressed GluR subtypes recognised by the autoantibodies in the serum samples using immunoblotting*

Membrane lysate fraction from transiently transfected HEK293 cells (30 µg) was added to equal volume of 2X loading buffer and subjected to polyacrylamide gel electrophoresis followed by transfer onto a PVDF membrane (Chapter two, section 2.3.9). The membrane was blocked in 5% milk for 1 hour and incubated overnight at 4^{o}C with human T1DM or control sera (1 in 250 diluted in 5% milk), anti-GluK2/3 (1 in 3000), anti-GluK5 (1 in 3000) and anti-pan-AMPAR (1 in 1000) primary antibodies.

The membranes were washed six times in TBS-T for 5 minutes each and incubated at RT for 45 minutes with HRP-conjugated anti-rabbit or anti-mouse IgG secondary antibody (dilution; 1:4000 in 5% milk).

After incubation, the membrane was washed six times in TBS-T for 5 minutes each and incubated with 2 mL of HRP substrate for 1 minute. Detection of immunopositive bands was performed using the enhanced chemiluminescence detection system and Syngene gel imaging and analysis system (Syngene, Cambridge, UK). (Storto *et al*., 2006; Whitehead *et al*., 2013; Diraison *et al*., 2010).

The membranes were stripped of all bound antibodies for 35 minutes at 50°C in stripping buffer (2% (w/v) SDS, 0.0625 M Tris, pH 6.8, 0.11 M 2-mercaptoethanol) before reprobing (Varadi *et al*., 1996).

3.3.8. *Statistical analysis*

Data are presented as means ± SEM of at least three independent experiments with number of replicates stated in respective experiments. Statistical comparisons were performed by one-tailed Student's *t*-test using Microsoft Excel or one-way *ANOVA* using Minitab data analysis software. Differences between means were considered statistically significant if the *p* value was less than 0.05.

3.4. Results

3.4.1. Investigation of the presence of autoantibodies against glutamate receptor subunits in serum of type 1 diabetic patients.

This current study identified functional KAR channels in pancreatic endocrine cells and have also established that these receptors play significant roles in β-cells including calcium influx and insulin secretion (Chapter two, sections 2.4.1-2.4.4). Also, these receptors have been shown to significantly influence the viability of pancreatic endocrine cells (Chapter two, section 2.4.5). Other studies have identified the other iGluR subtypes in pancreatic endocrine cells (Chapter one, Tables 1.6-1.8).

Evidence linking pathogenesis of neurological conditions to GluR autoantibodies (Chapter one, section 1.8) as well as the potential role of glutamate and GluRs in diabetes mellitus have been discussed (Chapter one, section 1.10). Furthermore, circumstantial evidence which is indicative of a possible relationship between TIDM pathogenesis and GluR antigens/autoantibodies has also been discussed (section 3.1). Thus, it was important to investigate the presence of autoantibodies against KARs and other GluR subtypes in serum of T1DM patients.

Serum samples from forty newly-diagnosed T1DM individuals as well as forty age-matched non diabetic healthy individuals were collected at the University Hospital of Wales. Details of the patients and healthy non-diabetic controls are shown in section 3.3.4, tables 3.1-3.2.

3.4.1a. *Optimisation of the amount of synaptosomal plasma membrane (SPM) fraction required for the coating of ELISA wells*

To select the optimal SPM concentration required to immobilise in ELISA plates, different amounts (0.25-4.0 µg) of the SPM were immobilised into ELISA plates, incubated with primary (anti-GluK2/3, anti-GluK5, anti-pan-AMPAR) and secondary (horseradish peroxidase-conjugated anti-rabbit IgG) antibodies. A TMB horseradish peroxidase substrate was added and incubated for 20 minutes followed by addition of 1 M HCl to stop the reaction. Optical density at 450 nm was measured immediately after addition of the HCl (section 3.3). A bar chart of optical density against concentration of the immobilised protein was plotted (Figure 3.2). From the results, coating the ELISA wells with 2-4 µg of SPM showed approximately the same antibody binding and approximately the same amount of bound protein hence 3 µg was selected as the amount of SPM protein to coat the wells.

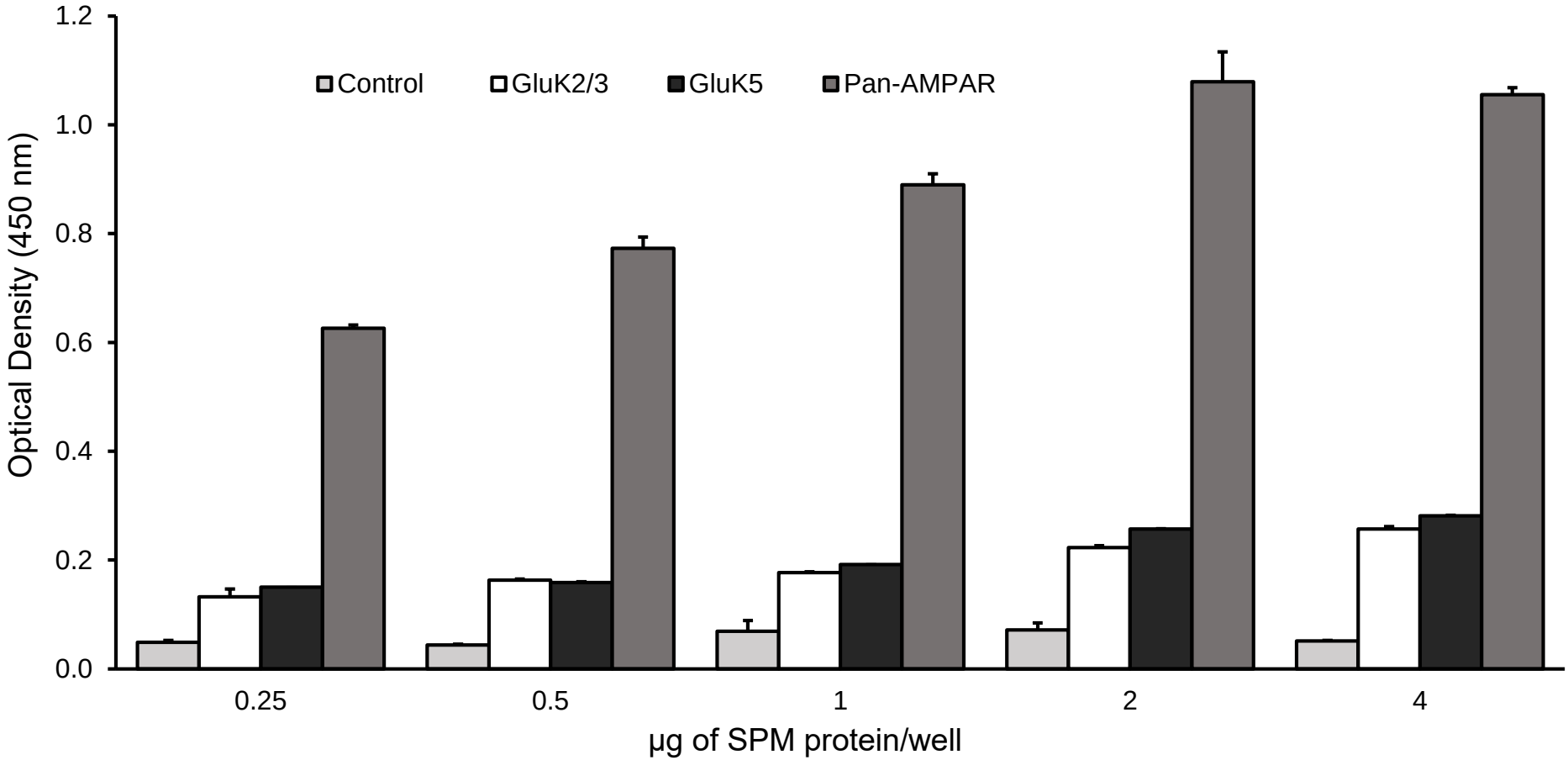

Figure 3.2. Optimisation of the amount of SPM required for immobilisation in ELISA plates. SPM fractions were prepared from rat whole brain tissue and immobilised onto ELISA wells. The coated wells were incubated with anti-GluK2/3, anti-GluK5 and anti-pan-AMPAR primary antibodies and then with HRP-conjugated anti-rabbit IgG secondary antibody. The wells were rinsed, incubated with enhanced K-blue TMB substrate and then optical density measured at 450 nm. Results are presented as means ± SEM from three separate experiments.

3.4.1b. *Selection of test sera that react with GluR-enriched SPM fraction proteins*

After optimising the amount of SPM fraction required to coat the wells for ELISA, the assay was used to select T1DM sera that react with GluR-enriched SPM proteins as described in section 3.3.4. Negative controls were set up by excluding the primary antibody incubation step. An image of a representative ELISA plate after addition of HCl stop solution is shown in Figure 3.3. Bar graph of optical density for 40 T1DM, 40 non-diabetic controls and 3 delipidated (free of cholesterol, triglycerides and most other lipids) human serum is shown in Figure 3.4 and a bar graph comparing optical density between T1DM patients and their age- and gender-matched controls is shown in Figure 3.5. Individual value plot was used to analyse the data distribution and also to compare the optical densities for T1DM and non-diabetic controls (Figure 3.6). The individual plots indicate that there is no significant differences in immunoreactivities between serum of T1DM and non-diabetic controls. Also, the plots show the same data distribution between immunoreactivities of T1DM and controls.

Serum of T1DM patients and non-diabetic controls with optical density above the mean optical density of the commercial human serum were selected for further analysis. In total, 34 sera representing approximately 43% of the samples were selected based on this approach.

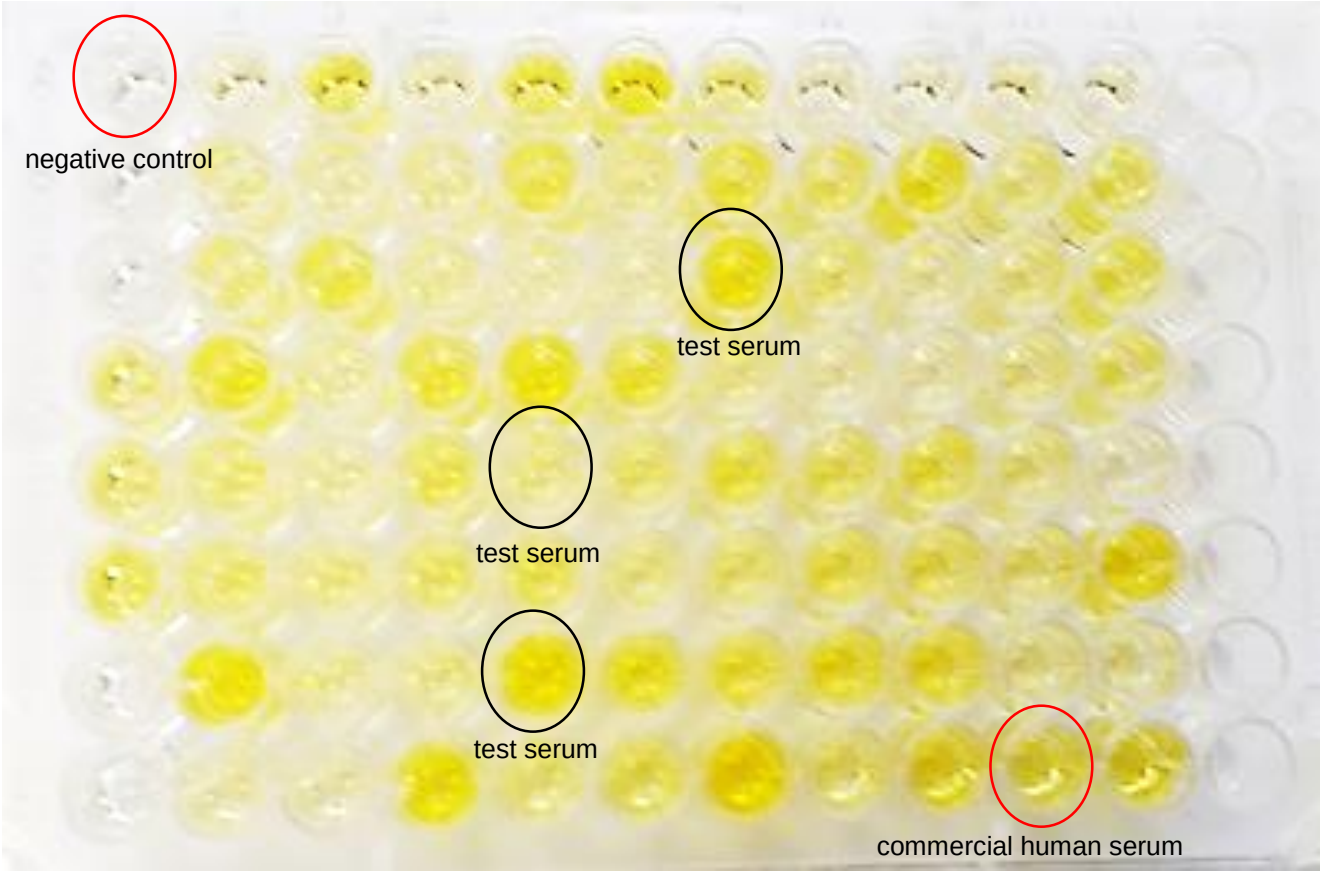

Figure 3.3. Representative ELISA for selection of sera from T1DM patients and non-diabetic controls that react with GluR-enriched SPM proteins. SPM proteins were immobilised in ELISA plates and incubated with serum of T1DM patients and non-diabetic controls and delipidated human serum followed by incubation with HRP-conjugated anti-human IgG secondary antibody. Negative control was set up by excluding the primary antibody step of the reaction. Image is representative of three independent experiments.

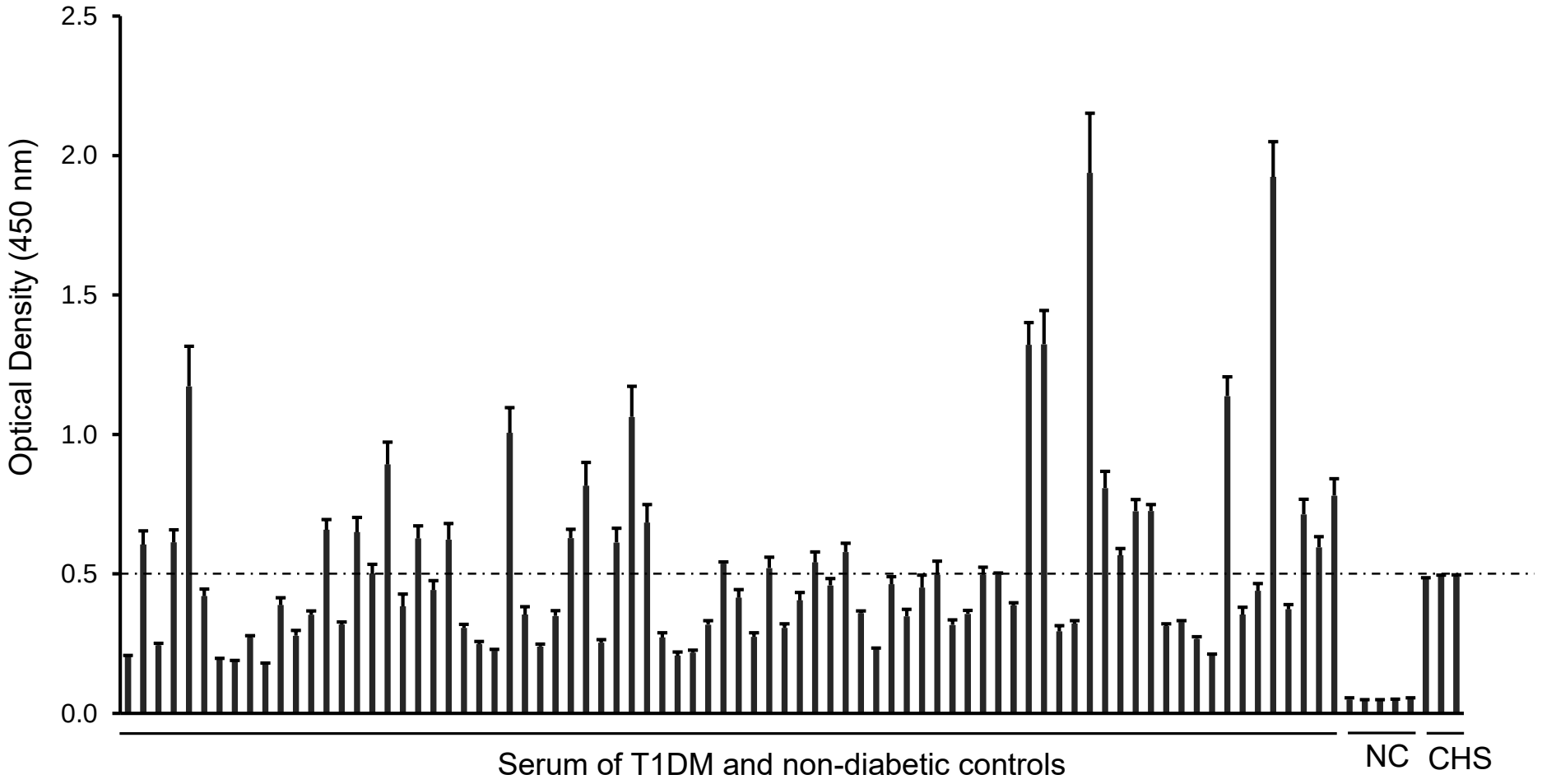

Figure 3.4. Selection of test sera that react with GluR-enriched SPM proteins. SPM fraction proteins were immobilised in ELISA plates and incubated with serum from T1DM patients and non-diabetic controls and delipidated human serum followed by incubation with HRP-conjugated anti-human IgG secondary antibody. Negative control (NC) was set up by excluding the primary antibody incubation step. Samples with optical densities above that of commercial human sera (CHS) were selected for further analysis. Results are presented as means ± SEM from three separate experiments.

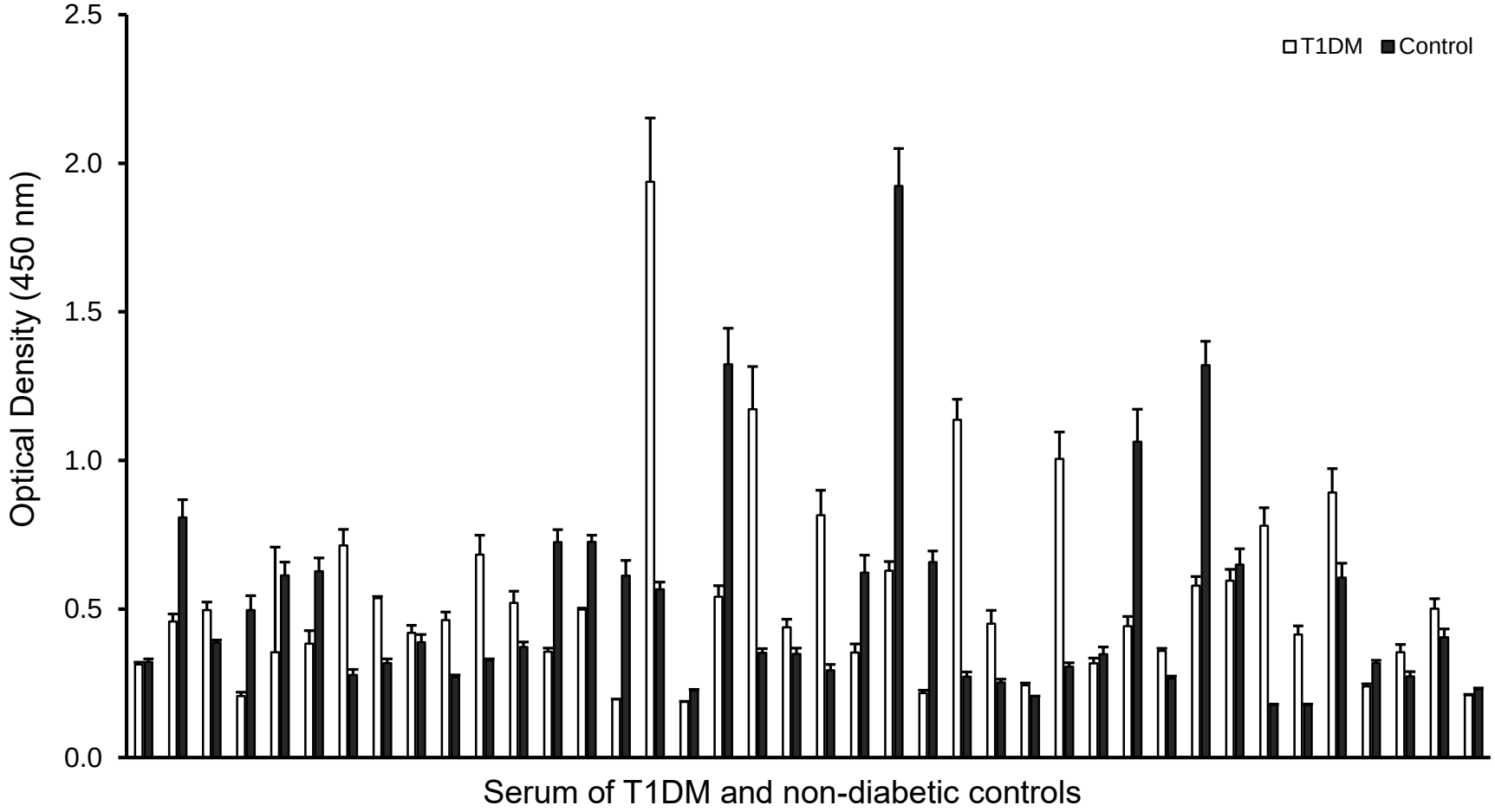

Figure 3.5. Bar graph showing optical densities for T1DM patients and aged- and gender-matched non-diabetic controls. SPM fraction proteins were immobilised in ELISA wells and incubated with serum of T1DM patients and non-diabetic controls followed by incubation with HRP-conjugated anti-human IgG secondary antibody. TMB ELISA substrate was added and optical density measured at 450 nm. Results are presented as means ± SEM from three separate experiments.

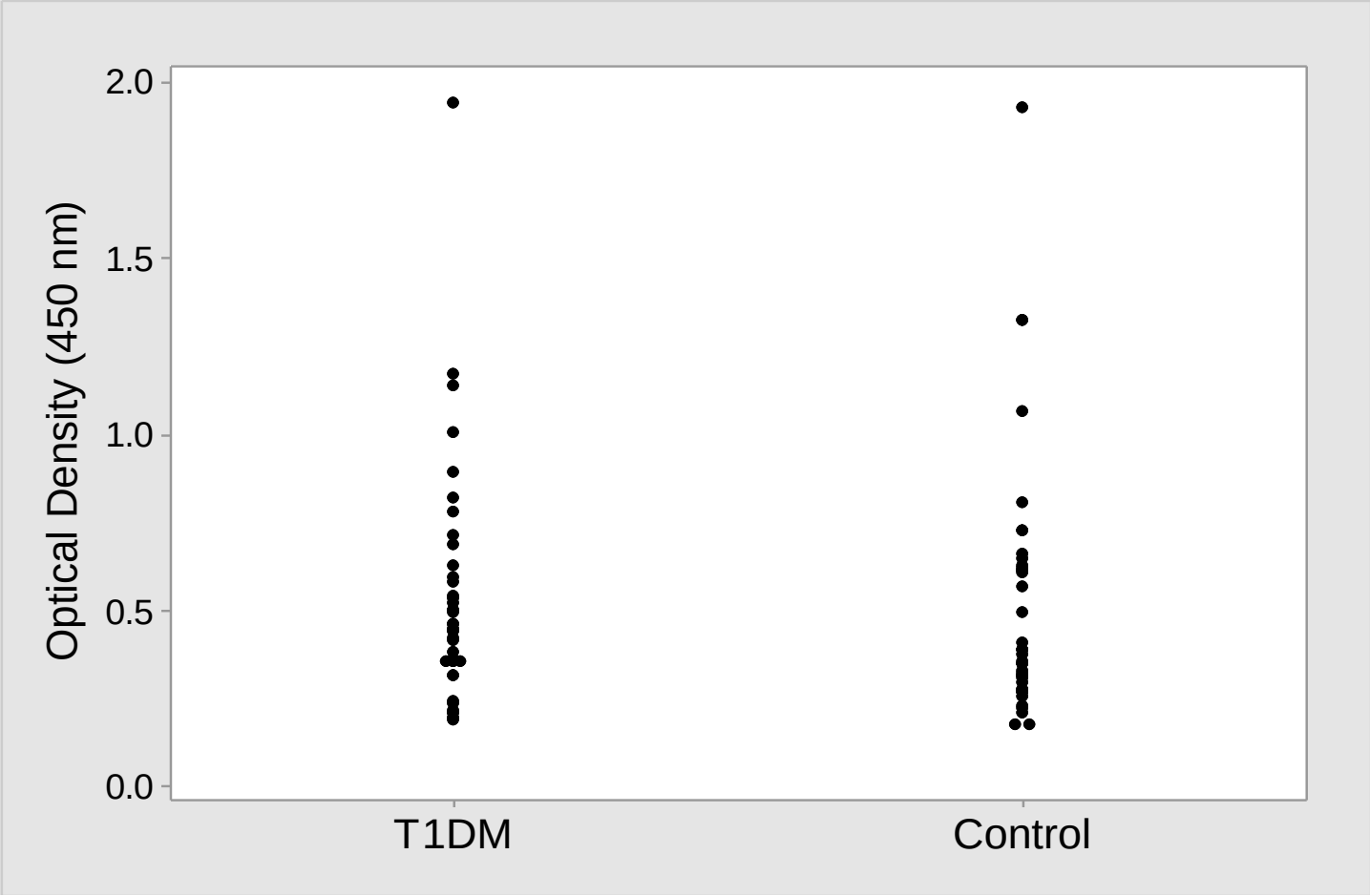

Figure 3.6. Individual value plots of optical densities for T1DM and non-diabetic control samples. SPM fraction proteins were immobilised in ELISA plates and incubated with serum from T1DM patients and non-diabetic controls followed by incubation with HRP-conjugated anti-human IgG secondary antibody. TMB ELISA substrate was added and optical density measured at 450 nm. Results are presented as means from three separate experiments.

3.4.1c. *Visualisation of the SPM target proteins recognised by autoantibodies in serum of T1DM patients and non-diabetic controls*

In addition to GluRs, several other proteins are present in synaptosomal plasma membrane fraction (Rodriguez-Moreno and Sihra, 2013; Biesemann *et al*., 2014). Thus, immunoblotting was used to investigate the type of SPM proteins which reacted with antibodies in the test samples. SPM protein (20 µg) was separated using SDS-PAGE, transferred onto PVDF membrane, incubated with 1:1000 dilution of serum of T1DM patients, non-diabetic controls and commercial human serum followed by incubation with HRP-conjugated anti-human IgG secondary antibody (1:10,000) as described in section 3.35. The immunoblot results are shown in Figure 3.7.

The results show immunopositive bands in the region between 100 and 150 kDa in some T1DM and non-diabetic control serum samples. This region (100-150 kDa) corresponds to the molecular weight range for GluR proteins. Membranes which were incubated with commercial human serum showed no immunopositive bands. Immunopositive bands were present in the region between 50 and 75 kDa for some of the membranes incubated with T1DM or non-diabetic control sera. Though the identity of these bands could not be elucidated from this technique, the method gave an indication that antibodies in the test sera target SPM proteins with molecular weight range between 100 and 150 kDa.

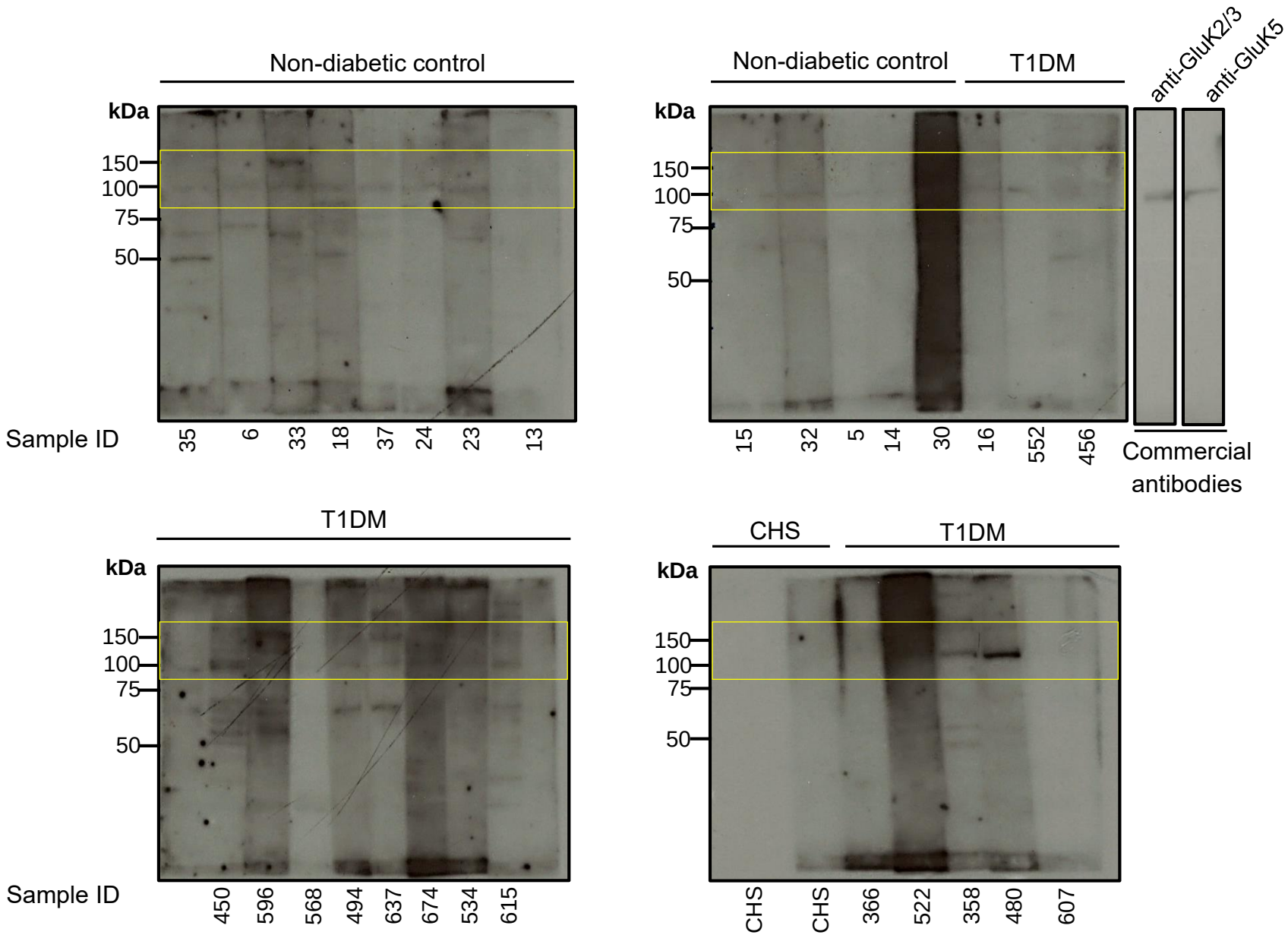

Figure 3.7. Immunoblotting of SPM proteins using serum of T1DM patients, non-diabetic controls and GluK antibodies. SPM proteins were separated using SDS-PAGE, transferred onto PVDF membrane and incubated with serum of T1DM, non-diabetic controls, anti-GluK2/3 or anti-GluK5 antibodies followed by HRP-conjugated anti-human/rabbit IgG secondary antibody. The region inside the yellow rectangle represents where GluR subunit proteins are expected. Figures are representative of two independent experiments. Sample ID and patient details are shown in tables 3.1-3.2. CHS: commercial human serum.

3.4.1d. *Identification of sera that specifically recognise overexpressed GluR subunits in HEK293 cells.*

Based on the results from section 3.4.1c, using immunoblotting to detect SPM proteins that are bound by antibodies in the serum samples was not specific. However, the technique was useful in selecting serum samples that reacted with separated SPM fraction proteins. Based on these observations, GluR subunits (GluK2, GluK5, GluA1, GluN2A and GluN2B) were overexpressed in HEK293 cells as described in section 3.3.6. Membrane lysates were prepared from the transfected HEK293 cells and 20 μg of protein was separated using SDS-PAGE, transferred onto PVDF membrane and then incubated with serum of T1DM or non-diabetic controls as described in sections 3.3.6-3.3.7. Negative controls were set up by reacting test serum with proteins from non-transfected HEK293 cells. Positive controls were set up by reacting anti-GluK2/3, anti-GluK5 and ant-pan-AMPAR antibodies with proteins from GluK2-, GluK5- and GluA1-tranfected HEK293 cells respectively. Four serum samples (sample ID: 358, 596, 18 and 615) were used in this experiment. These four samples were selected because they showed immunoreactive bands within a region corresponding to the molecular weight range for GluR proteins when they were incubated with SPM proteins in immunoblotting (Figure 3.7). However, not all the samples that showed immunoreactive bands with SPM were used at this stage due to time constraints.

The reaction between the overexpressed proteins and the commercial antibodies (anti-GluK2/3, anti-GluK5 and anti-pan-AMPAR) showed immunopositive bands in the region that corresponds to the molecular weights of these GluR subunit proteins (100-110 kDa) (Figure 3.8). This confirmed that the transfected GluK2, GluK5 and GluA1 were expressed in the HEK293 cells. However, due to unavailability of anti- GluN2A and anti-GluN2B antibodies, expression of these transfected subunits could not the confirmed.

There were no reactions between the commercial antibodies and membrane lysates from non-transfected HEK293 cells (Figure 3.8).

The reaction between membrane lysates from the transfected HEK293 and the test sera showed several immunopositive bands within the region which corresponds to the molecular weight range for GluR proteins (100-150 kDa). Some immunopositive bands were also outside the region that corresponds to the molecular weight range for GluR proteins (Figures 3.9-3.12). The presence of non-specific immunoreactive bands makes it difficult to conclude that the overexpressed proteins were specifically targeted by corresponding antibodies in the test samples.

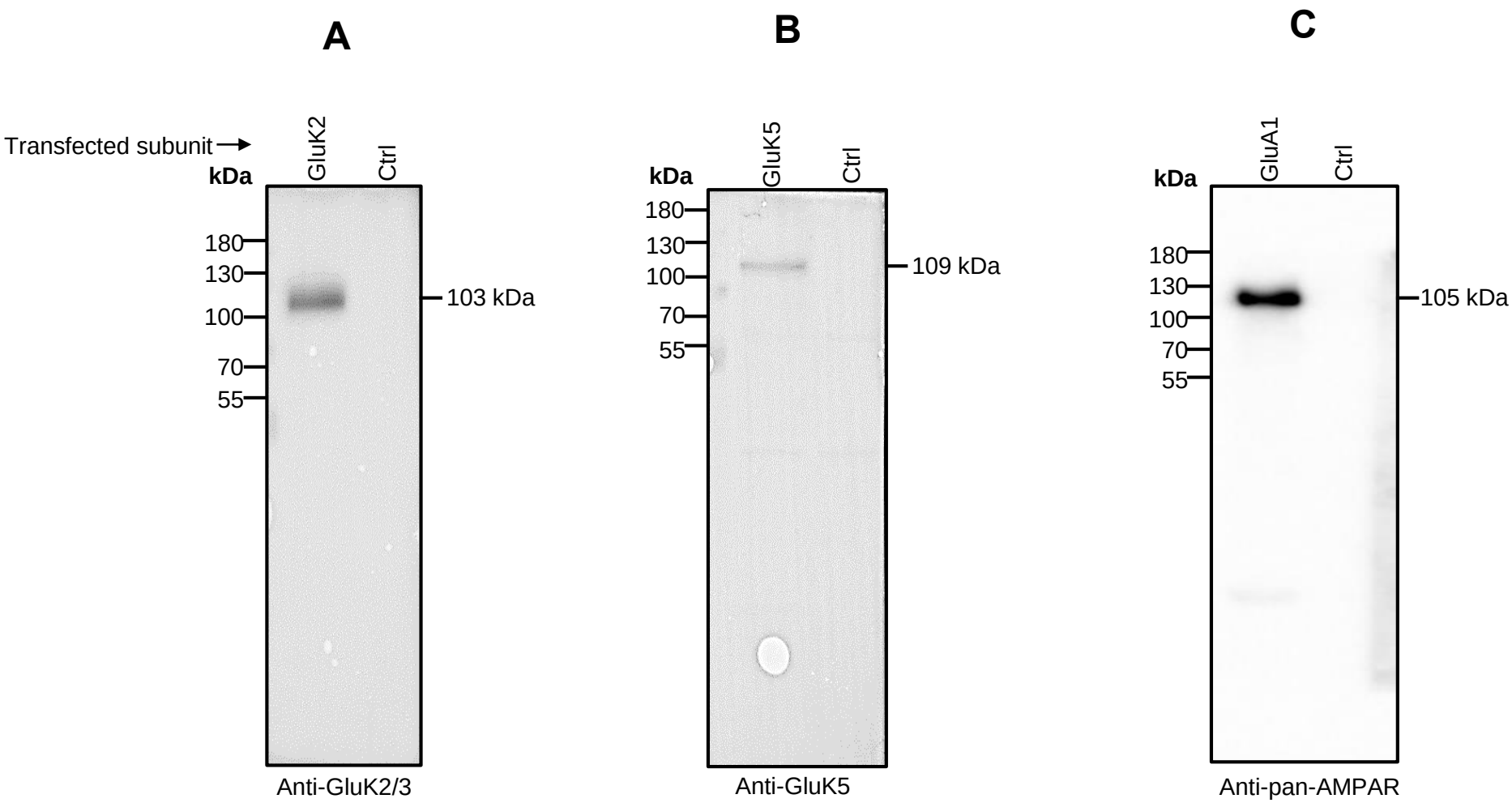

Figure 3.8. Confirmation of expression of GluR subunits in transfected HEK293 cells. Proteins prepared from HEK293 cells transfected with GluK2 (A), GluK5 (B) and GluA1 (C) were separated using SDS-PAGE, transferred onto PVDF membranes. The membranes were labelled with corresponding antibodies (anti-GluK2/3, anti-GluK5 and anti-pan-AMPAR) followed by incubation with corresponding HRP-conjugated anti-rabbit IgG secondary antibody. The immunopositive bands were visualised using enhanced chemiluminescence. One experiment was performed.

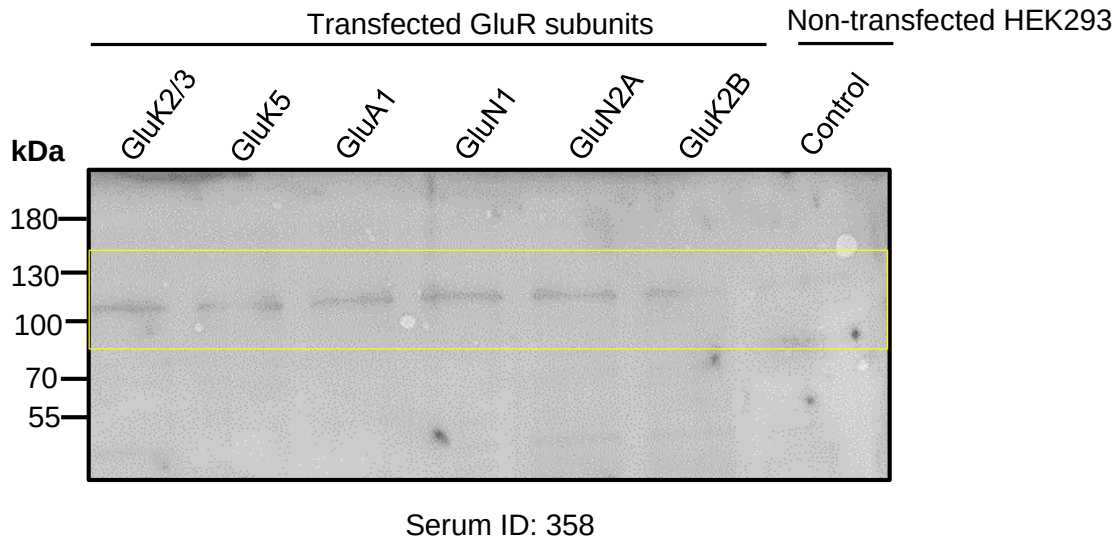

Figure 3.9. Identification of serum that specifically recognise overexpressed GluR subunits in HEK293 cells. Proteins prepared from GluR subunit-transfected HEK293 cells were separated using SDS-PAGE, transferred onto PVDF membrane. The membrane was incubated with test serum (1:200) followed by incubation with HRP-conjugated anti-human IgG secondary antibody. The immunopositive bands were visualised using enhanced chemiluminescence. The region inside the yellow rectangle represents where GluR subunit proteins are expected. Sample ID and patient details are shown in tables 3.1-3.2. One experiment was performed.

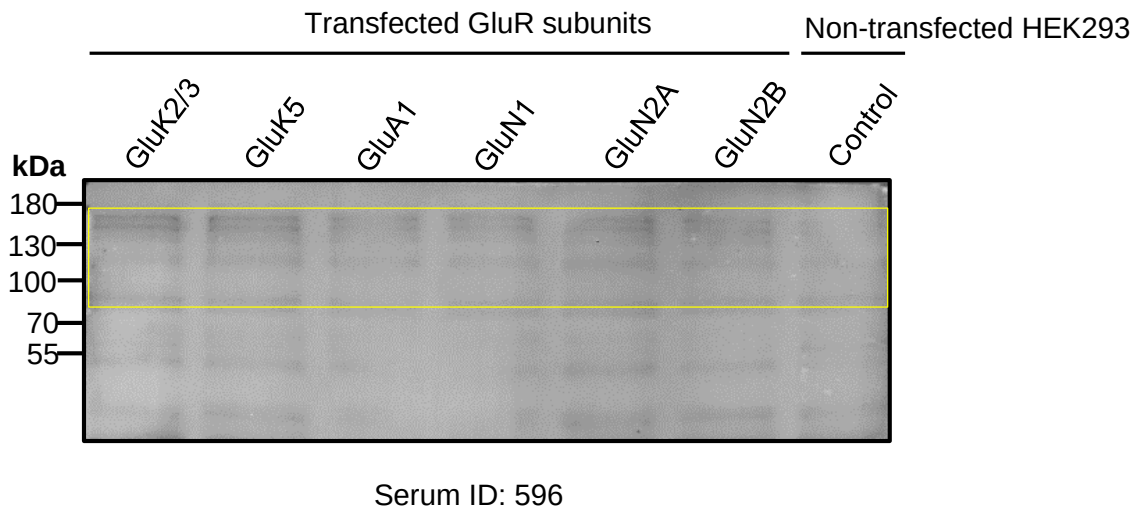

Figure 3.10. Identification of serum that specifically recognise overexpressed GluR subunits in HEK293 cells. Proteins prepared from GluR subunit-transfected HEK293 cells were separated using SDS-PAGE, transferred onto PVDF membrane. The membrane was incubated with test serum (1:200) followed by incubation with HRP-conjugated anti-human IgG secondary antibody. The immunopositive bands were visualised using enhanced chemiluminescence. The region inside the yellow rectangle represents where GluR subunit proteins are expected. Sample ID and patient details are shown in tables 3.1-3.2. One experiment was performed.

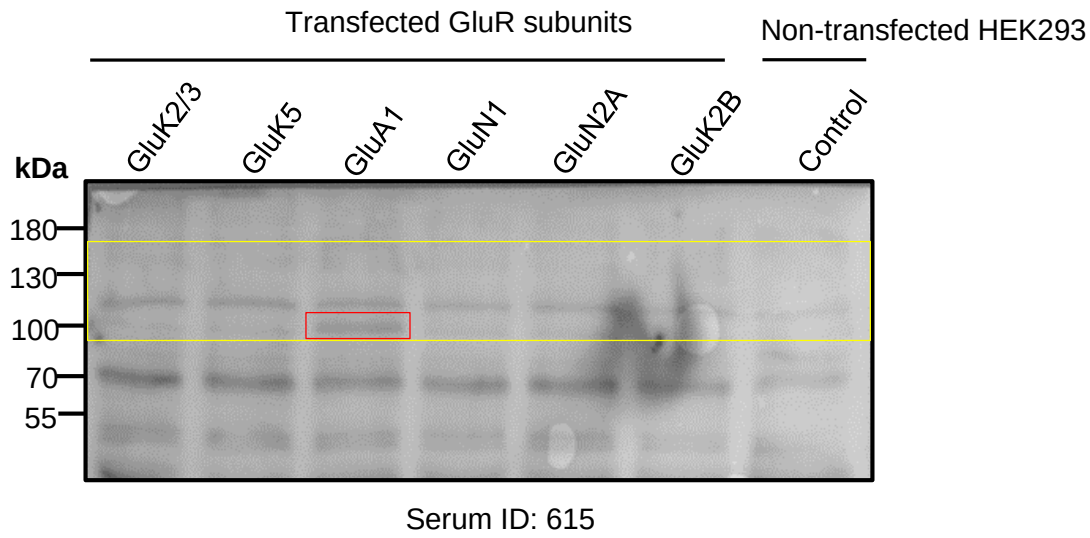

Figure 3.11. Identification of serum that specifically recognise overexpressed GluR subunits in HEK293 cells. Proteins prepared from GluR subunit-transfected HEK293 cells were separated using SDS-PAGE, transferred onto PVDF membrane. The membrane was incubated with test serum (1:200) followed by incubation with HRP-conjugated anti-human IgG secondary antibody. The immunopositive bands were visualised using enhanced chemiluminescence. The region inside the yellow rectangle represents where GluR subunit proteins are expected and the red rectangle indicates an immunopositive band of interest. Sample ID and patient details are shown in tables 3.1-3.2. One experiment was performed.

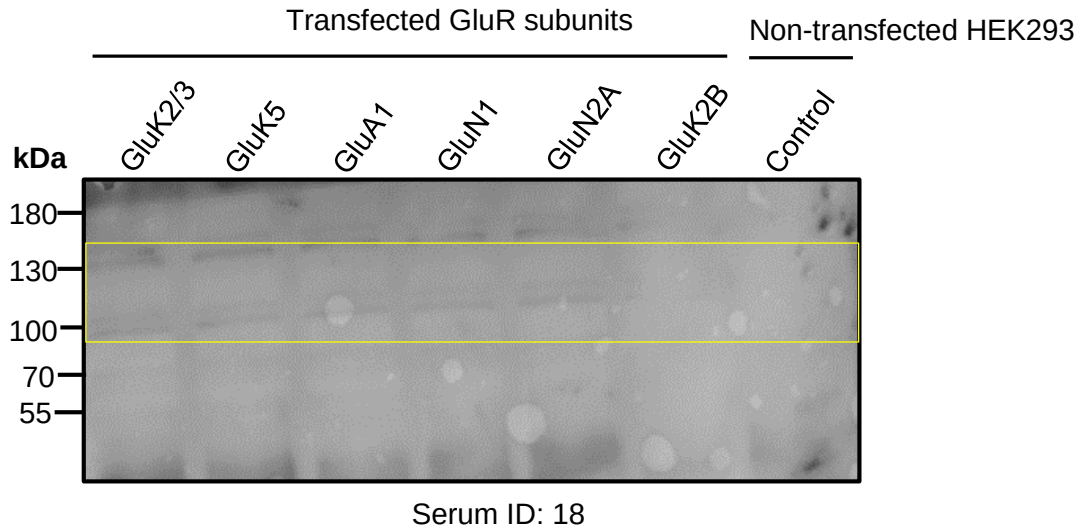

Figure 3.12. Identification of serum that specifically recognise overexpressed GluR subunits in HEK293 cells. Proteins prepared from GluR subunit-transfected HEK293 cells were separated using SDS-PAGE, transferred onto PVDF membrane. The membrane was incubated with test serum (1:200) followed by incubation with HRP-conjugated anti-human IgG secondary antibody. The immunopositive bands were visualised using enhanced chemiluminescence. The region inside the yellow rectangle represents where GluR subunit proteins are expected. Sample ID and patient details are shown in tables 3.1-3.2. One experiment was performed.

On the membrane labelled with serum with sample ID 615, an immunopositive band was present in the GluA1 lane (highlighted in red in Figure 3.11). This band was distinct from the other immunopositive bands. It was suggested from this observation that this immunopositive band could likely be the result of reaction between the overexpressed GluA1 protein and a corresponding antibody in the serum. A look at the patient details (Tables 3.1-3.2) showed that the serum with sample ID 615 is a T1DM patient.

To further investigate this observation, the membrane was stripped of the antibodies by incubating in a stripping buffer (2% SDS, 0.0625 M Tris, pH 6.8, 0.11 M 2-mercaptoethanol). The membrane was then reprobed with anti-pan-AMPAR antibody at 4^{o}C overnight followed by incubation with HRP-conjugated anti-rabbit IgG secondary antibody. The reprobed membrane is shown in Figure 3.13.

A crude method of band position analysis involving measuring the distance from the top of the gel to the middle of the band of interest was utilised. The distances from the top of the gel to the protein ladder markers were also measured. The log of molecular weights of the protein ladder against the distance was plotted to derive an equation (Figure 3.14). The distance measured from the top of the gel to the middle of the band of interest (14 mm) was used in the equation of the curve ($y = -0.38\ln(x) + 3.0457$) to determine the log of molecular weight of the band of interest (2.0428). The anti-log of this figure (approximately 110.2) represented the approximate molecular weight of the band of interest. From literature, the molecular weight of GluA1 is between 100 and 105 kDa (Hoftberger *et al*., 2015). Thus it can be inferred from these observations that immunoblotting of overexpressed GluR proteins with T1DM serum could be used to identify antibodies in serum that react with these GluR proteins.

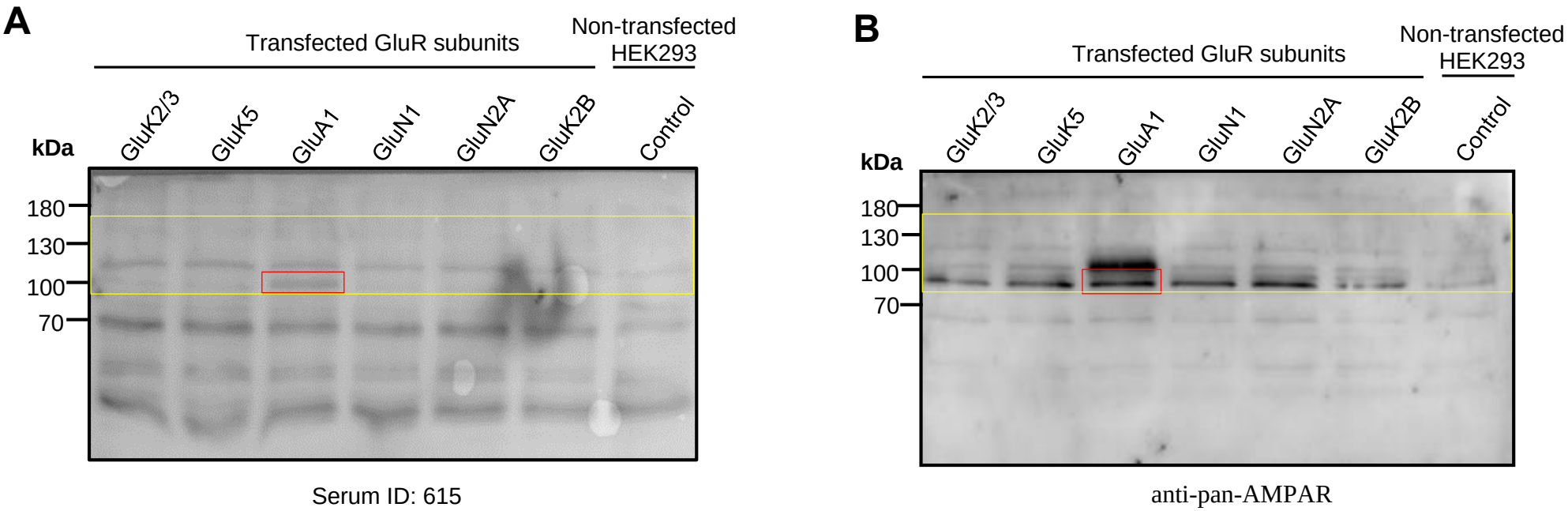

Figure 3.13. Reprobing of membrane of with anti-pan-AMPAR to investigate immunopositive band of interest. The membrane labelled with sample ID 615 (A) was incubated with stripping buffer and labelled with anti-pan-AMPAR antibody followed by incubation with HRP-conjugated anti-rabbit IgG secondary antibody. The immunopositive bands were visualised using enhanced chemiluminescence (B). The band in the red rectangle is the immunopositive band of interest. One experiment was performed.

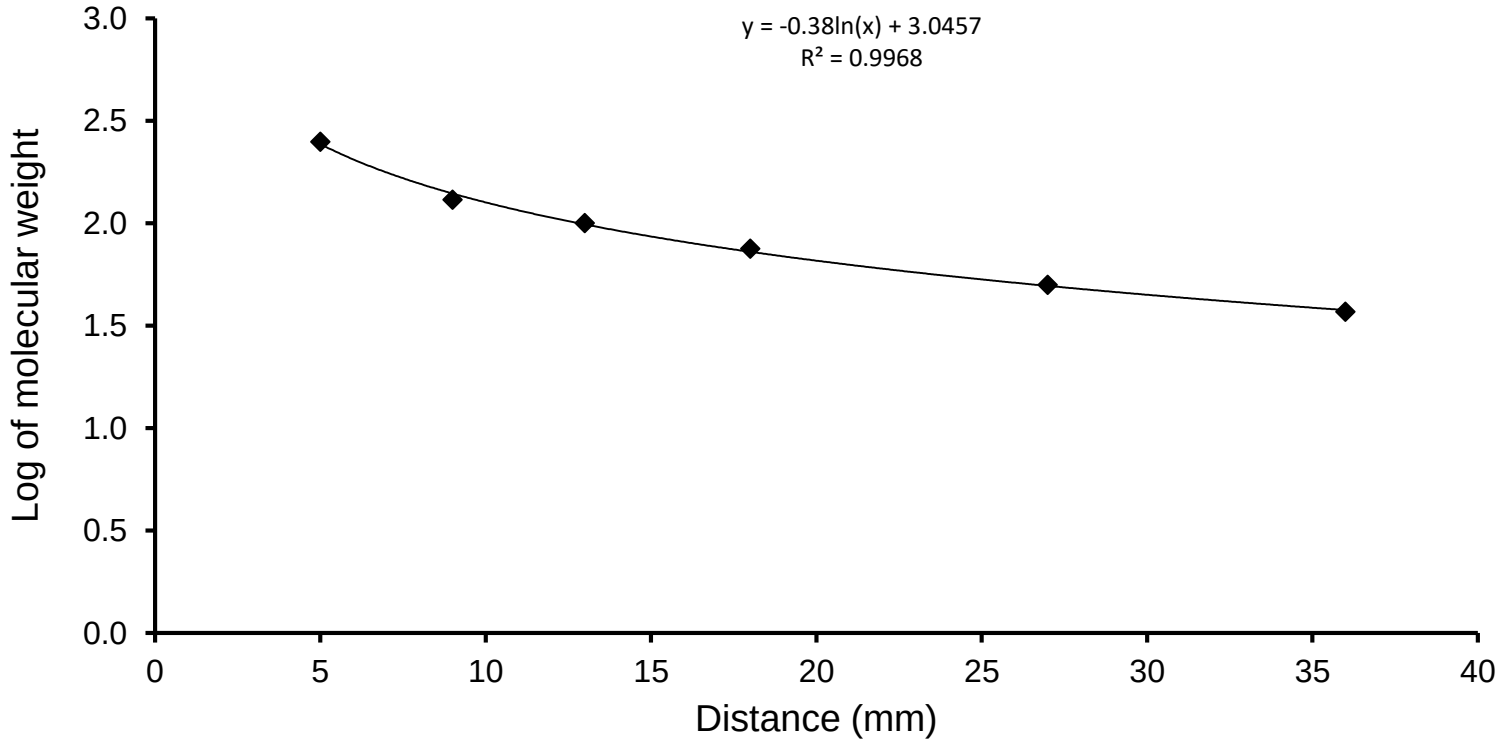

Figure 3.14. Determining the approximate molecular weight of an immunopositive band of interest. The membrane was stripped and reprobed with anti-pan-AMPAR followed by incubation with HRP-conjugated anti-rabbit IgG secondary antibody. The distance of the molecular weight markers from the top of the membrane were plotted against the log of their molecular weights. The equation of the logarithmic trendline was used to calculate the approximate molecular weight of the band of interest.

3.5. Summary of results

The aim of this chapter was to investigate the presence of autoantibodies against GluR subunits in serum of newly-diagnosed T1DM patients. The following is a summary of the results:

- Serum from both T1DM patients and non-diabetic controls reacted with synaptosomal plasma membrane proteins.
- Reaction between SPM proteins and serum samples from T1DM patients or non-diabetic controls in ELISA was useful in selecting samples for further analysis.
- Antibodies in serum from T1DM patients and non-diabetic controls reacted with SPM proteins in the region corresponding to the molecular weight range for GluR proteins. However, this reaction was not specific since other SPM proteins with molecular weights outside the molecular weight range for GluRs were also bound by antibodies in the test serum.
- GluR subunits (GluK2, GluK5, GluA1, GluN1, GluN2A and GluN2B) were expressed when transfected into HEK293 cells.
- Antibodies in serum from T1DM patients and non-diabetic controls reacted with proteins extracted from GluR-transfected HEK293 cells in the region corresponding to the molecular weight range for GluR proteins. However, this reaction was not specific since other immunoreactive bands were present in regions outside the molecular weight range for GluRs.
- The methods used in this chapter (ELISA and immunoblotting) could be further optimised and used in the identification of autoantibodies against GluR proteins.

3.6. Discussion

As discussed previously (Chapter one, section 1.10), there is no existing data to establish a direct link between T1DM and GluR subunit antigens or antibodies (Chapter one, section 1.10). However, previous studies have suggested indirect links between glutamate, GluRs and pathogenesis of T1DM (Chapter one, section 1.10). The investigation of anti-GluR autoantibodies in T1DM patients is essential considering that use of previously-identified T1DM autoantibodies has helped with prediction of the disease but has not helped significantly with prevention (Atkinson *et al*., 2014). Moreover, the well-established autoantigens in T1DM are involved in the secretory pathways and are predominantly located in β-cells hence these autoantigens could not likely be the first to be targeted by the autoimmune process in T1DM (Arvan *et al*., 2012). GluRs on the other hand are transmembrane proteins which could be targeted to initiate an autoimmune process (Willard and Koochekpour, 2013; Lodge, 2009). Thus investigation of autoantibodies to GluRs in T1DM could contribute to our understanding of the autoimmune process in T1DM and also provide significant information about the multifactorial nature of T1DM. Furthermore, results from this current study have shown that functional KAR subunits are present and modulate the functions and survival of pancreatic endocrine cells (Chapter two). Thus, an investigation into possible roles of GluR antigens and autoantibodies in the pathogenesis of T1DM was essential. Thus, this chapter investigated the presence of autoantibodies against KAR and other GluR subunits antigens in serum of newly-diagnosed T1DM patients and also in serum of age-matched non-diabetic controls.

3.6.1. *Reaction between serum from T1DM/controls and GluR-enriched SPM proteins in ELISA can be used to select samples from T1DM and controls for further analysis.*

Reaction between serum of T1DM patients or non-diabetic controls with SPM fraction showed that some serum from both T1DM and control serum reacted with proteins in the synaptosome fraction (Figure 3.3).

SPM fraction was used at this stage because studies have established that this fraction is rich in glutamatergic synaptic proteins including GluRs (Rodriguez-Moreno and Sihra, 2013; Biesemann *et al*., 2014). Synaptosomal preparations have also been used in several studies involving GluRs including identification and control of neurotransmitter release and role of GluRs in calcium ion influx (Rodriguez-Moreno and Sihra, 2013; Sumioka *et al*., 2011; Evans, 2015; Molnar *et al*., 1994).

Moreover, reactions between serum/CSF and crude preparations containing neuronal components has been used in previous studies to select samples that react against neuronal components for further analysis (Nibber *et al*., 2015; Gleichman *et al*., 2014; Fujita *et al*., 2012). For instance, in studies investigating autoantibodies to AMPARs, serum from Rasmussen's encephalitis and anti-AMPAR encephalitis were reacted against primary neuronal cultures to select samples that react against GluRs on the surface of these neurons for further investigations (Nibber *et al*., 2015; Gleichman *et al*., 2014). Another study used reaction between serum of Creutzfeldt–Jakob disease patients and rat hippocampal preparations to select samples which react against neuronal components in the preparation for further investigations to detect autoantibodies against NMDARs in the patients (Fujita *et al*., 2012). Thus, reaction between antibodies in the patient/control samples and glutamatergic synaptic proteins in SPM was useful selecting samples for further analysis in the current study.

Negative control which excluded primary antibody incubation confirmed that the secondary antibody (anti-human) alone did not bind to the SPM proteins. Furthermore, commercially-acquired delipidated human sera reacted with the SPM proteins implying that serum from both diabetic and non-diabetic controls may contain antibodies that react against SPM proteins. This observation does not necessarily indicate that the method used is not specific. In a previous study using ELISA, it was observed that serum from both diabetic patients and some non-diabetic healthy controls show strong immunopositivity with purified pancreatic duodenal homeobox protein 1 (Pdx1), a protein suggested to be a β-cell-specific autoantigen in T1DM (Li *et al*., 2010). Other studies have also shown the presence of autoantibodies against GluR antigens in serum of patients and healthy control individuals. In one study, autoantibodies against GluA3 were present in serum of both Rasmussen's encephalitis patients and health controls (Mantegazza *et al*., 2002). From these observations, it could be concluded that use of GluR-enriched SPM proteins in ELISA can be used to select samples from T1DM and controls for further analysis. However, as a limitation, this method of reacting serum samples and GluR-enriched SPM proteins is not specific for identification of autoantibodies in T1DM.

3.6.2. *Visualisation of the SPM target proteins recognised by the autoantibodies in serum of T1DM patients and non-diabetic controls*

To determine the specific SPM proteins that are targets for antibodies in the serum samples, SPM proteins were separated on a gel and then reacted against human serum in immunoblotting. The results indicate immunopositive bands that corresponds to the molecular weight range for glutamatergic proteins (100-150 kDa). In addition to this, there were bands with molecular weights outside the range of GluR proteins. This was observed in reactions between SPM proteins and both T1DM and non-diabetic controls

(Figure 3.6). This method has been used to detect serum autoantibodies in experimental autoimmune encephalomyelitis rats against myelin proteins in SPM fractions (Degano *et al*., 2004; Pedraza *et al*., 2006). Other studies have used immunoblotting of crude membrane fraction from mouse primary hippocampal neurons with serum to detect NMDA receptor antibodies in herpes simplex encephalitis patients (Pruss *et al*., 2013). Another study used crude homogenates of human basal ganglia to detect anti-basal ganglia antibodies in serum of individuals suffering from idiopathic movement disorders (Church *et al*., 2004). It can be concluded from the results that labelling SPM proteins with serum of T1DM or controls in immunoblot gives information about the nature of the proteins that are targeted by antibodies in the serum samples. Also, information derived from these reactions enabled the selection of serum samples which reacted against SPM proteins in the expected molecular weight range. A limitation of this method is that the immunopositive bands were not specific since in some of the samples, other immunopositive bands were present in regions outside the expected molecular weight range. However, this method was useful in screening and selecting serum samples for further analysis.

3.6.3. *T1DM and control serum samples react with and recognise overexpressed GluR subunits in HEK293 cells.*

This approach was aimed at increasing the sensitivity and specificity of the reaction between GluR antigens and corresponding autoantibodies in the serum of T1DM and control subjects. Immunopositive bands were present in the expected molecular weight range of 100-150kDa (Figures 3.9-3.12). However, there were other bands with molecular weights below or above the expected range which may be indicative non-specific binding. The presence of immunopositive band in the reactions between proteins from GluK2,

GluK5, GluA1 and their corresponding specific antibodies indicates that expression of these three GluR subunits in HEK293 cells was successful. Also, there were no immunopositive bands when proteins from non-transfected HEK293 cells were labelled with these specific antibodies indicating that HEK293 cells do not express native GluR subunits. However, unavailability of antibodies against GluN1, GluN2A and GluN2B in our laboratory meant that we could not verify if these subunits were expressed in HEK293 cells after transfections. Membranes which were incubated with T1DM sera showed more distinct immunopositive bands compared to membranes which were incubated with non-diabetic control serum (Figures 3.9-3.12). This observation may not be representative, since only one control serum was used in the immunoblotting compared to three T1DM sera. A similar method has been used in previous studies in which proteins from GluA1- and GluA2-transfected HEK293 cells were used in immunoblotting to detect autoantibodies in serum of anti-AMPAR encephalitis human patients (Gleichman *et al*., 2014). Another study used protein lysates from GluN1- and GluN2-transfected HEK293 cells to detect autoantibodies to these NMDAR subunits in serum of herpes simplex encephalitis patients using immunoblotting (Pruss *et al*., 2013). Similarly, in a study detect autoantibodies against Pdx1 proteins in serum of T1DM patients, proteins prepared from Pdx1-transfetced cells was separated using SDS-PAGE, transferred onto nitrocellulose membrane and labelled with serum of T1DM and controls (Li *et al*., 2010). However, in contrast to the current study, all three previous studies (Gleichman *et al*., 2014; Pruss *et al*., 2013; Li *et al*., 2010) purified the overexpressed proteins and also purified IgG from the patient serum for the immunoblotting. Thus, the non-specific immunopositive bands observed in this current study may be as result of using non-purified GluR subunit proteins or labelling the proteins with whole serum instead of purified IgG. In spite of these differences, it can be concluded that labelling overexpressed

GluR proteins with test serum can potentially help to determine if autoantibodies against GluRs are present in serum of T1DM and non-diabetic healthy controls provided that steps are taken to reduce non-specific reactions.

The membrane labelled with sample with ID 615 showed a distinct band in the GluA1 lane and was within the expected range of molecular weight for GluRs (Figure 3.11). The lane protein from non-transfected HEK293 cells did not show immunopositive band indicating that the observed immunopositive band in the GluA1-transfected lane could likely be as result of reaction between antibodies in the serum sample and GluA1. Re-probing of the membrane with anti-pan-AMPAR antibody showed that the immunopositive band was very distinct and within the expected molecular weight range for GluA1 protein (100-105) (Figure 3.13). Using a crude method of molecular weight analysis, the molecular weight of the band was estimated to be approximately 109.8 kDa. From literature, the molecular weight of GluA1 is between 100 and 105 kDa (Hoftberger *et al*., 2015). Based on the information available, serum sample 615 is from a 37-year old newly diagnosed T1DM female. Though this could be an indication of the presence of autoantibodies against GluA1 subunit protein in serum of this T1DM patient, no specific or direct conclusions can be made regarding this observation for two reasons. First, another method of detection including radioimmunoassay (Nibber *et al*., 2015), ELISA (Lai *et al*., 2009), immunohistochemistry (Barry *et al*, 2015) and immunofluorescence (Lauvsnes *et al*., 2014) could be used to confirm or verify that the immunopositive band is the result of reaction between GluA1 protein and corresponding autoantibody in the T1DM patient's serum. Secondly, autoantibodies against GluA1 subunit protein has been detected in serum of individuals suffering from anti-AMPAR encephalitis (Gleichman *et al*., 2014; Lai *et al*., 2009). Thus, detection of autoantibody against GluA1 antigen in the serum of the T1DM patient could potentially be as a result of T1DM and anti-AMPAR

encephalitis comorbidity. The likelihood of this comorbidity could not be investigated since there was not sufficient clinical information or medical history available for the T1DM patients whose sera were used in this study.

3.7. Conclusion

The primary aim of this part of the study was to determine if autoantibodies against KAR and other GluR subunits are present in serum of T1DM patients. By using SPM fractions and proteins from HEK293 cells transfected with GluR subunits as antigen targets, some of the serum samples from both T1DM and non-diabetic controls were shown to react against these antigen targets. Though some technical challenges including non-specific binding between antibodies and the target proteins were identified, the methods of autoantibody identification used in this study were useful in selecting test samples that reacted against proteins in SPM preparations as well as showing potential for detection of autoantibodies against over-expressed GluR subunits in HEK293 cell lines. Due to time-constraints, only four out of the selected thirty-four test samples were tested for presence of autoantibodies to overexpressed GluR subunits. Thus, there is the need for further optimisation of the techniques and for more samples to be tested.

Chapter Four

Thesis Discussion

4.1. Discussion

This study addressed three main areas; first, the identification of KAR subunits in pancreatic endocrine cells. The study identified four KAR subunits (GluK2, GluK3, GluK4, GluK5) in α- and β-cells and all five subunits (GluK1-5) in islets of Langerhans. In addition, the study showed that Neto 1 and Neto 2 auxiliary proteins are present in α- and β-cells and rat primary islets of Langerhans. Furthermore, this is the first study to show a preferential expression of Neto 1 for α-cells and Neto 2 for β-cells of the pancreas. Few studies have reported of KARs in the endocrine pancreas (Molnar *et al*., 1995; Inagaki *et al*., 1995; Gonoi *et al*, 1994; Cabrera *et al*., 2008; Weaver *et al*., 1996). In addition to contrasting observations from these previous studies, many questions remained unresolved about the specific molecular characterisation of these receptors. For instance, only GluK5 protein has previously been identified in pancreatic β-cells (Molnar *et al*., 1995). Thus, results from this current study has provided sufficient information to address these unresolved questions about KARs in pancreatic endocrine cells and has also show that functional homomeric or heteromeric units of KARs could assemble in α- and β-cells of the pancreas. The successful identification of KAR subunits and auxiliary proteins in pancreatic endocrine cells supports previous suggestions of similarities between cells of the endocrine pancreas and the CNS (Del Rosario *et al*., 2015; Marquard *et al*., 2015; Di Cairano *et al*., 2011; Cheng *et al*., 2015; Hanson *et al*., 2015) and also provide new insights into non-neuronal expression of KARs.

The second area which was addressed by this current study is the role of KARs in regulation of the $[Ca^{2+}]_i$ and GSIS in β-cells as well as the effect of KAR agonists on the

viability of α- and β-cells. The results show that activation of KARs by kainate results in increased $[Ca^{2+}]_i$ and GSIS in β-cells. Results from previous studies were inconclusive regarding how KAR activation affect $[Ca^{2+}]_i$ and GSIS in β-cells (Molnar *et al*., 1995; Inagaki *et al*., 1995; Gonoi *et al*, 1994) due to contrasting observations. Thus, results from this current study provides significant evidence for the important role of KARs pancreatic β-cell physiology. Furthermore, this study is the first to observe that prolonged exposure of α- and β-cells to kainate significantly reduce viability of these cells. The observation that prolonged activation of KARs by glutamate significantly reduces viability of β-cells supports previous observations (Di Cairano *et al*., 2011). However, the observation that prolonged exposure to glutamate causes significant reduction in viability of α-cells is in contrast to previous reports (Di Cairano *et al*., 2011). Thus results from this current study provides significant evidence to show that similar to neurons and other cells of the CNS, pancreatic endocrine cells are vulnerable to prolonged exposure to glutamate and other agonists of KARs.

In conclusion, results from previous studies have remained inconclusive regarding the molecular characterisation and function of KAR subunits in pancreatic cells. However, based on the confirmatory and novel observations from this current study, it can be concluded that functional homomeric and heteromeric units of KARs are present and can assemble in pancreatic endocrine cells. In addition, it can be concluded that similar to observations in the CNS, KARs play significant role in the function and survival of pancreatic endocrine cells. Thus, the presence of β-cell KARs should be considered when therapies are being developed to target neuronal KARs with the aim of managing neurological conditions since these therapies could potentially have beneficial or deleterious effects on pancreatic endocrine cells. Moreover, results from this study has contributed to understanding why antidiabetic drugs such as exenatide and glitazones

possess neuroprotective properties (Cunha *et al*., 2009; Tsunekawa *et al*., 2007) or why anti-epileptic drugs such as topiramate which attenuates glutamate-induced excitotoxicity also have antidiabetic properties and preserve β-cell survival and function (Davalli *et al*., 2012; Toplak *et al*., 2007; Angehagen *et al*., 2003). Thus, β-cell KARs could be considered as potential targets in the management or treatment of diabetes mellitus. In the same vein, it can be concluded based on novel results from this current study that significant considerations must be taken regarding the consumption of glutamate-rich food supplements and other salts of glutamate since these products have the potential to increase blood glutamate concentration resulting in exposure α- and β-cell KARs to increased plasma glutamate with potentially deleterious effects.

GluRs have been shown to be autoantibody targets in a number of autoimmune neurological conditions (Nibber *et al*., 2016; Lancaster, 2016). Thus, the third part of this study investigated the role of GluR antigens as potential targets of the autoimmune process in T1DM. Several procedures and techniques for the detection of anti-GluR autoantibodies in serum was used in this study and different techniques were optimised to identify autoantibodies in serum of T1DM patients and non-diabetic controls. The results showed indications that ELISA and immunoblotting using SPM proteins and overexpressed GluR proteins could be used to detect serum autoantibodies that react against GluR subunits in serum of patients. Thus, this is an area of further research.

4.2. Future work

4.2.1. *KARs in pancreatic endocrine cells*

Previous studies have shown that in isolated neurons and mouse models, Neto 1 and Neto 2 enhances the expression of GluK2 and GluK5 subunits (Sheng *et al*., 2015; Copits *et al*., 2011). Thus, in future studies, the amount of KAR subunit mRNA and proteins can be measured in α- and β-cells after Neto 1 and Neto 2 genes have been silenced. This will help to assess how auxiliary subunits proteins affect the surface expression of KARs in pancreatic endocrine cells. The presence of GluK1 mRNA and protein in pancreatic δ-cells and PP cells could also be investigated in future works to understand why GluK1 is expressed in the islets of Langerhans but not in α- cells or β-cells.

4.2.2. *Calcium imaging and glucose-stimulated insulin secretion*

In the current study, kainate was applied to MIN6 β-cells for two minutes and there was sustained rise in $[Ca^{2+}]_i$. In previous studies (Inagaki *et al*., 1995; Gonoi *et al,* 1994), kainate was applied to MIN6 β-cells for 40 seconds and then for 10-15 minutes. In both applications, there was sustained rise in $[Ca^{2+}]_i$. Sustained rise in $[Ca^{2+}]_i$ subsequent to application of kainate for a relatively long period could be due to sustained KAR activation and slow onset of desensitisation. Previous studies have suggested that KAR desensitisation is dependent on several factors including physicochemical properties of bound ligands as well as receptor internalisation (Dawe *et al*., 2013). Neto 1 and Neto 2 have been shown to enhances the surface expression of KARs particularly GluK2 (Sheng *et al*., 2015; Zhang *et al*., 2009) while Neto 2 slows onset of KAR desensitisation (Griffith and Swanson, 2015; Straub *et al*., 2011b; Zhang *et al*., 2009). Thus future studies could explore how silencing Neto 1 and Neto 2 could affect the response of β-cells or islets of Langerhans to sustained application of kainate. The idea behind this will be to determine

if Neto 1 and Neto 2 in β-cells play specific roles in agonist binding, onset of desensitisation or recovery from desensitisation of β-cell KARs. This could be determined by silencing Neto 1 and Neto 2 and then investigating how application of kainate for a relatively prolonged period (5-15 minutes) affect $[Ca^{2+}]_i$ and GSIS. The results from this study would provide more insights into mechanisms underlying the role of KARs and its auxiliary proteins in pancreatic β-cells.

4.2.3. *Detection of anti-GluR autoantibodies in serum of T1DM patients*

The serum samples used in this current study were from newly-diagnosed T1DM. In a previous study investigating the presence of autoantibodies against Pdx1 proteins in serum of T1DM patients and non-obese diabetic mice (Li *et al*., 2010), it was observed that levels of anti-Pdx1 autoantibodies in NOD mice were higher before onset of diabetes but reduced significantly or became undetectable after disease onset. The titres of other autoantibodies implicated in T1DM (IA-2, GAD65, insulin and ZnT8) have been shown to fluctuate before and after the onset of diabetes (Bonifacio, 2015; Mannering *et al*., 2015; Morran *et al*., 2015). Thus, it could be suggested that the presence and titres of autoantibodies against GluR antigens in serum of T1DM patients could be dependent on the stage of the disease. Thus, in addition to samples from newly-diagnosed T1DM patients, future work could include serum samples from individuals at different stages on T1DM as well as from individuals who are genetically at risk of developing T1DM.

To reduce background noise and increase sensitivity of the immunoblotting, GluR subunit proteins prepared from transfected HEK293 cells could be purified using protein tags such polyhistidine or FLAG-tags. This technique has been used to purify AMPAR proteins from transiently-transfected HEK293 cells in studies investigating presence of anti-AMPAR antibodies in CSF and serum (Gill and Madden, 2008; Shanks *et al*., 2014).

Furthermore, antibody purification methods could be used to enrich and concentrate antibodies from serum of T1DM and control subjects and used in both ELISA and immunoblotting. Though this method will require significantly large sample volume, this could potentially increase sensitivity of the technique and reduce background noise. Antibody purification methods have been used in previous studies where autoantibodies to GluR subunit proteins were investigated in serum and CSF of patients suffering from anti-NMDAR and anti-AMPAR encephalitis (Manto *et al*., 2010; Gleichman *et al*., 2014; Hughes *et al*., 2010). These methods enabled the use of several different methods to detect GluR subunit proteins.

Furthermore, in previous studies investigating autoantibodies against AMPAR subunits in patients with Rasmussen's Encephalitis (RE), there was no reactivity between RE serum samples and HEK293 cells which had been singly-transfected with AMPAR subunits (GluA1, GluA2, GluA3) (Nibber *et al*., 2015). However, there was reactivity between some of the RE serum samples and HEK293 cells co-transfected with GluA2 and GluA3 (Nibber *et al*., 2015). This implies that the antigenic epitope targeted by the autoantibodies is formed by contributions of the two AMPAR subunits (GluA2 and GluA3). Thus, a similar phenomenon or mechanism could be present in reactivity between autoantibodies in T1DM and GluR subunits whereby the antigenic epitope is formed or made stable as result of contribution of two or more subunits. For future works, HEK293 cells could be co-transfected with receptor combinations (GluK2/GluK5 for instance) and then reacted against the T1DM serum samples.

In addition, in future studies, immunopositive bands from the reaction between GluR subunit proteins and serum could be investigated further using mass spectroscopy to confirm if these bands contain sequences of the expected GluR subunit. This approach has been used to confirm autoantibodies to AMPAR in serum of patients suffering from

limbic encephalitis (Lai *et al*., 2009) and anti-NMDAR encephalitis (Gleichman *et al*., 2012). However, confirmation of immunopositive bands could only be done after the immunoblotting technique has been optimised.

Several issues remain unresolved with regards to the nature and mechanism of autoimmune T1DM. Mechanisms by which immune tolerance to β-cell antigens is compromised remain unclear. Moreover, the observation that all the autoantigen candidates in T1DM are intracellular present suggest that further studies are required to determine if a surface antigen is first targeted in the initial stages of the disease before the intracellular antigens are exposed to the immune system. This is essential to understand fully the autoimmune mechanisms of the disease and develop potential therapeutic and preventative strategies for T1DM.

Chapter Five

References

- Abd El-Aziz, S.A. and El-Serogy, H. (2013) Antinuclear antibodies and glutamic acid decarboxylase antibodies in children with refractory epilepsy. *Egyptian Pediatric Association Gazette*. 61 (1), pp.46-51.
- Aller, M.I., Pecoraro, V., Paternain, A.V., Canals, S. and Lerma, J. (2015) Increased Dosage of High-Affinity Kainate Receptor Gene grik4 Alters Synaptic Transmission and Reproduces Autism Spectrum Disorders Features. *The Journal of Neuroscience*. 35 (40), pp.13619-13628.
- Almasi, S., Aliparasti, M.R., Aliasgarzadeh, A., Abd-Nikfarjam, B., Hyoty, H., Knip, M., Feizi, H., Sioofy-Khojine, A. and Rahnama, B. (2015) Investigation of CTLA-4-318C/T gene polymorphism in cases with type 1 diabetes of Azerbaijan, Northwest Iran. *Immunology Letters*. 166 (2), pp.134-139.
- Amalric, M. (2015) Targeting metabotropic glutamate receptors (mGluRs) in Parkinson's disease. *Current Opinion in Pharmacology*. 20 pp.29-34.
- Amisten, S., Salehi, A., Rorsman, P., Jones, P.M. and Persaud, S.J. (2013) An atlas and functional analysis of G-protein coupled receptors in human islets of Langerhans. *Pharmacology & Therapeutics*. 139 (3), pp.359-391.
- Anderson, M., Suh, J.M., Kim, E.Y. and Dryer, S.E. (2011) Functional NMDA receptors with atypical properties are expressed in podocytes. *American Journal of Physiology-Cell Physiology*. 300 (1), pp.C22-C32.
- Andersson, L.E., Valtat, B., Bagge, A., Sharoyko, V.V., Nicholls, D.G., Ravassard, P., Scharfmann, R., Spegel, P. and Mulder, H. (2015) Characterization of stimulus-secretion coupling in the human pancreatic EndoC-betaH1 beta cell line. *PloS One*. 10 (3), pp.e0120879.
- Andrade-Talavera, Y., Feria, P.D., Negrete-Diaz, J.V., Sihra, T.S. and Rodriguez-Moreno, A. (2012) Presynaptic kainate receptor-mediated facilitation of glutamate release involves calcium-calmodulin at mossy fiber-CA3 synapses. *Febs Journal*. 279 pp.139-139.

- Andrianesis, V. and Doupis, J. (2013) The role of kidney in glucose homeostasis--SGLT2 inhibitors, a new approach in diabetes treatment. *Expert Review of Clinical Pharmacology*. 6 (5), pp.519-539.
- Angehagen, M., Ben-Menachem, E., Ronnback, L. and Hansson, E. (2003) Topiramate protects against glutamate- and kainate-induced neurotoxicity in primary neuronal-astroglial cultures. *Epilepsy Research*. 54 (1), pp.63-71.
- Anu, J., Peeyush Kumar, T., Nandhu, M.S. and Paulose, C.S. (2010) Enhanced NMDAR1, NMDA2B and mGlu5 receptors gene expression in the cerebellum of insulin induced hypoglycaemic and streptozotocin induced diabetic rats. *European Journal of Pharmacology*. 630 (1-3), pp.61-68.
- Artinian, J., Peret, A., Marti, G., Epsztein, J. and Crepel, V. (2011) Synaptic kainate receptors in interplay with INaP shift the sparse firing of dentate granule cells to a sustained rhythmic mode in temporal lobe epilepsy. *The Journal of Neuroscience*. 31 (30), pp.10811-10818.
- Arvan, P., Pietropaolo, M., Ostrov, D. and Rhodes, C.J. (2012) Islet Autoantigens: Structure, Function, Localization, and Regulation. *Cold Spring Harbor Perspectives in Biology*. 4 (9), pp.a007658.
- Ashcroft, F.M. and Rorsman, P. (2012) Diabetes mellitus and the beta cell: the last ten years. *Cell*. 148 (6), pp.1160-1171.
- Atkinson, M.A., Eisenbarth, G.S. and Michels, A.W. (2014) Type 1 diabetes. *Lancet*. 383 (9911), pp.69-82.
- Babic, T., Browning, K.N., Kawaguchi, Y., Tang, X. and Travagli, R.A. (2012) Pancreatic insulin and exocrine secretion are under the modulatory control of distinct subpopulations of vagal motoneurones in the rat. *The Journal of Physiology*. 590 (Pt 15), pp.3611-3622.
- Balfe, M., Doyle, F., Smith, D., Sreenan, S., Brugha, R., Hevey, D. and Conroy, R. (2013) What's distressing about having type 1 diabetes? A qualitative study of young adults' perspectives. *BMC Endocrine Disorders*. 13 pp.25.
- Balkowiec-Iskra, E., Vermehren-Schmaedick, A. and Balkowiec, A. (2011) Tumor necrosis factor-alpha increases brain-derived neurotrophic factor expression in

trigeminal ganglion neurons in an activity-dependent manner. *Neuroscience*. 180 pp.322-333.

- Barry, H., Byrne, S., Barrett, E., Murphy, K.C. and Cotter, D.R. (2015) Anti-N-methyl-d-aspartate receptor encephalitis: review of clinical presentation, diagnosis and treatment. *BJPsych Bulletin*. 39 (1), pp.19-23.
- Bellamy, L., Casas, J.P., Hingorani, A.D. and Williams, D. (2009) Type 2 diabetes mellitus after gestational diabetes: a systematic review and meta-analysis. *Lancet*. 373 (9677), pp.1773-1779.
- Bellin, M.D., Barton, F.B., Heitman, A., Harmon, J.V., Kandaswamy, R., Balamurugan, A.N., Sutherland, D.E., Alejandro, R. and Hering, B.J. (2012) Potent induction immunotherapy promotes long-term insulin independence after islet transplantation in type 1 diabetes. *American Journal of Transplantation*. 12 (6), pp.1576-1583.
- Benner, C., van der Meulen, T., Caceres, E., Tigyi, K., Donaldson, C.J. and Huising, M.O. (2014) The transcriptional landscape of mouse beta cells compared to human beta cells reveals notable species differences in long non-coding RNA and protein-coding gene expression. *BMC Genomics*. 15 pp.620-2164-15-620.
- Bertrand, G., Gross, R., Puech, R., Loubatieres-Mariani, M.M. and Bockaert, J. (1992) Evidence for a glutamate receptor of the AMPA subtype which mediates insulin release from rat perfused pancreas. *British Journal of Pharmacology*. 106 (2), pp.354-359.
- Biesemann, C., Gronborg, M., Luquet, E., Wichert, S.P., Bernard, V., Bungers, S.R., Cooper, B., Varoqueaux, F., Li, L., Byrne, J.A., Urlaub, H., Jahn, O., Brose, N. and Herzog, E. (2014) Proteomic screening of glutamatergic mouse brain synaptosomes isolated by fluorescence activated sorting. *The EMBO Journal*. 33 (2), pp.157-170.
- Black, M.H., Watanabe, R.M., Trigo, E., Takayanagi, M., Lawrence, J.M., Buchanan, T.A. and Xiang, A.H. (2013) High-fat diet is associated with obesity-mediated insulin resistance and beta-cell dysfunction in Mexican Americans. *The Journal of Nutrition*. 143 (4), pp.479-485.

- Blanc, F., Ruppert, E., Kleitz, C., Valenti, M.P., Cretin, B., Humbel, R.L., Honnorat, J., Namer, I.J., Hirsch, E., Manning, L. and de Seze, J. (2009) Acute limbic encephalitis and glutamic acid decarboxylase antibodies: a reality? *Journal of the Neurological Sciences*. 287 (1-2), pp.69-71.
- Bonfardin, V.D., Fossat, P., Theodosis, D.T. and Oliet, S.H. (2010) Glia-dependent switch of kainate receptor presynaptic action. *The Journal of Neuroscience*. 30 (3), pp.985-995.
- Bonifacio, E. (2015) Predicting type 1 diabetes using biomarkers. *Diabetes Care*. 38 (6), pp.989-996.
- Bonnet, C.S., Williams, A.S., Gilbert, S.J., Harvey, A.K., Evans, B.A. and Mason, D.J. (2015) AMPA/kainate glutamate receptors contribute to inflammation, degeneration and pain related behaviour in inflammatory stages of arthritis. *Annals of the Rheumatic Diseases*. 74 (1), pp.242-251.
- Boonnate, P., Waraasawapati, S., Hipkaeo, W., Pethlert, S., Sharma, A., Selmi, C., Prasongwattana, V. and Cha'on, U. (2015) Monosodium Glutamate Dietary Consumption Decreases Pancreatic beta-Cell Mass in Adult Wistar Rats. *PloS One*. 10 (6), pp.e0131595.
- Bosco, D., Armanet, M., Morel, P., Niclauss, N., Sgroi, A., Muller, Y.D., Giovannoni, L., Parnaud, G. and Berney, T. (2010) Unique arrangement of alpha- and beta-cells in human islets of Langerhans. *Diabetes*. 59 (5), pp.1202-1210.
- Bowie, D. (2008) Ionotropic glutamate receptors & CNS disorders. *CNS & Neurological Disorders Drug Targets*. 7 (2), pp.129-143.
- Bramswig, N.C., Everett, L.J., Schug, J., Dorrell, C., Liu, C., Luo, Y., Streeter, P.R., Naji, A., Grompe, M. and Kaestner, K.H. (2013) Epigenomic plasticity enables human pancreatic alpha to beta cell reprogramming. *The Journal of Clinical Investigation*. 123 (3), pp.1275-1284.
- Brereton, M.F., Iberl, M., Shimomura, K., Zhang, Q., Adriaenssens, A.E., Proks, P., Spiliotis, I.I., Dace, W., Mattis, K.K., Ramracheya, R., Gribble, F.M., Reimann, F., Clark, A., Rorsman, P. and Ashcroft, F.M. (2014) Reversible changes in pancreatic islet structure and function produced by elevated blood glucose. *Nature Communications*. 5 pp.4639.

- Brice, N.L., Varadi, A., Ashcroft, S.J.H. and Molnar, E. (2002) Metabotropic glutamate and GABA (B) receptors contribute to the modulation of glucose-stimulated insulin secretion in pancreatic beta cells. *Diabetologia. Pp.* 45 pp.242-252.
- Briley, P.A., Kouyoumdjian, J.C., Haidamous, M. and Gonnard, P. (1979) Effect of L-glutamate and kainate on rat cerebellar cGMP levels in vivo. *European Journal of Pharmacology*. 54 (1-2), pp.181-184.
- Brozzi, F., Diraison, F., Lajus, S., Rajatileka, S., Philips, T., Regazzi, R., Fukuda, M., Verkade, P., Molnar, E. and Varadi, A. (2012) Molecular mechanism of myosin Va recruitment to dense core secretory granules. *Traffic*. 13 (1), pp.54-69.
- Bush, N.C., Chandler-Laney, P.C., Rouse, D.J., Granger, W.M., Oster, R.A. and Gower, B.A. (2011) Higher maternal gestational glucose concentration is associated with lower offspring insulin sensitivity and altered beta-cell function. *The Journal of Clinical Endocrinology and Metabolism*. 96 (5), pp.E803-9.
- Bustin, S.A. and Nolan, T. (2004) Pitfalls of quantitative real-time reverse-transcription polymerase chain reaction. *Journal of Biomolecular Techniques*. 15 (3), pp.155-166.
- Cabrera, O., Jacques-Silva, M.C., Speier, S., Yang, S.N., Kohler, M., Fachado, A., Vieira, E., Zierath, J.R., Kibbey, R., Berman, D.M., Kenyon, N.S., Ricordi, C., Caicedo, A. and Berggren, P.O. (2008) Glutamate is a positive autocrine signal for glucagon release. *Cell Metabolism*. 7 (6), pp.545-554.
- Caiati, M.D., Sivakumaran, S. and Cherubini, E. (2010) In the developing rat hippocampus, endogenous activation of presynaptic kainate receptors reduces GABA release from mossy fiber terminals. *The Journal of Neuroscience*. 30 (5), pp.1750-1759.
- Campbell, J.E. and Drucker, D.J. (2015) Islet alpha cells and glucagon--critical regulators of energy homeostasis. *Nature Reviews Endocrinology*. 11 (6), pp.329-338.
- Cannarsa, R., Landuzzi, D., Cavina, C., Candeletti, S. and Romualdi, P. (2008) Kainic acid down-regulates NOP receptor density and gene expression in human

neuroblastoma SH-SY5Y cells. *Journal of Molecular Neuroscience:* 35 (2), pp.171-177.

- Cantley, J. and Ashcroft, F.M. (2015) Q&A: insulin secretion and type 2 diabetes: why do beta-cells fail? *BMC Biology*. 13 pp.33-015-0140-6.
- Cardwell, C.R., Stene, L.C., Joner, G., Davis, E.A., Cinek, O., Rosenbauer, J., Ludvigsson, J., Castell, C., Svensson, J., Goldacre, M.J., Waldhoer, T., Polanska, J., Gimeno, S.G.A., Chuang, L.-., Parslow, R.C., Wadsworth, E.J.K., Chetwynd, A., Pozzilli, P., Brigis, G., Urbonaite, B., Sipetic, S., Schober, E., Ionescu-Tirgoviste, C., de Beaufort, C.E., Stoyanov, D., Buschard, K. and Patterson, C.C. (2010) Birthweight and the risk of childhood-onset type 1 diabetes: a meta-analysis of observational studies using individual patient data. *Diabetologia*. 53 (4), pp.641-651.
- Cardwell, C.R., Stene, L.C., Joner, G., Bulsara, M.K., Cinek, O., Rosenbauer, J., Ludvigsson, J., Jane, M., Svensson, J., Goldacre, M.J., Waldhoer, T., Jarosz-Chobot, P., Gimeno, S.G.A., Chuang, L., Parslow, R.C., Wadsworth, E.J.K., Chetwynd, A., Pozzilli, P., Brigis, G., Urbonaite, B., Sipetic, S., Schober, E., Devoti, G., Ionescu-Tirgoviste, C., de Beaufort, C.E., Stoyanov, D., Buschard, K. and Patterson, C.C. (2010) Maternal Age at Birth and Childhood Type 1 Diabetes: A Pooled Analysis of 30 Observational Studies. *Diabetes*. 59 (2), pp.486-494.
- Cardwell, C.R., Stene, L.C., Joner, G., Bulsara, M.K., Cinek, O., Rosenbauer, J., Ludvigsson, J., Svensson, J., Goldacre, M.J., Waldhoer, T., Jarosz-Chobot, P., Gimeno, S.G.A., Chuang, L., Roberts, C.L., Parslow, R.C., Wadsworth, E.J.K., Chetwynd, A., Brigis, G., Urbonaite, B., Sipetic, S., Schober, E., Devoti, G., Ionescu-Tirgoviste, C., de Beaufort, C.E., Stoyanov, D., Buschard, K., Radon, K., Glatthaar, C. and Patterson, C.C. (2011) Birth order and childhood type 1 diabetes risk: a pooled analysis of 31 observational studies. *International Journal of Epidemiology*. 40 (2), pp.363-374.
- Cardwell, C.R., Stene, L.C., Ludvigsson, J., Rosenbauer, J., Cinek, O., Svensson, J., Perez-Bravo, F., Memon, A., Gimeno, S.G., Wadsworth, E.J.K., Strotmeyer, E.S., Goldacre, M.J., Radon, K., Chuang, L., Parslow, R.C., Chetwynd, A., Karavanaki, K., Brigis, G., Pozzilli, P., Urbonaite, B., Schober, E., Devoti, G., Sipetic, S., Joner,

G., Ionescu-Tirgoviste, C., de Beaufort, C.E., Harrild, K., Benson, V., Savilahti, E., Ponsonby, A., Salem, M., Rabiei, S. and Patterson, C.C. (2012) Breast-Feeding and Childhood-Onset Type 1 Diabetes A pooled analysis of individual participant data from 43 observational studies. *Diabetes Care*. 35 (11), pp.2215-2225.

- Carlin, R.K., Grab, D.J., Cohen, R.S. and Siekevitz, P. (1980) Isolation and characterization of postsynaptic densities from various brain regions: enrichment of different types of postsynaptic densities. *The Journal of Cell Biology*. 86 (3), pp.831-845.
- Carobbio, S., Frigerio, F., Rubi, B., Vetterli, L., Bloksgaard, M., Gjinovci, A., Pournourmohammadi, S., Herrera, P.L., Reith, W., Mandrup, S. and Maechler, P. (2009) Deletion of glutamate dehydrogenase in beta-cells abolishes part of the insulin secretory response not required for glucose homeostasis. *The Journal of Biological Chemistry*. 284 (2), pp.921-929.
- Carta, M., Fievre, S., Gorlewicz, A. and Mulle, C. (2014) Kainate receptors in the hippocampus. *The European Journal of Neuroscience*. 39 (11), pp.1835-1844.
- Cerf, M.E. (2013) Beta cell dysfunction and insulin resistance. *Frontiers in Endocrinology*. 4 pp.37.
- Chater, T.E. and Goda, Y. (2014) The role of AMPA receptors in postsynaptic mechanisms of synaptic plasticity. *Frontiers in Cellular Neuroscience*. 8 pp.401.
- Cheng, K., Delghingaro-Augusto, V., Nolan, C.J., Turner, N., Hallahan, N., Andrikopoulos, S. and Gunton, J.E. (2012) High Passage MIN6 Cells Have Impaired Insulin Secretion with Impaired Glucose and Lipid Oxidation. *Plos One*. 7 (7), pp.e40868.
- Cheng, Q., Diez Beltran, V., Chan, S.M., Brown, J.R., Bevington, A. and Herbert, T.P. (2015) System-L amino acid transporters play a key role in pancreatic beta-cell signalling and function. *Journal of Molecular Endocrinology*. 56 (3), pp.175-187.
- Cheng, X.L., Ding, F., Li, H., Tan, X.Q., Liu, X., Cao, J.M. and Gao, X. (2015) Activation of AMPA receptor promotes TNF-alpha release via the ROS-cSrc-NFkappaB signaling cascade in RAW264.7 macrophages. *Biochemical and Biophysical Research Communications*. 461 (2), pp.275-280.

- Chew, L.J., Yuan, X., Scherer, S.E., Qie, L., Huang, F., Hayes, W.P. and Gallo, V. (2001) Characterization of the rat GRIK5 kainate receptor subunit gene promoter and its intragenic regions involved in neural cell specificity. *The Journal of Biological Chemistry*. 276 (45), pp.42162-42171.
- Chiodo, F., Marradi, M., Tefsen, B., Snippe, H., van Die, I. and Penades, S. (2013) High sensitive detection of carbohydrate binding proteins in an ELISA-solid phase assay based on multivalent glyconanoparticles. *PloS One*. 8 (8), pp.e73027.
- Chittajallu, R., Vignes, M., Dev, K.K., Barnes, J.M., Collingridge, G.L. and Henley, J.M. (1996) Regulation of glutamate release by presynaptic kainate receptors in the hippocampus. *Nature*. 379 (6560), pp.78-81.
- Cho, J.H., Chen, L., Kim, M.H., Chow, R.H., Hille, B. and Koh, D.S. (2010) Characteristics and functions of {alpha}-amino-3-hydroxy-5-methyl-4-isoxazolepropionate receptors expressed in mouse pancreatic {alpha}-cells. *Endocrinology*. 151 (4), pp.1541-1550.
- Cho, K., Francis, J.C., Hirbec, H., Dev, K., Brown, M.W., Henley, J.M. and Bashir, Z.I. (2003) Regulation of kainate receptors by protein kinase C and metabotropic glutamate receptors. *The Journal of Physiology*. 548 (Pt 3), pp.723-730.
- Cho, K.O., Hunt, C.A. and Kennedy, M.B. (1992) The rat brain postsynaptic density fraction contains a homolog of the Drosophila discs-large tumor suppressor protein. *Neuron*. 9 (5), pp.929-942.
- Choudhuri, S.P., Delay, R.J. and Delay, E.R. (2016) Metabotropic glutamate receptors are involved in the detection of IMP and l-amino acids by mouse taste sensory cells. *Neuroscience*. 316, pp.94-108.
- Christensen, G.L., Jacobsen, M.L., Wendt, A., Mollet, I.G., Friberg, J., Frederiksen, K.S., Meyer, M., Bruun, C., Eliasson, L. and Billestrup, N. (2015) Bone morphogenetic protein 4 inhibits insulin secretion from rodent beta cells through regulation of calbindin1 expression and reduced voltage-dependent calcium currents. *Diabetologia*. 58 (6), pp.1282-1290.
- Chung, C.H., Hao, E., Piran, R., Keinan, E. and Levine, F. (2010) Pancreatic beta-cell neogenesis by direct conversion from mature alpha-cells. *Stem Cells*. 28 (9), pp.1630-1638.

- Church, A.J., Dale, R.C. and Giovannoni, G. (2004) Anti-basal ganglia antibodies: a possible diagnostic utility in idiopathic movement disorders? *Archives of Disease in Childhood*. 89 (7), pp.611-614.
- Cnop, M., Igoillo-Esteve, M., Hughes, S.J., Walker, J.N., Cnop, I. and Clark, A. (2011) Longevity of human islet alpha- and beta-cells. *Diabetes, Obesity & Metabolism*. 13 Suppl 1 pp.39-46.
- Collombat, P., Xu, X., Ravassard, P., Sosa-Pineda, B., Dussaud, S., Billestrup, N., Madsen, O.D., Serup, P., Heimberg, H. and Mansouri, A. (2009) The ectopic expression of Pax4 in the mouse pancreas converts progenitor cells into alpha and subsequently beta cells. *Cell*. 138 (3), pp.449-462.
- Contractor, A., Mulle, C. and Swanson, G.T. (2011) Kainate receptors coming of age: milestones of two decades of research. *Trends in Neurosciences*. 34 (3), pp.154-163.
- Copik, A.J., Baldys, A., Nguyen, K., Sahdeo, S., Ho, H., Kosaka, A., Dietrich, P.J., Fitch, B., Raymond, J.R., Ford, A.P., Button, D. and Milla, M.E. (2015) Isoproterenol acts as a biased agonist of the alpha-1A-adrenoceptor that selectively activates the MAPK/ERK pathway. *PloS One*. 10 (1), pp.e0115701.
- Copits, B.A., Robbins, J.S., Frausto, S. and Swanson, G.T. (2011) Synaptic targeting and functional modulation of GluK1 kainate receptors by the auxiliary neuropilin and tolloid-like (NETO) proteins. *The Journal of Neuroscience*. 31 (20), pp.7334-7340.
- Copits, B.A. and Swanson, G.T. (2013) Lateral thinking: CaMKII uncouples kainate receptors from mossy fibre synapses. *The EMBO Journal*. 32 (4), pp.487-489.
- Costes, S., Langen, R., Gurlo, T., Matveyenko, A.V. and Butler, P.C. (2013) beta-Cell failure in type 2 diabetes: a case of asking too much of too few? *Diabetes*. 62 (2), pp.327-335.
- Craig, M.E., Nair, S., Stein, H. and Rawlinson, W.D. (2013) Viruses and type 1 diabetes: a new look at an old story. *Pediatric Diabetes*. 14 (3), pp.149-158.
- Crepel, V. and Mulle, C. (2015) Physiopathology of kainate receptors in epilepsy. *Current Opinion in Pharmacology*. 20 pp.83-88.

- Crepel, V. (2013) Kainate receptors in epilepsy. *Wiley Interdisciplinary Reviews: Membrane Transport and Signaling*. 2 (2), pp.75-83.
- Crevecoeur, I., Rondas, D., Mathieu, C. and Overbergh, L. (2015) The beta-cell in type 1 diabetes: What have we learned from proteomic studies? *Proteomics-Clinical Applications*. 9 (7-8), pp.755-766.
- Cunha, D.A., Ladriere, L., Ortis, F., Igoillo-Esteve, M., Gurzov, E.N., Eizirik, D.L. and Cnop, M. (2009) Exendin-4 and cAMP protect pancreatic beta cells from lipotoxic ER stress via induction of antiapoptotic defense mechanisms. *Diabetologia*. 52 pp.S149-S149.
- Dalmau, J., Tuzun, E., Wu, H.Y., Masjuan, J., Rossi, J.E., Voloschin, A., Baehring, J.M., Shimazaki, H., Koide, R., King, D., Mason, W., Sansing, L.H., Dichter, M.A., Rosenfeld, M.R. and Lynch, D.R. (2007) Paraneoplastic anti-N-methyl-D-aspartate receptor encephalitis associated with ovarian teratoma. *Annals of Neurology*. 61 (1), pp.25-36.
- Dalmau, J., Lancaster, E., Martinez-Hernandez, E., Rosenfeld, M.R. and Balice-Gordon, R. (2011) Clinical experience and laboratory investigations in patients with anti-NMDAR encephalitis. *Lancet Neurology*. 10 (1), pp.63-74.
- Davalli, A.M., Perego, C. and Folli, F.B. (2012) The potential role of glutamate in the current diabetes epidemic. *Acta Diabetologica* . 49 (3), pp.167-183.
- Dawe, G.B., Musgaard, M., Andrews, E.D., Daniels, B.A., Aurousseau, M.R., Biggin, P.C. and Bowie, D. (2013) Defining the structural relationship between kainate-receptor deactivation and desensitization. *Nature Structural & Molecular Biology*. 20 (9), pp.1054-1061.
- de Jong, V.,M., Zaldumbide, A., van der Slik, A.,R., Laban, S., Koeleman, B.,P.C. and Roep, B.,O. (2016) Variation in the CTLA4 3prime]UTR has phenotypic consequences for autoreactive T cells and associates with genetic risk for type 1 diabetes. *Genes and Immunity*. 17 (1), pp.75-78.
- De Leon, D.D. and Stanley, C.A. (2007) Mechanisms of Disease: advances in diagnosis and treatment of hyperinsulinism in neonates. *Nature Clinical Practice Endocrinology & Metabolism*. 3 (1), pp.57-68.

- De Marinis, Y.Z., Salehi, A., Ward, C.E., Zhang, Q., Abdulkader, F., Bengtsson, M., Braha, O., Braun, M., Ramracheya, R., Amisten, S., Habib, A.M., Moritoh, Y., Zhang, E., Reimann, F., Rosengren, A.H., Shibasaki, T., Gribble, F., Renstrom, E., Seino, S., Eliasson, L. and Rorsman, P. (2010) GLP-1 inhibits and adrenaline stimulates glucagon release by differential modulation of N- and L-type $Ca2^{+}$ channel-dependent exocytosis. *Cell Metabolism*. 11 (6), pp.543-553.
- Dean, B.J., Snelling, S.J., Dakin, S.G., Murphy, R.J., Javaid, M.K. and Carr, A.J. (2015) Differences in glutamate receptors and inflammatory cell numbers are associated with the resolution of pain in human rotator cuff tendinopathy. *Arthritis Research & Therapy*. 17 pp.176-015-0691-5.
- Degano, A.L., Ditamo, Y. and Roth, G.A. (2004) Neuronal antigens modulate the immune response associated with experimental autoimmune encephalomyelitis. *Immunology and Cell Biology*. 82 (1), pp.17-23.
- Del Rosario, J.S., Feldmann, K.G., Ahmed, T., Amjad, U., Ko, B., An, J., Mahmud, T., Salama, M., Mei, S., Asemota, D. and Mano, I. (2015) Death Associated Protein Kinase (DAPK) -mediated neurodegenerative mechanisms in nematode excitotoxicity. *BMC Neuroscience*. 16 pp.25-015-0158-2.
- Di Cairano, E.S., Davalli, A.M., Perego, L., Sala, S., Sacchi, V.F., La Rosa, S., Finzi, G., Placidi, C., Capella, C., Conti, P., Centonze, V.E., Casiraghi, F., Bertuzzi, F., Folli, F. and Perego, C. (2011) The Glial Glutamate Transporter 1 (GLT1) Is Expressed by Pancreatic beta-Cells and Prevents Glutamate-induced beta-Cell Death. *Journal of Biological Chemistry*. 286 (16), pp.14007-14018.
- Diguet, E., Fernagut, P.O., Normand, E., Centelles, L., Mulle, C. and Tison, F. (2004) Experimental basis for the putative role of GluR6/kainate glutamate receptor subunit in Huntington's disease natural history. *Neurobiology of Disease*. 15 (3), pp.667-675.
- Ding, L., Gysemans, C. and Mathieu, C. (2013) β -Cell differentiation and regeneration in type 1 diabetes. *Diabetes, Obesity and Metabolism*. 15 (Suppl. 3) pp.98-104.
- Diraison, F., Hayward, K., Sanders, K.L., Brozzi, F., Lajus, S., Hancock, J., Francis, J.E., Ainscow, E., Bommer, U.A., Molnar, E., Avent, N.D. and Varadi, A. (2011)

Translationally controlled tumour protein (TCTP) is a novel glucose-regulated protein that is important for survival of pancreatic beta cells. *Diabetologia*. 54 (2), pp.368-379.

- Dirice, E. and Kulkarni, R.N. (2016) Harnessing immune cells to enhance beta-cell mass in type 1 diabetes. *Journal of Investigative Medicine*. 64 (1), pp.14-20.
- Dohare, P., Zia, M.T., Ahmed, E., Ahmed, A., Yadala, V., Schober, A.L., Ortega, J.A., Kayton, R., Ungvari, Z., Mongin, A.A. and Ballabh, P. (2016) AMPA-Kainate Receptor Inhibition Promotes Neurologic Recovery in Premature Rabbits with Intraventricular Hemorrhage. *The Journal of Neuroscience*. 36 (11), pp.3363-3377.
- Dolensek, J., Rupnik, M.S. and Stozer, A. (2015) Structural similarities and differences between the human and the mouse pancreas. *Islets*. 7 (1), pp.e1024405.
- Domin, H., Zieba, B., Golembiowska, K., Kowalska, M., Dziubina, A. and Smialowska, M. (2010) Neuroprotective potential of mGluR5 antagonist MTEP: effects on kainate-induced excitotoxicity in the rat hippocampus. *Pharmacological Reports*. 62 (6), pp.1051-1061.
- Donevan, S.D. and Rogawski, M.A. (1993) GYKI 52466, a 2,3-benzodiazepine, is a highly selective, noncompetitive antagonist of AMPA/kainate receptor responses. *Neuron*. 10 (1), pp.51-59.
- Dong, X.X., Wang, Y.R., Qin, S., Liang, Z.Q., Liu, B.H., Qin, Z.H. and Wang, Y. (2012) P53 Mediates Autophagy Activation and Mitochondria Dysfunction in Kainic Acid-Induced Excitotoxicity in Primary Striatal Neurons. *Neuroscience*. 207 pp.52-64.
- Dor, Y., Brown, J., Martinez, O.I. and Melton, D.A. (2004) Adult pancreatic beta-cells are formed by self-duplication rather than stem-cell differentiation. *Nature*. 429 (6987), pp.41-46.
- Dorrell, C., Grompe, M.T., Pan, F.C., Zhong, Y., Canaday, P.S., Shultz, L.D., Greiner, D.L., Wright, C.V., Streeter, P.R. and Grompe, M. (2011) Isolation of mouse pancreatic alpha, beta, duct and acinar populations with cell surface markers. *Molecular and Cellular Endocrinology*. 339 (1-2), pp.144-150.

- Dosemeci, A., Tao-Cheng, J.H., Vinade, L. and Jaffe, H. (2006) Preparation of postsynaptic density fraction from hippocampal slices and proteomic analysis. *Biochemical and Biophysical Research Communications*. 339 (2), pp.687-694.
- Dou, H., Wang, C., Wu, X., Yao, L., Zhang, X., Teng, S., Xu, H., Liu, B., Wu, Q., Zhang, Q., Hu, M., Wang, Y., Wang, L., Wu, Y., Shang, S., Kang, X., Zheng, L., Zhang, J., Raoux, M., Lang, J., Li, Q., Su, J., Yu, X., Chen, L. and Zhou, Z. (2015) Calcium influx activates adenylyl cyclase 8 for sustained insulin secretion in rat pancreatic beta cells. *Diabetologia*. 58 (2), pp.324-333.
- Downs, C.A. and Faulkner, M.S. (2015) Toxic stress, inflammation and symptomatology of chronic complications in diabetes. *World Journal of Diabetes*. 6 (4), pp.554-565.
- Dryer, S.E. (2015) Glutamate receptors in the kidney. *Nephrology, Dialysis, Transplantation.* 30 (10), pp.1630-1638.
- Dunning, B.E. and Gerich, J.E. (2007) The role of alpha-cell dysregulation in fasting and postprandial hyperglycemia in type 2 diabetes and therapeutic implications. *Endocrine Reviews*. 28 (3), pp.253-283.
- Edgerton, D.S. and Cherrington, A.D. (2013) Glucagon's yin and yang effects on hepatic glucose production. *Nature Medicine*. 19 (6), pp.674-675.
- Edgerton, D.S., Lautz, M., Scott, M., Everett, C.A., Stettler, K.M., Neal, D.W., Chu, C.A. and Cherrington, A.D. (2006) Insulin's direct effects on the liver dominate the control of hepatic glucose production. *The Journal of Clinical Investigation*. 116 (2), pp.521-527.
- Edwards, R.H. (2015) Mobile binding sites regulate glutamate clearance. *Nature Neuroscience*. 18 (2), pp.166-168.
- Ehlers, M.R. (2016) Immune Interventions to preserve beta cell function in type 1 diabetes. *Journal of Investigative Medicine*. 64 (1), pp.7-13.
- Eizirik, D.L., Sammeth, M., Bouckenooghe, T., Bottu, G., Sisino, G., Igoillo-Esteve, M., Ortis, F., Santin, I., Colli, M.L., Barthson, J., Bouwens, L., Hughes, L., Gregory, L., Lunter, G., Marselli, L., Marchetti, P., McCarthy, M.I. and Cnop, M. (2012) The human pancreatic islet transcriptome: expression of candidate genes for

type 1 diabetes and the impact of pro-inflammatory cytokines. *PLoS Genetics*. 8 (3), pp.e1002552.

- Eldh, M., Lotvall, J., Malmhall, C. and Ekstrom, K. (2012) Importance of RNA isolation methods for analysis of exosomal RNA: Evaluation of different methods. *Molecular Immunology*. 50 (4), pp.278-286.
- Evans, G.J. (2015) The synaptosome as a model system for studying synaptic physiology. *Cold Spring Harbor Protocols*. 2015 (5), pp.421-424.
- Fan, F., Ji, C., Wu, Y., Ferguson, S.M., Tamarina, N., Philipson, L.H. and Lou, X. (2015) Dynamin 2 regulates biphasic insulin secretion and plasma glucose homeostasis. *The Journal of Clinical Investigation*. 125 (11), pp.4026-4041.
- Fauser, S., Uttner, I., Arino, H., Scherbaum, W.A., Saiz, A. and Lewerenz, J. (2015) Long latency between GAD-antibody detection and development of limbic encephalitis--a case report. *BMC Neurology*. 15 pp.177-015-0435-9.
- Feldmann, N., del Rio, R.M., Gjinovci, A., Tamarit-Rodriguez, J., Wollheim, C.B. and Wiederkehr, A. (2011) Reduction of plasma membrane glutamate transport potentiates insulin but not glucagon secretion in pancreatic islet cells. *Molecular and Cellular Endocrinology*. 338 (1-2), pp.46-57.
- Felizola, S.J., Nakamura, Y., Satoh, F., Morimoto, R., Kikuchi, K., Nakamura, T., Hozawa, A., Wang, L., Onodera, Y., Ise, K., McNamara, K.M., Midorikawa, S., Suzuki, S. and Sasano, H. (2014) Glutamate receptors and the regulation of steroidogenesis in the human adrenal gland: the metabotropic pathway. *Molecular and Cellular Endocrinology*. 382 (1), pp.170-177.
- Feng, Y., He, D., Yao, Z. and Klionsky, D.J. (2014) The machinery of macroautophagy. *Cell Research*. 24 (1), pp.24-41.
- Fernandes, H.B., Catches, J.S., Petralia, R.S., Copits, B.A., Xu, J., Russell, T.A., Swanson, G.T. and Contractor, A. (2009) High-Affinity Kainate Receptor Subunits Are Necessary for Ionotropic but Not Metabotropic Signaling. *Neuron*. 63 (6), pp.818-829.
- Fisher, J.L. (2015) The auxiliary subunits Neto1 and Neto2 have distinct, subunit-dependent effects at recombinant GluK1- and GluK2-containing kainate receptors. *Neuropharmacology*. 99 pp.471-480.

- Fisher, J.L. (2014) The neurotoxin domoate causes long-lasting inhibition of the kainate receptor GluK5 subunit. *Neuropharmacology*. 85 pp.9-17.
- Fisher, J.L. and Housley, P.R. (2013) Agonist binding to the GluK5 subunit is sufficient for functional surface expression of heteromeric GluK2/GluK5 kainate receptors. *Cellular and Molecular Neurobiology*. 33 (8), pp.1099-1108.
- Fisher, J.L. and Mott, D.D. (2013) Modulation of homomeric and heteromeric kainate receptors by the auxiliary subunit Neto1. *The Journal of Physiology*. 591 (Pt 19), pp.4711-4724.
- Fisher, J.L. and Mott, D.D. (2011) Distinct functional roles of subunits within the heteromeric kainate receptor. *The Journal of Neuroscience*. 31 (47), pp.17113-17122.
- Fisher, M.T. and Fisher, J.L. (2014) Contributions of different kainate receptor subunits to the properties of recombinant homomeric and heteromeric receptors. *Neuroscience*. 278 pp.70-80.
- Franklin, I., Gromada, J., Gjinovci, A., Theander, S. and Wollheim, C.B. (2005) Beta-cell secretory products activate alpha-cell ATP-dependent potassium channels to inhibit glucagon release. *Diabetes*. 54 (6), pp.1808-1815.
- Freeborn, D., Dyches, T., Roper, S.O. and Mandleco, B. (2013) Identifying challenges of living with type 1 diabetes: child and youth perspectives. *Journal of Clinical Nursing*. 22 (13-14), pp.1890-1898.
- Freitag, C.M. (2007) The genetics of autistic disorders and its clinical relevance: a review of the literature. *Molecular Psychiatry*. 12 (1), pp.2-22.
- Fritsch, B., Reis, J., Gasior, M., Kaminski, R.M. and Rogawski, M.A. (2014) Role of GluK1 kainate receptors in seizures, epileptic discharges, and epileptogenesis. *The Journal of Neuroscience*. 34 (17), pp.5765-5775.
- Fu, Z., Gilbert, E.R. and Liu, D. (2013) Regulation of insulin synthesis and secretion and pancreatic Beta-cell dysfunction in diabetes. *Current Diabetes Reviews*. 9 (1), pp.25-53.
- Fuerstenau-Sharp, M., Zimmermann, M.E., Stark, K., Jentsch, N., Klingenstein, M., Drzymalski, M., Wagner, S., Maier, L.S., Hehr, U., Baessler, A., Fischer, M. and Hengstenberg, C. (2015) Generation of highly purified human cardiomyocytes from

peripheral blood mononuclear cell-derived induced pluripotent stem cells. *PloS One*. 10 (5), pp.e0126596.

- Fujita, K., Yuasa, T., Takahashi, Y., Tanaka, K., Sako, W., Koizumi, H., Iwasaki, Y., Yoshida, M., Izumi, Y. and Kaji, R. (2012) Antibodies to N-methyl-D-aspartate glutamate receptors in Creutzfeldt-Jakob disease patients. *Journal of Neuroimmunology*. 251 (1-2), pp.90-93.
- Gammelsaeter, R., Coppola, T., Marcaggi, P., Storm-Mathisen, J., Chaudhry, F.A., Attwell, D., Regazzi, R. and Gundersen, V. (2011) A role for glutamate transporters in the regulation of insulin secretion. *PloS One*. 6 (8), pp.e22960.
- Gao, F., Li, F., Miao, Y., Dong, L.D., Zhang, S.H., Wu, J., Sun, X.H. and Wang, Z. (2015) Group I metabotropic glutamate receptor agonist DHPG modulates Kir4.1 protein and mRNA in cultured rat retinal Muller cells. *Neuroscience Letters*. 588 pp.12-17.
- Garey, L.J., Von Bussmann, K.A. and Hirsch, S.R. (2006) Decreased numerical density of kainate receptor-positive neurons in the orbitofrontal cortex of chronic schizophrenics. *Experimental Brain Research*. 173 (2), pp.234-242.
- Gelsomino, G., Menna, E., Antonucci, F., Rodighiero, S., Riganti, L., Mulle, C., Benfenati, F., Valtorta, F., Verderio, C. and Matteoli, M. (2013) Kainate induces mobilization of synaptic vesicles at the growth cone through the activation of protein kinase A. *Cerebral Cortex*. 23 (3), pp.531-541.
- Gheni, G., Ogura, M., Iwasaki, M., Yokoi, N., Minami, K., Nakayama, Y., Harada, K., Hastoy, B., Wu, X., Takahashi, H., Kimura, K., Matsubara, T., Hoshikawa, R., Hatano, N., Sugawara, K., Shibasaki, T., Inagaki, N., Bamba, T., Mizoguchi, A., Fukusaki, E., Rorsman, P. and Seino, S. (2014) Glutamate acts as a key signal linking glucose metabolism to incretin/cAMP action to amplify insulin secretion. *Cell Reports*. 9 (2), pp.661-673.
- Gill, A. and Madden, D.R. (2008) Purification and crystallization of a non-GluR2 AMPA-receptor ligand-binding domain: a case of cryo-incompatibility addressed by room-temperature data collection. *Acta Crystallographica.Section F, Structural Biology and Crystallization Communications*. 64 (Pt 9), pp.831-835.

- Gilon, P., Chae, H.Y., Rutter, G.A. and Ravier, M.A. (2014) Calcium signaling in pancreatic beta-cells in health and in Type 2 diabetes. *Cell Calcium*. 56 (5), pp.340-361.
- Giugliano, D., Ceriello, A. and Esposito, K. (2008) Glucose metabolism and hyperglycemia. *The American Journal of Clinical Nutrition*. 87 (1), pp.217S-222S.
- Gleichman, A.J., Panzer, J.A., Baumann, B.H., Dalmau, J. and Lynch, D.R. (2014) Antigenic and mechanistic characterization of anti-AMPA receptor encephalitis. *Annals of Clinical and Translational Neurology*. 1 (3), pp.180-189.
- Gleichman, A.J., Spruce, L.A., Dalmau, J., Seeholzer, S.H. and Lynch, D.R. (2012) Anti-NMDA receptor encephalitis antibody binding is dependent on amino acid identity of a small region within the GluN1 amino terminal domain. *The Journal of Neuroscience: The Official Journal of the Society for Neuroscience*. 32 (32), pp.11082-11094.
- Goginashvili, A., Zhang, Z., Erbs, E., Spiegelhalter, C., Kessler, P., Mihlan, M., Pasquier, A., Krupina, K., Schieber, N., Cinque, L., Morvan, J., Sumara, I., Schwab, Y., Settembre, C. and Ricci, R. (2015) Insulin granules. Insulin secretory granules control autophagy in pancreatic beta cells. *Science*. 347 (6224), pp.878-882.
- Goldberg-Stern, H., Ganor, Y., Cohen, R., Pollak, L., Teichberg, V. and Levite, M. (2014) Glutamate receptor antibodies directed against AMPA receptors subunit 3 peptide B (GluR3B) associate with some cognitive/psychiatric/behavioral abnormalities in epilepsy patients. *Psychoneuroendocrinology*. 40 pp.221-231.
- Gonoi, T., Mizuno, N., Inagaki, N., Kuromi, H., Seino, Y., Miyazaki, J. and Seino, S. (1994) Functional Neuronal Ionotropic Glutamate Receptors are Expressed in the Nonneuronal Cell-Line Min6. *Journal of Biological Chemistry*. 269 (25), pp.16989-16992.
- Gonzalez, M.P., Herrero, M.T., Vicente, S. and Oset-Gasque, M.J. (1998) Effect of glutamate receptor agonists on catecholamine secretion in bovine chromaffin cells. *Neuroendocrinology*. 67 (3), pp.181-189.
- Gonzalez-Gonzalez, I.M. and Henley, J.M. (2013) Postsynaptic Kainate Receptor Recycling and Surface Expression Are Regulated by Metabotropic Autoreceptor Signalling. *Traffic*. 14 (7), pp.810-822.

- Gotoh, K., Masaki, T., Chiba, S., Ando, H., Fujiwara, K., Shimasaki, T., Mitsutomi, K., Katsuragi, I., Kakuma, T., Sakata, T. and Yoshimatsu, H. (2013) Hypothalamic brain-derived neurotrophic factor regulates glucagon secretion mediated by pancreatic efferent nerves. *Journal of Neuroendocrinology*. 25 (3), pp.302-311.
- Graham, T.E., Sgro, V., Friars, D. and Gibala, M.J. (2000) Glutamate ingestion: the plasma and muscle free amino acid pools of resting humans. *American Journal of Physiology.Endocrinology and Metabolism*. 278 (1), pp.E83-9.
- Grarup, N., Sandholt, C.H., Hansen, T. and Pedersen, O. (2014) Genetic susceptibility to type 2 diabetes and obesity: from genome-wide association studies to rare variants and beyond. *Diabetologia*. 57 (8), pp.1528-1541.
- Griffith, T.N. and Swanson, G.T. (2015) Identification of critical functional determinants of kainate receptor modulation by auxiliary protein Neto2. *The Journal of Physiology*. 593 (22), pp.4815-4833.
- Guemes, M., Rahman, S.A. and Hussain, K. (2015) What is a normal blood glucose? *Archives of Disease in Childhood*. 0, pp.1-6.
- Guemez-Gamboa, A., Estrada-Sanchez, A.M., Montiel, T., Paramo, B., Massieu, L. and Moran, J. (2011) Activation of NOX2 by the Stimulation of Ionotropic and Metabotropic Glutamate Receptors Contributes to Glutamate Neurotoxicity In Vivo Through the Production of Reactive Oxygen Species and Calpain Activation. *Journal of Neuropathology and Experimental Neurology*. 70 (11), pp.1020-1035.
- Guerriero, R.M., Giza, C.C. and Rotenberg, A. (2015) Glutamate and GABA imbalance following traumatic brain injury. *Current Neurology and Neuroscience Reports*. 15 (5), pp.27-015-0545-1.
- Gylfe, E. (2013) Glucose control of glucagon secretion: there is more to it than KATP channels. *Diabetes*. 62 (5), pp.1391-1393.
- Gylfe, E. and Gilon, P. (2014) Glucose regulation of glucagon secretion. *Diabetes Research and Clinical Practice*. 103 (1), pp.1-10.
- Hahn, C.G., Banerjee, A., Macdonald, M.L., Cho, D.S., Kamins, J., Nie, Z., Borgmann-Winter, K.E., Grosser, T., Pizarro, A., Ciccimaro, E., Arnold, S.E., Wang, H.Y. and Blair, I.A. (2009) The post-synaptic density of human postmortem

brain tissues: an experimental study paradigm for neuropsychiatric illnesses. *PloS One*. 4 (4), pp.e5251.

- Hall, K., Frederiksen, B., Rewers, M. and Norris, J.M. (2015) Daycare attendance, breastfeeding, and the development of type 1 diabetes: the diabetes autoimmunity study in the young. *BioMed Research International*. 2015 pp.203947.
- Hanson, E., Armbruster, M., Cantu, D., Andresen, L., Taylor, A., Danbolt, N.C. and Dulla, C.G. (2015) Astrocytic glutamate uptake is slow and does not limit neuronal NMDA receptor activation in the neonatal neocortex. *Glia*. 63 (10), pp.1784-1796.
- Hawkins, R.A. (2009) The blood-brain barrier and glutamate. *The American Journal of Clinical Nutrition*. 90 (3), pp.867S-874S.
- Henquin, J.C., Nenquin, M., Stiernet, P. and Ahren, B. (2006) In vivo and in vitro glucose-induced biphasic insulin secretion in the mouse: pattern and role of cytoplasmic Ca2+ and amplification signals in beta-cells. *Diabetes*. 55 (2), pp.441-451.
- Herold, K.C., Usmani-Brown, S., Ghazi, T., Lebastchi, J., Beam, C.A., Bellin, M.D., Ledizet, M., Sosenko, J.M., Krischer, J.P., Palmer, J.P. and Type 1 Diabetes TrialNet Study Group (2015) Beta Cell Death and Dysfunction during Type 1 Diabetes Development in At-Risk Individuals. *The Journal of Clinical Investigation*. 125 (3), pp.1163-1173.
- Herring, R., Jones, R.H. and Russell-Jones, D.L. (2014) Hepatoselectivity and the evolution of insulin. *Diabetes, Obesity & Metabolism*. 16 (1), pp.1-8.
- Hinoi, E., Fujimori, S., Takemori, A., Kurabayashi, H., Nakamura, Y. and Yoneda, Y. (2002) Demonstration of expression of mRNA for particular AMPA and kainate receptor subunits in immature and mature cultured rat calvarial osteoblasts. *Brain Research*. 943 (1), pp.112-116.
- Hod, M., Hadar, E. and Cabero-Roura, L. (2015) Prevention of type 2 diabetes among women with prior gestational diabetes mellitus. *International Journal of Gynaecology and Obstetrics*. 131 Suppl 1 pp.S16-8.
- Hoftberger, R., van Sonderen, A., Leypoldt, F., Houghton, D., Geschwind, M., Gelfand, J., Paredes, M., Sabater, L., Saiz, A., Titulaer, M.J., Graus, F. and Dalmau,

J. (2015) Encephalitis and AMPA receptor antibodies: Novel findings in a case series of 22 patients. *Neurology*. 84 (24), pp.2403-2412.

- Hou, J.C., Min, L. and Pessin, J.E. (2009) Insulin Granule Biogenesis, Trafficking and Exocytosis. *Vitamins and Hormones Insulin and Igfs*. 80 pp.473-506.
- Hovelso, N., Sotty, F., Montezinho, L.P., Pinheiro, P.S., Herrik, K.F. and Mork, A. (2012) Therapeutic potential of metabotropic glutamate receptor modulators. *Current Neuropharmacology*. 10 (1), pp.12-48.
- Howe, J.R. (2015) Auxiliary subunits highlight a role for the LBD-TMD linkers in glutamate receptor desensitization. *The Journal of Physiology*. 593 (22), pp.4813-4814.
- Hughes, E.G., Peng, X., Gleichman, A.J., Lai, M., Zhou, L., Tsou, R., Parsons, T.D., Lynch, D.R., Dalmau, J. and Balice-Gordon, R.J. (2010) Cellular and synaptic mechanisms of anti-NMDA receptor encephalitis. *The Journal of Neuroscience*. 30 (17), pp.5866-5875.
- Hussain, M.A., Akalestou, E. and Song, W.J. (2016) Inter-organ communication and regulation of beta cell function. *Diabetologia*. 59 (4), pp.659-667.
- Hussen, H.I., Persson, M. and Moradi, T. (2015) Maternal overweight and obesity are associated with increased risk of type 1 diabetes in offspring of parents without diabetes regardless of ethnicity. *Diabetologia*. 58 (7), pp.1464-1473.
- Imamura, M., Maeda, S., Yamauchi, T., Hara, K., Yasuda, K., Morizono, T., Takahashi, A., Horikoshi, M., Nakamura, M., Fujita, H., Tsunoda, T., Kubo, M., Watada, H., Maegawa, H., Okada-Iwabu, M., Iwabu, M., Shojima, N., Ohshige, T., Omori, S., Iwata, M., Hirose, H., Kaku, K., Ito, C., Tanaka, Y., Tobe, K., Kashiwagi, A., Kawamori, R., Kasuga, M., Kamatani, N., Diabetes Genetics Replication and Meta-analysis (DIAGRAM) Consortium, Nakamura, Y. and Kadowaki, T. (2012) A single-nucleotide polymorphism in ANK1 is associated with susceptibility to type 2 diabetes in Japanese populations. *Human Molecular Genetics*. 21 (13), pp.3042-3049.
- Imperatore, G., Boyle, J.P., Thompson, T.J., Case, D., Dabelea, D., Hamman, R.F., Lawrence, J.M., Liese, A.D., Liu, L.L., Mayer-Davis, E.J., Rodriguez, B.L., Standiford, D. and SEARCH for Diabetes in Youth Study Group (2012) Projections

of type 1 and type 2 diabetes burden in the U.S. population aged <20 years through 2050: dynamic modeling of incidence, mortality, and population growth. *Diabetes Care*. 35 (12), pp.2515-2520.

- Inagaki, N., Kuromi, H., Gonoi, T., Okamoto, Y., Ishida, H., Seino, Y., Kaneko, T., Iwanaga, T. and Seino, S. (1995) Expression and Role of Ionotropic Glutamate Receptors in Pancreatic-Islet Cells. *Faseb Journal*. 9 (8), pp.686-691.
- International Diabetes Federation. IDF Diabetes, 7 ed. Brussels, Belgium: International Diabetes Federation, 2015. http://www.diabetesatlas.org.
- Jane, D.E., Lodge, D. and Collingridge, G.L. (2009) Kainate receptors: Pharmacology, function and therapeutic potential. *Neuropharmacology*. 56 (1), pp.90-113.
- Julio-Pieper, M., O'Connor, R.M., Dinan, T.G. and Cryan, J.F. (2013) Regulation of the brain-gut axis by group III metabotropic glutamate receptors. *European Journal of Pharmacology*. 698 (1-3), pp.19-30.
- Kalev-Zylinska, M.L., Green, T.N., Morel-Kopp, M.C., Sun, P.P., Park, Y.E., Lasham, A., During, M.J. and Ward, C.M. (2014) N-methyl-D-aspartate receptors amplify activation and aggregation of human platelets. *Thrombosis Research*. 133 (5), pp.837-847.
- Keenan, H.A., Sun, J.K., Levine, J., Doria, A., Aiello, L.P., Eisenbarth, G., Bonner-Weir, S. and King, G.L. (2010) Residual insulin production and pancreatic ss-cell turnover after 50 years of diabetes: Joslin Medalist Study. *Diabetes*. 59 (11), pp.2846-2853.
- Keezer, M.R., Novy, J. and Sander, J.W. (2015) Type 1 diabetes mellitus in people with pharmacoresistant epilepsy: Prevalence and clinical characteristics. *Epilepsy Research*. 115 pp.55-57.
- Kharroubi, A.T. and Darwish, H.M. (2015) Diabetes mellitus: The epidemic of the century. *World Journal of Diabetes*. 6 (6), pp.850-867.
- Kim, A., Miller, K., Jo, J., Kilimnik, G., Wojcik, P. and Hara, M. (2009) Islet architecture: A comparative study. *Islets*. 1 (2), pp.129-136.
- Klein, D., Misawa, R., Bravo-Egana, V., Vargas, N., Rosero, S., Piroso, J., Ichii, H., Umland, O., Zhijie, J., Tsinoremas, N., Ricordi, C., Inverardi, L., Dominguez-

Bendala, J. and Pastori, R.L. (2013) MicroRNA expression in alpha and beta cells of human pancreatic islets. *PloS One*. 8 (1), pp.e55064.

- Klieverik, L.P., Janssen, S.F., van Riel, A., Foppen, E., Bisschop, P.H., Serlie, M.J., Boelen, A., Ackermans, M.T., Sauerwein, H.P., Fliers, E. and Kalsbeek, A. (2009) Thyroid hormone modulates glucose production via a sympathetic pathway from the hypothalamic paraventricular nucleus to the liver. *Proceedings of the National Academy of Sciences of the United States of America*. 106 (14), pp.5966-5971.
- Kniazeff, J., Prezeau, L., Rondard, P., Pin, J.P. and Goudet, C. (2011) Dimers and beyond: The functional puzzles of class C GPCRs. *Pharmacology & Therapeutics*. 130 (1), pp.9-25.
- Krogvold, L., Edwin, B., Buanes, T., Frisk, G., Skog, O., Anagandula, M., Korsgren, O., Undlien, D., Eike, M.C., Richardson, S.J., Leete, P., Morgan, N.G., Oikarinen, S., Oikarinen, M., Laiho, J.E., Hyoty, H., Ludvigsson, J., Hanssen, K.F. and Dahl-Jorgensen, K. (2015) Detection of a low-grade enteroviral infection in the islets of langerhans of living patients newly diagnosed with type 1 diabetes. *Diabetes*. 64 (5), pp.1682-1687.
- Krogvold, L., Skog, O., Sundstrom, G., Edwin, B., Buanes, T., Hanssen, K.F., Ludvigsson, J., Grabherr, M., Korsgren, O. and Dahl-Jorgensen, K. (2015) Function of isolated pancreatic islets from patients at onset of type 1 diabetes: insulin secretion can be restored after some days in a nondiabetogenic environment in vitro: results from the DiViD Study. *Diabetes*. 64 (7), pp.2506-2512.
- Kurihara, K. (2015) Umami the Fifth Basic Taste: History of Studies on Receptor Mechanisms and Role as a Food Flavor. *BioMed Research International*. 2015 pp.10-20.
- Kutlu, B., Burdick, D., Baxter, D., Rasschaert, J., Flamez, D., Eizirik, D.L., Welsh, N., Goodman, N. and Hood, L. (2009) Detailed transcriptome atlas of the pancreatic beta cell. *BMC Medical Genomics*. 2 pp.3-8794-2-3.
- Lai, M., Hughes, E.G., Peng, X., Zhou, L., Gleichman, A.J., Shu, H., Mata, S., Kremens, D., Vitaliani, R., Geschwind, M.D., Bataller, L., Kalb, R.G., Davis, R., Graus, F., Lynch, D.R., Balice-Gordon, R. and Dalmau, J. (2009) AMPA receptor

antibodies in limbic encephalitis alter synaptic receptor location. *Annals of Neurology*. 65 (4), pp.424-434.

- Lamb, M.M., Miller, M., Seifert, J.A., Frederiksen, B., Kroehl, M., Rewers, M. and Norris, J.M. (2015) The effect of childhood cow's milk intake and HLA-DR genotype on risk of islet autoimmunity and type 1 diabetes: the Diabetes Autoimmunity Study in the Young. *Pediatric Diabetes*. 16 (1), pp.31-38.
- Lammert, E., Gu, G., McLaughlin, M., Brown, D., Brekken, R., Murtaugh, L.C., Gerber, H.P., Ferrara, N. and Melton, D.A. (2003) Role of VEGF-A in vascularization of pancreatic islets. *Current Biology*. 13 (12), pp.1070-1074.
- Lamy, C.M., Sanno, H., Labouebe, G., Picard, A., Magnan, C., Chatton, J.Y. and Thorens, B. (2014) Hypoglycemia-activated GLUT2 neurons of the nucleus tractus solitarius stimulate vagal activity and glucagon secretion. *Cell Metabolism*. 19 (3), pp.527-538.
- Lancaster, E. (2016) The Diagnosis and Treatment of Autoimmune Encephalitis. *Journal of Clinical Neurology*. 12 (1), pp.1-13.
- Lancaster, E., Martinez-Hernandez, E., Titulaer, M.J., Boulos, M., Weaver, S., Antoine, J.C., Liebers, E., Kornblum, C., Bien, C.G., Honnorat, J., Wong, S., Xu, J., Contractor, A., Balice-Gordon, R. and Dalmau, J. (2011) Antibodies to metabotropic glutamate receptor 5 in the Ophelia syndrome. *Neurology*. 77 (18), pp.1698-1701.
- Languren, G., Montiel, T., Julio-Amilpas, A. and Massieu, L. (2013) Neuronal damage and cognitive impairment associated with hypoglycemia: An integrated view. *Neurochemistry International*. 63 (4), pp.331-343.
- Lanore, F., Labrousse, V.F., Szabo, Z., Normand, E., Blanchet, C. and Mulle, C. (2012) Deficits in morphofunctional maturation of hippocampal mossy fiber synapses in a mouse model of intellectual disability. *The Journal of Neuroscience*. 32 (49), pp.17882-17893.
- Lauvsnes, M.B., Maroni, S.S., Appenzeller, S., Beyer, M.K., Greve, O.J., Kvaloy, J.T., Harboe, E., Goransson, L.G., Tjensvoll, A.B. and Omdal, R. (2013) Memory dysfunction in primary Sjogren's syndrome is associated with anti-NR2 antibodies. *Arthritis and Rheumatism*. 65 (12), pp.3209-3217.

- Lee, C.J., Labrakakis, C., Joseph, D.J. and Macdermott, A.B. (2004) Functional similarities and differences of AMPA and kainate receptors expressed by cultured rat sensory neurons. *Neuroscience*. 129 (1), pp.35-48.
- Lee, J.H., Lee, J.M., Ramos, E.M., Gillis, T., Mysore, J.S., Kishikawa, S., Hadzi, T., Hendricks, A.E., Hayden, M.R., Morrison, P.J., Nance, M., Ross, C.A., Margolis, R.L., Squitieri, F., Gellera, C., Gomez-Tortosa, E., Ayuso, C., Suchowersky, O., Trent, R.J., McCusker, E., Novelletto, A., Frontali, M., Jones, R., Ashizawa, T., Frank, S., Saint-Hilaire, M.H., Hersch, S.M., Rosas, H.D., Lucente, D., Harrison, M.B., Zanko, A., Abramson, R.K., Marder, K., Sequeiros, J., Landwehrmeyer, G.B., Registry Study of the European Huntington's Disease Network, Shoulson, I., Huntington Study Group COHORT project, Myers, R.H., MacDonald, M.E. and Gusella, J.F. (2012) TAA repeat variation in the GRIK2 gene does not influence age at onset in Huntington's disease. *Biochemical and Biophysical Research Communications*. 424 (3), pp.404-408.
- Lee, J.M., Seo, W.Y., Han, H.S., Oh, K.J., Lee, Y.S., Kim, D.K., Choi, S., Choi, B.H., Harris, R.A., Lee, C.H., Koo, S.H. and Choi, H.S. (2016) Insulin-Inducible SMILE Inhibits Hepatic Gluconeogenesis. *Diabetes*. 65 (1), pp.62-73.
- Lee, K.M., Yang, S.J., Kim, Y.D., Choi, Y.D., Nam, J.H., Choi, C.S., Choi, H.S. and Park, C.S. (2013) Disruption of the cereblon gene enhances hepatic AMPK activity and prevents high-fat diet-induced obesity and insulin resistance in mice. *Diabetes*. 62 (6), pp.1855-1864.
- Lerma, J. and Marques, J.M. (2013) Kainate receptors in health and disease. *Neuron*. 80 (2), pp.292-311.
- Leslie, R.D., Palmer, J., Schloot, N.C. and Lernmark, A. (2016) Diabetes at the crossroads: relevance of disease classification to pathophysiology and treatment. *Diabetologia*. 59 (1), pp.13-20.
- Levetan, C. (2010) Distinctions between islet neogenesis and beta-cell replication: implications for reversal of Type 1 and 2 diabetes. *Journal of Diabetes*. 2 (2), pp.76-84.

- Levite, M. (2014) Glutamate receptor antibodies in neurological diseases: anti-AMPA-GluR3 antibodies, anti-NMDA-NR1 antibodies, anti-NMDA-NR2A/B antibodies, anti-mGluR1 antibodies or anti-mGluR5 antibodies are present in subpopulations of patients with either: epilepsy, encephalitis, cerebellar ataxia, systemic lupus erythematosus (SLE) and neuropsychiatric SLE, Sjogren's syndrome, schizophrenia, mania or stroke. These autoimmune anti-glutamate receptor antibodies can bind neurons in few brain regions, activate glutamate receptors, decrease glutamate receptor's expression, impair glutamate-induced signaling and function, activate blood brain barrier endothelial cells, kill neurons, damage the brain, induce behavioral/psychiatric/cognitive abnormalities and ataxia in animal models, and can be removed or silenced in some patients by immunotherapy. *Journal of Neural Transmission*. 121 (8), pp.1029-1075.
- Li, J.M., Zeng, Y.J., Peng, F., Li, L., Yang, T.H., Hong, Z., Lei, D., Chen, Z. and Zhou, D. (2010) Aberrant glutamate receptor 5 expression in temporal lobe epilepsy lesions. *Brain Research*. 1311 pp.166-174.
- Li, R., Lu, W., Jiang, Q.W., Li, Y.Y., Zhao, G.M., Shi, L., Yang, Q.D., Ruan, Y., Jiang, J., Zhang, S.N., Xu, W.H. and Zhong, W.J. (2012) Increasing prevalence of type 2 diabetes in Chinese adults in Shanghai. *Diabetes Care*. 35 (5), pp.1028-1030.
- Li, S.W., Koya, V., Li, Y., Donelan, W., Lin, P., Reeves, W.H. and Yang, L.J. (2010) Pancreatic duodenal homeobox 1 protein is a novel beta-cell-specific autoantigen for type I diabetes. *Laboratory Investigation; a Journal of Technical Methods and Pathology*. 90 (1), pp.31-39.
- Liimatainen, S. and Peltola, J. (2012) Epilepsy associated with glutamic acid decarboxylase antibody (GADA). *European Journal of Neurology*. 19 (6), pp.799-799.
- Liimatainen, S., Peltola, M., Sabater, L., Fallah, M., Kharazmi, E., Haapala, A.M., Dastidar, P., Knip, M., Saiz, A. and Peltola, J. (2010) Clinical significance of glutamic acid decarboxylase antibodies in patients with epilepsy. *Epilepsia*. 51 (5), pp.760-767.

- Likhite, N. and Warawdekar, U.M. (2011) A unique method for isolation and solubilization of proteins after extraction of RNA from tumor tissue using trizol. *Journal of Biomolecular Techniques*. 22 (1), pp.37-44.
- Lima Nda, S., de Moura, E.G., Passos, M.C., Nogueira Neto, F.J., Reis, A.M., de Oliveira, E. and Lisboa, P.C. (2011) Early weaning causes undernutrition for a short period and programmes some metabolic syndrome components and leptin resistance in adult rat offspring. *The British Journal of Nutrition*. 105 (9), pp.1405-1413.
- Lin, B., White, J.T., Lu, W., Xie, T., Utleg, A.G., Yan, X., Yi, E.C., Shannon, P., Khrebtukova, I., Lange, P.H., Goodlett, D.R., Zhou, D., Vasicek, T.J. and Hood, L. (2005) Evidence for the presence of disease-perturbed networks in prostate cancer cells by genomic and proteomic analyses: a systems approach to disease. *Cancer Research*. 65 (8), pp.3081-3091.
- Linnemann, A.K., Baan, M. and Davis, D.B. (2014) Pancreatic beta-cell proliferation in obesity. *Advances in Nutrition*. 5 (3), pp.278-288.
- Lodge, D. (2009) The history of the pharmacology and cloning of ionotropic glutamate receptors and the development of idiosyncratic nomenclature. *Neuropharmacology*. 56 (1), pp.6-21.
- Longo, P.A., Kavran, J.M., Kim, M.S. and Leahy, D.J. (2013) Transient mammalian cell transfection with polyethylenimine (PEI). *Methods in Enzymology*. 529 pp.227-240.
- Lowry, E.R., Kruyer, A., Norris, E.H., Cederroth, C.R. and Strickland, S. (2013) The GluK4 kainate receptor subunit regulates memory, mood, and excitotoxic neurodegeneration. *Neuroscience*. 235 pp.215-225.
- Lu, W., Shi, Y., Jackson, A.C., Bjorgan, K., During, M.J., Sprengel, R., Seeburg, P.H. and Nicoll, R.A. (2009) Subunit composition of synaptic AMPA receptors revealed by a single-cell genetic approach. *Neuron*. 62 (2), pp.254-268.
- Lund-Blix, N.A., Stene, L.C., Rasmussen, T., Torjesen, P.A., Andersen, L.F. and Ronningen, K.S. (2015) Infant feeding in relation to islet autoimmunity and type 1 diabetes in genetically susceptible children: the MIDIA Study. *Diabetes Care*. 38 (2), pp.257-263.

- Luther, M.J., Davies, E., Muller, D., Harrison, M., Bone, A.J., Persaud, S.J. and Jones, P.M. (2005) Cell-to-cell contact influences proliferative marker expression and apoptosis in MIN6 cells grown in islet-like structures. *American Journal of Physiology-Endocrinology and Metabolism*. 288 (3), pp.E502-E509.
- Luyt, K., Slade, T.P., Dorward, J.J., Durant, C.F., Wu, Y., Shigemoto, R., Mundell, S.J., Varadi, A. and Molnar, E. (2007) Developing oligodendrocytes express functional GABA(B) receptors that stimulate cell proliferation and migration. *Journal of Neurochemistry*. 100 (3), pp.822-840.
- Lyon, L., Borel, M., CarriÓn, M., Kew, J.N.C., Corti, C., Harrison, P.J., Burnet, P.W.J., Paulsen, O. and RodrÍGuez-Moreno, A. (2011) Hippocampal mossy fiber long-term depression in Grm2/3 double knockout mice. *Synapse*. 65 (9), pp.945-954.
- Maechler, P. and Wollheim, C.B. (1999) Mitochondrial glutamate acts as a messenger in glucose-induced insulin exocytosis. *Nature*. 402 (6762), pp.685-689.
- Maioli, E., Torricelli, C., Fortino, V., Carlucci, F., Tommassini, V. and Pacini, A. (2009) Critical appraisal of the MTT assay in the presence of rottlerin and uncouplers. *Biological Procedures Online*. 11 pp.227-240.
- Mannering, S.I., Pathiraja, V. and Kay, T.W. (2016) The case for an autoimmune aetiology of type 1 diabetes. *Clinical and Experimental Immunology*. 183 (1), pp.8-15.
- Mantegazza, R., Bernasconi, P., Baggi, F., Spreafico, R., Ragona, F., Antozzi, C., Bernardi, G. and Granata, T. (2002) Antibodies against GluR3 peptides are not specific for Rasmussen's encephalitis but are also present in epilepsy patients with severe, early onset disease and intractable seizures. *Journal of Neuroimmunology*. 131 (1-2), pp.179-185.
- Manto, M., Dalmau, J., Didelot, A., Rogemond, V. and Honnorat, J. (2010) In vivo effects of antibodies from patients with anti-NMDA receptor encephalitis: further evidence of synaptic glutamatergic dysfunction. *Orphanet Journal of Rare Diseases*. 5 pp.31-1172-5-31.

- Maraschi, A., Ciammola, A., Folci, A., Sassone, F., Ronzitti, G., Cappelletti, G., Silani, V., Sato, S., Hattori, N., Mazzanti, M., Chieregatti, E., Mulle, C., Passafaro, M. and Sassone, J. (2014) Parkin regulates kainate receptors by interacting with the GluK2 subunit. *Nature Communications*. 5 pp.5182.
- Marciniak, M., Chruscicka, B., Lech, T., Burnat, G. and Pilc, A. (2014) Expression of group III metabotropic glutamate receptors in the reproductive system of male mice. *Reproduction, Fertility, and Development*. 28 (3), pp.369-374.
- Marignier, R., Chenevier, F., Rogemond, V., Sillevis Smitt, P., Renoux, C., Cavillon, G., Androdias, G., Vukusic, S., Graus, F., Honnorat, J. and Confavreux, C. (2010) Metabotropic glutamate receptor type 1 autoantibody-associated cerebellitis: a primary autoimmune disease? *Archives of Neurology*. 67 (5), pp.627-630.
- Marone, M., Mozzetti, S., De Ritis, D., Pierelli, L. and Scambia, G. (2001) Semiquantitative RT-PCR analysis to assess the expression levels of multiple transcripts from the same sample. *Biological Procedures Online*. 3 pp.19-25.
- Marquard, J., Otter, S., Welters, A., Stirban, A., Fischer, A., Eglinger, J., Herebian, D., Kletke, O., Klemen, M.S., Stozer, A., Wnendt, S., Piemonti, L., Kohler, M., Ferrer, J., Thorens, B., Schliess, F., Rupnik, M.S., Heise, T., Berggren, P.O., Klocker, N., Meissner, T., Mayatepek, E., Eberhard, D., Kragl, M. and Lammert, E. (2015) Characterization of pancreatic NMDA receptors as possible drug targets for diabetes treatment. *Nature Medicine*. 21 (4), pp.363-372.
- Martin-Timon, I. and Del Canizo-Gomez, F.J. (2015) Mechanisms of hypoglycemia unawareness and implications in diabetic patients. *World Journal of Diabetes*. 6 (7), pp.912-926.
- Mat, A., Adler, H., Merwick, A., Chadwick, G., Gullo, G., Dalmau, J.O. and Tubridy, N. (2013) Ophelia syndrome with metabotropic glutamate receptor 5 antibodies in CSF. *Neurology*. 80 (14), pp.1349-1350.
- Mattsson, K., Jonsson, I., Malmqvist, E., Larsson, H.E. and Rylander, L. (2015) Maternal smoking during pregnancy and offspring type 1 diabetes mellitus risk: accounting for HLA haplotype. *European Journal of Epidemiology*. 30 (3), pp.231-238.

- Matute, C. (2011) Therapeutic potential of kainate receptors. *CNS Neuroscience & Therapeutics*. 17 (6), pp.661-669.
- Mayeda, E.R., Whitmer, R.A. and Yaffe, K. (2015) Diabetes and cognition. *Clinics in Geriatric Medicine*. 31 (1), pp.101-15, ix.
- McCorry, D., Nicolson, A., Smith, D., Marson, A., Feltbower, R.G. and Chadwick, D.W. (2006) An association between type 1 diabetes and idiopathic generalized epilepsy. *Annals of Neurology*. 59 (1), pp.204-206.
- Meabon, J.S., Lee, A., Meeker, K.D., Bekris, L.M., Fujimura, R.K., Yu, C.E., Watson, G.S., Pow, D.V., Sweet, I.R. and Cook, D.G. (2012) Differential expression of the glutamate transporter GLT-1 in pancreas. *The Journal of Histochemistry and Cytochemistry*. 60 (2), pp.139-151.
- Melyan, Z., Wheal, H.V. and Lancaster, B. (2002) Metabotropic-mediated kainate receptor regulation of IsAHP and excitability in pyramidal cells. *Neuron*. 34 (1), pp.107-114.
- Menge, B.A., Tannapfel, A., Belyaev, O., Drescher, R., Muller, C., Uhl, W., Schmidt, W.E. and Meier, J.J. (2008) Partial pancreatectomy in adult humans does not provoke beta-cell regeneration. *Diabetes*. 57 (1), pp.142-149.
- Merkle, F.T., Maroof, A., Wataya, T., Sasai, Y., Studer, L., Eggan, K. and Schier, A.F. (2015) Generation of neuropeptidergic hypothalamic neurons from human pluripotent stem cells. *Development*. 142 (4), pp.633-643.
- Mezza, T. and Kulkarni, R.N. (2014) The regulation of pre- and post-maturational plasticity of mammalian islet cell mass. *Diabetologia*. 57 (7), pp.1291-1303.
- Miura, K., Orcutt, A.C., Muratova, O.V., Miller, L.H., Saul, A. and Long, C.A. (2008) Development and characterization of a standardized ELISA including a reference serum on each plate to detect antibodies induced by experimental malaria vaccines. *Vaccine*. 26 (2), pp.193-200.
- Miyatsuka, T. (2016) Chronology of endocrine differentiation and beta-cell neogenesis [Review. *Endocrine Journal*. 63 (3), pp.205-211.

- Mohd Sairazi, N.S., Sirajudeen, K.N., Asari, M.A., Muzaimi, M., Mummedy, S. and Sulaiman, S.A. (2015) Kainic Acid-Induced Excitotoxicity Experimental Model: Protective Merits of Natural Products and Plant Extracts. *Evidence-Based Complementary and Alternative Medicine*. pp.972623.
- Moller, N. and Jorgensen, J.O. (2009) Effects of growth hormone on glucose, lipid, and protein metabolism in human subjects. *Endocrine Reviews*. 30 (2), pp.152-177.
- Molnar, E. (2013) Are Neto1 and APP auxiliary subunits of NMDA receptors? *Journal of Neurochemistry*. 126 (5), pp.551-553.
- Molnar, E., Varadi, A., Mcilhinney, R.A.J. and Ashcroft, S.J.H. (1995) Identification of Functional Ionotropic Glutamate-Receptor Proteins in Pancreatic Beta-Cells and in Islets of Langerhans. *FEBS Letters*. 371 (3), pp.253-257.
- Molnár, E., McIlhinney, R.A.J., Baude, A., Nusser, Z. and Somogyi, P. (1994) Membrane Topology of the GluR1 Glutamate Receptor Subunit: Epitope Mapping by Site-Directed Antipeptide Antibodies. *Journal of Neurochemistry*. 63 (2), pp.683-693.
- Mondin, M., Carta, M., Normand, E., Mulle, C. and Coussen, F. (2010) Profilin II regulates the exocytosis of kainate glutamate receptors. *The Journal of Biological Chemistry*. 285 (51), pp.40060-40071.
- Monyer, H. and von Engelhardt, J. (2015) Modulation of AMPA receptor function by auxiliary subunits. *e-Neuroforum*. 6 (2), pp.39-48.
- Morley, P., MacLean, S., Gendron, T.F., Small, D.L., Tremblay, R., Durkin, J.P. and Mealing, G. (2000) Pharmacological and molecular characterization of glutamate receptors in the MIN6 pancreatic beta-cell line. *Neurological Research*. 22 (4), pp.379-385.
- Morran, M.P., Vonberg, A., Khadra, A. and Pietropaolo, M. (2015) Immunogenetics of type 1 diabetes mellitus. *Molecular Aspects of Medicine*. 42 pp.42-60.

- Morrell, C.N., Sun, H., Ikeda, M., Beique, J.C., Swaim, A.M., Mason, E., Martin, T.V., Thompson, L.E., Gozen, O., Ampagoomian, D., Sprengel, R., Rothstein, J., Faraday, N., Huganir, R. and Lowenstein, C.J. (2008) Glutamate mediates platelet activation through the AMPA receptor. *The Journal of Experimental Medicine*. 205 (3), pp.575-584.
- Mothet, J.P., Le Bail, M. and Billard, J.M. (2015) Time and space profiling of NMDA receptor co-agonist functions. *Journal of Neurochemistry*. 135 (2), pp.210-225.
- Mott, D.D., Rojas, A., Fisher, J.L., Dingledine, R.J. and Benveniste, M. (2010) Subunit-specific desensitization of heteromeric kainate receptors. *The Journal of Physiology*. 588 (Pt 4), pp.683-700.
- Muller, A., Gunzel, D. and Schlue, W.R. (2003) Activation of AMPA/kainate receptors but not acetylcholine receptors causes Mg^{2+} influx into Retzius neurones of the leech Hirudo medicinalis. *The Journal of General Physiology*. 122 (6), pp.727-739.
- Muller, W.A., Faloona, R.H. and Unger, R.H. (1973) Hyperglucagonemia in diabetic ketoacidosis: its prevalence and significance. *The American Journal of Medicine*. 54 pp.52-57.
- Muroyama, A., Uehara, S., Yatsushiro, S., Echigo, N., Morimoto, R., Morita, M., Hayashi, M., Yamamoto, A., Koh, D.S. and Moriyama, Y. (2004) A novel variant of ionotropic glutamate receptor regulates somatostatin secretion from delta-cells of islets of Langerhans. *Diabetes*. 53 (7), pp.1743-1753.
- Nagata, M., Suzuki, W., Iizuka, S., Tabuchi, M., Maruyama, H., Takeda, S., Aburada, M. and Miyamoto, K. (2006) Type 2 diabetes mellitus in obese mouse model induced by monosodium glutamate. *Experimental Animals*. 55 (2), pp.109-115.
- Nakatsu, D., Horiuchi, Y., Kano, F., Noguchi, Y., Sugawara, T., Takamoto, I., Kubota, N., Kadowaki, T. and Murata, M. (2015) L-cysteine reversibly inhibits glucose-induced biphasic insulin secretion and ATP production by inactivating PKM2. *Proceedings of the National Academy of Sciences of the United States of America*. 112 (10), pp.E1067-76.

- Negrete-Diaz, J.V., Sihra, T.S., Delgado-Garcia, J.M. and Rodriguez-Moreno, A. (2006) Kainate receptor-mediated inhibition of glutamate release involves protein kinase A in the mouse hippocampus. *Journal of Neurophysiology*. 96 (4), pp.1829-1837.
- Newsholme, P., Cruzat, V., Arfuso, F. and Keane, K. (2014) Nutrient regulation of insulin secretion and action. *The Journal of Endocrinology*. 221 (3), pp.R105-20.
- Ng, D., Pitcher, G.M., Szilard, R.K., Sertie, A., Kanisek, M., Clapcote, S.J., Lipina, T., Kalia, L.V., Joo, D., McKerlie, C., Cortez, M., Roder, J.C., Salter, M.W. and McInnes, R.R. (2009) Neto1 is a novel CUB-domain NMDA receptor-interacting protein required for synaptic plasticity and learning. *PLoS Biology*. 7 (2), pp.e41.
- Nibber, A., Clover, L., Pettingill, P., Waters, P., Elger, C.E., Bien, C.G., Vincent, A. and Lang, B. (2016) Antibodies to AMPA receptors in Rasmussen's encephalitis. *European Journal of Paediatric Neurology*. 20 (2), pp.222-227.
- Nica, A.C., Ongen, H., Irminger, J.C., Bosco, D., Berney, T., Antonarakis, S.E., Halban, P.A. and Dermitzakis, E.T. (2013) Cell-type, allelic, and genetic signatures in the human pancreatic beta cell transcriptome. *Genome Research*. 23 (9), pp.1554-1562.
- Nicoletti, F., Bruno, V., Ngomba, R.T., Gradini, R. and Battaglia, G. (2015) Metabotropic glutamate receptors as drug targets: what's new? *Current Opinion in Pharmacology*. 20 pp.89-94.
- Niimi, M., Sato, M., Murao, K., Takahara, J. and Kawanishi, K. (1994) Effect of excitatory amino acid receptor agonists on secretion of growth hormone as assessed by the reverse hemolytic plaque assay. *Neuroendocrinology*. 60 (2), pp.173-178.
- Niinisto, S., Takkinen, H.M., Uusitalo, L., Rautanen, J., Vainio, N., Ahonen, S., Nevalainen, J., Kenward, M.G., Lumia, M., Simell, O., Veijola, R., Ilonen, J., Knip, M. and Virtanen, S.M. (2015) Maternal intake of fatty acids and their food sources during lactation and the risk of preclinical and clinical type 1 diabetes in the offspring. *Acta Diabetologica*. 52 (4), pp.763-772.
- Niswender, C.M. and Conn, P.J. (2010) Metabotropic Glutamate Receptors: Physiology, Pharmacology, and Disease. *Annual Review of Pharmacology and Toxicology*. 50 pp.295-322.

- Noble, J.A. (2015) Immunogenetics of type 1 diabetes: A comprehensive review. *Journal of Autoimmunity*. 64 pp.101-112.
- O'Connell, M.A., Harvey, A.S., Mackay, M.T. and Cameron, F.J. (2008) Does epilepsy occur more frequently in children with Type 1 diabetes? *Journal of Paediatrics and Child Health*. 44 (10), pp.586-589.
- Oh, S. and McCaslin, P.P. (1996) Kainate produces concentration-dependent elevation of glutamate release but not cGMP levels in cultured neuron. *General Pharmacology*. 27 (1), pp.83-87.
- Omote, H., Miyaji, T., Hiasa, M., Juge, N. and Moriyama, Y. (2016) Structure, Function, and Drug Interactions of Neurotransmitter Transporters in the Postgenomic Era. *Annual Review of Pharmacology and Toxicology*. 56 pp.385-402.
- Oram, R.A., McDonald, T.J., Shields, B.M., Hudson, M.M., Shepherd, M.H., Hammersley, S., Pearson, E.R., Hattersley, A.T. and UNITED Team (2015) Most people with long-duration type 1 diabetes in a large population-based study are insulin microsecretors. *Diabetes Care*. 38 (2), pp.323-328.
- Oresic, M., Simell, S., Sysi-Aho, M., Nanto-Salonen, K., Seppanen-Laakso, T., Parikka, V., Hekkalal, A., Mattila, I., Katajamaa, M., Keskinen, P., Simell, T., Veijola, R., Ilonen, J., Knip, M. and Simell, O. (2008) Dysregulation of lipid and amino acid metabolism precedes islet autoimmunity in children who later progress to type 1 diabetes. *Diabetologia*. 51 pp.S27-S27.
- Otter, S. and Lammert, E. (2016) Exciting Times for Pancreatic Islets: Glutamate Signaling in Endocrine Cells. *Trends in Endocrinology and Metabolism*. 27 (3), pp.177-188.
- Pagliuca, F.W., Millman, J.R., Gurtler, M., Segel, M., Van Dervort, A., Ryu, J.H., Peterson, Q.P., Greiner, D. and Melton, D.A. (2014) Generation of functional human pancreatic beta cells in vitro. *Cell*. 159 (2), pp.428-439.
- Pahl, S., Tapken, D., Haering, S.C. and Hollmann, M. (2014) Trafficking of kainate receptors. *Membranes*. 4 (3), pp.565-595.
- Palacios-Filardo, J., Aller, M.I. and Lerma, J. (2016) Synaptic Targeting of Kainate Receptors. *Cerebral Cortex*. 26 (4), pp.1464-1472.

- Paoletti, P., Bellone, C. and Zhou, Q. (2013) NMDA receptor subunit diversity: impact on receptor properties, synaptic plasticity and disease. *Nature Reviews Neuroscience*. 14 (6), pp.383-400.
- Papouin, T. and Oliet, S.H. (2014) Organization, control and function of extrasynaptic NMDA receptors. *Philosophical Transactions of the Royal Society of London Series B, Biological Sciences*. 369 (1654), pp.20130601.
- Paranjape, S.A., Chan, O., Zhu, W., Horblitt, A.M., McNay, E.C., Cresswell, J.A., Bogan, J.S., McCrimmon, R.J. and Sherwin, R.S. (2010) Influence of insulin in the ventromedial hypothalamus on pancreatic glucagon secretion in vivo. *Diabetes*. 59 (6), pp.1521-1527.
- Park, Y.H., Mueller, B.H., McGrady, N.R., Ma, H.Y. and Yorio, T. (2015) AMPA receptor desensitization is the determinant of AMPA receptor mediated excitotoxicity in purified retinal ganglion cells. *Experimental Eye Research*. 132 pp.136-150.
- Parpura, V. and Verkhratsky, A. (2013) Astrogliopathology: could nanotechnology restore aberrant calcium signalling and pathological astroglial remodelling? *Biochimica et Biophysica Acta*. 1833 (7), pp.1625-1631.
- Pasca, A.M., Sloan, S.A., Clarke, L.E., Tian, Y., Makinson, C.D., Huber, N., Kim, C.H., Park, J.Y., O'Rourke, N.A., Nguyen, K.D., Smith, S.J., Huguenard, J.R., Geschwind, D.H., Barres, B.A. and Pasca, S.P. (2015) Functional cortical neurons and astrocytes from human pluripotent stem cells in 3D culture. *Nature Methods*. 12 (7), pp.671-678.
- Patterson, C., Guariguata, L., Dahlquist, G., Soltesz, G., Ogle, G. and Silink, M. (2014) Diabetes in the young - a global view and worldwide estimates of numbers of children with type 1 diabetes. *Diabetes Research and Clinical Practice*. 103 (2), pp.161-175.
- Patterson, S., Irwin, N., Guo-Parke, H., Moffett, R.C., Scullion, S.M., Flatt, P.R. and McClenaghan, N.H. (2015) Evaluation of the role of N-methyl-d-aspartate (NMDA) receptors in insulin secreting beta-cells. *European Journal of Pharmacology*. 771, pp.107-113.

- Pedersen, M.G., Cortese, G. and Eliasson, L. (2011) Mathematical modeling and statistical analysis of calcium-regulated insulin granule exocytosis in beta-cells from mice and humans. *Progress in Biophysics & Molecular Biology*. 107 (2), pp.257-264.
- Pedraza, L.T., Roth, G.A. and Cumar, F.A. (1988) Identification as synapsin of a synaptosomal protein immunoreacting with anti-myelin basic protein antiserum. *Journal of Neurochemistry*. 51 (2), pp.413-420.
- Pepaj, M., Bredahl, M.K., Gjerlaugsen, N., Bornstedt, M.E. and Thorsby, P.M. (2014) Discovery of novel vitamin D-regulated proteins in INS-1 cells: a proteomic approach. *Diabetes/metabolism Research and Reviews*. 31 (5), pp.481-491.
- Peret, A., Christie, L.A., Ouedraogo, D.W., Gorlewicz, A., Epsztein, J., Mulle, C. and Crepel, V. (2014) Contribution of aberrant GluK2-containing kainate receptors to chronic seizures in temporal lobe epilepsy. *Cell Reports*. 8 (2), pp.347-354.
- Perrais, D., Veran, J. and Mulle, C. (2010) Gating and permeation of kainate receptors: differences unveiled. *Trends in Pharmacological Sciences*. 31 (11), pp.516-522.
- Pfeifer, C.R., Shomorony, A., Aronova, M.A., Zhang, G., Cai, T., Xu, H., Notkins, A.L. and Leapman, R.D. (2015) Quantitative analysis of mouse pancreatic islet architecture by serial block-face SEM. *Journal of Structural Biology*. 189 (1), pp.44-52.
- Phonnok, S., Uthaisang-Tanechpongtamb, W. and Wongsatayanon, B.T. (2010) Anticancer and apoptosis-inducing activities of microbial metabolites. *European Journal of Biotechnology*. 13 (5), pp.732-744.
- Pillai, S.C., Hacohen, Y., Tantsis, E., Prelog, K., Merheb, V., Kesson, A., Barnes, E., Gill, D., Webster, R., Menezes, M., Ardern-Holmes, S., Gupta, S., Procopis, P., Troedson, C., Antony, J., Ouvrier, R.A., Polfrit, Y., Davies, N.W., Waters, P., Lang, B., Lim, M.J., Brilot, F., Vincent, A. and Dale, R.C. (2015) Infectious and autoantibody-associated encephalitis: clinical features and long-term outcome. *Pediatrics*. 135 (4), pp.e974-84.
- Pinheiro, P. and Mulle, C. (2006) Kainate receptors. *Cell and Tissue Research*. 326 (2), pp.457-482.

- Piro, S., Mascali, L.G., Urbano, F., Filippello, A., Malaguarnera, R., Calanna, S., Rabuazzo, A.M. and Purrello, F. (2014) Chronic exposure to GLP-1 increases GLP-1 synthesis and release in a pancreatic alpha cell line (alpha-TC1): evidence of a direct effect of GLP-1 on pancreatic alpha cells. *PloS One*. 9 (2), pp.e90093.
- Prasad, R.B. and Groop, L. (2015) Genetics of type 2 diabetes-pitfalls and possibilities. *Genes*. 6 (1), pp.87-123.
- Pratt, E.P., Salyer, A.E., Guerra, M.L. and Hockerman, G.H. (2016) Ca2+ influx through L-type Ca2+ channels and Ca2+-induced Ca^{2+} release regulate cAMP accumulation and Epac1-dependent ERK 1/2 activation in INS-1 cells. *Molecular and Cellular Endocrinology*. 419 pp.60-71.
- Pruss, H., Finke, C., Holtje, M., Hofmann, J., Klingbeil, C., Probst, C., Borowski, K., Ahnert-Hilger, G., Harms, L., Schwab, J.M., Ploner, C.J., Komorowski, L., Stoecker, W., Dalmau, J. and Wandinger, K.P. (2012) N-methyl-D-aspartate receptor antibodies in herpes simplex encephalitis. *Annals of Neurology*. 72 (6), pp.902-911.
- Pruss, H., Finke, C., Holtje, M., Hofmann, J., Klingbeil, C., Probst, C., Borowski, K., Ahnert-Hilger, G., Harms, L., Schwab, J.M., Ploner, C.J., Komorowski, L., Stoecker, W., Dalmau, J. and Wandinger, K.P. (2012) N-methyl-D-aspartate receptor antibodies in herpes simplex encephalitis. *Annals of Neurology*. 72 (6), pp.902-911.
- Psychiatric GWAS Consortium Bipolar Disorder Working Group (2011) Large-scale genome-wide association analysis of bipolar disorder identifies a new susceptibility locus near ODZ4. *Nature Genetics*. 43 (10), pp.977-983.
- Puff, R., D'Orlando, O., Heninger, A.K., Kuhn, D., Krause, S., Winkler, C., Beyerlein, A., Bonifacio, E. and Ziegler, A.G. (2015) Compromised immune response in infants at risk for type 1 diabetes born by Caesarean Section. *Clinical Immunology*. 160 (2), pp.282-285.
- Raiteri, L. and Raiteri, M. (2015) Multiple functions of neuronal plasma membrane neurotransmitter transporters. *Progress in Neurobiology*. 134 pp.1-16.

- Rajatileka, S., Luyt, K., El-Bokle, M., Williams, M., Kemp, H., Molnar, E. and Varadi, A. (2013) Isolation of human genomic DNA for genetic analysis from premature neonates: a comparison between newborn dried blood spots, whole blood and umbilical cord tissue. *BMC Genetics*. 14 pp.105-2156-14-105.
- Ramirez, T., Tong, M., Chen, W.C., Nguyen, Q.G., Wands, J.R. and de la Monte, S.M. (2013) Chronic alcohol-induced hepatic insulin resistance and endoplasmic reticulum stress ameliorated by peroxisome-proliferator activated receptor-delta agonist treatment. *Journal of Gastroenterology and Hepatology*. 28 (1), pp.179-187.
- Razavi, R., Najafabadi, H.S., Abdullah, S., Smukler, S., Arntfield, M. and van der Kooy, D. (2015) Diabetes enhances the proliferation of adult pancreatic multipotent progenitor cells and biases their differentiation to more beta-cell production. *Diabetes*. 64 (4), pp.1311-1323.
- Reinhardt, F., Schultz, J., Waterstradt, R. and Baltrusch, S. (2016) Drp1 guarding of the mitochondrial network is important for glucose-stimulated insulin secretion in pancreatic beta cells. *Biochemical and Biophysical Research Communications*. 474 (4), pp.646-651.
- Reynisdottir, I., Thorleifsson, G., Benediktsson, R., Sigurdsson, G., Emilsson, V., Einarsdottir, A.S., Hjorleifsdottir, E.E., Orlygsdottir, G.T., Bjornsdottir, G.T., Saemundsdottir, J., Halldorsson, S., Hrafnkelsdottir, S., Sigurjonsdottir, S.B., Steinsdottir, S., Martin, M., Kochan, J.P., Rhees, B.K., Grant, S.F., Frigge, M.L., Kong, A., Gudnason, V., Stefansson, K. and Gulcher, J.R. (2003) Localization of a susceptibility gene for type 2 diabetes to chromosome 5q34-q35.2. *American Journal of Human Genetics*. 73 (2), pp.323-335.
- Rio, D.C., Ares, M.J., Hannon, G.J. and Nilsen, T.W. (2010) Purification of RNA using TRIzol (TRI reagent). *Cold Spring Harbor Protocols*. (6), pp. 5439- 5439.
- Robinson, M.B. and Jackson, J.G. (2016) Astroglial glutamate transporters coordinate excitatory signaling and brain energetics. *Neurochemistry International*. S0197-0186 (16), pp.30040-30047.
- Rodriguez-Diaz, R., Abdulreda, M.H., Formoso, A.L., Gans, I., Ricordi, C., Berggren, P.O. and Caicedo, A. (2011) Innervation patterns of autonomic axons in the human endocrine pancreas. *Cell Metabolism*. 14 (1), pp.45-54.

- Rodriguez-Moreno, A., Herreras, O. and Lerma, J. (1997) Kainate receptors presynaptically downregulate GABAergic inhibition in the rat hippocampus. *Neuron*. 19 (4), pp.893-901.
- Rodriguez-Moreno, A. and Sihra, T.S. (2013) Presynaptic kainate receptor-mediated facilitation of glutamate release involves Ca2+-calmodulin and PKA in cerebrocortical synaptosomes. *FEBS Letters*. 587 (6), pp.788-792.
- Rogawski, M.A. (2011) Revisiting AMPA receptors as an antiepileptic drug target. *Epilepsy Currents / American Epilepsy Society*. 11 (2), pp.56-63.
- Rogawski, M.A. and Hanada, T. (2013) Preclinical pharmacology of perampanel, a selective non-competitive AMPA receptor antagonist. *Acta Neurologica Scandinavica Supplementum*. 197, pp.19-24.
- Rogers, S.W., Andrews, P.I., Gahring, L.C., Whisenand, T., Cauley, K., Crain, B., Hughes, T.E., Heinemann, S.F. and McNamara, J.O. (1994) Autoantibodies to glutamate receptor GluR3 in Rasmussen's encephalitis. *Science*. 265 (5172), pp.648-651.
- Rohrer, T.R., Wolf, J., Liptay, S., Zimmer, K.P., Frohlich-Reiterer, E., Scheuing, N., Marg, W., Stern, M., Kapellen, T.M., Hauffa, B.P., Wolfle, J., Holl, R.W. and DPV Initiative and the German BMBF Competence Network Diabetes Mellitus (2015) Microvascular Complications in Childhood-Onset Type 1 Diabetes and Celiac Disease: A Multicenter Longitudinal Analysis of 56,514 Patients From the German-Austrian DPV Database. *Diabetes Care*. 38 (5), pp.801-807.
- Rojas, A., Wetherington, J., Shaw, R., Serrano, G., Swanger, S. and Dingledine, R. (2013) Activation of group I metabotropic glutamate receptors potentiates heteromeric kainate receptors. *Molecular Pharmacology*. 83 (1), pp.106-121.
- Rojas, J.M. and Schwartz, M.W. (2014) Control of hepatic glucose metabolism by islet and brain. *Diabetes, Obesity & Metabolism*. 16 Suppl 1 pp.33-40.
- Roland, A.V., Nunemaker, C.S., Keller, S.R. and Moenter, S.M. (2010) Prenatal androgen exposure programs metabolic dysfunction in female mice. *The Journal of Endocrinology*. 207 (2), pp.213-223.

- Roman-Ramos, R., Almanza-Perez, J.C., Garcia-Macedo, R., Blancas-Flores, G., Fortis-Barrera, A., Jasso, E.I., Garcia-Lorenzana, M., Campos-Sepulveda, A.E., Cruz, M. and Alarcon-Aguilar, F.J. (2011) Monosodium glutamate neonatal intoxication associated with obesity in adult stage is characterized by chronic inflammation and increased mRNA expression of peroxisome proliferator-activated receptors in mice. *Basic & Clinical Pharmacology & Toxicology*. 108 (6), pp.406-413.
- Rondard, P. and Pin, J.P. (2015) Dynamics and modulation of metabotropic glutamate receptors. *Current Opinion in Pharmacology*. 20, pp.95-101.
- Rorsman, P. and Braun, M. (2013) Regulation of Insulin Secretion in Human Pancreatic Islets. *Annual Review of Physiology*. 75, pp.155-179.
- Rubinsztein, D.C., Leggo, J., Chiano, M., Dodge, A., Norbury, G., Rosser, E. and Craufurd, D. (1997) Genotypes at the GluR6 kainate receptor locus are associated with variation in the age of onset of Huntington disease. *Proceedings of the National Academy of Sciences of the United States of America*. 94 (8), pp.3872-3876.
- Rutkowska-Wlodarczyk, I., Aller, M.I., Valbuena, S., Bologna, J.C., Prezeau, L. and Lerma, J. (2015) A proteomic analysis reveals the interaction of GluK1 ionotropic kainate receptor subunits with Go proteins. *The Journal of Neuroscience*. 35 (13), pp.5171-5179.
- Saisho, Y., Butler, A.E., Manesso, E., Elashoff, D., Rizza, R.A. and Butler, P.C. (2013) Beta-Cell Mass and Turnover in Humans: Effects of Obesity and Aging. *Diabetes Care*. 36 (1), pp.111-117.
- Sakha, P., Vesikansa, A., Orav, E., Heikkinen, J., Kukko-Lukjanov, T.K., Shintyapina, A., Franssila, S., Jokinen, V., Huttunen, H.J. and Lauri, S.E. (2016) Axonal Kainate Receptors Modulate the Strength of Efferent Connectivity by Regulating Presynaptic Differentiation. *Frontiers in Cellular Neuroscience*. 10, pp.3.
- Salmen, B., Beed, P.S., Ozdogan, T., Maier, N., Johenning, F.W., Winterer, J., Breustedt, J. and Schmitz, D. (2012) GluK1 inhibits calcium dependent and

independent transmitter release at associational/commissural synapses in area CA3 of the hippocampus. *Hippocampus*. 22 (1), pp.57-68.

- Sarmiento, J., Wallis, R.H., Ning, T., Marandi, L., Chao, G., Veillette, A., Lernmark, A., Paterson, A.D. and Poussier, P. (2015) A functional polymorphism of Ptpn22 is associated with type 1 diabetes in the BioBreeding rat. *Journal of Immunology*. 194 (2), pp.615-629.
- Sasaki, Y., Shimada, T., Iizuka, S., Suzuki, W., Makihara, H., Teraoka, R., Tsuneyama, K., Hokao, R. and Aburada, M. (2011) Effects of bezafibrate in nonalcoholic steatohepatitis model mice with monosodium glutamate-induced metabolic syndrome. *European Journal of Pharmacology*. 662 (1-3), pp.1-8.
- Sato, K., Kiyama, H., Shimada, S. and Tohyama, M. (1993) Gene expression of KA type and NMDA receptors and of a glycine transporter in the rat pineal gland. *Neuroendocrinology*. 58 (1), pp.77-79.
- Schauwecker, P.E. (2010) Neuroprotection by glutamate receptor antagonists against seizure-induced excitotoxic cell death in the aging brain. *Experimental Neurology*. 224 (1), pp.207-218.
- Schober, E., Otto, K.P., Dost, A., Jorch, N., Holl, R., German Austrian DPV Initiative and BMBF Competence Network Diab (2012) Association of Epilepsy and Type 1 Diabetes Mellitus in Children and Adolescents: Is There an Increased Risk for Diabetic Ketoacidosis? *Journal of Pediatrics*. 160 (4), pp.662-+.
- Seino, S., Shibasaki, T. and Minami, K. (2011) Dynamics of insulin secretion and the clinical implications for obesity and diabetes. *The Journal of Clinical Investigation*. 121 (6), pp.2118-2125.
- Selway, J.L., Moore, C.E., Mistry, R., Challiss, R.A.J. and Herbert, T.P. (2012) Molecular mechanisms of muscarinic acetylcholine receptor-stimulated increase in cytosolic free Ca2+ concentration and ERK1/2 activation in the MIN6 pancreatic beta-cell line. *Acta Diabetologica*. 49 (4), pp.277-289.

- Shanks, N.F., Cais, O., Maruo, T., Savas, J.N., Zaika, E.I., Azumaya, C.M., Yates, J.R., Greger, I. and Nakagawa, T. (2014) Molecular dissection of the interaction between the AMPA receptor and cornichon homolog-3. *The Journal of Neuroscience*. 34 (36), pp.12104-12120.
- Sharma, R.B., O'Donnell, A.C., Stamateris, R.E., Ha, B., McCloskey, K.M., Reynolds, P.R., Arvan, P. and Alonso, L.C. (2015) Insulin demand regulates beta cell number via the unfolded protein response. *The Journal of Clinical Investigation*. 125 (10), pp.3831-3846.
- Sharp, R.C., Abdulrahim, M., Naser, E.S. and Naser, S.A. (2015) Genetic Variations of PTPN2 and PTPN22: Role in the Pathogenesis of Type 1 Diabetes and Crohn's Disease. *Frontiers in Cellular and Infection Microbiology*. 5 pp.95.
- Shaw, J.E., Sicree, R.A. and Zimmet, P.Z. (2010) Global estimates of the prevalence of diabetes for 2010 and 2030. *Diabetes Research and Clinical Practice*. 87 (1), pp.4-14.
- Sheng, N., Shi, Y.S., Lomash, R.M., Roche, K.W. and Nicoll, R.A. (2015) Neto auxiliary proteins control both the trafficking and biophysical properties of the kainate receptor GluK1. *Elife*. 4 pp. 11682-11701.
- Shi, Z., Taylor, A.W. and Wittert, G.A. (2013) Re. Association between monosodium glutamate intake and sleep-disordered breathing among Chinese adults with normal body weight: emerging opportunities for research on monosodium glutamate intake and health at a population level. *Nutrition*. 29 (10), pp.1276-1277.
- Shimo, N., Matsuoka, T.A., Miyatsuka, T., Takebe, S., Tochino, Y., Takahara, M., Kaneto, H. and Shimomura, I. (2015) Short-term selective alleviation of glucotoxicity and lipotoxicity ameliorates the suppressed expression of key beta-cell factors under diabetic conditions. *Biochemical and Biophysical Research Communications*. 467 (4), pp.948-954.
- Siafarikas, A., Johnston, R.J., Bulsara, M.K., O'Leary, P., Jones, T.W. and Davis, E.A. (2012) Early loss of the glucagon response to hypoglycemia in adolescents with type 1 diabetes. *Diabetes Care*. 35 (8), pp.1757-1762.
- Sihra, T.S., Flores, G. and Rodriguez-Moreno, A. (2014) Kainate receptors: multiple roles in neuronal plasticity. *The Neuroscientist*. 20 (1), pp.29-43.

- Sillevis Smitt, P., Kinoshita, A., De Leeuw, B., Moll, W., Coesmans, M., Jaarsma, D., Henzen-Logmans, S., Vecht, C., De Zeeuw, C., Sekiyama, N., Nakanishi, S. and Shigemoto, R. (2000) Paraneoplastic cerebellar ataxia due to autoantibodies against a glutamate receptor. *The New England Journal of Medicine*. 342 (1), pp.21-27.
- Silva, H.,P.V., Ururahy, M.,A.G., Souza, K.,S.C., Loureiro, M.,B., Oliveira, Y.,M.C., Oliveira, G.,H.M., Luchessi, A.,D., Carvalho, K.,T.C., Freitas, J.,C.O.C., Donadi, E.,A., Hirata, R.,D.C., Almeida, M.,G., Arrais, R.,F., Hirata, M.,H. and Rezende, A.,A. (2016) The association between the HLA-G 14-bp insertion/deletion polymorphism and type 1 diabetes. *Genes and Immunity*. 17 (1), pp.13-18.
- Singh, S. (2015) Genetics of type 2 diabetes: advances and future prospect. *Journal of Diabetes & Metabolism*. 6 (4), pp.518-525.
- Skrzypski, M., Khajavi, N., Mergler, S., Szczepankiewicz, D., Kolodziejski, P.A., Metzke, D., Wojciechowicz, T., Billert, M., Nowak, K.W. and Strowski, M.Z. (2015) TRPV6 channel modulates proliferation of insulin secreting INS-1E beta cell line. *Biochimica Et Biophysica Acta*. 1853 (12), pp.3202-3210.
- Sladek, R., Rocheleau, G., Rung, J., Dina, C., Shen, L., Serre, D., Boutin, P., Vincent, D., Belisle, A., Hadjadj, S., Balkau, B., Heude, B., Charpentier, G., Hudson, T.J., Montpetit, A., Pshezhetsky, A.V., Prentki, M., Posner, B.I., Balding, D.J., Meyre, D., Polychronakos, C. and Froguel, P. (2007) A genome-wide association study identifies novel risk loci for type 2 diabetes. *Nature*. 445 (7130), pp.881-885.
- Smolders, I., Bortolotto, Z.A., Clarke, V.R., Warre, R., Khan, G.M., O'Neill, M.J., Ornstein, P.L., Bleakman, D., Ogden, A., Weiss, B., Stables, J.P., Ho, K.H., Ebinger, G., Collingridge, G.L., Lodge, D. and Michotte, Y. (2002) Antagonists of GLU(K5)-containing kainate receptors prevent pilocarpine-induced limbic seizures. *Nature Neuroscience*. 5 (8), pp.796-804.
- Soni, A., Amisten, S., Rorsman, P. and Salehi, A. (2013) GPRC5B a putative glutamate-receptor candidate is negative modulator of insulin secretion. *Biochemical and Biophysical Research Communications*. 291 (13), pp.1780-1784.

- Spijker, H.S., Ravelli, R.B., Mommaas-Kienhuis, A.M., van Apeldoorn, A.A., Engelse, M.A., Zaldumbide, A., Bonner-Weir, S., Rabelink, T.J., Hoeben, R.C., Clevers, H., Mummery, C.L., Carlotti, F. and de Koning, E.J. (2013) Conversion of mature human beta-cells into glucagon-producing alpha-cells. *Diabetes*. 62 (7), pp.2471-2480.
- Spijker, H.S., Song, H., Ellenbroek, J.H., Roefs, M.M., Engelse, M.A., Bos, E., Koster, A.J., Rabelink, T.J., Hansen, B.C., Clark, A., Carlotti, F. and de Koning, E.J. (2015) Loss of beta-Cell Identity Occurs in Type 2 Diabetes and Is Associated With Islet Amyloid Deposits. *Diabetes*. 64 (8), pp.2928-2938.
- Steup-Beekman, G., Steens, S., van Buchem, M. and Huizinga, T. (2007) Anti-NMDA receptor autoantibodies in patients with systemic lupus erythematosus and their first-degree relatives. *Lupus*. 16 (5), pp.329-334.
- Storto, M., Capobianco, L., Battaglia, G., Molinaro, G., Gradini, R., Riozzi, B., Di Mambro, A., Mitchell, K.J., Bruno, V., Vairetti, M.P., Rutter, G.A. and Nicoletti , F. (2006) Insulin secretion is controlled by mGlu5 metabotropic glutamate receptors. *Molecular Pharmacology*. 69 pp.1234-1241.
- Straub, C., Hunt, D.L., Yamasaki, M., Kim, K.S., Watanabe, M., Castillo, P.E. and Tomita, S. (2011) Distinct functions of kainate receptors in the brain are determined by the auxiliary subunit Neto1. *Nature Neuroscience*. 14 (7), pp.866-873.
- Straub, C., Zhang, W. and Howe, J.R. (2011) Neto2 modulation of kainate receptors with different subunit compositions. *The Journal of Neuroscience*. 31 (22), pp.8078-8082.
- Sturgill, J.L., Mathews, J., Scherle, P. and Conrad, D.H. (2011) Glutamate signaling through the kainate receptor enhances human immunoglobulin production. *Journal of Neuroimmunology*. 233 (1-2), pp.80-89.
- Sumioka, A., Brown, T.E., Kato, A.S., Bredt, D.S., Kauer, J.A. and Tomita, S. (2011) PDZ binding of TARPgamma-8 controls synaptic transmission but not synaptic plasticity. *Nature Neuroscience*. 14 (11), pp.1410-1412.

- Sun, H., Swaim, A., Herrera, J.E., Becker, D., Becker, L., Srivastava, K., Thompson, L.E., Shero, M.R., Perez-Tamayo, A., Suktitipat, B., Mathias, R., Contractor, A., Faraday, N. and Morrell, C.N. (2009) Platelet kainate receptor signaling promotes thrombosis by stimulating cyclooxygenase activation. *Circulation Research*. 105 (6), pp.595-603.
- Suzuki, E. and Kamiya, H. (2015) PSD-95 regulates synaptic kainate receptors at mouse hippocampal mossy fiber-CA3 synapses. *Neuroscience Research*. 107, pp.14-19.
- Suzuki, K., Sato, Y., Kai, S., Nishi, K., Adachi, T., Matsuo, Y. and Hirota, K. (2015) Volatile anesthetics suppress glucose-stimulated insulin secretion in MIN6 cells by inhibiting glucose-induced activation of hypoxia-inducible factor 1. *Peerj*. 3 pp.1498-1515.
- Taborsky, G.J.,Jr and Mundinger, T.O. (2012) Minireview: The role of the autonomic nervous system in mediating the glucagon response to hypoglycemia. *Endocrinology*. 153 (3), pp.1055-1062.
- Tamayo, T., Christian, H. and Rathmann, W. (2010) Impact of early psychosocial factors (childhood socioeconomic factors and adversities) on future risk of type 2 diabetes, metabolic disturbances and obesity: a systematic review. *BMC Public Health*. 10, pp.525-540.
- Tamayo, T., Rosenbauer, J., Wild, S.H., Spijkerman, A.M., Baan, C., Forouhi, N.G., Herder, C. and Rathmann, W. (2014) Diabetes in Europe: an update. *Diabetes Research and Clinical Practice*. 103 (2), pp.206-217.
- Tang, B.L. (2009) Neuronal protein trafficking associated with Alzheimer disease: from APP and BACE1 to glutamate receptors. *Cell Adhesion & Migration*. 3 (1), pp.118-128.
- Tang, M., Ivakine, E., Mahadevan, V., Salter, M.W. and McInnes, R.R. (2012) Neto2 interacts with the scaffolding protein GRIP and regulates synaptic abundance of kainate receptors. *PloS One*. 7 (12), pp.51433-51441.

- Tarasov, A.I., Semplici, F., Li, D., Rizzuto, R., Ravier, M.A., Gilon, P. and Rutter, G.A. (2013) Frequency-dependent mitochondrial Ca2+ accumulation regulates ATP synthesis in pancreatic beta cells. *Pflugers Archiv-European Journal of Physiology*. 465 (4), pp.543-554.
- Tarry-Adkins, J.L., Chen, J.H., Jones, R.H., Smith, N.H. and Ozanne, S.E. (2010) Poor maternal nutrition leads to alterations in oxidative stress, antioxidant defense capacity, and markers of fibrosis in rat islets: potential underlying mechanisms for development of the diabetic phenotype in later life. *FASEB Journal*. 24 (8), pp.2762-2771.
- Taylor, B.L., Benthuysen, J. and Sander, M. (2015) Postnatal beta-cell proliferation and mass expansion is dependent on the transcription factor Nkx6.1. *Diabetes*. 64 (3), pp.897-903.
- Thiering, E., Bruske, I., Kratzsch, J., Thiery, J., Sausenthaler, S., Meisinger, C., Koletzko, S., Bauer, C.P., Schaaf, B., von Berg, A., Berdel, D., Lehmann, I., Herbarth, O., Kramer, U., Wichmann, H.E., Heinrich, J. and GINIplus and LISAplus Study Groups (2011) Prenatal and postnatal tobacco smoke exposure and development of insulin resistance in 10 year old children. *International Journal of Hygiene and Environmental Health*. 214 (5), pp.361-368.
- Thorel, F., Nepote, V., Avril, I., Kohno, K., Desgraz, R., Chera, S. and Herrera, P.L. (2010) Conversion of adult pancreatic alpha-cells to beta-cells after extreme beta-cell loss. *Nature*. 464 (7292), pp.1149-1154.
- Thorn, P., Zorec, R., Rettig, J. and Keating, D.J. (2016) Exocytosis in non-neuronal cells. *Journal of Neurochemistry*. 137 (6), pp.849-859.
- Tom, R., Bisson, L. and Durocher, Y. (2008) Transfection of HEK293-EBNA1 Cells in Suspension with Linear PEI for Production of Recombinant Proteins. *CSH Protocols*. 4977-4982.
- Tomita, S. and Castillo, P.E. (2012) Neto1 and Neto2: auxiliary subunits that determine key properties of native kainate receptors. *Journal of Physiology*. 590 (10), pp.2217-2223.

- Toplak, H., Hamann, A., Moore, R., Masson, E., Gorska, M., Vercruysse, F., Sun, X., Fitchet, M. and OBDM-002 Study Grp (2007) Efficacy and safety of topiramate in combination with metformin in the treatment of obese subjects with type 2 diabetes: a randomized, double-blind, placebo-controlled study. *International Journal of Obesity*. 31 (1), pp.138-146.
- Toselli, C., Hyslop, C.M., Hughes, M., Natale, D.R., Santamaria, P. and Huang, C.T. (2014) Contribution of a non-beta-cell source to beta-cell mass during pregnancy. *PloS One*. 9 (6), pp. 100398-100410.
- Traynelis, S.F., Wollmuth, L.P., McBain, C.J., Menniti, F.S., Vance, K.M. and Ogden, K.K. (2010) Glutamate receptor ion channels: structure, regulation, and function. . 62, pp. 405–496. *Pharmacology Reviews*. 62 pp.405-496.
- Tsunekawa, S., Yamamoto, N., Tsukamoto, K., Itoh, Y., Kaneko, Y., Kimura, T., Ariyoshi, Y., Miura, Y., Oiso, Y. and Niki, I. (2007) Protection of pancreatic beta-cells by exendin-4 may involve the reduction of endoplasmic reticulum stress; in vivo and in vitro studies. *Journal of Endocrinology*. 193 (1), pp.65-74.
- Tuomi, T., Santoro, N., Caprio, S., Cai, M., Weng, J. and Groop, L. (2014) The many faces of diabetes: a disease with increasing heterogeneity. *Lancet*. 383 (9922), pp.1084-1094.
- Twele, F., Bankstahl, M., Klein, S., Romermann, K. and Loscher, W. (2015) The AMPA receptor antagonist NBQX exerts anti-seizure but not antiepileptogenic effects in the intrahippocampal kainate mouse model of mesial temporal lobe epilepsy. *Neuropharmacology*. 95 pp.234-242.
- Uhlen, M., Fagerberg, L., Hallstrom, B.M., Lindskog, C., Oksvold, P., Mardinoglu, A., Sivertsson, A., Kampf, C., Sjostedt, E., Asplund, A., Olsson, I., Edlund, K., Lundberg, E., Navani, S., Szigyarto, C.A., Odeberg, J., Djureinovic, D., Takanen, J.O., Hober, S., Alm, T., Edqvist, P.H., Berling, H., Tegel, H., Mulder, J., Rockberg, J., Nilsson, P., Schwenk, J.M., Hamsten, M., von Feilitzen, K., Forsberg, M., Persson, L., Johansson, F., Zwahlen, M., von Heijne, G., Nielsen, J. and Ponten, F. (2015) Proteomics. Tissue-based map of the human proteome. *Science*. 347 (6220), pp.1260419-1260432.

- Uil, T.G., Vellinga, J., de Vrij, J., van den Hengel, S.K., Rabelink, M.J.W.E., Cramer, S.J., Eekels, J.J.M., Ariyurek, Y., van Galen, M. and Hoeben, R.C. (2011) Directed adenovirus evolution using engineered mutator viral polymerases. *Nucleic Acids Research*. 39 (5), pp.30-44.
- Unger, R.H. and Cherrington, A.D. (2012) Glucagonocentric restructuring of diabetes: a pathophysiologic and therapeutic makeover. *The Journal of Clinical Investigation*. 122 (1), pp.4-12.
- van Praag, H., Fleshner, M., Schwartz, M.W. and Mattson, M.P. (2014) Exercise, energy intake, glucose homeostasis, and the brain. *The Journal of Neuroscience*. 34 (46), pp.15139-15149.
- Vandal, M., White, P.J., Tremblay, C., St-Amour, I., Chevrier, G., Emond, V., Lefrancois, D., Virgili, J., Planel, E., Giguere, Y., Marette, A. and Calon, F. (2014) Insulin reverses the high-fat diet-induced increase in brain Abeta and improves memory in an animal model of Alzheimer disease. *Diabetes*. 63 (12), pp.4291-4301.
- Vandenberg, R.J. and Ryan, R.M. (2013) Mechanisms of glutamate transport. *Physiological Reviews*. 93 (4), pp.1621-1657.
- Varadi, A., Cirulli, V. and Rutter, G.A. (2004) Mitochondrial localization as a determinant of capacitative Ca^{2+} entry in HeLa cells. *Cell Calcium*. 36 (6), pp.499-508.
- Varadi, A., Molnar, E., Ostenson, C.G. and Ashcroft, S.J. (1996) Isoforms of endoplasmic reticulum Ca(2+)-ATPase are differentially expressed in normal and diabetic islets of Langerhans. *The Biochemical Journal*. 319 (2), pp.521-527.
- Varadi, A. and Rutter, G.A. (2002) Dynamic imaging of endoplasmic reticulum Ca^{2+} concentration in insulin-secreting MIN6 cells using recombinant targeted cameleons - Roles of sarco(endo)plasmic reticulum Ca^{2+}-ATPase (SERCA)-2 and ryanodine receptors. *Diabetes*. 51 pp.S190-S201.
- Varadkar, S., Bien, C.G., Kruse, C.A., Jensen, F.E., Bauer, J., Pardo, C.A., Vincent, A., Mathern, G.W. and Cross, J.H. (2014) Rasmussen's encephalitis: clinical features, pathobiology, and treatment advances. *The Lancet. Neurology*. 13 (2), pp.195-205.

- Vargas, J.R., Takahashi, D.K., Thomson, K.E. and Wilcox, K.S. (2013) The expression of kainate receptor subunits in hippocampal astrocytes after experimentally induced status epilepticus. *Journal of Neuropathology and Experimental Neurology*. 72 (10), pp.919-932.
- Varma, A. and Sapra, M. (2015) Anti-NMDA Receptor Encephalitis: A need for increased awareness among psychiatrists. *Psychiatric Annals*. 45 pp.572-576.
- Vehik, K., Ajami, N.J., Hadley, D., Petrosino, J.F. and Burkhardt, B.R. (2013) The changing landscape of type 1 diabetes: recent developments and future frontiers. *Current Diabetes Reports*. 13 (5), pp.642-650.
- Verbeeten, K.C., Elks, C.E., Daneman, D. and Ong, K.K. (2011) Association between childhood obesity and subsequent Type 1 diabetes: a systematic review and meta-analysis. *Diabetic Medicine*. 28 (1), pp.10-18.
- Vetere, A., Choudhary, A., Burns, S.M. and Wagner, B.K. (2014) Targeting the pancreatic beta-cell to treat diabetes. *Nature Reviews Drug Discovery*. 13 (4), pp.278-289.
- Vetterli, L., Carobbio, S., Pournourmohammadi, S., Martin-Del-Rio, R., Skytt, D.M., Waagepetersen, H.S., Tamarit-Rodriguez, J. and Maechler, P. (2012) Delineation of glutamate pathways and secretory responses in pancreatic islets with beta-cell-specific abrogation of the glutamate dehydrogenase. *Molecular Biology of the Cell*. 23 (19), pp.3851-3862.
- Vimalananda, V.G., Palmer, J.R., Gerlovin, H., Wise, L.A., Rosenzweig, J.L., Rosenberg, L. and Ruiz Narvaez, E.A. (2015) Night-shift work and incident diabetes among African-American women. *Diabetologia*. 58 (4), pp.699-706.
- Vincent, P. and Mulle, C. (2009) Kainate receptors in epilepsy and excitotoxicity. *Neuroscience*. 158 (1), pp.309-323.
- Virk, J., Li, J., Vestergaard, M., Obel, C., Kristensen, J.K. and Olsen, J. (2012) Prenatal exposure to bereavement and type-2 diabetes: a Danish longitudinal population based study. *PloS One*. 7 (8), pp.e43508.

- Viswaprakash, N., Vaithianathan, T., Viswaprakash, A., Judd, R., Parameshwaran, K. and Suppiramaniam, V. (2015) Insulin treatment restores glutamate (alpha-amino-3-hydroxy-5-methyl-4-isoxazolepropionic acid) receptor function in the hippocampus of diabetic rats. *Journal of Neuroscience Research*. 93 (9), pp.1442-1450.
- Vyklicky, V., Korinek, M., Smejkalova, T., Balik, A., Krausova, B., Kaniakova, M., Lichnerova, K., Cerny, J., Krusek, J., Dittert, I., Horak, M. and Vyklicky, L. (2014) Structure, function, and pharmacology of NMDA receptor channels. *Physiological Research / Academia Scientiarum Bohemoslovaca*. 63 Suppl 1 pp.S191-203.
- Wallis, J.L., Irvine, M.W., Jane, D.E., Lodge, D., Collingridge, G.L. and Bortolotto, Z.A. (2015) An interchangeable role for kainate and metabotropic glutamate receptors in the induction of rat hippocampal mossy fiber long-term potentiation in vivo. *Hippocampus*. 25 (11), pp.1407-1417.
- Wang, L.G., Zeng, J., Yuan, W.J., Su, D.F. and Wang, W.Z. (2007) Comparative study of NMDA and AMPA/kainate receptors involved in cardiovascular inhibition produced by imidazoline-like drugs in anaesthetized rats. *Experimental Physiology*. 92 (5), pp.849-858.
- Wang, P., Henning, S.M. and Heber, D. (2010) Limitations of MTT and MTS-based assays for measurement of antiproliferative activity of green tea polyphenols. *PloS One*. 5 (4), pp.e10202.
- Weaver, C.D., Yao, T.L., Powers, A.C. and Verdoorn, T.A. (1996) Differential expression of glutamate receptor subtypes in rat pancreatic islets. *Journal of Biological Chemistry*. 271 (22), pp.12977-12984.
- Weir, G.C. and Bonner-Weir, S. (2013) Islet beta cell mass in diabetes and how it relates to function, birth, and death. *Annals of the New York Academy of Sciences*. 1281 pp.92-105.
- Weskamp, G., Ford, J.W., Sturgill, J., Martin, S., Docherty, A.J.P., Swendeman, S., Broadway, N., Hartmann, D., Saftig, P., Umland, S., Sehara-Fujisawa, A., Black, R.A., Ludwig, A., Becherer, J.D., Conrad, D.H. and Blobel, C.P. (2006) ADAM10 is a principal 'sheddase' of the low-affinity immunoglobulin E receptor CD23. *Nature Immunology*. 7 (12), pp.1293-1298.

- Whitehead, G., Jo, J., Hogg, E.L., Piers, T., Kim, D.H., Seaton, G., Seok, H., Bru-Mercier, G., Son, G.H., Regan, P., Hildebrandt, L., Waite, E., Kim, B.C., Kerrigan, T.L., Kim, K., Whitcomb, D.J., Collingridge, G.L., Lightman, S.L. and Cho, K. (2013) Acute stress causes rapid synaptic insertion of Ca^{2+}-permeable AMPA receptors to facilitate long-term potentiation in the hippocampus. *Brain*. 136 (Pt 12), pp.3753-3765.
- Wicht, H., Maronde, E., Olcese, J. and Korf, H.W. (1999) A semiquantitative image-analytical method for the recording of dose-response curves in immunocytochemical preparations. *The Journal of Histochemistry and Cytochemistry*. 47 (3), pp.411-420.
- Willard, S.S. and Koochekpour, S. (2013) Glutamate, glutamate receptors, and downstream signaling pathways. *International Journal of Biological Sciences*. 9 (9), pp.948-959.
- Wollheim, C.B. and Maechler, P. (2015) Beta cell glutamate receptor antagonists: novel oral antidiabetic drugs? *Nature Medicine*. 21 (4), pp.310-311.
- Wu, Z.-., Zhu, L.-., Zou, N., Bombek, L.K., Shao, C.-., Wang, N., Wang, X.-., Liang, L., Xia, J., Rupnik, M. and Shen, Y. (2012) AMPA Receptors Regulate Exocytosis and Insulin Release in Pancreatic β Cells. *Traffic*. 13 pp.1124-1139.
- Wyeth, M.S., Pelkey, K.A., Petralia, R.S., Salter, M.W., McInnes, R.R. and McBain, C.J. (2014) Neto auxiliary protein interactions regulate kainate and NMDA receptor subunit localization at mossy fiber-CA3 pyramidal cell synapses. *The Journal of Neuroscience*. 34 (2), pp.622-628.
- Xie, L., Dolai, S., Kang, Y., Liang, T., Xie, H., Qin, T., Yang, L., Chen, L. and Gaisano, H.Y. (2016) Syntaxin-3 Binds and Regulates Both R- and L-Type Calcium Channels in Insulin-Secreting INS-1 832/13 Cells. *Plos One*. 11 (2), pp.e0147862.
- Xu, Y., Wang, L., He, J., Bi, Y., Li, M., Wang, T., Wang, L., Jiang, Y., Dai, M., Lu, J., Xu, M., Li, Y., Hu, N., Li, J., Mi, S., Chen, C.S., Li, G., Mu, Y., Zhao, J., Kong, L., Chen, J., Lai, S., Wang, W., Zhao, W., Ning, G. and 2010 China Noncommunicable Disease Surveillance Group (2013) Prevalence and control of diabetes in Chinese adults. *Jama*. 310 (9), pp.948-959.

- Yan, D. and Tomita, S. (2012) Defined criteria for auxiliary subunits of glutamate receptors. *The Journal of Physiology*. 590 (Pt 1), pp.21-31.
- Yang, K., Jackson, M.F. and MacDonald, J.F. (2014) Recent progress in understanding subtype specific regulation of NMDA receptors by G Protein Coupled Receptors (GPCRs). *International Journal of Molecular Sciences*. 15 (2), pp.3003-3024.
- Yasumatsu, K., Manabe, T., Yoshida, R., Iwatsuki, K., Uneyama, H., Takahashi, I. and Ninomiya, Y. (2015) Involvement of multiple taste receptors in umami taste: analysis of gustatory nerve responses in metabotropic glutamate receptor 4 knockout mice. *The Journal of Physiology*. 593 (4), pp.1021-1034.
- Ye, L., Robertson, M.A., Hesselson, D., Stainier, D.Y. and Anderson, R.M. (2015) Glucagon is essential for alpha cell transdifferentiation and beta cell neogenesis. *Development.* 142 (8), pp.1407-1417.
- Yeo, R. and Sawdon, M. (2013) Hormonal control of metabolism: regulation of plasma glucose. *Anaesthesia & Intensive Care Medicine*. 14 (7), pp.296-300.
- Yi, P., Park, J.S. and Melton, D.A. (2013) Betatrophin: a hormone that controls pancreatic β cell proliferation. *Cell*. 153 (4), pp.747-758.
- Yin, S. and Niswender, C.M. (2014) Progress toward advanced understanding of metabotropic glutamate receptors: structure, signaling and therapeutic indications. *Cellular Signalling*. 26 (10), pp.2284-2297.
- Yu, L., Boulware, D.C., Beam, C.A., Hutton, J.C., Wenzlau, J.M., Greenbaum, C.J., Bingley, P.J., Krischer, J.P., Sosenko, J.M., Skyler, J.S., Eisenbarth, G.S., Mahon, J.L. and Type 1 Diabet TrialNet Study Grp (2012) Zinc Transporter-8 Autoantibodies Improve Prediction of Type 1 Diabetes in Relatives Positive for the Standard Biochemical Autoantibodies. *Diabetes Care*. 35 (6), pp.1213-1218.
- Yuchi, Y., Cai, Y., Legein, B., De Groef, S., Leuckx, G., Coppens, V., Van Overmeire, E., Staels, W., De Leu, N., Martens, G., Van Ginderachter, J.A., Heimberg, H. and Van de Casteele, M. (2015) Estrogen Receptor alpha Regulates beta-Cell Formation During Pancreas Development and Following Injury. *Diabetes*. 64 (9), pp.3218-3228.

- Zanisi, M., Galbiati, M., Messi, E. and Martini, L. (1994) The anterior pituitary gland as a possible site of action of kainic acid. *Proceedings of the Society for Experimental Biology and Medicine*. 206 (4), pp.431-437.
- Zhang, W., Devi, S.P., Tomita, S. and Howe, J.R. (2014) Auxiliary proteins promote modal gating of AMPA- and kainate-type glutamate receptors. *The European Journal of Neuroscience*. 39 (7), pp.1138-1147.
- Zhang, W., St-Gelais, F., Grabner, C.P., Trinidad, J.C., Sumioka, A., Morimoto-Tomita, M., Kim, K.S., Straub, C., Burlingame, A.L., Howe, J.R. and Tomita, S. (2009) A Transmembrane Accessory Subunit that Modulates Kainate-Type Glutamate Receptors. *Neuron*. 61 (3), pp.385-396.
- Zhang, X.M. and Zhu, J. (2011) Kainic Acid-induced neurotoxicity: targeting glial responses and glia-derived cytokines. *Current Neuropharmacology*. 9 (2), pp.388-398.
- Zheng, X.L., Xie, Z.H., Zhu, Z.Y., Liu, Z., Wang, Y., Wei, L.F., Yang, H., Yang, H.N., Liu, Y.Q. and Bi, J.Z. (2014) Methyllycaconitine Alleviates Amyloid-Î² Peptides-Induced Cytotoxicity in SH-SY5Y Cells. *Plos One*. 9 (10), 111536-111543.
- Zhou, Y. and Danbolt, N.C. (2014) Glutamate as a neurotransmitter in the healthy brain. *Journal of Neural Transmission*. 121 (8), pp.799-817.
- Zhu, X., Wang, K., Zhang, K., Lin, X., Zhu, L. and Zhou, F. (2016) Puerarin Protects Human Neuroblastoma SH-SY5Y Cells against Glutamate-Induced Oxidative Stress and Mitochondrial Dysfunction. *Journal of Biochemical and Molecular Toxicology*. 30 (1), pp.22-28.
- Zurawek, M., Fichna, M., Fichna, P., Skowronska, B., Dzikiewicz-Krawczyk, A., Januszkiewicz, D. and Nowak, J. (2015) Cumulative effect of IFIH1 variants and increased gene expression associated with type 1 diabetes. *Diabetes Research and Clinical Practice*. 107 (2), pp.259-266.

2-mercaptoethanol	Sigma M6250
Advanced DMEM	Thermo-Fisher 12491-015
Agarose	Sigma A9539
BCA Protein Assay Reagent kit	Thermo-Fisher 23227
BIOTAQ DNA polymerase	Bioline BIO-21040
BSA	Sigma A9418
cDNA synthesis kit	Bioline BIO-65043
Chloroform	Sigma 288306
DEPC-treated water	Sigma 95284
DHPG	Tocris 0805
DMEM 25 mM Glucose	Sigma D5671
DMEM no Glucose	Thermo-Fisher 11966-025
DMSO	SigmaD8418
EDTA	Sigma E9884
Enhanced K-Blue® TMB substrate	Oxford Biosystems 308177
EZ-Link™ Sulfo-NHS-SS-Biotin	Thermo-Fisher 21331
FBS	Thermo-Fisher 16000-044
FURA-2AM	Thermo-Fisher F-1221
Glycine	Sigma G8898
Gyki-52466	Tocris 1454
HRP substrate	Millipore WBKLS0500
HRP-conjugated anti-mouse antibody	Sigma A9044
HRP-conjugated anti-rabbit antibody	Sigma A0545
Human Serum Stabilised - Delipidated	TCS Biosciences DR750-500
IGEPAL® or Nonidet P-40	Sigma I3021
Kainate	Tocris 0222
L-glutamic acid	Sigma G1251
L-glutamine solution	Sigma G7513
Low melting point agarose	Sigma A9414
Mouse Insulin ELISA kit	Diagenics 10-1247-01
MTT powder	Sigma M5655
NBQX	Tocris 0373
Nuclease-free water	Sigma W4502
Nunc-Immuno™ MicroWell™ 96-well ELISA plates	Sigma M9410-1CS
Opti-MEM® I Reduced Serum Media	Thermo-Fisher 31985-062
Penicillin/streptomycin	Sigma P4333
Phenol-free DMEM	Thermo-Fisher 21063-029
PMSF	Sigma P7626
Polyethylenimine (PEI)	Sigma 408727
Poly-L-lysine hydrobromide	Sigma P1399
Ponceau red	Sigma P7170
Protease inhibitor cocktail	Roche 04693116001
Rabbit anti-GluK2/3	Millipore 07-598
Rabbit GluK5 antibodies	Millipore 06-315
Rat Insulin ELISA kit	Diagenics 10-1250-01
RPMI amino acid solution	Sigma R7131
RPMI-1640	Sigma R5886

SDS	Sigma L3771
Sodium deoxycholate	Sigma D6750
Sodium orthovanadate	Sigma S6508
Sodium pyruvate	Sigma P2256
StreptaAvidin agarose beads	Thermo-Fisher 20353
Treated cell culture dishes	Thermo-Fisher 150288
Tri reagent	Sigma T9424
Triton X-100	Sigma T8787
Trypsin-EDTA	Sigma T3924
Wizard® SV PCR Clean-Up kit	Promega A9281

Appendix II

DNA Sequencing Results

5 ng/µl of purified PCR product together with its specific forward or reverse primers were sent to Eurofins MWG (Ebersberg, Germany) to be sequenced.

1.1. *KAR subunit expression in MIN6 mouse β-cells*

GluK2: Reverse primer (CAGAGCAGCATCAGTCGTCA)

Sequence of gene amplified:

TGAGTCAGGTTTTGGAGGTGCCTGTAACCGTTCCATCGACCACTTCTCGATGATGGAGGA
GACTTGGGTATTCTCTGTATTTAGTATTCTGAACCCTGTCATATTTACGCCACTGTATCT
GTAGGGCTCCACATCAAGAGCGAAGAGGTCCAGAGTCGTAAATATATAGTGGTAGTATTC
TGTCATCATTCCCATAGCTAATGCCTGCTTTAAAATGCCTGCTGCCATTTCATGGCTGCA
GTCGAAGATCACGTGGAACTCCTTGCCCCTCTTCATCTCTTTCAGCAAAGGCTTTGCATC
TTTTGTATCAGCTGGCAGCTGACGAATTTTAAGTCGAAGATTGTACCTTGATGGAGCTTT
GATGAGCTCTTGCAAGCGAATGAGACCAGTGCTGTCGTCATACACAACTGTGACAGTTTT
CCACTTAAAAAACTGCACCAAATCCAAGATGGCACGGCTGAGGAAAAAG

GluK3: Forward primer (GGTTCCGCATACTCAACGTG)

Sequence of gene amplified:

CTAGCATTGTGGAGAGTGGGCCATGGAGCGACTGCAGGCAGCTCCCCGGGCAGAGTCAGG
CCTGCTGGATGGTGTGATGATGACGGATGCTGCCCTGCTCTATGACGCGGTCCACATTGT
GTCTGTGTGCTACCAGCGAGCGCCACAGATGACCGTGAACTCCCTGCAGTGCCATCGGCA
CAAGGCCTGGCGCTTTGGTGGCCGCTTCATGAACTTCATCAAGGAGGCTCAATGGGAAGG
ATTAACTGGACGGATTGTGTTCAACAAAACCAGTGGCTTGCGGACTGATTTTGATCTGGA
CATCATCAGCCTGAAGGAAGATGGCCTCGAGAAGGTTGGAGTATGGAGTCCAGCTGACGG
TCTCAATATCACTGAGGTTGCCAAAGGCCGAGGTCCTAATGTCACTGACTCTCTGACCAA
TAGGTCACTCATCGTCACCACTGTGCTGGAGGAGCCTTTTGTCATGTTCCGCAAGTCTGA
TAGGACCCTTTATGGCAATGACCGGTTTGAGGGCTACTGCATAA

GluK4: Forward primer (ATCCGGGATGACAAGACAGC)

Sequence of gene amplified:

CTCCATGTCGCACACCATCCTCCTGAAGGCAGCTGAACTGGGGATGGTGTCAGCCTATTA
CACATACATCTTCACCAATCTGGAGTTCTCCCTCCAGAGAATGGACAGCCTTGTGGATGA
TAGAGTCAACATCTTAGGATTTTCCATTTTCAACCAATCCCATGCATTCTTCCAAGAGTT
CTCCCAGAGCCTCAACCAATCCTGGCAGGAGAACTGTGACCATGTGCCCTTCACCGGCCC
TGCGTTGTCCTCAGCCCTGCTGTTTGACGCTGTCTATGCTGTGGTGACAGCGGTACAGGA
ACTGAACCGGAGCCAAGAGATTGGTGTGAAGCCCCTGTCCTGTGGCTCAGCCCAGATCTG
GCAGCATGGCACCAGCCTCATGAACTACCTTCGCATGGTAGAATTGGAAGGTCTTACCGG
CCACATTA

Gluk5: Reverse primer (TACCACACCCCTATCTCACG)

Sequence of gene amplified:

CTCTCAGGATGCGTAGTGTGTAGTTGGTCCTCTGCCCTTTGCTGTTGAACTCAACCCGCC
CGGTCAGCCCGTCATACTCTACCATTCGAAGGTAGTTCATAAGGCTGGTCCCATGGGGCC
AAATGTTGGCCGAAGTGCAGGCCAGTGGCTTGACGCCAATCTCCTGGCTTCGGTTCAGTT
CTCGGACAGCGCTTACCACCACGTGCACAGCGTCAAACATCAGGGCTGCGGACAGCGCAG
GGCCAGGATAGGTGCTGGCTTCACAGTTCTCCCTCCAGGACATGTTGAGGCTGCGCACAA
ACTCTGGGTAGAAGGGGTGGGAGGTGTTGAACATGGAAAAGCCCAGGATGTTGGAGGAGT
CCTCCACGATACCATCCAGATGCAGGATGGGAAAGTCCATGGTGGTGAGGATGTACTTGT
AAAACGCTGAGGTCATTCCCAGCTCCGAAGCCTTAC

1.2. *Neto 1 and Neto 2 expression in MIN6 mouse β-cells*

Neto 1: Forward primer (CACCAGTGGGACTGTCATTG)

Sequence amplified:

GGGATGGCTGTGATCATCCTTATTATCGTTTCTGTCATTGTACAGATCAAACAGCCTCGT
AAAAAATACGTCCAAAGGAAGTCAGACTTTGACCAGACCGTTTTCCAGGAGGTGTTTGAG
CCTCCCCACTATGAGTTATGTACGCTCAGAGGAACTGGAGCAACAGCCGACTTTGCAGAT
GTGGCAGAGAACGATAATTCGGATGATCACAATGCAGGAAGTCACGCCGATGACAGTCCC
ACTCAGGGCGCCCCCGCACTGCTGATCTATTTCTTCTACTATATACTTACCACAAGGGAC
ATCTTCCTTCTTGATGGCCAGCCCTACATATTCAGAGTTAAAAAAATGAGGGGGTTCAG

Neto 2: Forward primer (CACCAGTGGGACTGTCATTG)

Sequence amplified:

GGGTCAAACATGAGTGTATCTATATTTTGGAAGCTGCTCCTCGTCAACGAATAGAGCTGA
CCTTTGATGAACGCTATTATATAGAGCCATCATTCGAATGTCGGTTTGATCACTTGGAAA
TTCGAGACGGGCCATTTGGTTTTTCTCCTCTTATAGATCGTTACTGTGGCGTGAAAAGCC
CTCCATTAAAAAGAGGGGGTTGAGTCGAAGACTGGTGGGATCCTCTGGGTTTCAAGGGCT
CCAATAACGATCCTGCCCCCTCCTGCTCAATTTCTTGTATTTCATTCCTTCCGCGGAGAA
CAATCTTGGCTCCCCGCAAGCCCGGCCTCCCTTCTGTTATTTATAGAAGCCCAGGGAGGG
AAAGTGATGCCCTGTCCATCAAACAGACCCCGAGGAAAGTCTCCCCTGGGGAAGATACTT
ATTCCTCCGACTTGTTGCC

1.3. *KAR subunit expression in INS-1 rat β-cells*

GluK2: Reverse primer (CGGTTCTTCCAAAATGGTGGT)

Sequence of gene amplified:

GTTTTTTAGTGGAACTGTCACAGTTGTGTATGACGACAGCACTGGTCTCATTCGCTTGCA
AGAGCTCATCAAAGCTCCATCAAGGTACAATCTTCGACTTAAAATTCGTCAGCTGCCAGC
TGATACAAAAGATGCAAAGCCTTTGCTGAAAGAGATGAAGAGGGGCAAGGAGTTCCACGT
GATCTTCGACTGCAGCCATGAAATGGCAGCAGGCATTTTAAAGCAGGCATTAGCTATGGG
AATGATGACAGAATACTACCACTATATATTTACGACTCTGGACCTCTTCGCTCTTGATGT
GGAGCCCTACAGATACAGTGGCGTAAATATGACAGGGTTCAGAATACTAAATACAGAGAA
TACCCAAGTCTCCTCCATCATCGAGAAGTGGTCGATGGAACGGTTACAGGCACCTCCAAA
ACCTGACTCAGGTTTGCTGGATGGATTTATGACGACTGATGCTGCTCTAAT

GluK3: Forward primer (CCGAGGTCCTAATGTCACCG)

Sequence of gene amplified:

TAGCCATTGTGGAGAGTGGTCCATGGAGCGGCTACAGGCAGCTCCCCGGGCAGAGTCAGG
CCTGCTGGATGGAGTGATGATGACCGATGCAGCCCTGCTCTACGATGCGGTCCACATTGT
GTCTGTGTGCTACCAGCGAGCGCCGCAGATGACTGTGAACTCCCTACAGTGCCATCGGCA
CAAGGCCTGGCGCTTCGGTGGCCGCTTCATGAACTTCATCAAGGAGGCTCAATGGGAAGG
ATTAACTGGACGGATTGTTTTCAACAAAACCAGTGGCTTGCGGACTGATTTTGATCTGGA
CATCATCAGCCTCAAGGAAGATGGCCTCGAGAAGGTCGGGGTGTGGAGTCCAGCTGACGG
TCTCAATATCACTGAGGTTGCCAAAGGCCGAGGTCCTAATGTCACCGACTCTCTGACCAA
CAGGTCAC

GluK4: Forward primer (CCAGGTTGGCTGTGTACGAT)

Sequence of gene amplified:

GGCCCGTGGGTATGCCGACTGAGCACACACCTTGGACCCAAAATTTGTCTTGACTATAAG
ATGTACAGGGGTAAAAAATGGAACAGAATTTGAGGGTATGGCCAATCAATTCCTGGCCCA
GAATGAGATCTACGAGAGAGAGCTCACCCCTGCAACTATTAATGATATTCTGATATATTT
GAAGACAGGAGCCGAGCATAAGTGTCATCAGTGAGGTTTCACCCAGCAACTGCGGGAAAA
TGTTGCAAAGACCCATAACCAAATCCTGTGGAATCCCTTTGGCGATTCTGTGGAAGAGGG
GAGTTGAGGACCGAACATGGTACAAGGGTCAAGGACAACACGAGGGAAACTACATTATTG
ATTAATCCGGGCTCAAATGGGTTTATAGTGAATCAACTG

Gluk5: Reverse primer (GGACTTCCCCATCCTGCATC)

Sequence of gene amplified:

ACGGAGCTGGGATGACCTCAGCGTTTTACAAGTACATCCTCACCACCATGGACTTTCCCA
TCCTGCATCTGGATGGTATCGTGGAGGACTCCTCCAACATCCTGGGCTTTTCCATGTTCA
ACACCTCCCACCCCTTCTACCCAGAGTTTGTGCGCAGCCTCAACATGTCCTGGAGGGAGA
ACTGTGAAGCCAGCACCTATCCTGGCCCTGCGCTGTCCGCAGCCCTGATGTTTGACGCTG
TGCACGTGGTGGTAAGCGCTGTCCGAGAACTGAACCGAAGCCAGGAGATTGGCGTCAAGC
CACTGGCCTGCACTTCGGCCAACATTTGGCCCCATGGGACCAGCCTTATGAACTACCTTC
GAATGGTAGAGTATGACGGGCTGACCGGGCGGGTTGAGTTCAACAGCAAAGGGCAGAGGA
CCAACTACACACTACCCATCCTGGAGAAGTCCCGCCAGGGCCACCG

1.4. *Neto 1 and Neto 2 expression in INS-1 rat β-cells*

Neto 1: Forward primer (CACCAGTGGGACTGTCATTG)

Sequence amplified:

TGATCTCCTTATTATCGTTTCTGTCATTGTACAGATCAAACAGCCTCGTAAAAAATACGT
CCAAAGGAAGTCAGACTTTGACCAGACCGTTTTCCAGGAGGTGTTTGAGCCTCCCCACTA
TGAGTTATGTACGCTCAGAGGAACTGGAGCAACAGCCGACTTTGCAGATGTGGCAGAA

Neto 2: Forward primer (TTTGCTTCGCCAAATTATCC)

Sequence amplified:

AGGAGTGTATCTATATTTTGGAAGCTGCTCCTCGTCAACGAATAGAGCTGACCTTTGATG
AACGCTATTATATAGAGCCATCATTCGAATGTCGGTTTGATCACTTGGAAATTCGAGACG
GGCCATTTGGTTTTTCTCCTCTTATAGATCGTTACTGTGGCGTGAAAAGCCCTCCATTAA

1.5. *KAR subunit expression in α-TC1 clone 6 mouse α-cells*

GluK2: Forward primer (GACTTCTCTTCCCTCAGCCG)

Sequence amplified:

GACGTCATGGTGCAGCTTTTAGTGGAACTGTCACAGTTGTGTATGACGACAGCACTGGTC
TCATTCGCTTGCAAGAGCTCATCAAAGCTCCATCAAGGTACAATCTTCGACTTAAAATTC
GTCAGCTGCCAGCTGATACAAAAGATGCAAAGCCTTTGCTGAAAGAGATGAAGAGGGGCA
AGGAGTTCCACGTGATCTTCGACTGCAGCCATGAAATGGCAGCAGGCATTTTAAAGCAGG
CATTAGCTATGGGAATGATGACAGAATACTACCACTATATATTTACGACTCTGGACCTCT
TCGCTCTTGATGTGGAGCCCTACAGATACAGTGGCGTAAATATGACAGGGTTCAGAATAC
TAAATACAGAGAATACCCAAGTCTCCTCCATCATCGAGAAGTGGTCGATGGAACGGTTAC
AGGCACCTCCAAAACCTGACTCAGGTTTGCTGGATGGATTTATGACGACTGTGCCTTGCT
CTA

GluK3: Reverse primer (ATGCAGTAGCCCTCAAACCG)

Sequence amplified:

CACTTTATCTACCTAGGCTCTGTCAGACTTGCGGAACATGACAAAAGGCTCCTCCAGCAC
AGTGGTGACGATGAGTGACCTATTGGTCAGAGAGTCAGTGACATTAGGACCTCGGCCTTT
GGCAACCTCAGTGATATTGAGACCGTCAGCTGGACTCCATACTCCAACCTTCTCGAGGCC
ATCTTCCTTCAGGCTGATGATGTCCAGATCAAAATCAGTCCGCAAGCCACTGGTTTTGTT
GAACACAATCCGTCCAGTTAATCCTTCCCATTGAGCCTCCTTGATGAAGTTCATGAAGCG
GCCACCAAAGCGCCAGGCCTTGTGCCGATGGCACTGCAGGGAGTTCACGGTCATCTGTGG
CGCTCGCTGGTAGCACACAGACACAATGTGGACCGCGTCATAGAGCAGGGCAGCATCCGT
CATCATCACACCATCCAGCAGGCCTGACTCTGCCCGGGGAGCTGCCTGCAGTCGCTCCAT
GGCCCACTTCTCCACAATGGCTGAGACATGGGGATTGTCCACGTTGAGTATGCGGAACCA
ACT

GluK4: Forward primer (ATCCGGGATGACAAGACAGC)

Sequence amplified:

CCAAATTTTTTGTAATTTATTATGCTGGTGCGATCCTGCTGACCTATCTCTGACTCACCC
GACAGACACTTCCTTCCATCTCTTGCTTGCGTCTCGTTTCCTGCCCGGATGTCTGCAACC
CATACATAGACTCCAACAAACAGCCTGACTAAAGACCACGCCCGGTGAAGGAAAGATGCA
TGCACTTCTCTCGCCTGGCTTGATTGATTGACTGTCTGAAATATTTCTTGAAAGAATGGA
TGTGATTGAATGAAAATGATCCATCCATGTATGTTCTCTCTTTCATCCAGCTGGCTGTTC
TTTCTCTGGAGAAATACCTATTGATTGATAAGTATGTGTAAGAAATTGACTCACTCCCTC
CCCCATTTGCCTTCCTTAAGAAGGAGGGCGAGCTACATGCATTGGTTGGCATGAATAATG
AAACTGTCTTGCTTGCCCTCATAGATA

GluK5: Forward primer (TGATGCCAATGCGTCCATCT)

Sequence amplified:

AAAGTCCTCGTAGCTTCGGAGCTGGGATGACCTCAGCGTTTTACAAGTACATCCTCACCA
CCATGGACTTTCCCATCCTGCATCTGGATGGTATCGTGGAGGACTCCTCCAACATCCTGG
GCTTTTCCATGTTCAACACCTCCCACCCCTTCTACCCAGAGTTTGTGCGCAGCCTCAACA
TGTCCTGGAGGGAGAACTGTGAAGCCAGCACCTATCCTGGCCCTGCGCTGTCCGCAGCCC
TGATGTTTGACGCTGTGCACGTGGTGGTAAGCGCTGTCCGAGAACTGAACCGAAGCCAGG
AGATTGGCGTCAAGCCACTGGCCTGCACTTCGGCCAACATTTGGCCCCATGGGACCAGCC
TTATGAACTACCTTCGAATGGTAGAGTATGACGGGCTGACCGGGCGGGTTGAGTTCAACA
GCAAAGGGCAGAGGACCAACTACACACTACGCATCCTGGAGAAGTCCCGCCAGGGCCACC
GTGAGATAGGGGTGTGGTAA

1.6. *Neto 1 and Neto 2 expression in α-TC1 clone 6 mouse α-cells*

Neto 1: Forward primer (CACCAGTGGGACTGTCATTG)

Sequence amplified:

GGGTGCATGTGATATCCTTATTATCGTTTCTGTCATTGTACAGATCAAACAGCCTCGTAA
AAAATACGTCCAAAGGAAGTCAGACTTTGACCAGACCGTTTTCCAGGAGGTGTTTGAGCC
TCCCCACTATGAGTTATGTACGCTCAGAGGAACTGGAGCAACAGCCGACTTTGCAGATGT
GGCAGAAACGATAATACGGCTGCTGCCATGCCGGATCCCGCCGCTGTCAGACCCAAGCGC
GCTCCTCCACCCTGCTGATCTATTTCTTGTCCTATATCCCTACGACTCGGGTCCTCTTCG
CTCTCGCTGTGGAGCCTTACATTATCTATGGTTTGAGGCCCAGGGGGTGAAGAGATGTAA
ACACTCGAATACCCCCTCATCCTGCCTCCGCTAGAAATATTCGATGGTTCCGGTACTGGC
CCATCCCAGACCTGACTCTTGCCCCTTGGACGAAATACGACGACCGTACGTGCTATGCA

Neto 2: Forward primer (CACCAGTGGGACTGTCATTG)

Sequence amplified:

GAGTCCAAACATGAGTGTATCTATATTTTGGAGCTGCTCCTCGTCAACGAATAGAGCTGA
CCTTTGATGAACGCTATTATATAGAGCCATCATTCGAATGTCGGTTTGATCACTTGGAAA
TTCGAGACGGGCCATTTGGTTTTTCTCCTCTTATAGATCGTTACTGTGGCGTGAAAAGCC
CTCCATTAACAAGTCTGGATGGCGGCCTCGCTGGGCGGGCCCGCTTTTCTCAAGGCGTTT
CACAACCCTCCTCCCCCCTCCTGCTCCCTTTCTTGTATCTCTTGCCTTCCGCGAAGTACC
ATCTCCCTGCTCGGCAGCCTTACCTAACCTCCGTAATTAAATCCCTCAGGGGATGAAATG
ATGCTTTGATTGCAACCAGACCCGTATGCTACCGTCCCTGAGTAGATTCTATTCCTCCAC
CATTCACAGCACCTGACTCAACTCCTTCCCCTGCGTAAACAAATCGACACTGCTATTTGC
TCCAAAATAAAGAA

1.7. *KAR subunit expression in rat islets of Langerhans*

GluK1: Forward primer (GGAAGGAACTGAAAAGATTGGG)

Sequence amplified:

ACGTGGGCTGACATGACGGATGGCAACAGAGACAGGTCCAACAATATCACGGACTCGCTG
GCTAACCGCACACTCATTGTCACCACTATTCTGGAAGAGCCCTACGTGATGTACAGGAAA
TCCGATAAGCCCTTGTATGGAAACGACAGGTTTGAAGGATATTGCCTGGATCTGCTGAAA
GAACTGTCCAATATCCTGGGTTTTCTTTACGATGTTAAACTGGTTCCTGATGGCAAATAT
GGAGCACAGAATGACAAAGGGGAATGGAATGGGATGGTAAAAGAACTCATCGACCACAGA
GCTGACCTGGCAGTGGCCCCTCTCACCATCACATACGTACGGGAGAAAGTCATTGACTTC
TCCAAGCCCTTCATGACCCTGGGCATTAGCATCCTTTACCGGAAGCCCAATGGACACATT
CT

GluK2: Forward primer (CTTGACGTGGAGCCCTACAG)

Sequence amplified:

GATTCAGGATACTAAATACAGAGAATACCCAAGTCTCCTCCATCATCGAAAAGTGGTCTA
TGGAACGGTTACAGGCGCCTCCAAAACCTGACTCAGGTTTGCTGGATGGATTTATGACGA
CTGATGCTGCTCTGATGTATGATGCAGTGCACGTTGTGTCTGTGGCTGTCCAACAGTTTC
CCCAGATGACAGTCAGCTCCTTGCAATGCAATCGACACAAACCCTGGCGCTTTGGGACCC
GCTTCATGAGTCTAATTAAAGAGGCTCACTGGGAAGGTCTCACAGGCAGAATAACATTTA
ACAAAACCAATGGATTACGGACAGATTTTGATTTGGATGTGATCAGTCTCAAGGAAGAAG
GTCTGGAGAAGATTGGAACTTGGGATCCAGCCAGTGGCCTGAATATGACAGAAAGTCAGA
AAGGAAAGCCAGCAAATATCACAGACTCATTGTCTAATCGTTCTTTGATTGTTACCACCA
TTTTGGAAGAACCGACAGAAATC

GluK3: Forward primer (CCGAGGTCCTAATGTCACCG)

Sequence amplified:

CTCATCGTCACCACTCTGCTGGAGGAGCCTTTTGTCATGTTCCGCAAGTCTGATAGGACC
CTTTACGGCAATGACCGGTTCGAGGGCTACTGCATCGACTTGCTCAAGGAGCTGGCGCAC
ATCCTGGGCTTCTCCTACGAGATCCGGCTGGTGGAAGACGGCAAGTACGGGGCACAGGAC
GACAAGGGCCAGTGGAACGGCATGGTCAAGGAACTCATTGACCACAAAGCAGATCTGGCT
GTGGCTCCCCTGACCATCACCCATGTCCGAGAGAAGGCCATTGACTTCTCTAAGCCTTTT
ATGACCCTCGGAGTGAGCATCTTATATCGAAAACCCAATGGCACCAACCCCAGTGTCTTC
TCCTTCCTCAACCCCCTGTCCCCAGACATCTGGATGTACGTGCTACTCGCCTACCTGGGT
GTCAGCTGTGTCCTCTTCGTCATTGCCAGTTTCAG

GluK4: Forward primer (CCACCATCCTGGAAAACCCA)

Sequence amplified:

GGACATGGAAGGCAATGACCGGTACGAGGGATTCTGCGTGGACATGCTCAAGGAGTTGGC
TGAGATCCTACGGTTCAACTACAAGATCCGCCTCGTTGGGGATGGTGTTTACGGCGTACC
TGAGGCCAACGGCACCTGGACGGGCATGGTTGGGGAGCTGATCGCTCGGAAAGCAGATCT
GGCTGTGGCGGGCCTCACCATCACAGCTGAACGTGAGAAAGTGATTGATTTCTCCAAGCC
GTTCATGACGCTGGGAATTAGTATTCTTTACAGAGTTCATATGGGCC

GluK5: Reverse primer (TGATGCCAATGCGTCCATCT)

Sequence amplified:

TCTCCACATCTTGGGCTTTTCCATGTTCAACACCTCCCATCCCTTCTACCCGGAGTTTGT
GCGCAGCCTCAACATGTCCTGGAGGGAGAACTGCGAAGCCAGCACCTACCCTGGCCCTGC
GCTGTCGGCAGCCCTGATGTTTGATGCCGTGCATGTGGTGGTAAGCGCTGTCCGAGAGCT
GAACCGGAGCCAGGAGATTGGTGTCAAGCCACTGGCTTGCACTTCGGCCAACATCTGGCC
CCATGGGACCAGCCTCATGAACTACCTGCGCATGGTAGAGTATGACGGGCTGACTGGGCG
GGTTGAGTTCAACAGCAAAGGGCAGAGGACCAACTACACACTGCGCATCCTGGAGAAGTC
CCGCCAGGGCCACCGTGAGATAGGGGTGTGGACTTCATT

1.8. *Neto 1 and Neto 2 expression in rat islets of Langerhans*

Neto 1: Reverse primer (TCTGCCACATCTGCAAAGTC)

Sequence amplified:

CTTGGCATTCTATGCTCTGAGCGTGCATACTCATAGTGAGGAGGCTCAAACACCTCCTGG
AAAACGGTCTGGTCAAAGTCTGACTTCCTTTGGACGTATTTTTTACGAGGCTGTTTGATC
TGTACAATGACAGAAACGATATTAAGGAAGATCACAATGCAGGAAGTCACGCCAATGACA
GTCCCACTGGTGATAAAAACAGTCTGGTTGATTATCTACTTTTTCCGTTCCCCGCCTCCC
CAAGGCGTTTAAAATGCCTCCCCCCCTCTCCTCCTCCATTTCTTATATTTCTTGCCTTCT
CCGCGGTACCTTCTTCGTCCCTGCCCGGTCTGGCCCATCTTCCCTAAGGTTATTCCCTCG
GGGGGTGAAATGATGCCCTGGCACCAAATACCTCCCTTCGCTCCTGCTCCTGGGCATATT
GGGAAGTTCCGCCTTGTT

Neto 1: Forward primer (CACCAGTGGGACTGTCATTG)

Sequence amplified:

CTGGACTGCAACATGAGTGTATCTATATTTTGGAAGCTGCTCCTCGTCAACGGATAGAGC
TGACCTTTGATGAACGATATTATATAGAGCCATCATTTGAATGCCGGTTTGATCACTTGG
AAGTTCGAGACGGGCCATTTGGCTTCTCTCCTCTTATAGATCGTTACTGTGGCGTGAAAA
GCCCTCCATTAAGAAGATGGGGACTGTAGCCTTGTTCTGGCCCTGGGCGTTTTAAAGCCC
GCATTAGCTCTCCTACCCCCGCCTCCATACTTTCTTGTATATATTGCCTACTGCAGACAA
CTATGCTCTTGCAGTGTAGCCTTACCTATATTCTGTAATTATATGAGCCAAGGGCAATGA
ACTAAGCCACAGAATCGCCAAGTTTCCTCCCTTGCCGTCCCTGGGTATATGAAATTCTTA
AGGGCACCCCCAAAATCTGACTCAACTTCTCCCCCTGGATTCGTGACGTTAGCACTCCTT
TGTGCTTTAATTAATG

Clip. 1 BQ 20 WL 10 Sequence: GluK 2 B_GluK-2-R

Clipped length:	469	Samples:	13659	Quality:	0 - 9
Left clip:	10	Bases:	486		10 - 19
Right clip:	478	Average spacing:	29.0		20 - 29
Avg. qual. in clip.:	57.12	Average quality >=	10: 9, 20: 7, 30: 452		>= 30

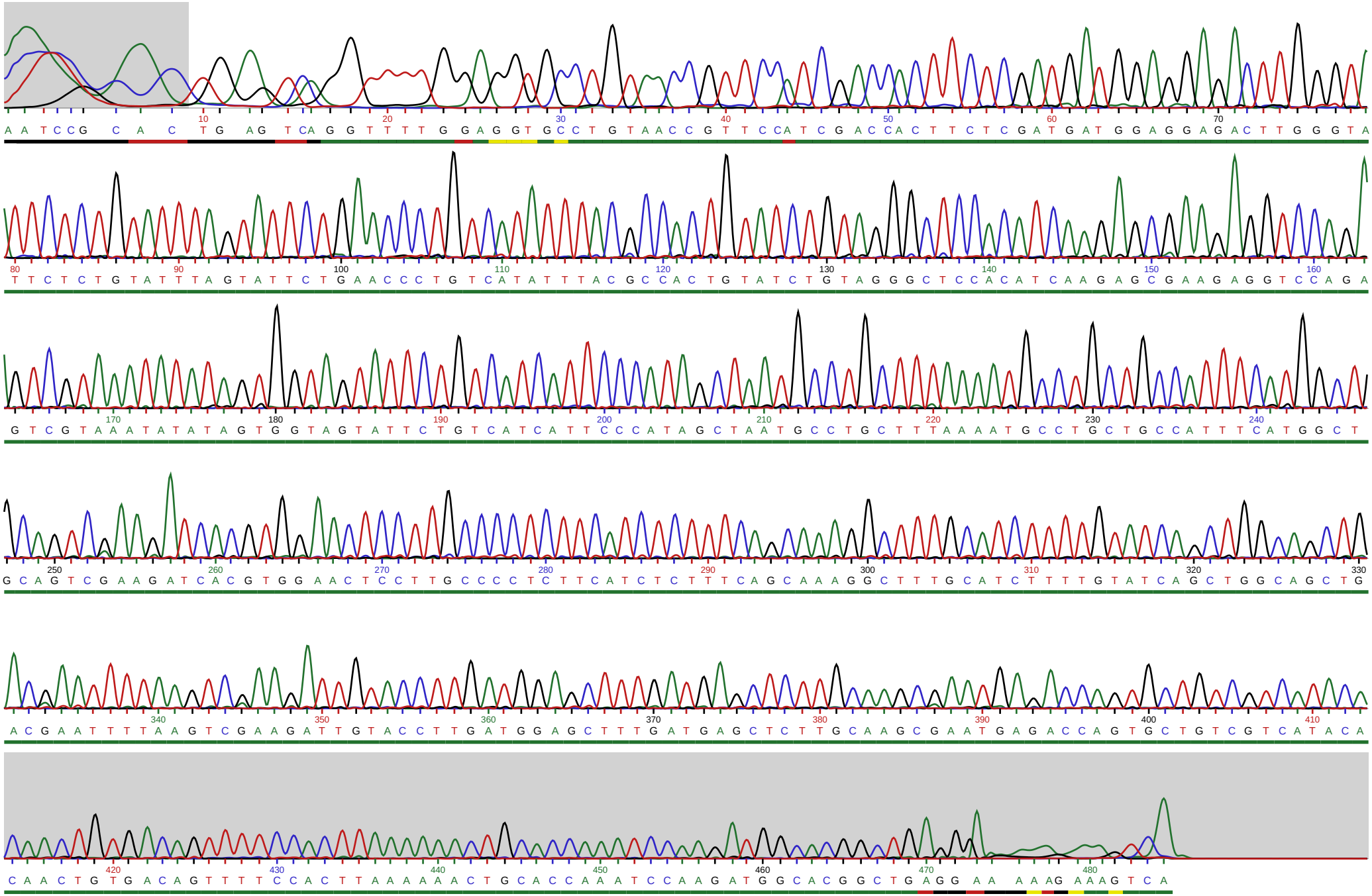

Clip. 1 BQ 20 WL 10

Sequence: GluK 2 B_GluK-2-R

Clipped length:	469	Samples:	13659	Quality:	0 - 9
Left clip:	10	Bases:	486		10 - 19
Right clip:	478	Average spacing:	29.0		20 - 29
Avg. qual. in clip.:	57.12	Average quality >=	10: 9, 20: 7, 30: 452		>= 30

Clip. 1 BQ 20 WL 10

Sequence: GluK 2 B_GluK-2-R

Clipped length:	469	Samples:	13659	Quality:	0 - 9
Left clip:	10	Bases:	486		10 - 19
Right clip:	478	Average spacing:	29.0		20 - 29
Avg. qual. in clip.:	57.12	Average quality >=	10: 9, 20: 7, 30: 452		>= 30

Clip. 1 BQ 20 WL 10 Sequence: GluK 3 A_GluK-3-F

Clipped length:	524	Samples:	13400	Quality:	0 - 9
Left clip:	10	Bases:	533		10 - 19
Right clip:	533	Average spacing:	26.0		20 - 29
Avg. qual. in clip.:	58.7	Average quality >=	10: 5, 20: 6, 30: 505		>= 30

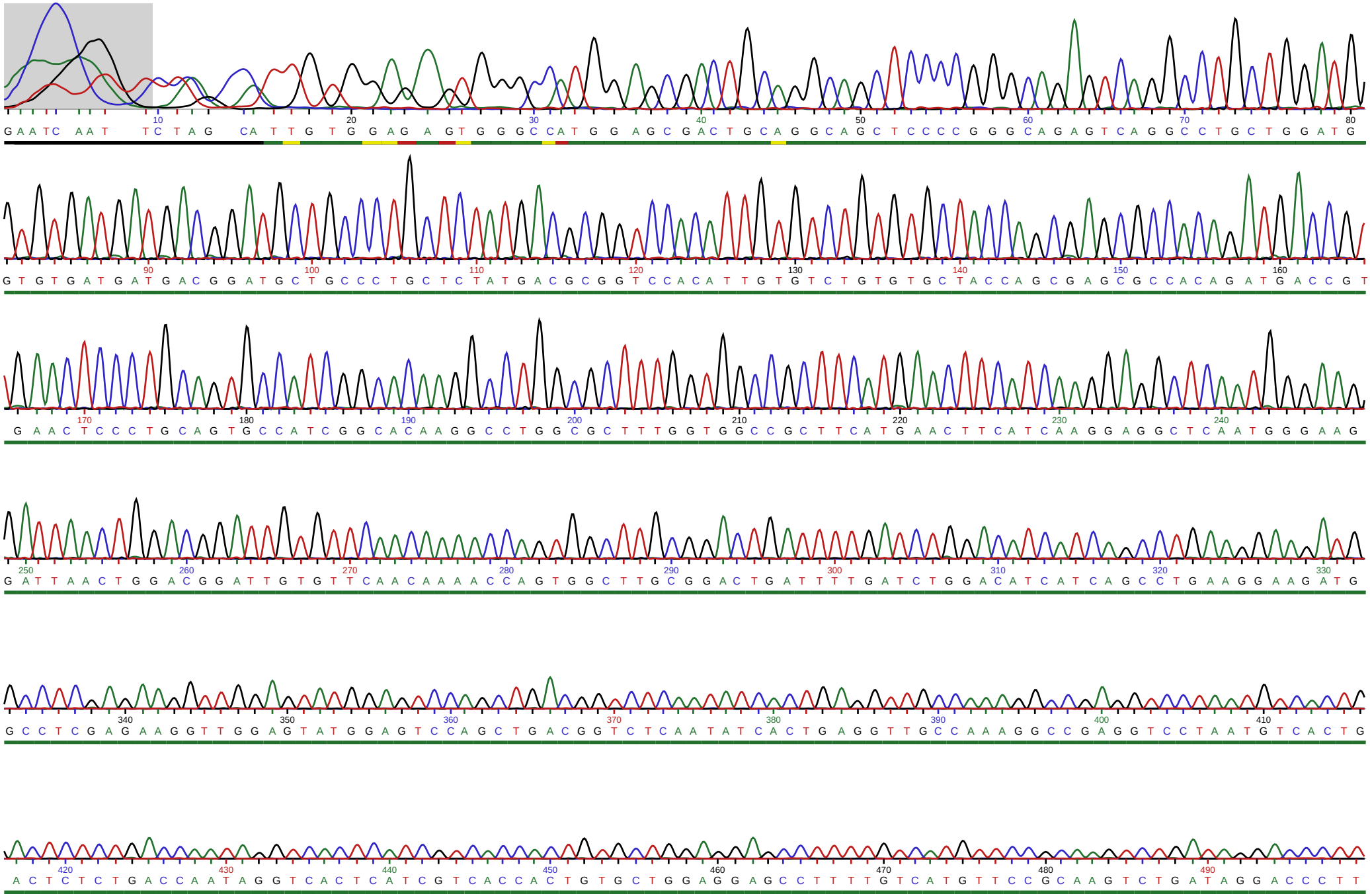

Clip. 1 BQ 20 WL 10 Sequence: GluK 3 A_GluK-3-F

Clipped length:	524	Samples:	13400	Quality:	0 - 9
Left clip:	10	Bases:	533		10 - 19
Right clip:	533	Average spacing:	26.0		20 - 29
Avg. qual. in clip.:	58.7	Average quality >=	10: 5, 20: 6, 30: 505		>= 30

Clip. 1 BQ 20 WL 10

Sequence: GluK 3 A_GluK-3-F

Clipped length:	524	Samples:	13400	Quality:	0 - 9
Left clip:	10	Bases:	533		10 - 19
Right clip:	533	Average spacing:	26.0		20 - 29
Avg. qual. in clip.:	58.7	Average quality >=	10: 5, 20: 6, 30: 505		>= 30

Clip. 1 BQ 20 WL 10 Sequence: GluK 4 A_GluK-4-F

Clipped length:	428	Samples:	13360	Quality:	0 - 9
Left clip:	18	Bases:	449		10 - 19
Right clip:	445	Average spacing:	30.0		20 - 29
Avg. qual. in clip.:	56.97	Average quality >=	10: 12, 20: 2, 30: 408		>= 30

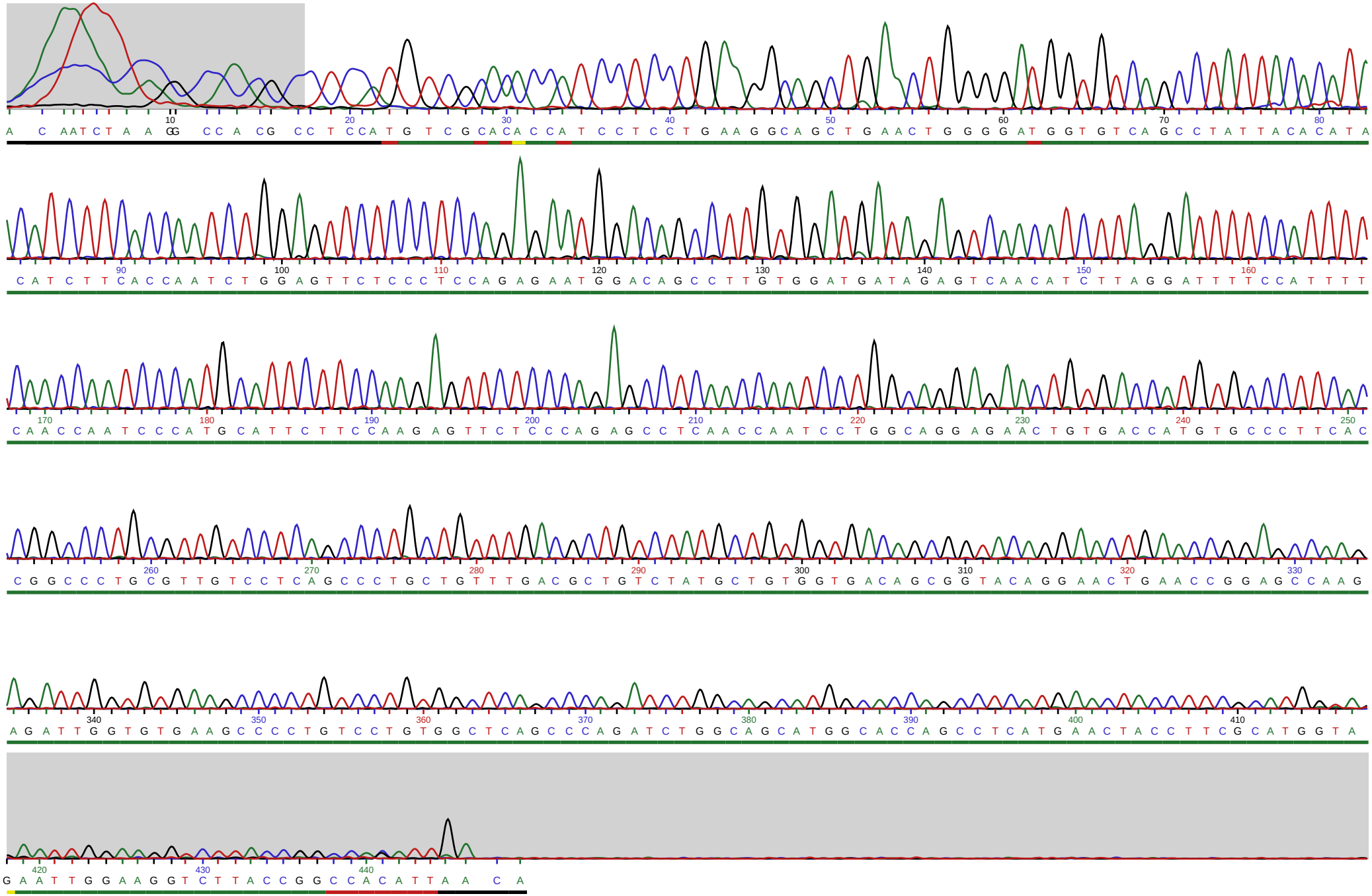

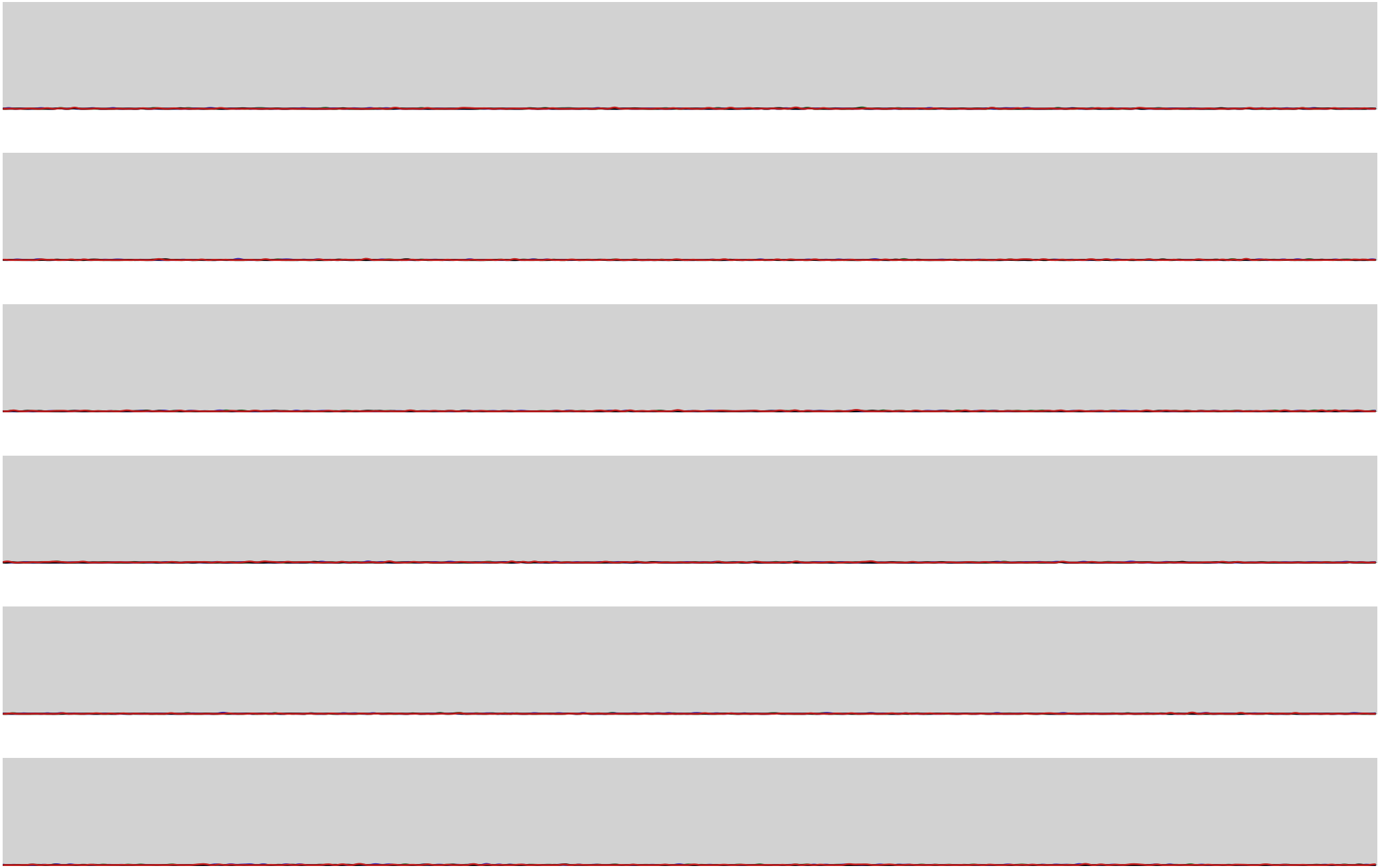

Clip. 1 BQ 20 WL 10

Sequence: GluK 4 A_GluK-4-F

Clipped length:	428	Samples:	13360	Quality:	0 - 9
Left clip:	18	Bases:	449		10 - 19
Right clip:	445	Average spacing:	30.0		20 - 29
Avg. qual. in clip.:	56.97	Average quality >=	10: 12, 20: 2, 30: 408		>= 30

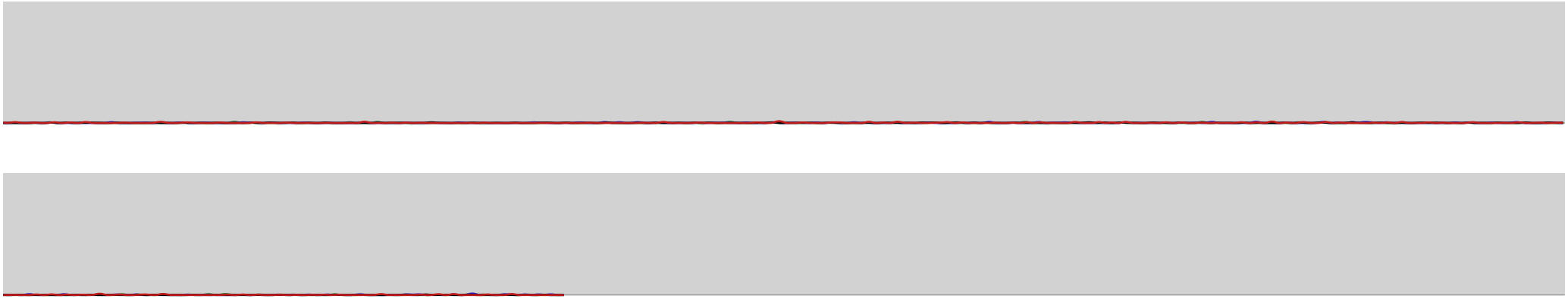

Clip. 1 BQ 20 WL 10 Sequence: GluK 5 B_GluK-5-R

Clipped length:	456	Samples:	13514	Quality:	0 - 9
Left clip:	8	Bases:	463		10 - 19
Right clip:	463	Average spacing:	30.0		20 - 29
Avg. qual. in clip.:	53.97	Average quality >=	10: 8, 20: 7, 30: 438		>= 30

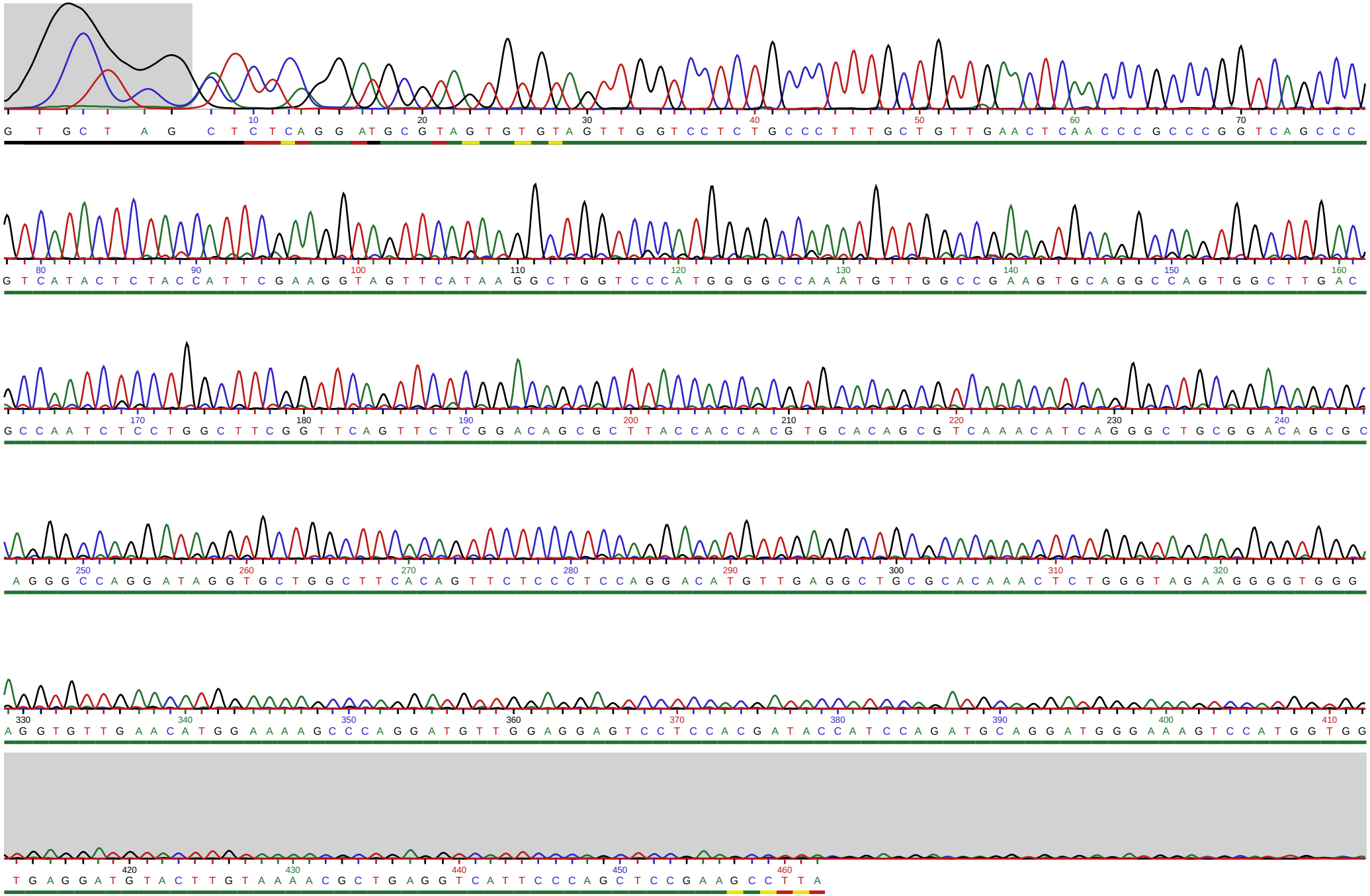

Clip. 1 BQ 20 WL 10

Sequence: GluK 5 B_GluK-5-R

Clipped length:	456	Samples:	13514	Quality:	0 - 9
Left clip:	8	Bases:	463		10 - 19
Right clip:	463	Average spacing:	30.0		20 - 29
Avg. qual. in clip.:	53.97	Average quality >=	10: 8, 20: 7, 30: 438		>= 30

Clip. 1 BQ 20 WL 10

Sequence: GluK 5 B_GluK-5-R

Clipped length:	456	Samples:	13514	Quality:	0 - 9
Left clip:	8	Bases:	463		10 - 19
Right clip:	463	Average spacing:	30.0		20 - 29
Avg. qual. in clip.:	53.97	Average quality >=	10: 8, 20: 7, 30: 438		>= 30

Clip. 1 BQ 20 WL 10 Sequence: MIN6 NETO 1_NETO-1-F

Clipped length:	180	Samples:	14340	Quality:	0 - 9
Left clip:	15	Bases:	359		10 - 19
Right clip:	194	Average spacing:	40.0		20 - 29
Avg. qual. in clip.:	51.46	Average quality >=	10: 119, 20: 33, 30: 178		>= 30

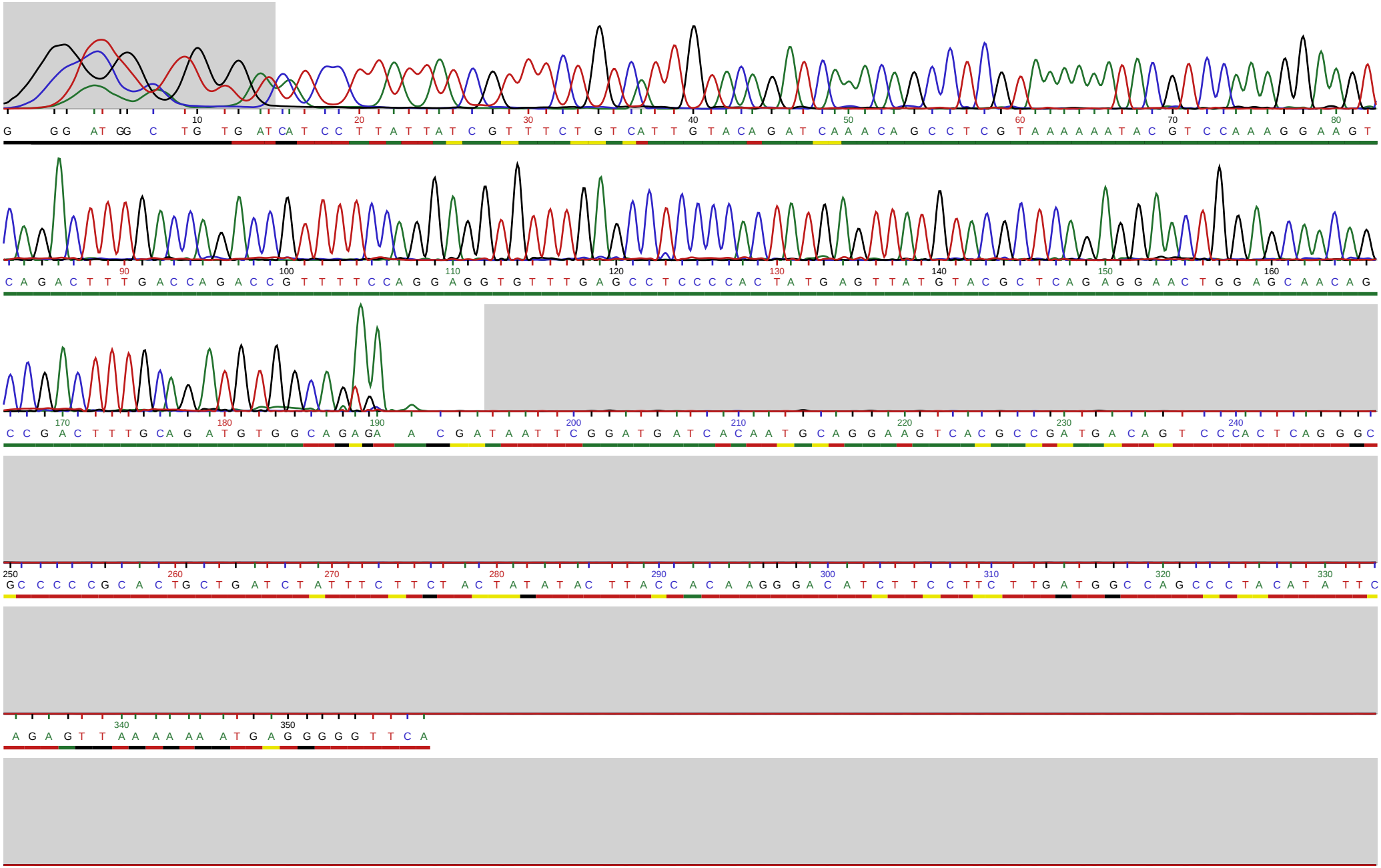

Clip. 1 BQ 20 WL 10

Sequence: MIN6 NETO 1_NETO-1-F

Clipped length:	180	Samples:	14340	Quality:	0 - 9
Left clip:	15	Bases:	359		10 - 19
Right clip:	194	Average spacing:	40.0		20 - 29
Avg. qual. in clip.:	51.46	Average quality >=	10: 119, 20: 33, 30: 178		>= 30

Clip. 1 BQ 20 WL 10

Sequence: MIN6 NETO 1_NETO-1-F

Clipped length:	180	Samples:	14340	Quality:	0 - 9
Left clip:	15	Bases:	359		10 - 19
Right clip:	194	Average spacing:	40.0		20 - 29
Avg. qual. in clip.:	51.46	Average quality >=	10: 119, 20: 33, 30: 178		>= 30

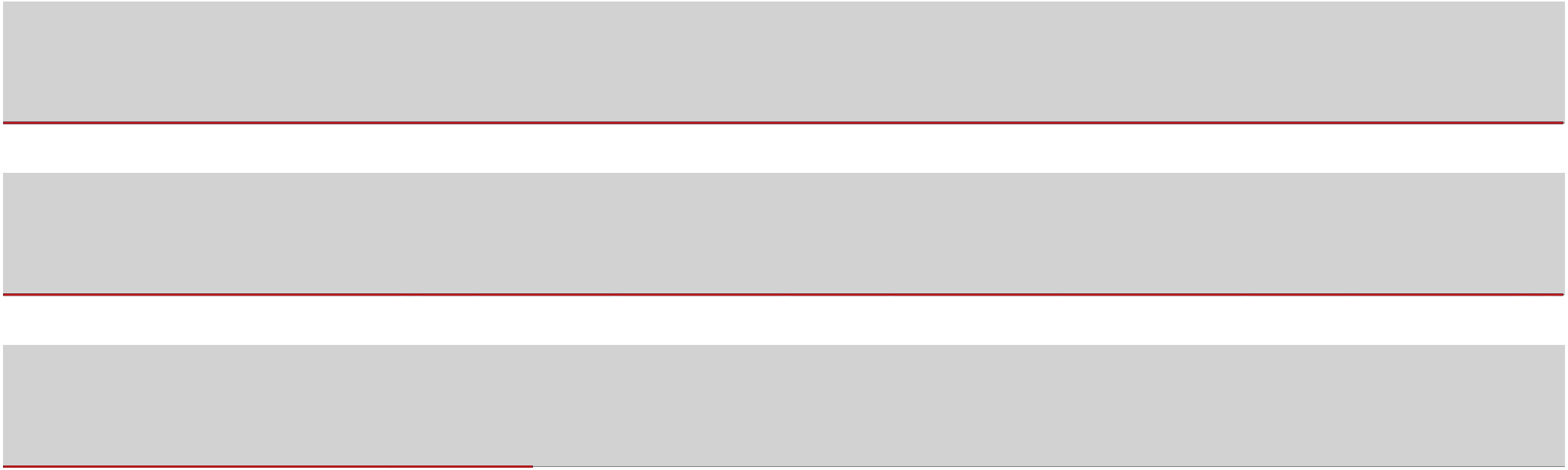

Clip. 1 BQ 20 WL 10 Sequence: MIN6 NETO 2_NETO-2-F

Clipped length:	189	Samples:	16300	Quality:	0 - 9
Left clip:	11	Bases:	439		10 - 19
Right clip:	199	Average spacing:	38.0		20 - 29
Avg. qual. in clip.:	53.3	Average quality >=	10: 196, 20: 34, 30: 178		>= 30

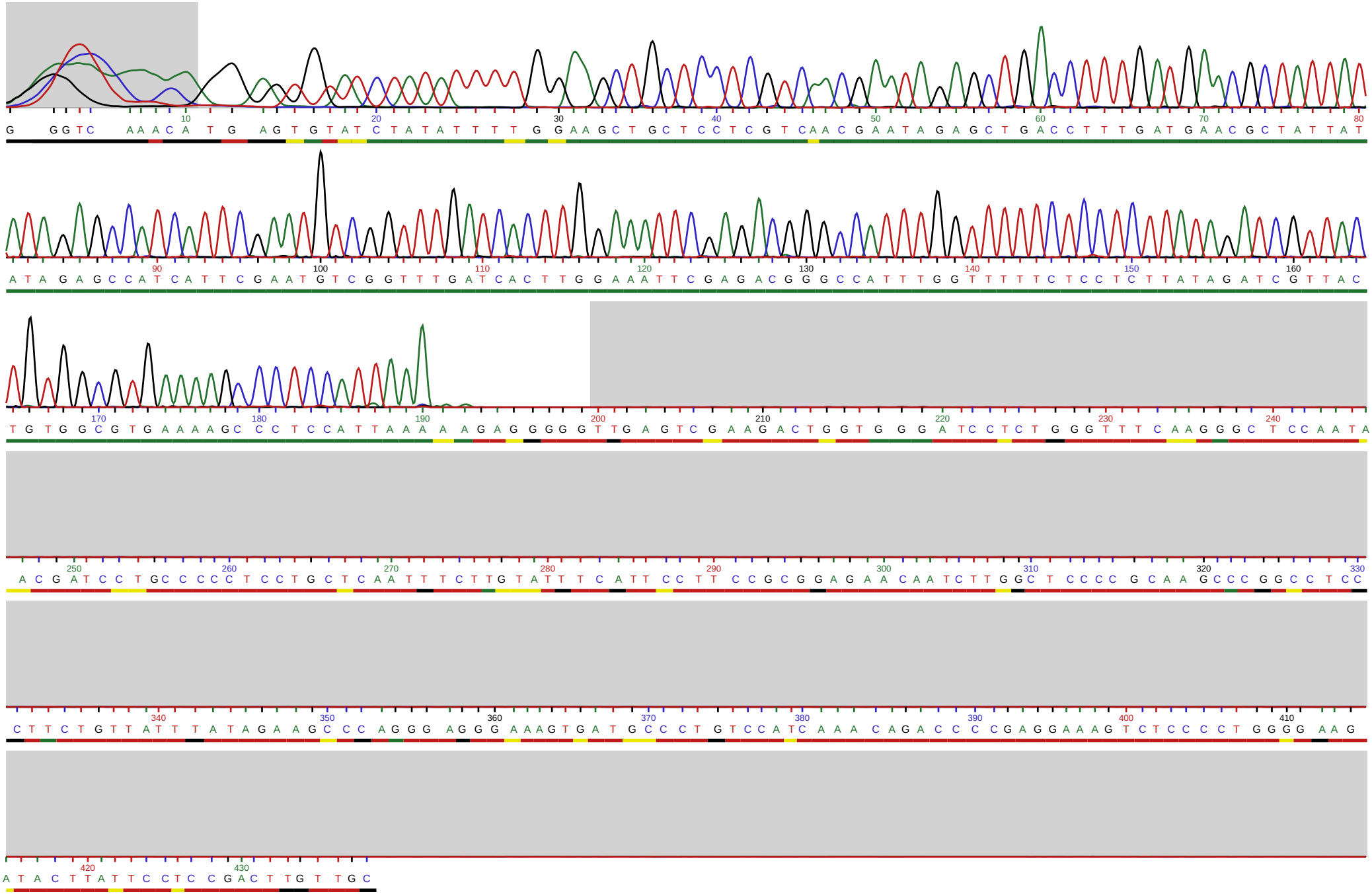

Clip. 1 BQ 20 WL 10

Sequence: MIN6 NETO 2_NETO-2-F

Clipped length:	189	Samples:	16300	Quality:	0 - 9
Left clip:	11	Bases:	439		10 - 19
Right clip:	199	Average spacing:	38.0		20 - 29
Avg. qual. in clip.:	53.3	Average quality >=	10: 196, 20: 34, 30: 178		>= 30

Clip. 1 BQ 20 WL 10

Sequence: MIN6 NETO 2_NETO-2-F

Clipped length:	189	Samples:	16300	Quality:	0 - 9
Left clip:	11	Bases:	439		10 - 19
Right clip:	199	Average spacing:	38.0		20 - 29
Avg. qual. in clip.:	53.3	Average quality >=	10: 196, 20: 34, 30: 178		>= 30

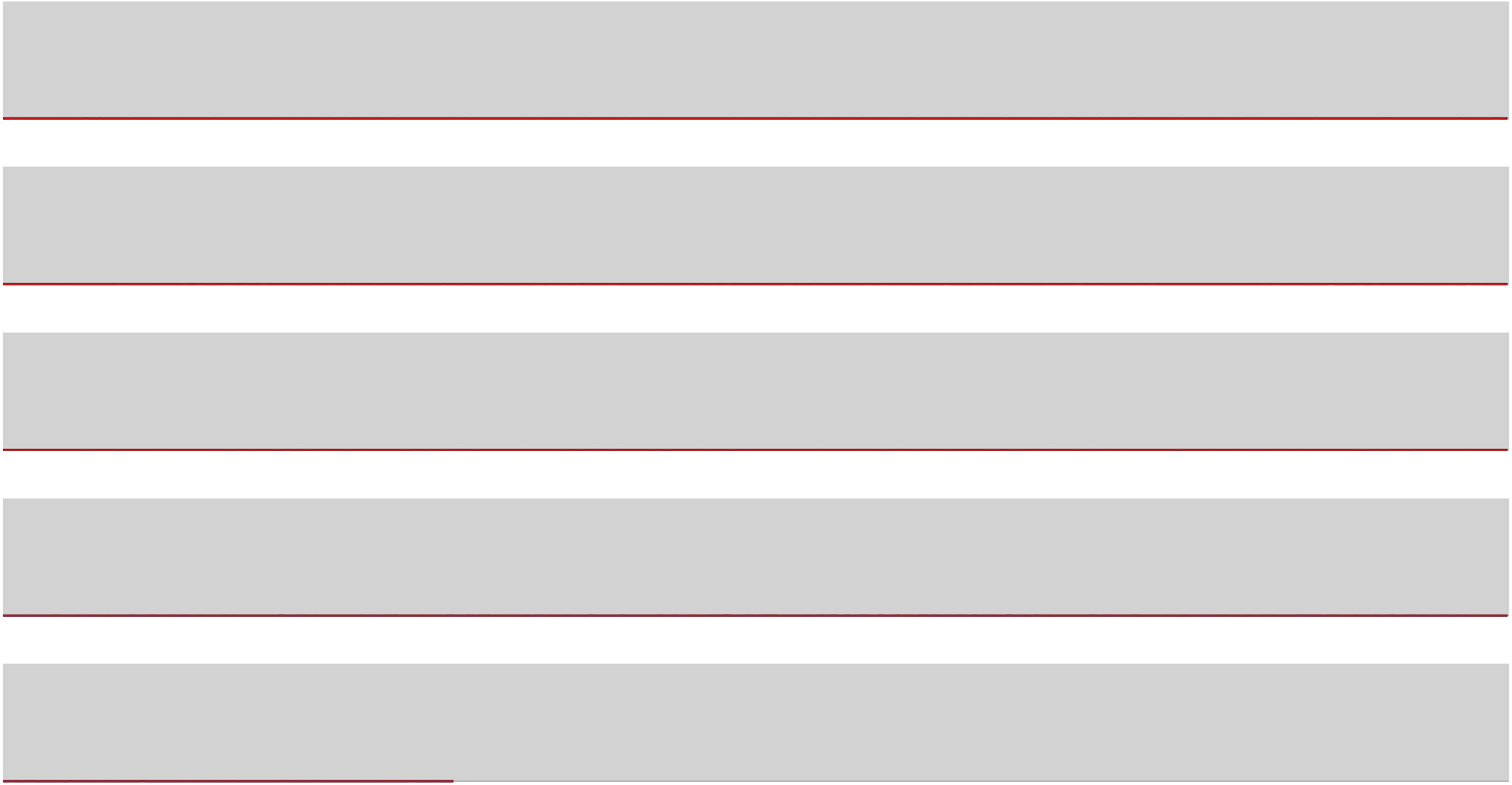

Clip. 1 BQ 20 WL 10 Sequence: INS1 GluK2_GluK2-F

Clipped length:	471	Samples:	16164	Quality:	0 - 9
Left clip:	15	Bases:	494		10 - 19
Right clip:	485	Average spacing:	33.0		20 - 29
Avg. qual. in clip.:	56.26	Average quality >=	10: 13, 20: 10, 30: 447		>= 30

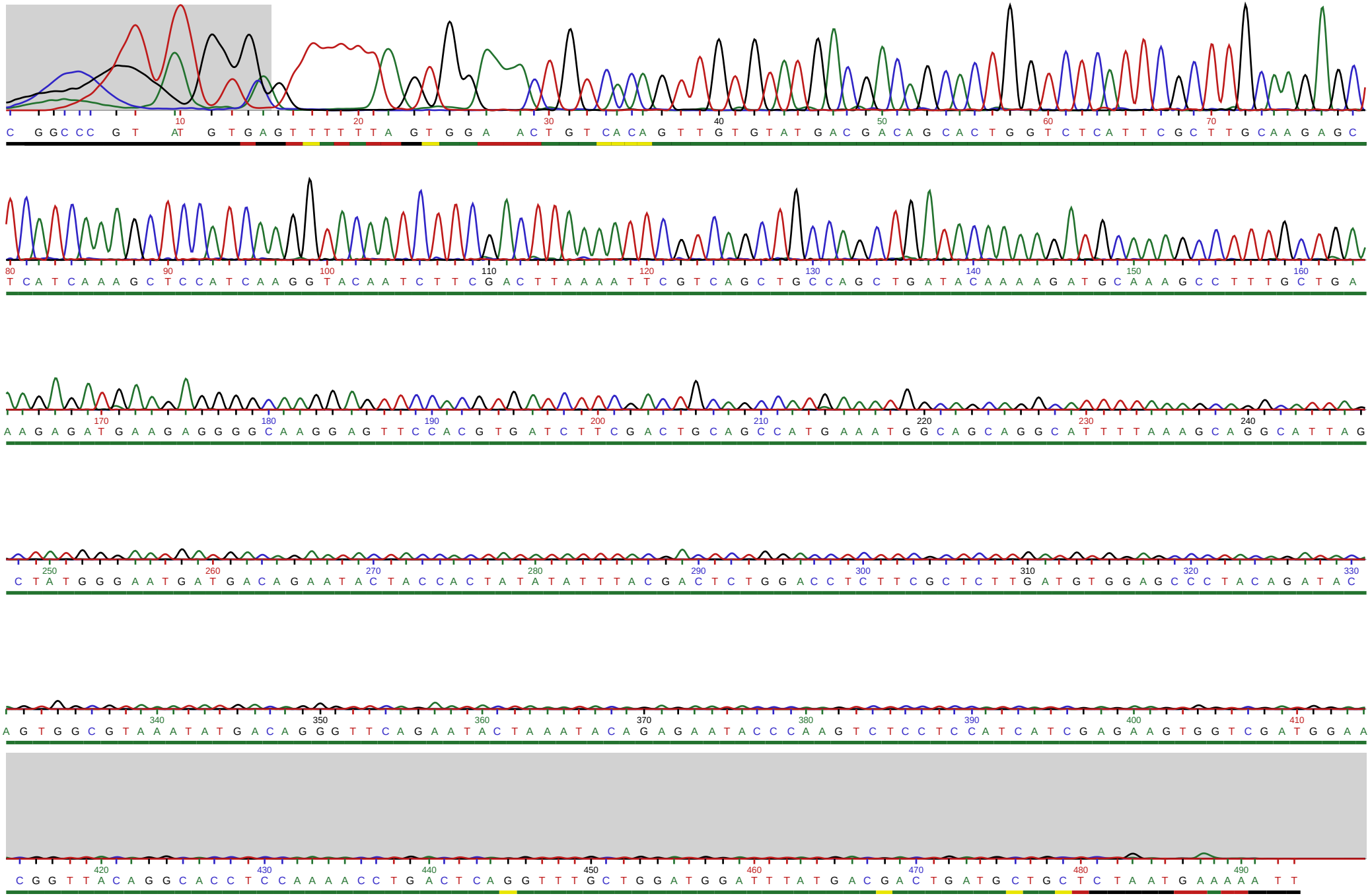

Clip. 1 BQ 20 WL 10

Sequence: INS1 GluK2_GluK2-F

Clipped length:	471	Samples:	16164	Quality:	0 - 9
Left clip:	15	Bases:	494		10 - 19
Right clip:	485	Average spacing:	33.0		20 - 29
Avg. qual. in clip.:	56.26	Average quality >=	10: 13, 20: 10, 30: 447		>= 30

Clip. 1 BQ 20 WL 10

Sequence: INS1 GluK2_GluK2-F

Clipped length:	471	Samples:	16164	Quality:	0 - 9
Left clip:	15	Bases:	494		10 - 19
Right clip:	485	Average spacing:	33.0		20 - 29
Avg. qual. in clip.:	56.26	Average quality >=	10: 13, 20: 10, 30: 447		>= 30

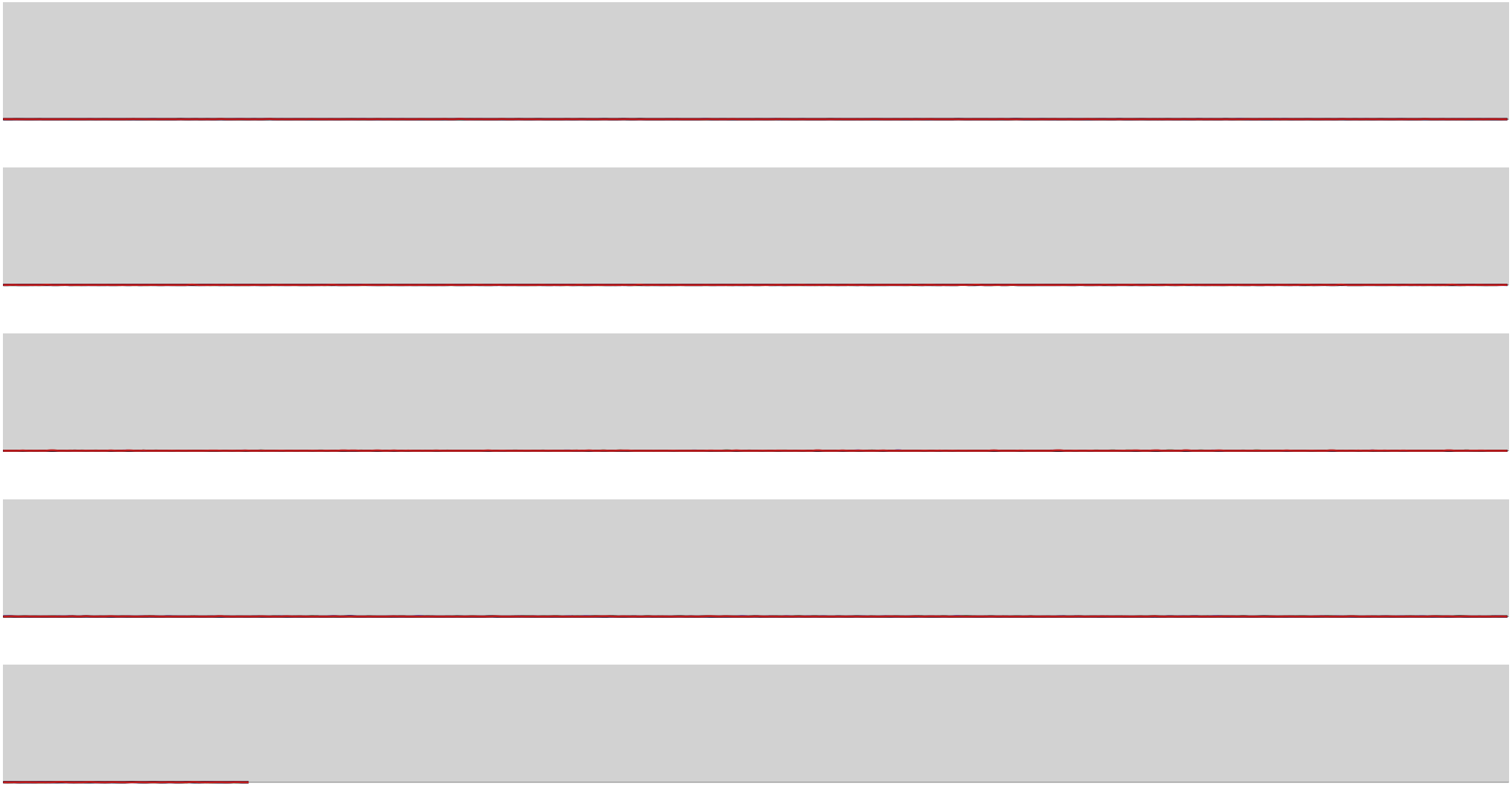

Clip. 1 BQ 20 WL 10 Sequence: INS1 Gluk3_GluK3-F

Clipped length:	428	Samples:	12297	Quality:	0 - 9
Left clip:	11	Bases:	537		10 - 19
Right clip:	438	Average spacing:	23.0		20 - 29
Avg. qual. in clip.:	55.28	Average quality >=	10: 18, 20: 35, 30: 455		>= 30

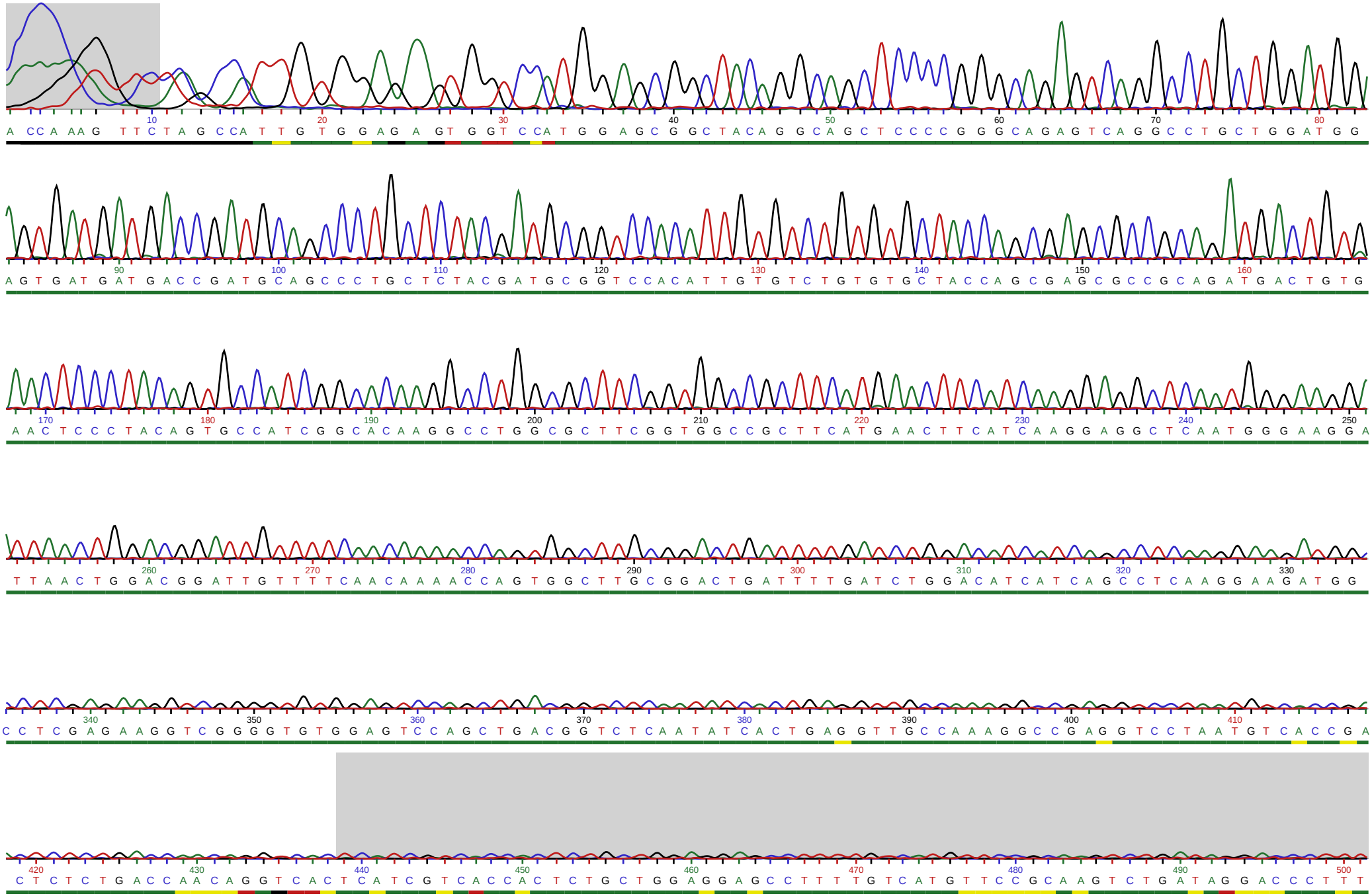

Clip. 1 BQ 20 WL 10 Sequence: INS1 Gluk3_GluK3-F

Clipped length:	428	Samples:	12297	Quality:	0 - 9
Left clip:	11	Bases:	537		10 - 19
Right clip:	438	Average spacing:	23.0		20 - 29
Avg. qual. in clip.:	55.28	Average quality >=	10: 18, 20: 35, 30: 455		>= 30

Clip. 1 BQ 20 WL 10

Sequence: INS1 Gluk3_GluK3-F

Clipped length:	428	Samples:	12297	Quality:	0 - 9
Left clip:	11	Bases:	537		10 - 19
Right clip:	438	Average spacing:	23.0		20 - 29
Avg. qual. in clip.:	55.28	Average quality >=	10: 18, 20: 35, 30: 455		>= 30

Clip. 1 BQ 20 WL 10 Sequence: RatGluk42_Rat-GluK4R

Clipped length:	38	Samples:	12961	Quality:	0 - 9
Left clip:	55	Bases:	248		10 - 19
Right clip:	92	Average spacing:	53.0		20 - 29
Avg. qual. in clip.:	27.31	Average quality >=	10: 103, 20: 49, 30: 31		>= 30

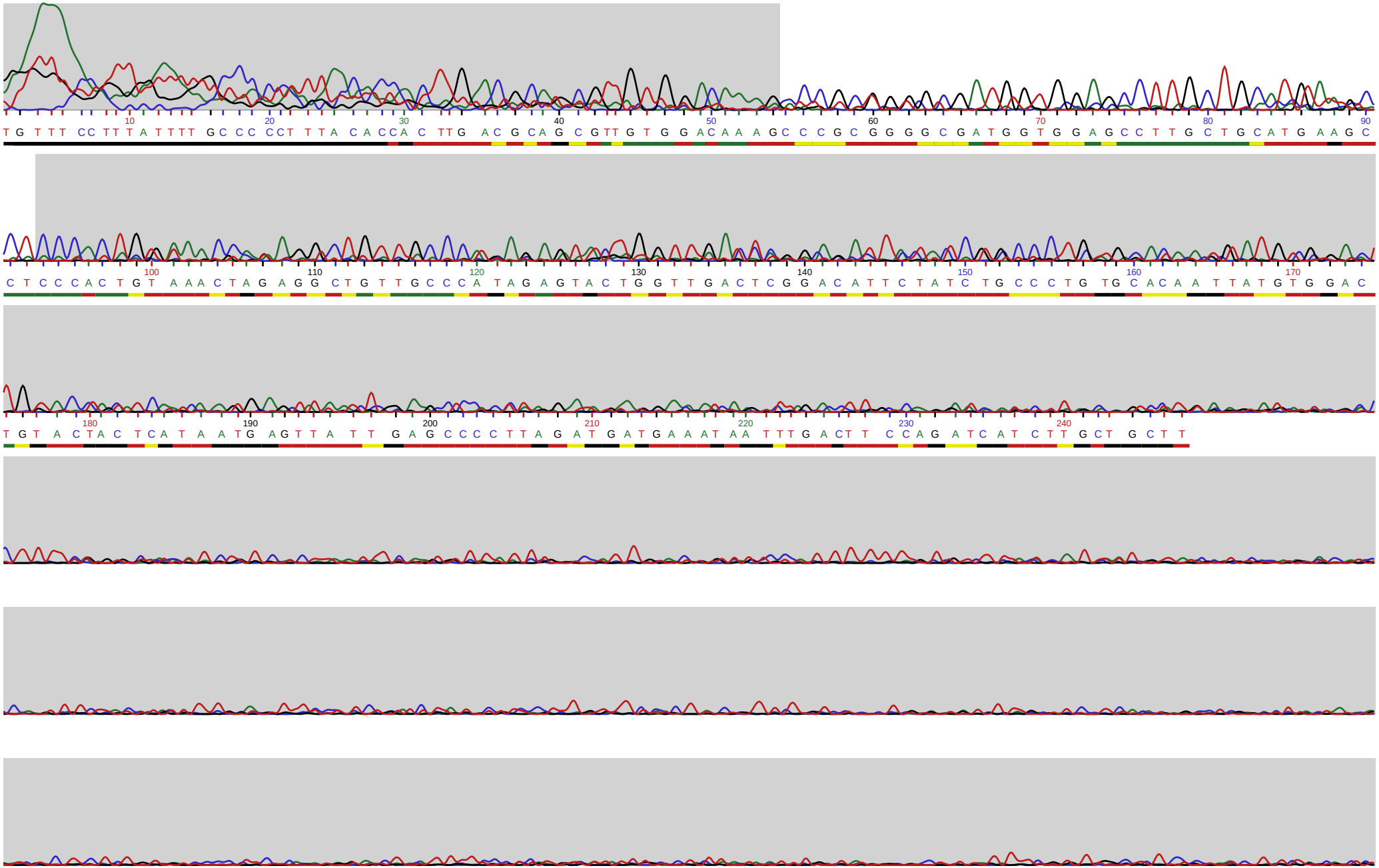

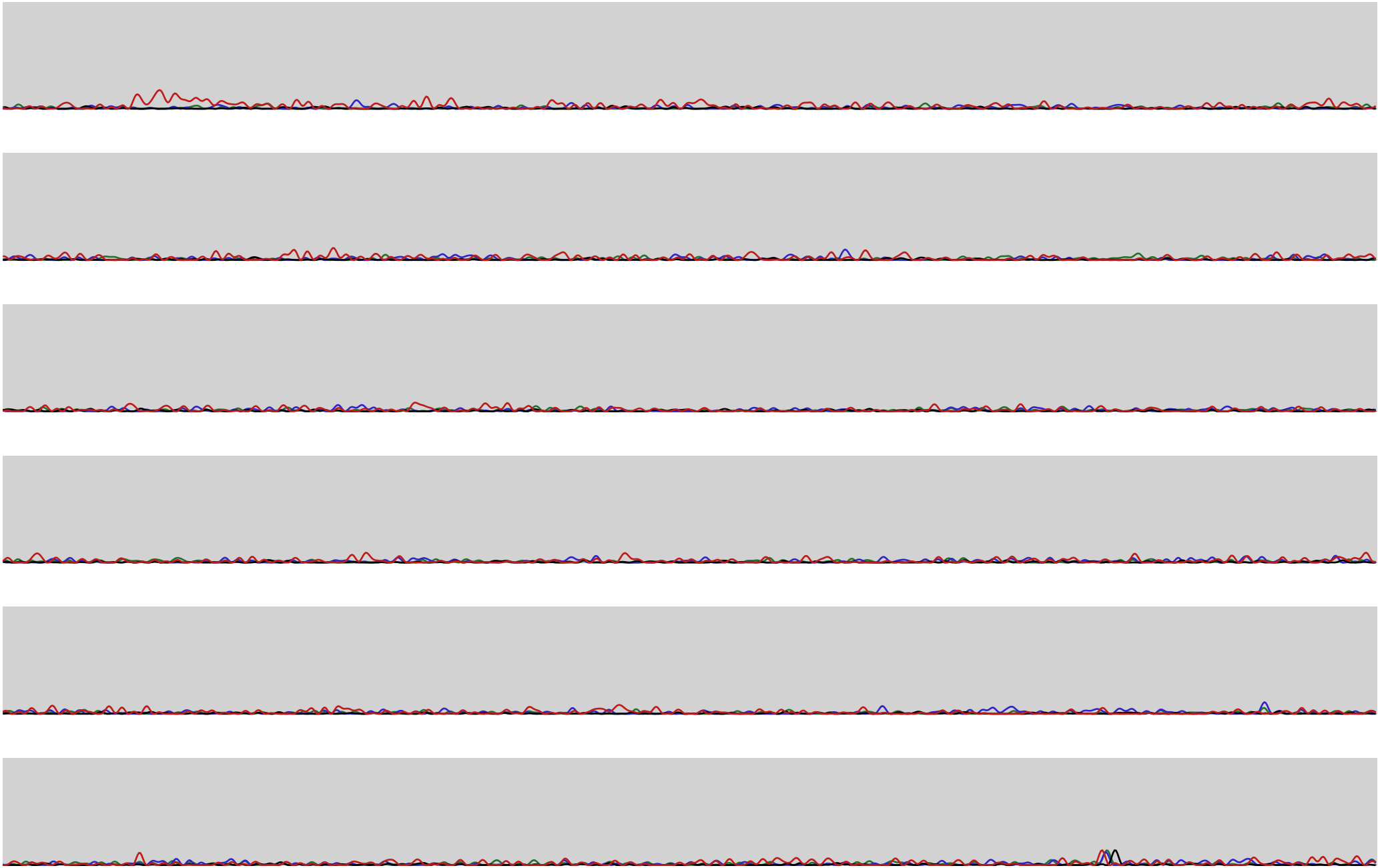

Clip. 1 BQ 20 WL 10

Sequence: RatGluk42_Rat-GluK4R

Clipped length:	38	Samples:	12961	Quality:	0 - 9
Left clip:	55	Bases:	248		10 - 19
Right clip:	92	Average spacing:	53.0		20 - 29
Avg. qual. in clip.:	27.31	Average quality >=	10: 103, 20: 49, 30: 31		>= 30

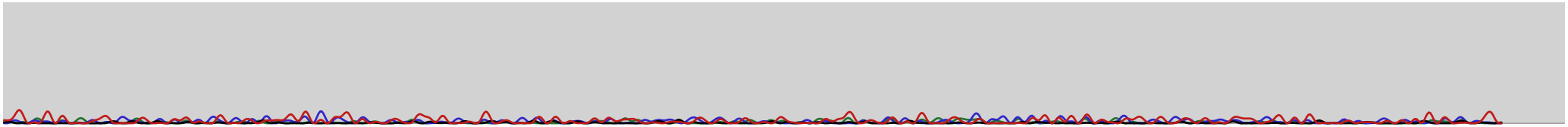

Clip. 1 BQ 20 WL 10 Sequence: INS1 GluK5_GluK5-F

Clipped length:	471	Samples:	12702	Quality:	0 - 9
Left clip:	23	Bases:	503		10 - 19
Right clip:	493	Average spacing:	26.0		20 - 29
Avg. qual. in clip.:	35.3	Average quality >=	10: 52, 20: 81, 30: 347		>= 30

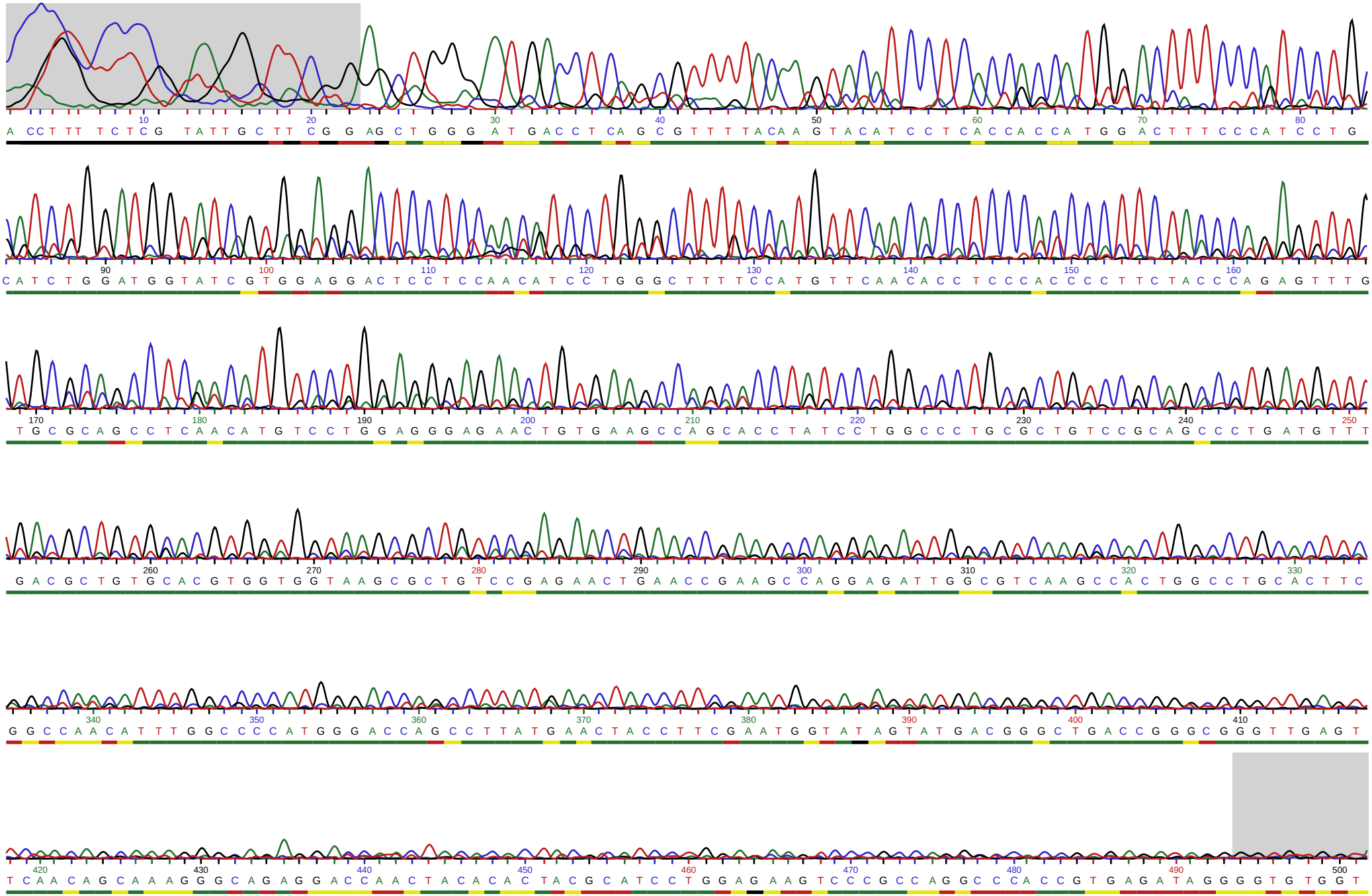

Clip. 1 BQ 20 WL 10

Sequence: INS1 GluK5_GluK5-F

Clipped length:	471	Samples:	12702	Quality:	0 - 9
Left clip:	23	Bases:	503		10 - 19
Right clip:	493	Average spacing:	26.0		20 - 29
Avg. qual. in clip.:	35.3	Average quality >=	10: 52, 20: 81, 30: 347		>= 30

Clip. 1 BQ 20 WL 10

Sequence: INS1 GluK5_GluK5-F

Clipped length:	471	Samples:	12702	Quality:	0 - 9
Left clip:	23	Bases:	503		10 - 19
Right clip:	493	Average spacing:	26.0		20 - 29
Avg. qual. in clip.:	35.3	Average quality >=	10: 52, 20: 81, 30: 347		>= 30

Clip. 1 BQ 20 WL 10 Sequence: INS1 Neto1o_Neto1-F

Clipped length:	178	Samples:	12177	Quality:	0 - 9
Left clip:	12	Bases:	189		10 - 19
Right clip:	189	Average spacing:	65.0		20 - 29
Avg. qual. in clip.:	53.16	Average quality >=	10: 7, 20: 11, 30: 158		>= 30

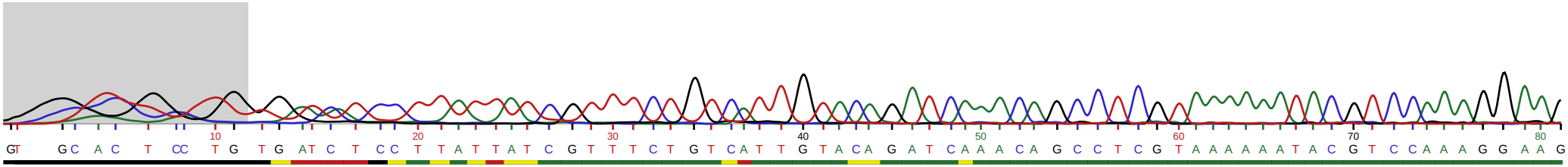

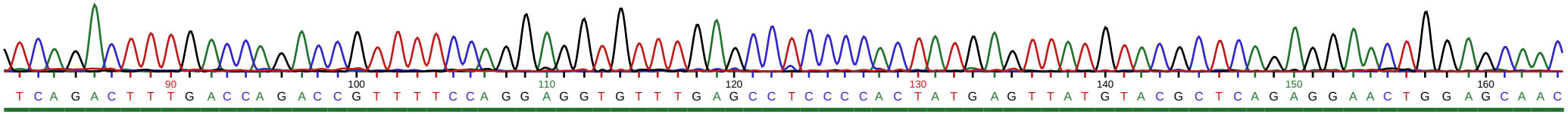

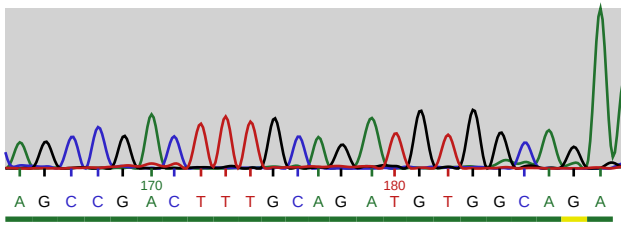

Clip. 1 BQ 20 WL 10

Sequence: INS1 Neto1o_Neto1-F

Clipped length:	178	Samples:	12177	Quality:	0 - 9
Left clip:	12	Bases:	189		10 - 19
Right clip:	189	Average spacing:	65.0		20 - 29
Avg. qual. in clip.:	53.16	Average quality >=	10: 7, 20: 11, 30: 158		>= 30

Clip. 1 BQ 20 WL 10

Sequence: INS1 Neto1o_Neto1-F

Clipped length:	178	Samples:	12177	Quality:	0 - 9
Left clip:	12	Bases:	189		10 - 19
Right clip:	189	Average spacing:	65.0		20 - 29
Avg. qual. in clip.:	53.16	Average quality >=	10: 7, 20: 11, 30: 158		>= 30

Clip. 1 BQ 20 WL 10 Sequence: INS1 Neto2o_Neto2-F

Clipped length:	180	Samples:	12159	Quality:	0 - 9
Left clip:	12	Bases:	191		10 - 19
Right clip:	191	Average spacing:	64.0		20 - 29
Avg. qual. in clip.:	55.78	Average quality >=	10: 4, 20: 1, 30: 170		>= 30

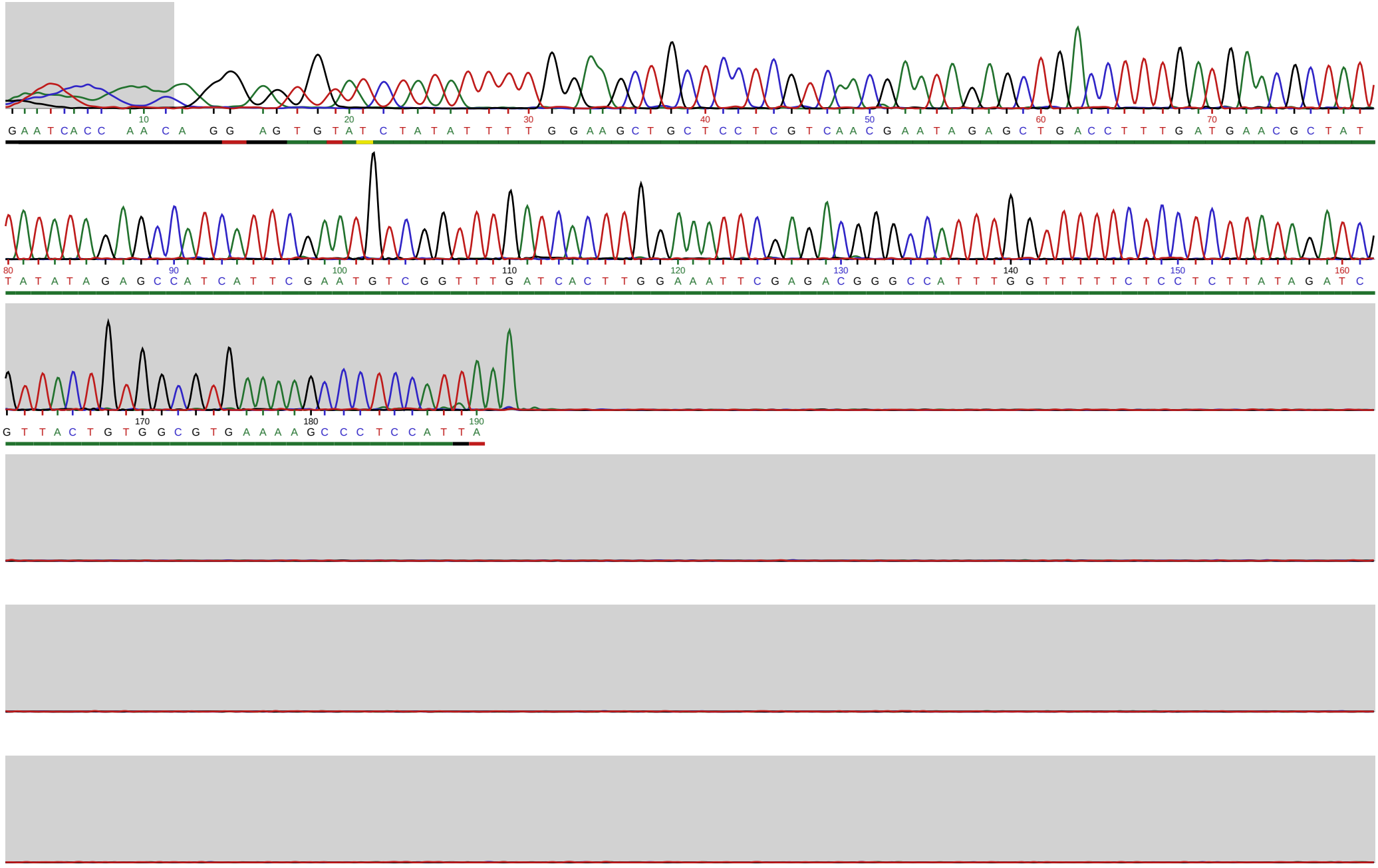

Clip. 1 BQ 20 WL 10

Sequence: INS1 Neto2o_Neto2-F

Clipped length:	180	Samples:	12159	Quality:	0 - 9
Left clip:	12	Bases:	191		10 - 19
Right clip:	191	Average spacing:	64.0		20 - 29
Avg. qual. in clip.:	55.78	Average quality >=	10: 4, 20: 1, 30: 170		>= 30

Clip. 1 BQ 20 WL 10

Sequence: INS1 Neto2o_Neto2-F

Clipped length:	180	Samples:	12159	Quality:	0 - 9
Left clip:	12	Bases:	191		10 - 19
Right clip:	191	Average spacing:	64.0		20 - 29
Avg. qual. in clip.:	55.78	Average quality >=	10: 4, 20: 1, 30: 170		>= 30

Clip. 1 BQ 20 WL 10 Sequence: ALPHA GLUK2_mGLUK2-F

Clipped length:	458	Samples:	12073	Quality: 0 - 9	
Left clip:	19	Bases:	483	10 - 19	
Right clip:	476	Average spacing:	25.0	20 - 29	
Avg. qual. in clip.:	58.65	Average quality >=	10: 14, 20: 5, 30: 442	>= 30	

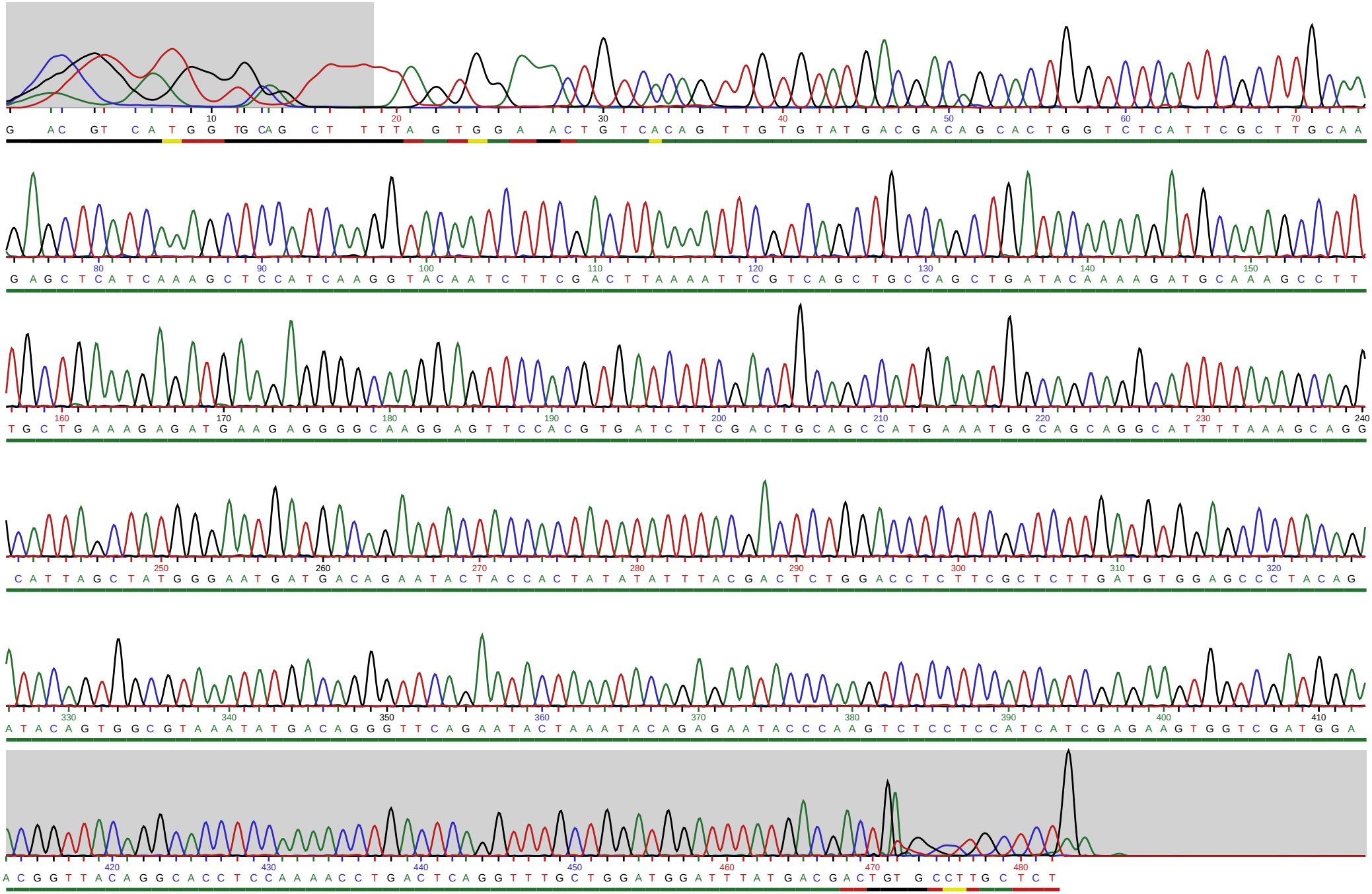

Clip. 1 BQ 20 WL 10

Sequence: ALPHA GLUK2_mGLUK2-F

Clipped length:	458	Samples:	12073	Quality:	0 - 9
Left clip:	19	Bases:	483		10 - 19
Right clip:	476	Average spacing:	25.0		20 - 29
Avg. qual. in clip.:	58.65	Average quality >=	10: 14, 20: 5, 30: 442		>= 30

Clip. 1 BQ 20 WL 10

Sequence: ALPHA GLUK2_mGLUK2-F

Clipped length:	458	Samples:	12073	Quality:	0 - 9
Left clip:	19	Bases:	483		10 - 19
Right clip:	476	Average spacing:	25.0		20 - 29
Avg. qual. in clip.:	58.65	Average quality >=	10: 14, 20: 5, 30: 442		>= 30

Clip. 1 BQ 20 WL 10 Sequence: ALPHA GLUK3_mGLUK3-R

Clipped length:	514	Samples:	13737	Quality:	0 - 9
Left clip:	30	Bases:	543		10 - 19
Right clip:	543	Average spacing:	26.0		20 - 29
Avg. qual. in clip.:	42.03	Average quality >=	10: 33, 20: 56, 30: 425		>= 30

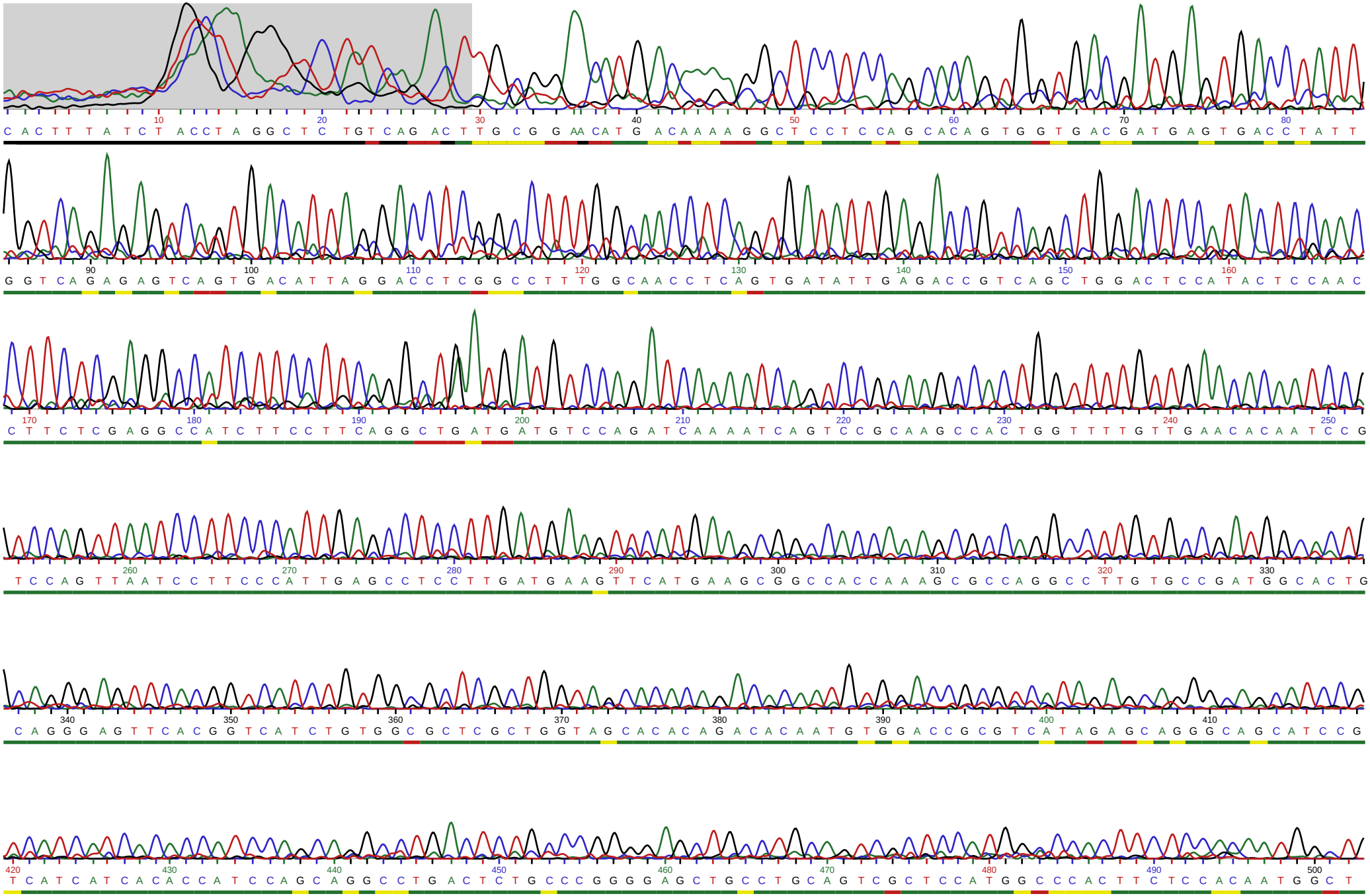

Clip. 1 BQ 20 WL 10 Sequence: ALPHA GLUK3_mGLUK3-R

Clipped length:	514	Samples:	13737	Quality:	0 - 9
Left clip:	30	Bases:	543		10 - 19
Right clip:	543	Average spacing:	26.0		20 - 29
Avg. qual. in clip.:	42.03	Average quality >=	10: 33, 20: 56, 30: 425		>= 30

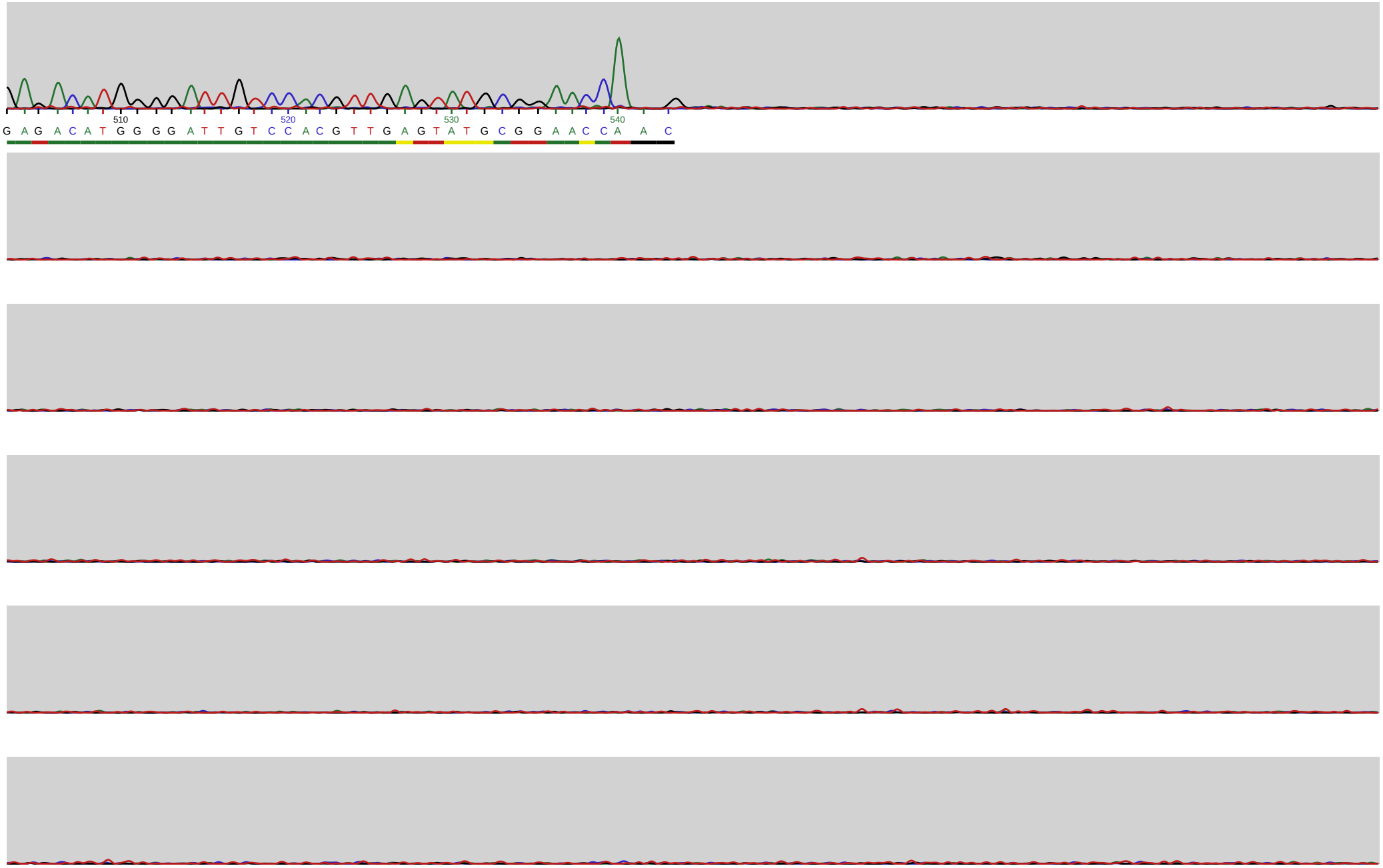

Clip. 1 BQ 20 WL 10

Sequence: ALPHA GLUK3_mGLUK3-R

Clipped length:	514	Samples:	13737	Quality:	0 - 9
Left clip:	30	Bases:	543		10 - 19
Right clip:	543	Average spacing:	26.0		20 - 29
Avg. qual. in clip.:	42.03	Average quality >=	10: 33, 20: 56, 30: 425		>= 30

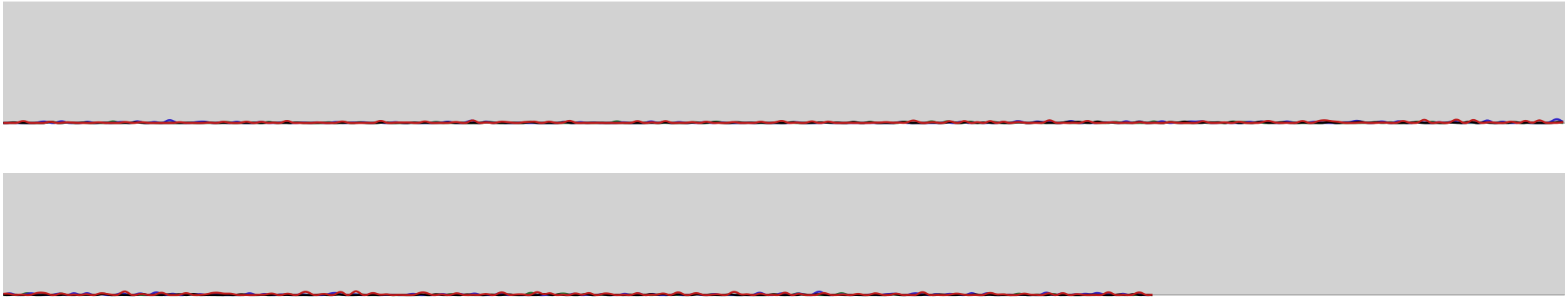

Clip. 1 BQ 20 WL 10 Sequence: alpha GluK 4 R_GluK-4-R

Clipped length:	266	Samples:	15889	Quality:	0 - 9
Left clip:	179	Bases:	453		10 - 19
Right clip:	444	Average spacing:	36.0		20 - 29
Avg. qual. in clip.:	37.48	Average quality >=	10: 54, 20: 67, 30: 303		>= 30

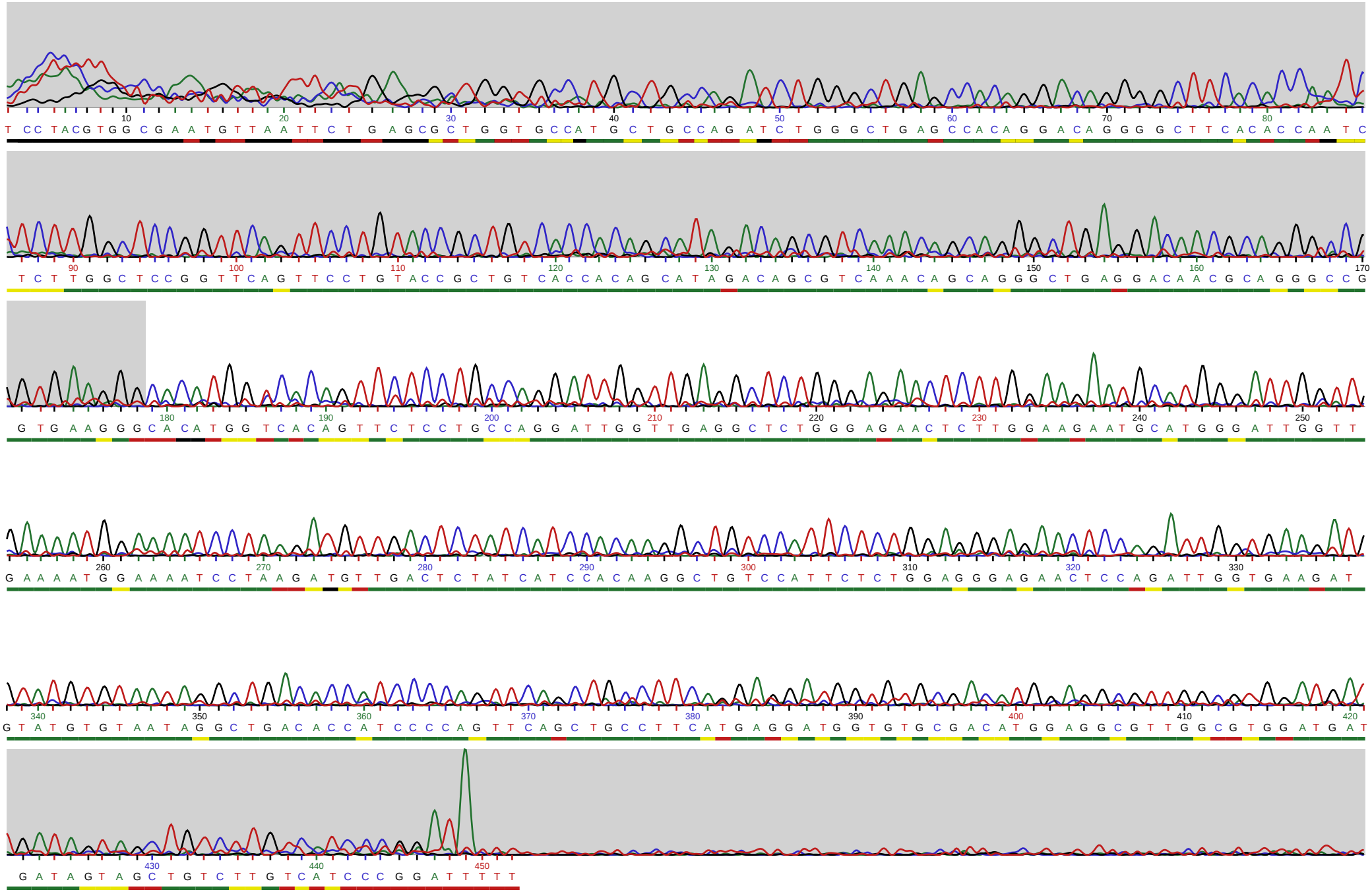

Sequence: alpha GluK 4 R_GluK-4-R

Clipped length:	266	Samples:	15889	Quality:	0 - 9
Left clip:	179	Bases:	453		10 - 19
Right clip:	444	Average spacing:	36.0		20 - 29
Avg. qual. in clip.:	37.48	Average quality >=	10: 54, 20: 67, 30: 303		>= 30

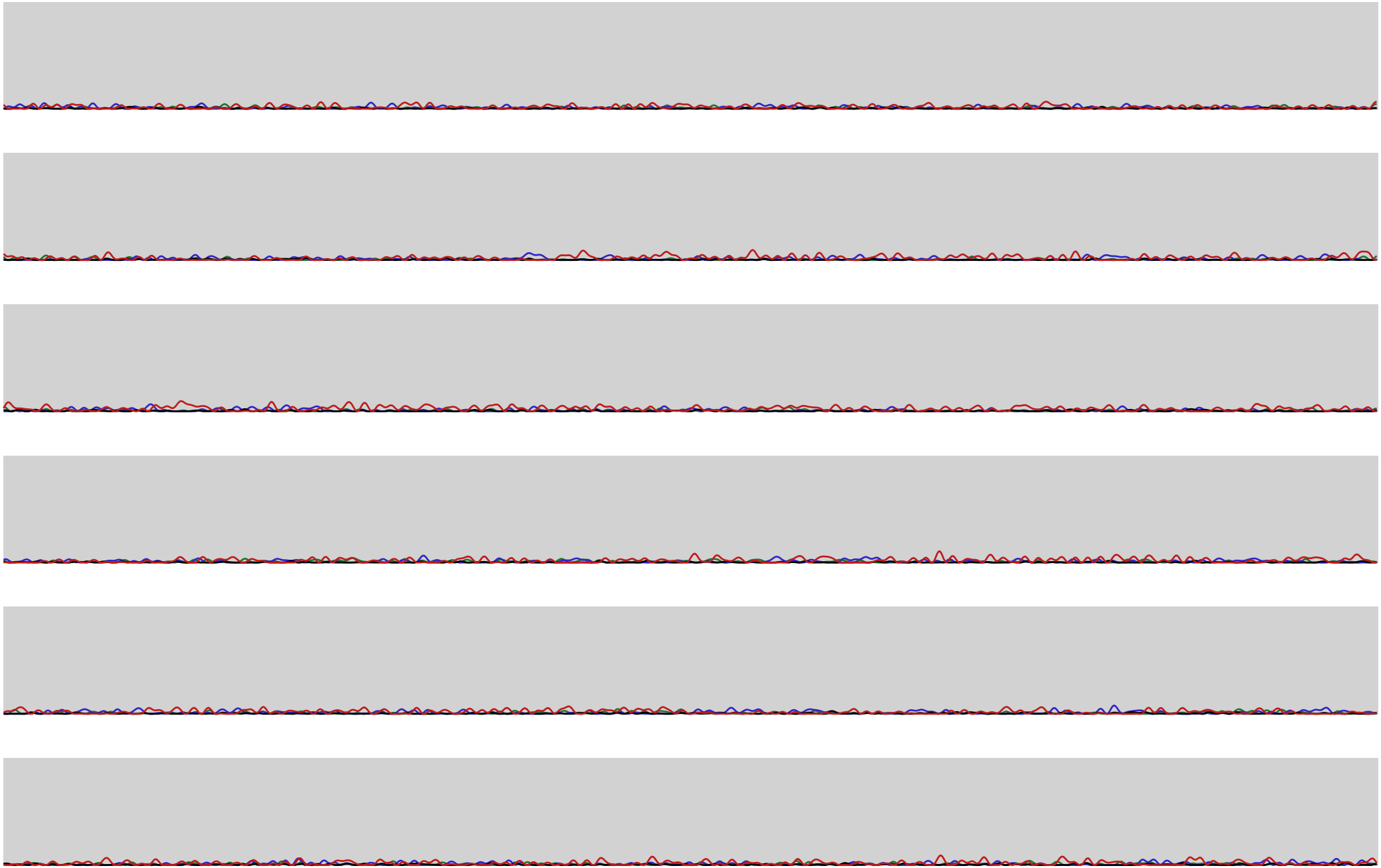

Clip. 1 BQ 20 WL 10

Sequence: alpha GluK 4 R_GluK-4-R

Clipped length:	266	Samples:	15889	Quality:	0 - 9
Left clip:	179	Bases:	453		10 - 19
Right clip:	444	Average spacing:	36.0		20 - 29
Avg. qual. in clip.:	37.48	Average quality >=	10: 54, 20: 67, 30: 303		>= 30

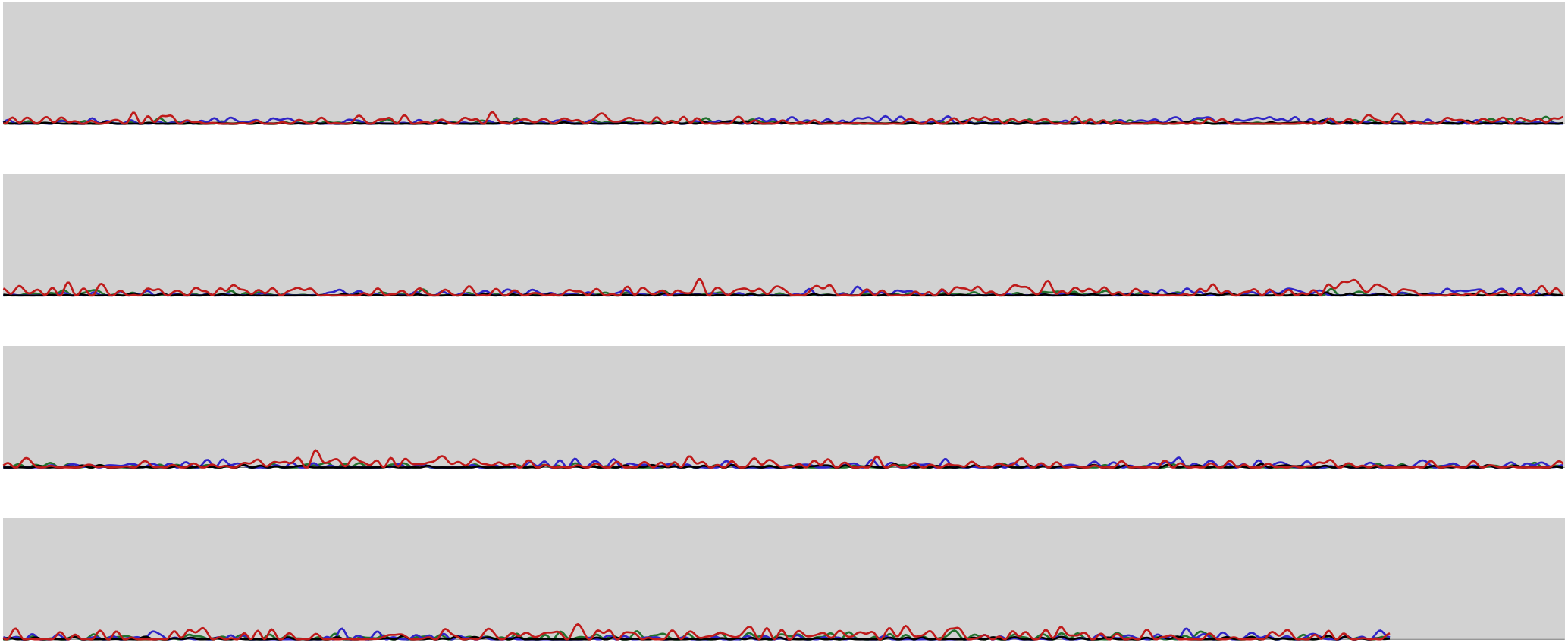

Clip. 1 BQ 20 WL 10 Sequence: ALPHA GLUK5_mGLUK5-F

Clipped length:	488	Samples:	13938	Quality:	0 - 9
Left clip:	13	Bases:	500		10 - 19
Right clip:	500	Average spacing:	28.0		20 - 29
Avg. qual. in clip.:	48.41	Average quality >=	10: 13, 20: 22, 30: 450		>= 30

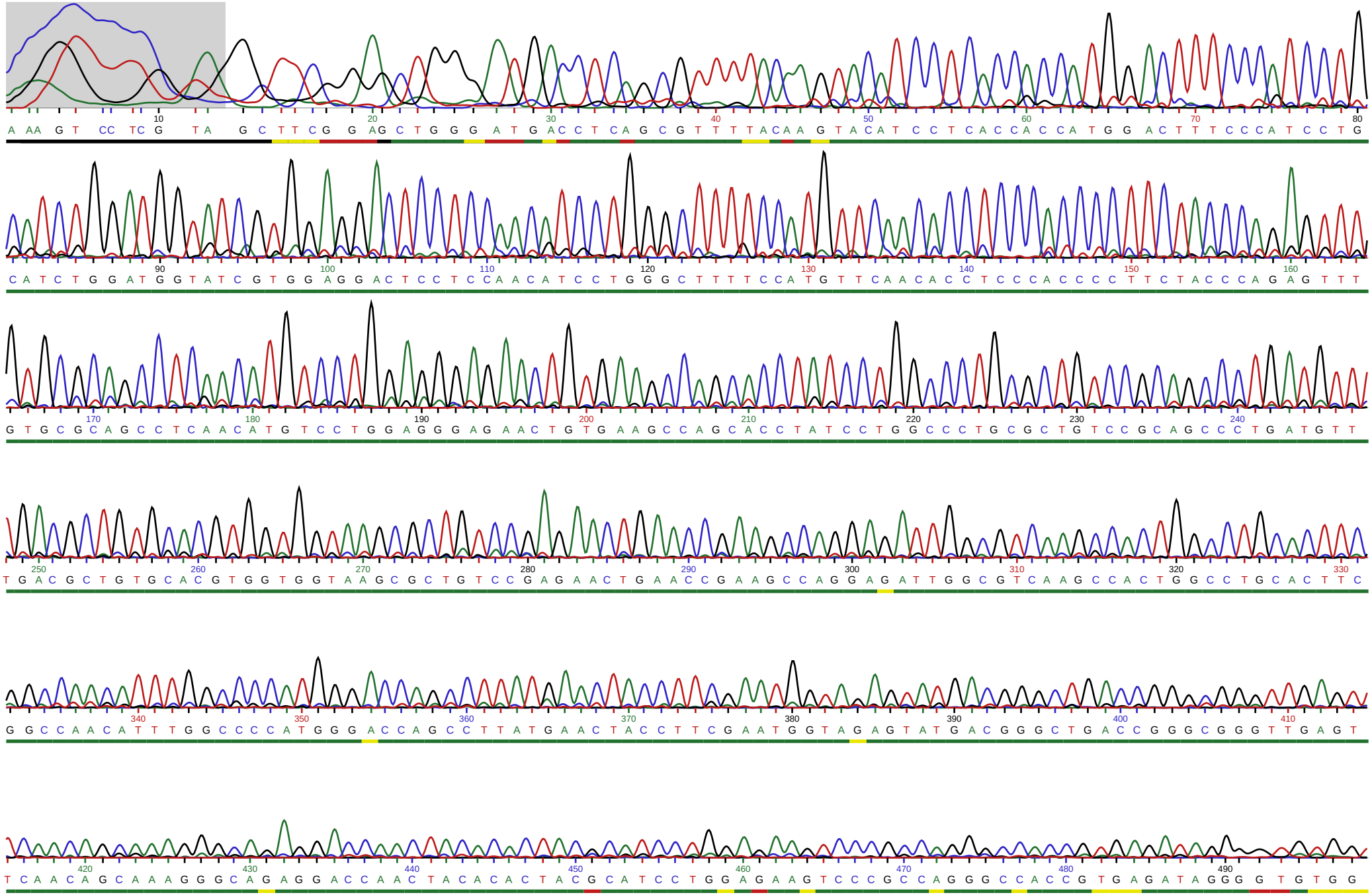

Clip. 1 BQ 20 WL 10

Sequence: ALPHA GLUK5_mGLUK5-F

Clipped length:	488	Samples:	13938	Quality:	0 - 9
Left clip:	13	Bases:	500		10 - 19
Right clip:	500	Average spacing:	28.0		20 - 29
Avg. qual. in clip.:	48.41	Average quality >=	10: 13, 20: 22, 30: 450		>= 30

Clip. 1 BQ 20 WL 10

Sequence: ALPHA GLUK5_mGLUK5-F

Clipped length:	488	Samples:	13938	Quality:	0 - 9
Left clip:	13	Bases:	500		10 - 19
Right clip:	500	Average spacing:	28.0		20 - 29
Avg. qual. in clip.:	48.41	Average quality >=	10: 13, 20: 22, 30: 450		>= 30

Clip. 1 BQ 20 WL 10 Sequence: ALPHA NETO 1_NETO-1-F

Clipped length:	179	Samples:	14835	Quality: 0 - 9	
Left clip:	13	Bases:	479	10 - 19	
Right clip:	191	Average spacing:	31.0	20 - 29	
Avg. qual. in clip.:	51.9	Average quality >=	10: 212, 20: 39, 30: 158	>= 30	

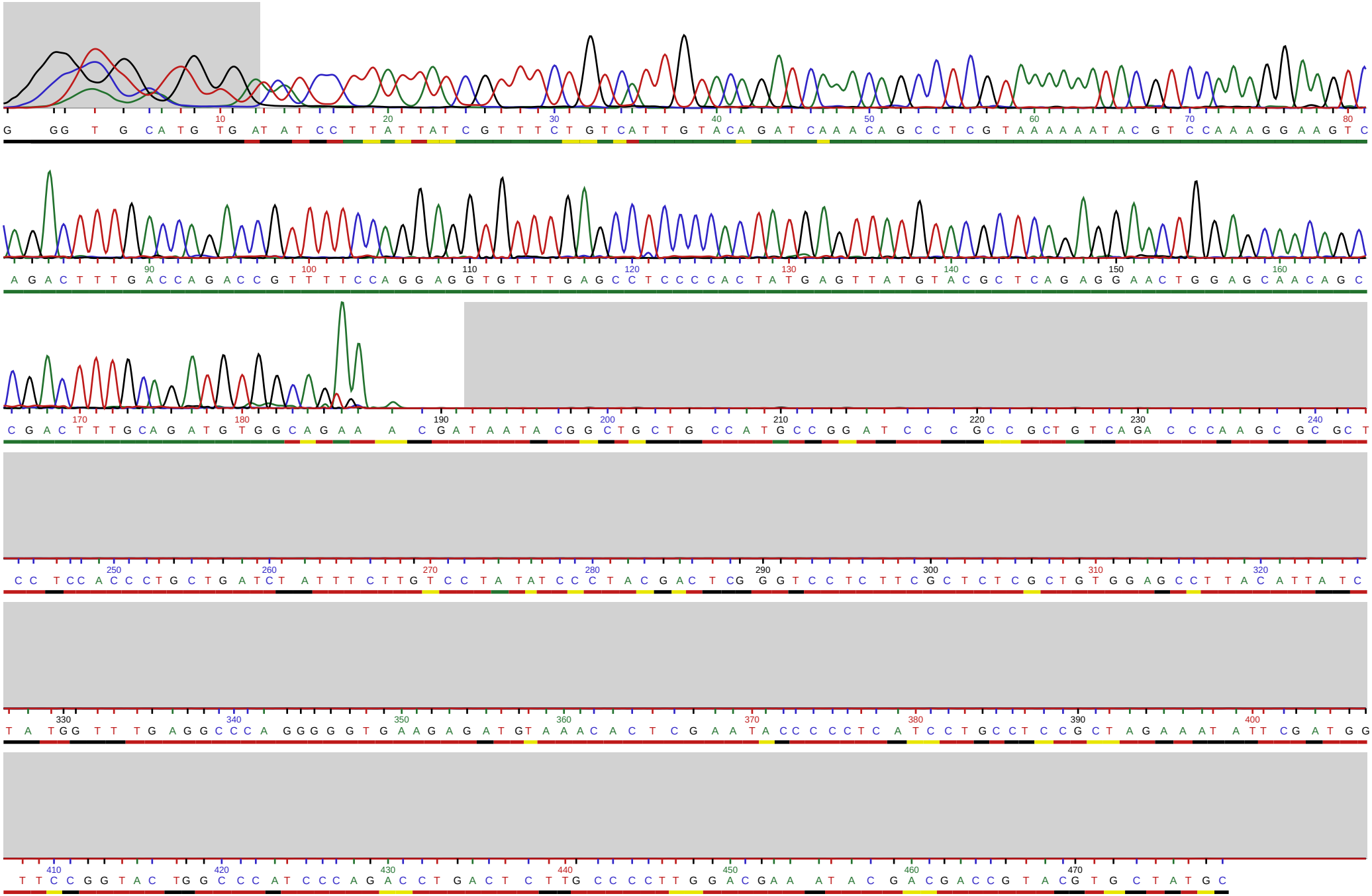

Clip. 1 BQ 20 WL 10

Sequence: ALPHA NETO 1_NETO-1-F

Clipped length:	179	Samples:	14835	Quality:	0 - 9
Left clip:	13	Bases:	479		10 - 19
Right clip:	191	Average spacing:	31.0		20 - 29
Avg. qual. in clip.:	51.9	Average quality >=	10: 212, 20: 39, 30: 158		>= 30

Clip. 1 BQ 20 WL 10 Sequence: ALPHA NETO 2_NETO-2-F

Clipped length:	185	Samples:	16280	Quality:	0 - 9
Left clip:	11	Bases:	494		10 - 19
Right clip:	195	Average spacing:	33.0		20 - 29
Avg. qual. in clip.:	53.98	Average quality >=	10: 228, 20: 30, 30: 163		>= 30

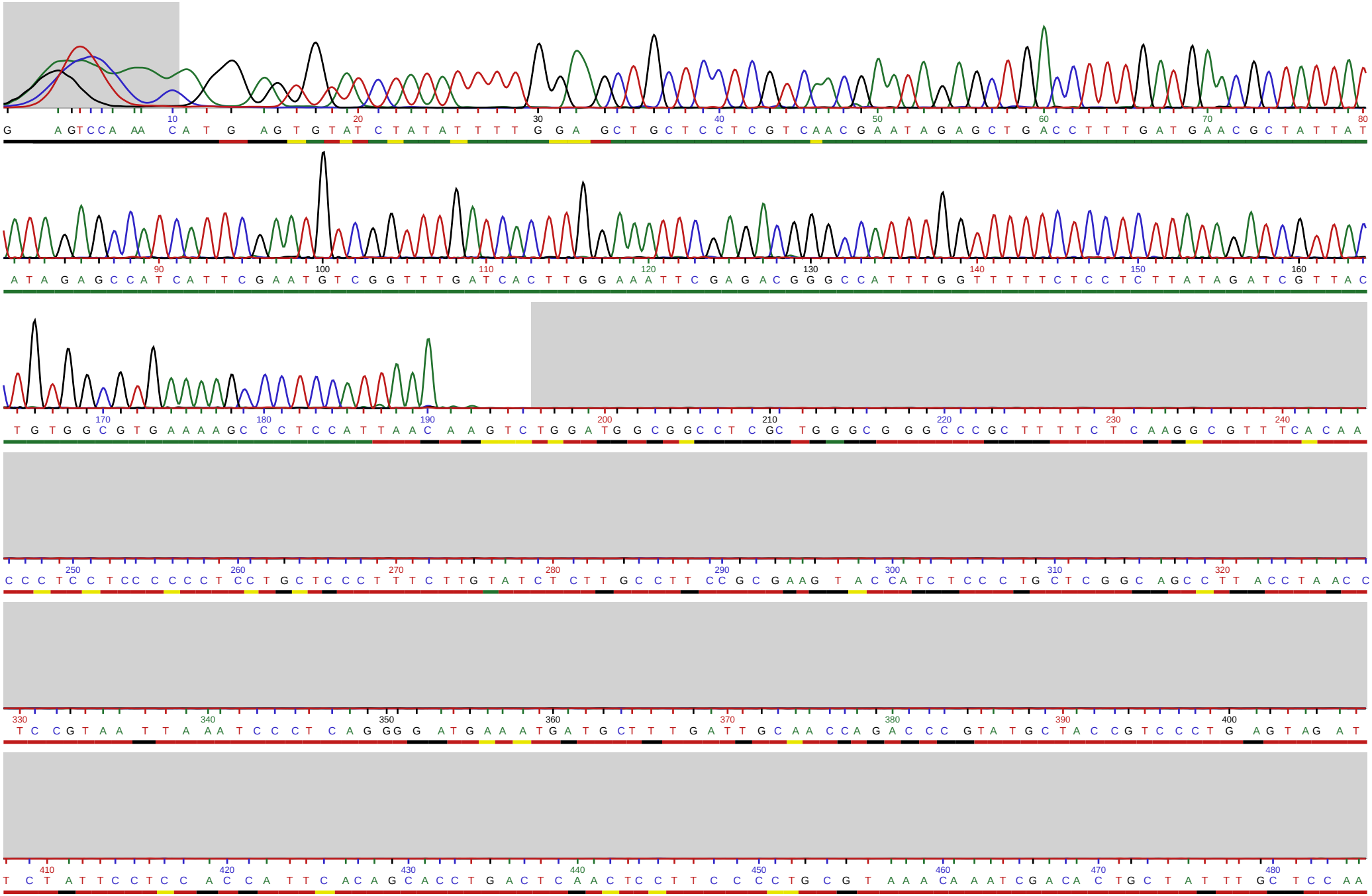

Clip. 1 BQ 20 WL 10 Sequence: ALPHA NETO 2_NETO-2-F

Clipped length:	185	Samples:	16280	Quality:	0 - 9
Left clip:	11	Bases:	494		10 - 19
Right clip:	195	Average spacing:	33.0		20 - 29
Avg. qual. in clip.:	53.98	Average quality >=	10: 228, 20: 30, 30: 163		>= 30

Clip. 1 BQ 20 WL 10

Sequence: ALPHA NETO 2_NETO-2-F

Clipped length:	185	Samples:	16280	Quality:	0 - 9
Left clip:	11	Bases:	494		10 - 19
Right clip:	195	Average spacing:	33.0		20 - 29
Avg. qual. in clip.:	53.98	Average quality >=	10: 228, 20: 30, 30: 163		>= 30

Clip. 1 BQ 20 WL 10 Sequence: Rat Islet GluK1_RK1-F

Clipped length:	422	Samples:	13340	Quality:	0 - 9
Left clip:	9	Bases:	663		10 - 19
Right clip:	430	Average spacing:	21.0		20 - 29
Avg. qual. in clip.:	57.22	Average quality >=	10: 170, 20: 26, 30: 398		>= 30

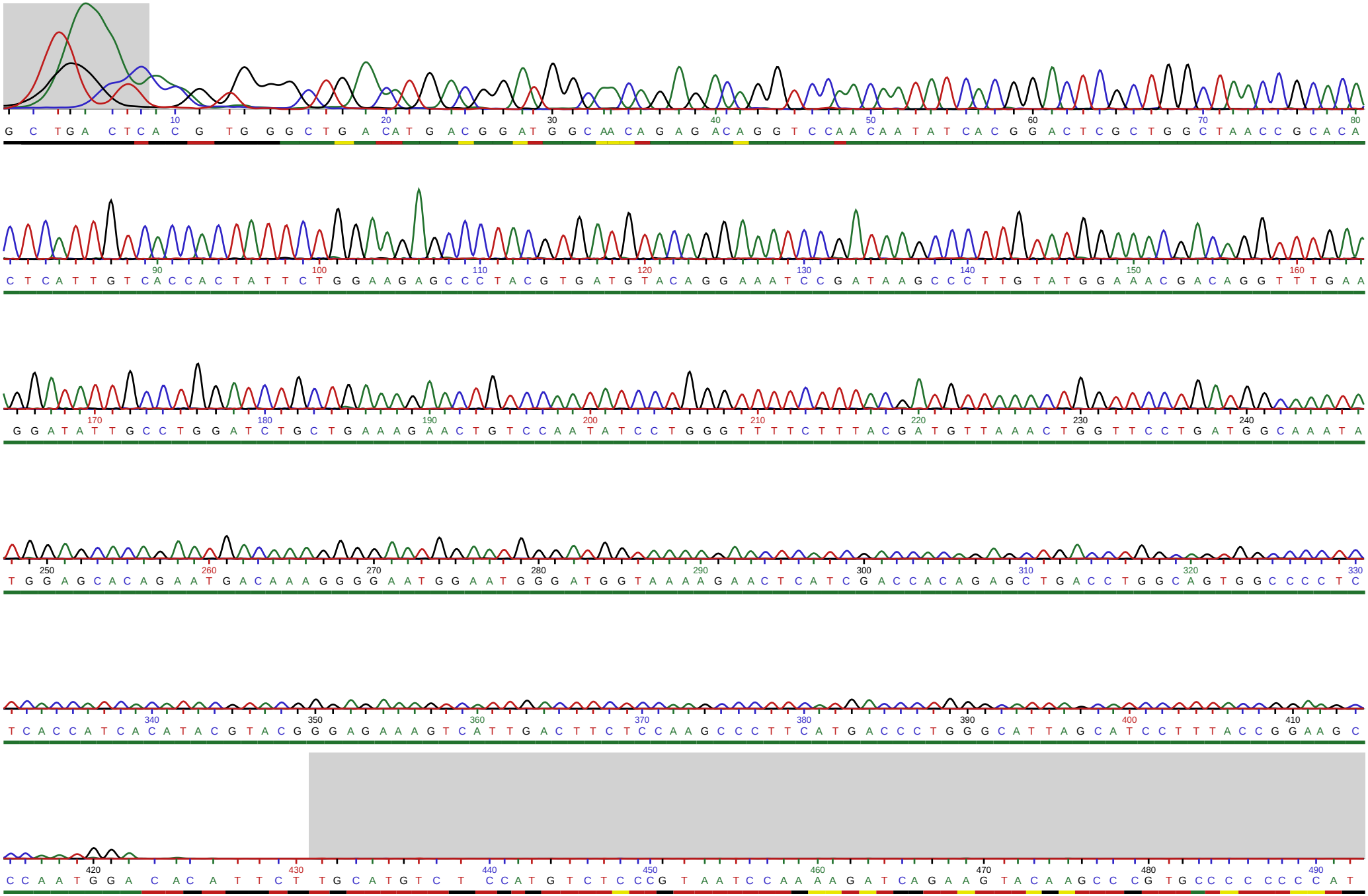

Clip. 1 BQ 20 WL 10 Sequence: Rat Islet GluK1_RK1-F

Clipped length:	422	Samples:	13340	Quality:	0 - 9
Left clip:	9	Bases:	663		10 - 19
Right clip:	430	Average spacing:	21.0		20 - 29
Avg. qual. in clip.:	57.22	Average quality >=	10: 170, 20: 26, 30: 398		>= 30

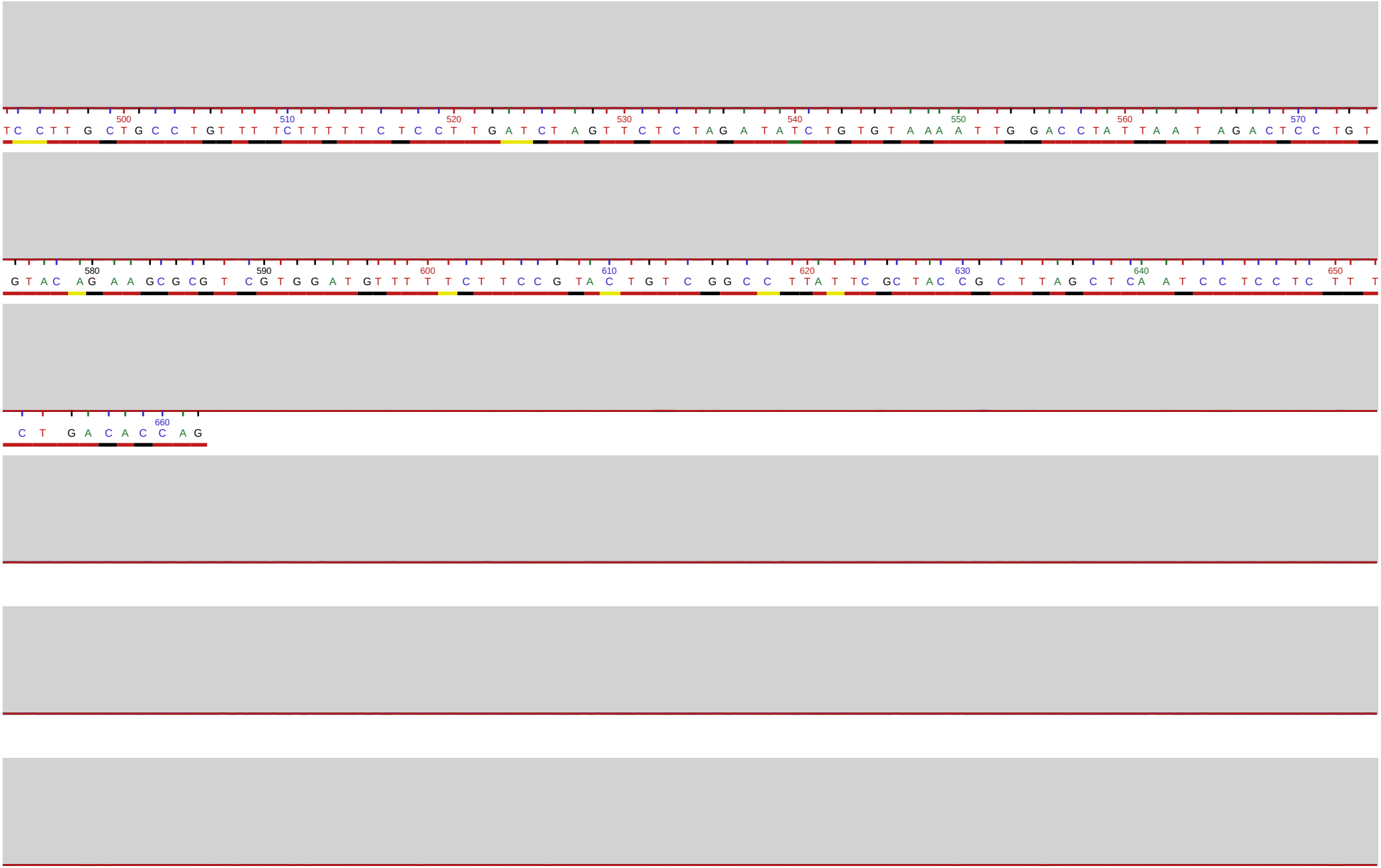

Clip. 1 BQ 20 WL 10

Sequence: Rat Islet GluK1_RK1-F

Clipped length:	422	Samples:	13340	Quality:	0 - 9
Left clip:	9	Bases:	663		10 - 19
Right clip:	430	Average spacing:	21.0		20 - 29
Avg. qual. in clip.:	57.22	Average quality >=	10: 170, 20: 26, 30: 398		>= 30

Clip. 1 BQ 20 WL 10 Sequence: Rat Islet GluK2_RK2-F

Clipped length:	503	Samples:	13516	Quality:	0 - 9
Left clip:	18	Bases:	910		10 - 19
Right clip:	520	Average spacing:	15.0		20 - 29
Avg. qual. in clip.:	57.0	Average quality >=	10: 276, 20: 76, 30: 474		>= 30

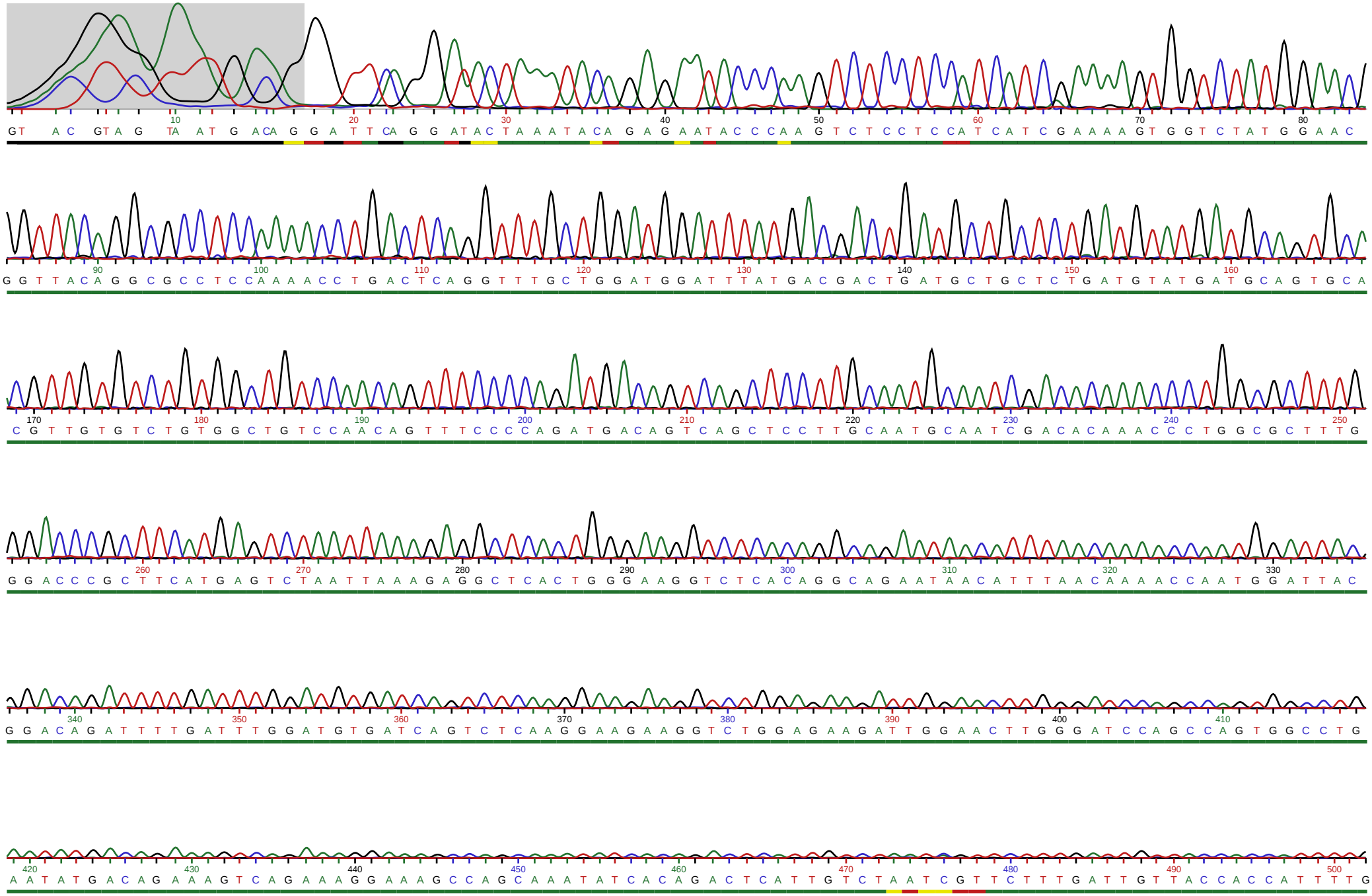

Clip. 1 BQ 20 WL 10 Sequence: Rat Islet GluK2_RK2-F

Clipped length:	503	Samples:	13516	Quality:	0 - 9
Left clip:	18	Bases:	910		10 - 19
Right clip:	520	Average spacing:	15.0		20 - 29
Avg. qual. in clip.:	57.0	Average quality >=	10: 276, 20: 76, 30: 474		>= 30

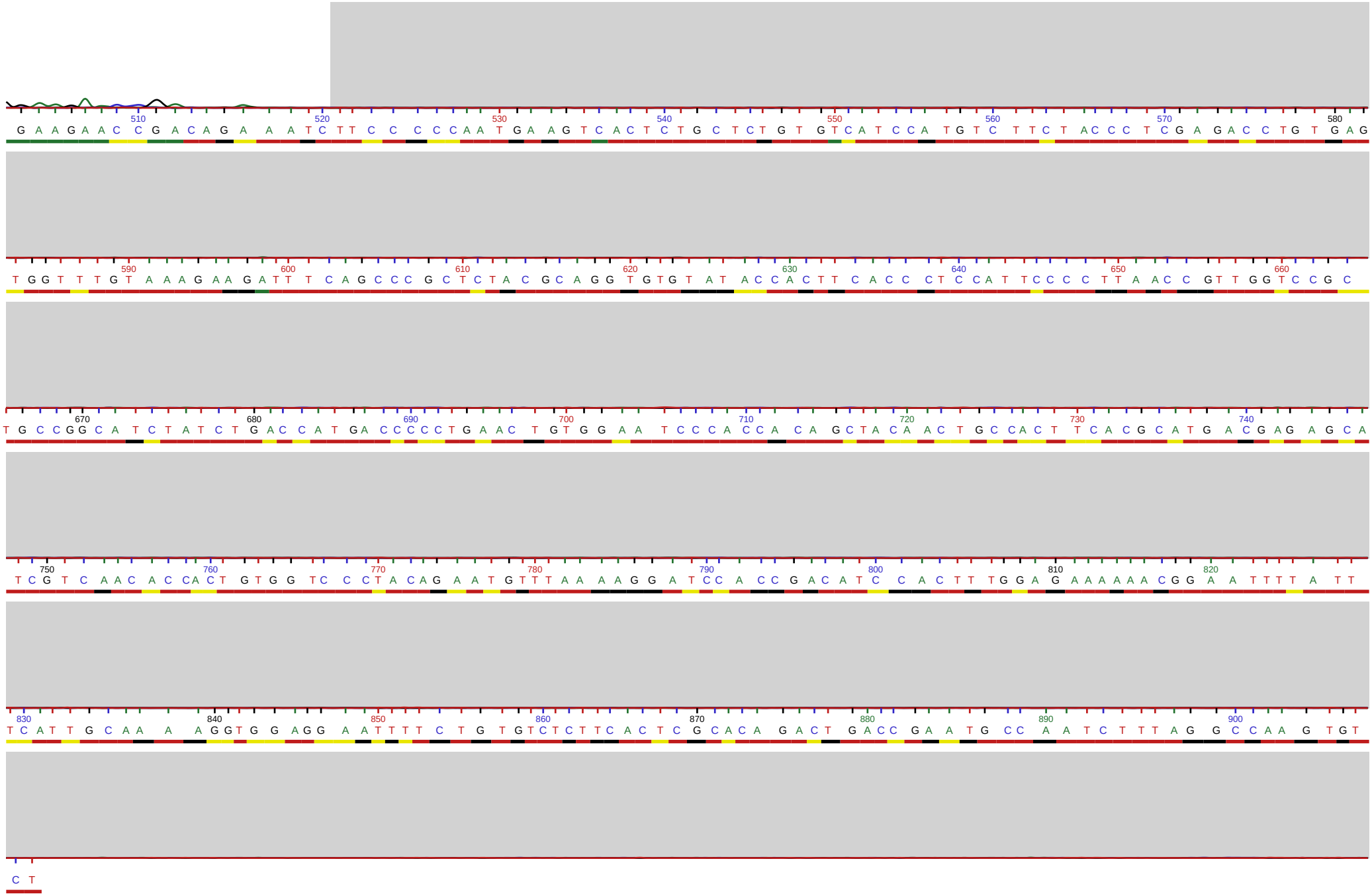

Clip. 1 BQ 20 WL 10

Sequence: Rat Islet GluK2_RK2-F

Clipped length:	503	Samples:	13516	Quality:	0 - 9
Left clip:	18	Bases:	910		10 - 19
Right clip:	520	Average spacing:	15.0		20 - 29
Avg. qual. in clip.:	57.0	Average quality >=	10: 276, 20: 76, 30: 474		>= 30

Clip. 1 BQ 20 WL 10 Sequence: Rat Islet GluK3_RK3-F

Clipped length:	455	Samples:	13428	Quality:	0 - 9
Left clip:	12	Bases:	704		10 - 19
Right clip:	466	Average spacing:	20.0		20 - 29
Avg. qual. in clip.:	57.0	Average quality >=	10: 173, 20: 29, 30: 443		>= 30

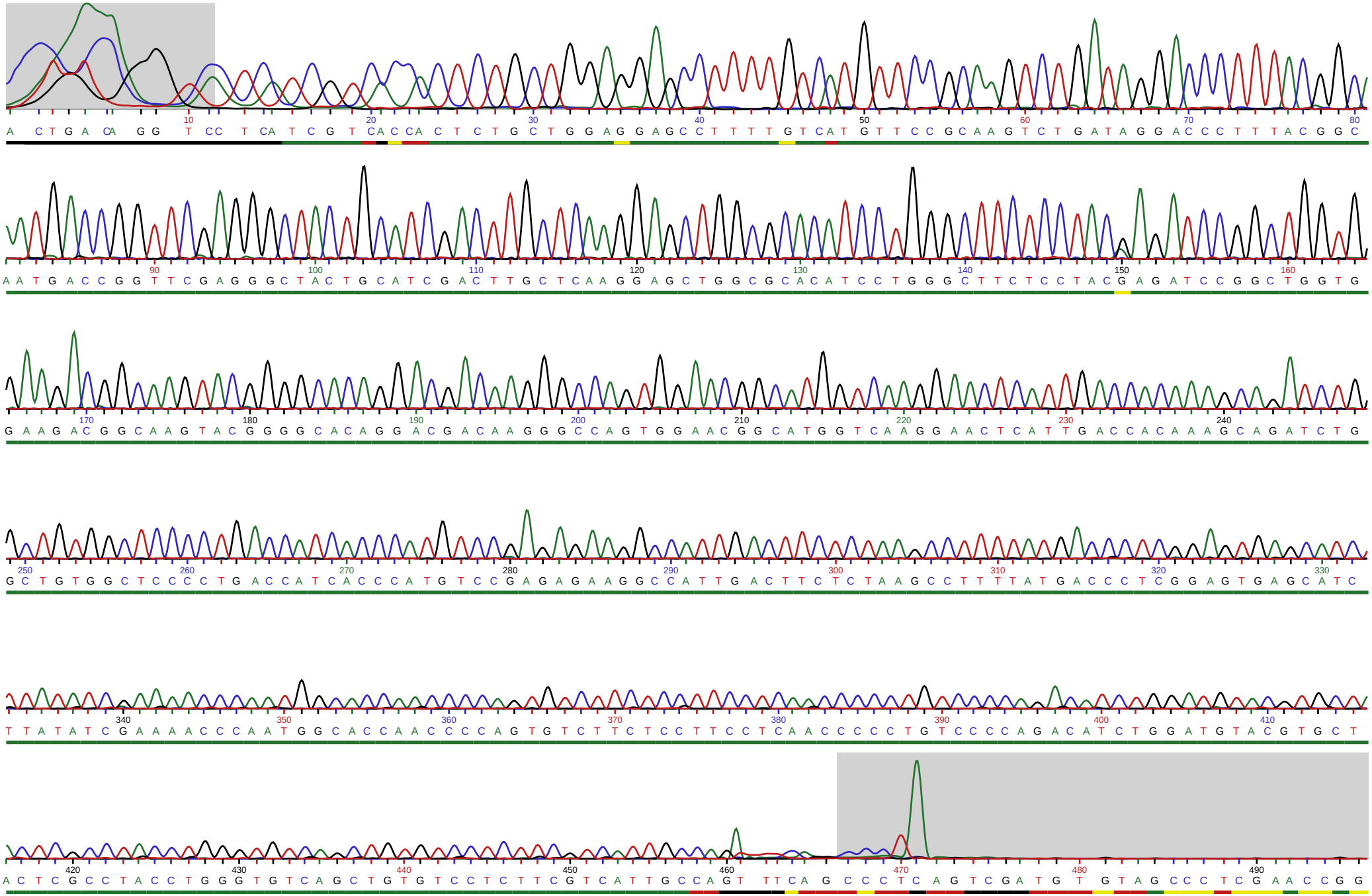

Clip. 1 BQ 20 WL 10 Sequence: Rat Islet GluK3_RK3-F

Clipped length:	455	Samples:	13428	Quality:	0 - 9
Left clip:	12	Bases:	704		10 - 19
Right clip:	466	Average spacing:	20.0		20 - 29
Avg. qual. in clip.:	57.0	Average quality >=	10: 173, 20: 29, 30: 443		>= 30

Clip. 1 BQ 20 WL 10

Sequence: Rat Islet GluK3_RK3-F

Clipped length:	455	Samples:	13428	Quality:	0 - 9
Left clip:	12	Bases:	704		10 - 19
Right clip:	466	Average spacing:	20.0		20 - 29
Avg. qual. in clip.:	57.0	Average quality >=	10: 173, 20: 29, 30: 443		>= 30

Clip. 1 BQ 20 WL 10 Sequence: Rat Islet GluK4_RK4-F

Clipped length:	287	Samples:	16304	Quality:	0 - 9
Left clip:	22	Bases:	360		10 - 19
Right clip:	308	Average spacing:	46.0		20 - 29
Avg. qual. in clip.:	45.25	Average quality >=	10: 49, 20: 44, 30: 236		>= 30

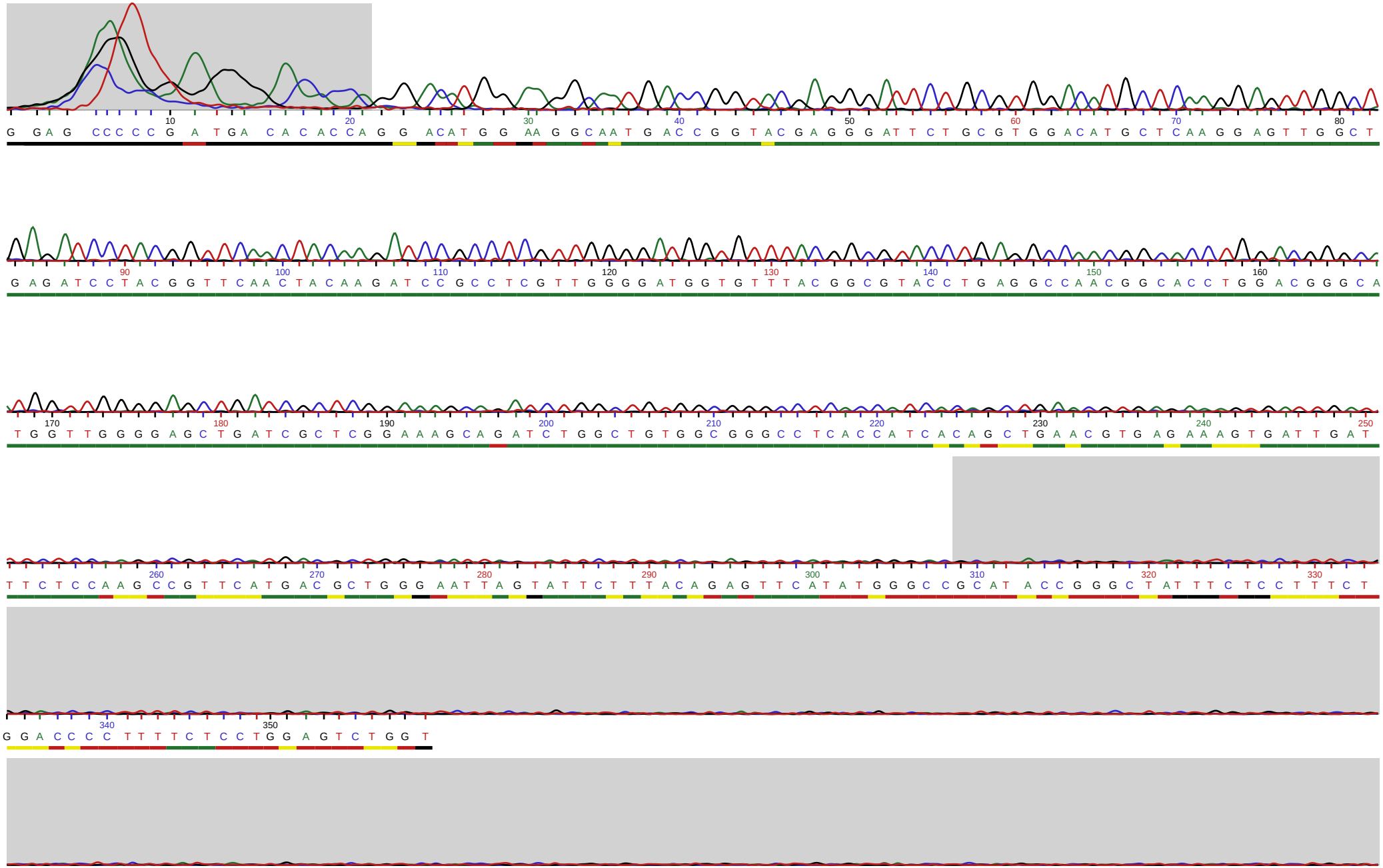

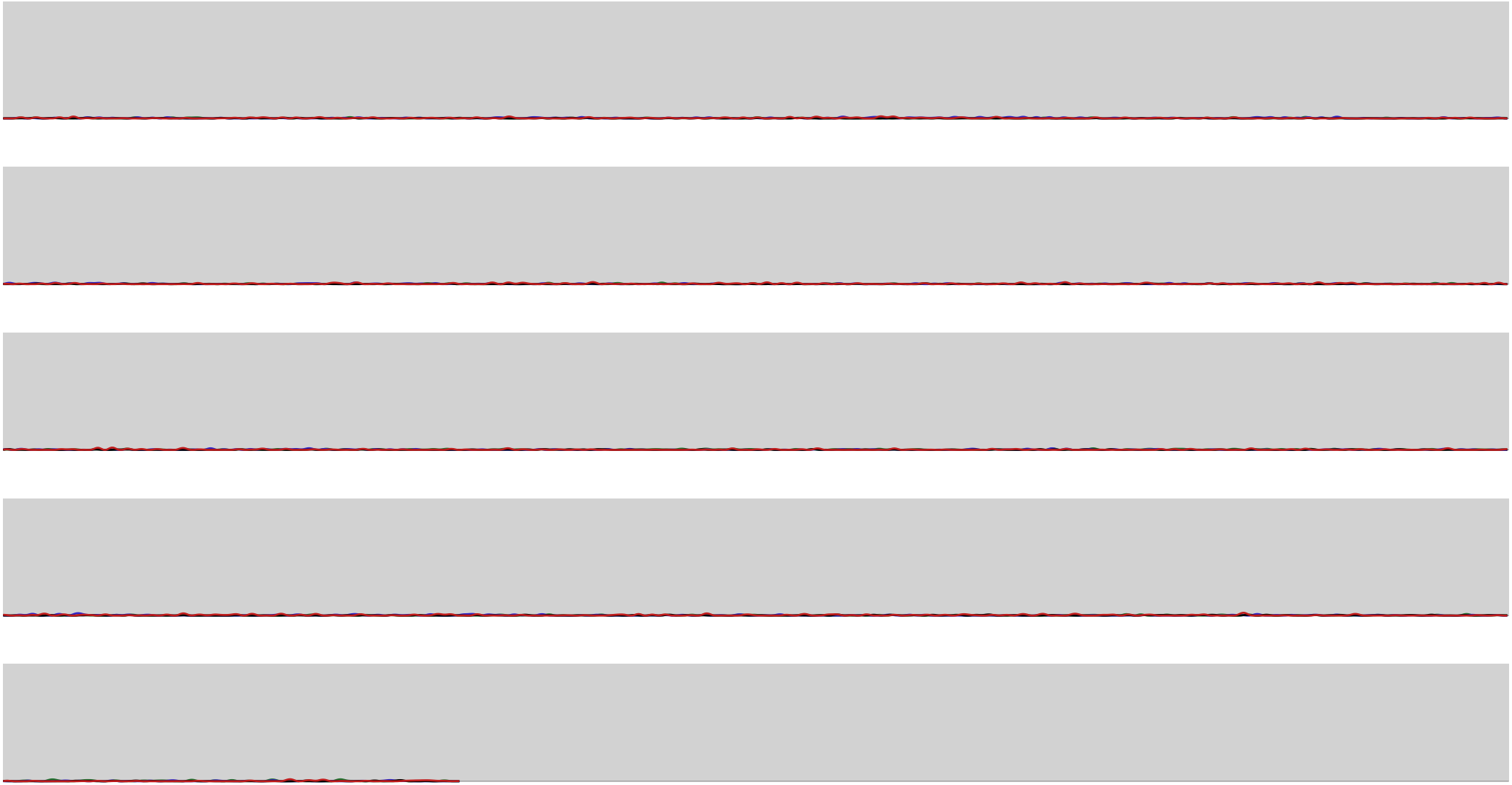

Clip. 1 BQ 20 WL 10 Sequence: Rat Islet GluK5_RK5-F

Clipped length:	399	Samples:	13713	Quality:	0 - 9
Left clip:	12	Bases:	515		10 - 19
Right clip:	410	Average spacing:	27.0		20 - 29
Avg. qual. in clip.:	56.03	Average quality >=	10: 87, 20: 12, 30: 374		>= 30

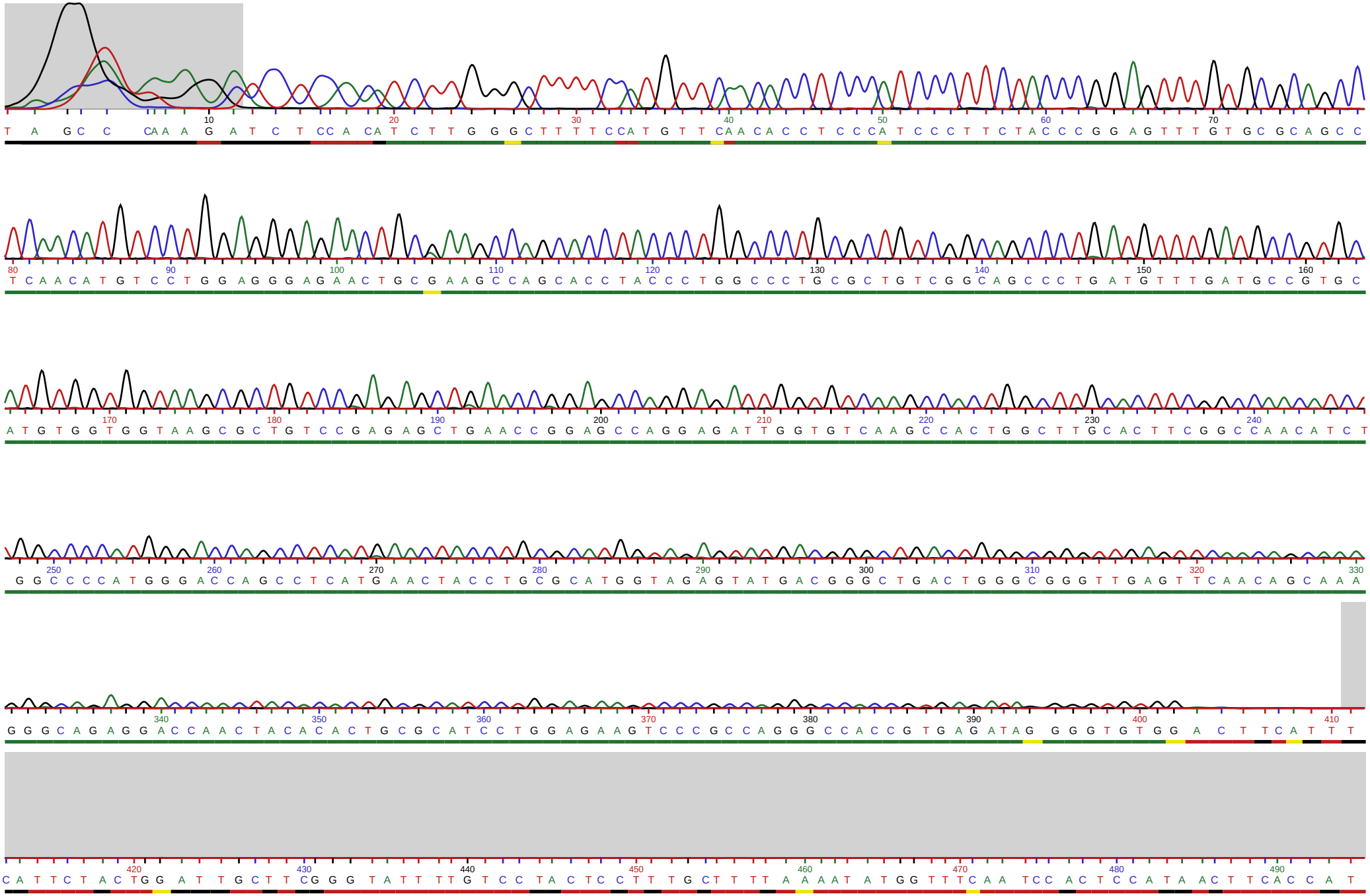

Clip. 1 BQ 20 WL 10 Sequence: Rat Islet GluK5_RK5-F

Clipped length:	399	Samples:	13713	Quality:	0 - 9
Left clip:	12	Bases:	515		10 - 19
Right clip:	410	Average spacing:	27.0		20 - 29
Avg. qual. in clip.:	56.03	Average quality >=	10: 87, 20: 12, 30: 374		>= 30

Clip. 1 BQ 20 WL 10

Sequence: Rat Islet GluK5_RK5-F

Clipped length:	399	Samples:	13713	Quality:	0 - 9
Left clip:	12	Bases:	515		10 - 19
Right clip:	410	Average spacing:	27.0		20 - 29
Avg. qual. in clip.:	56.03	Average quality >=	10: 87, 20: 12, 30: 374		>= 30

Clip. 1 BQ 20 WL 10 Sequence: RI Neto 1 A_Neto-1-F

Clipped length:	172	Samples:	12348	Quality:	0 - 9
Left clip:	20	Bases:	191		10 - 19
Right clip:	191	Average spacing:	65.0		20 - 29
Avg. qual. in clip.:	38.43	Average quality >=	10: 17, 20: 32, 30: 124		>= 30

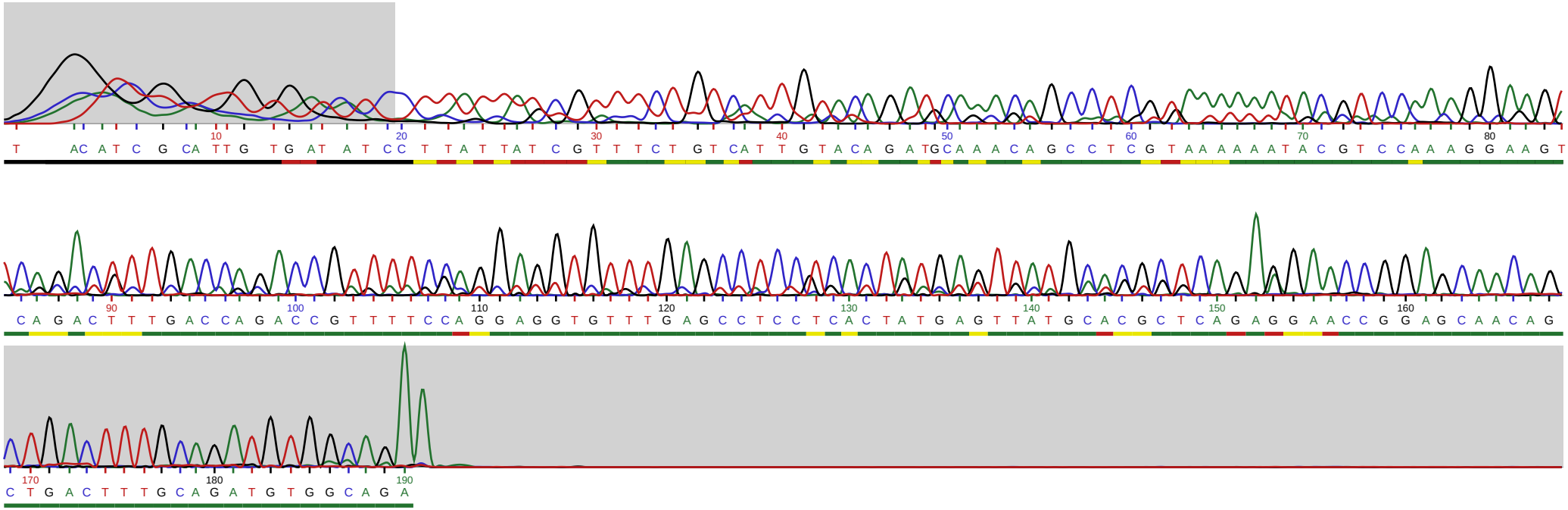

Clip. 1 BQ 20 WL 10 Sequence: RI Neto 1 A_Neto-1-F

Clipped length:	172	Samples:	12348	Quality:	0 - 9
Left clip:	20	Bases:	191		10 - 19
Right clip:	191	Average spacing:	65.0		20 - 29
Avg. qual. in clip.:	38.43	Average quality >=	10: 17, 20: 32, 30: 124		>= 30

Clip. 1 BQ 20 WL 10

Sequence: RI Neto 1 A_Neto-1-F

Clipped length:	172	Samples:	12348	Quality:	0 - 9
Left clip:	20	Bases:	191		10 - 19
Right clip:	191	Average spacing:	65.0		20 - 29
Avg. qual. in clip.:	38.43	Average quality >=	10: 17, 20: 32, 30: 124		>= 30

Clip. 1 BQ 20 WL 10 Sequence: RAT ISLET NETO 2_NETO-2.ab1

Clipped length:	183	Samples:	15510	Quality:	0 - 9
Left clip:	15	Bases:	496		10 - 19
Right clip:	197	Average spacing:	32.0		20 - 29
Avg. qual. in clip.:	53.79	Average quality >=	10: 231, 20: 28, 30: 169		>= 30

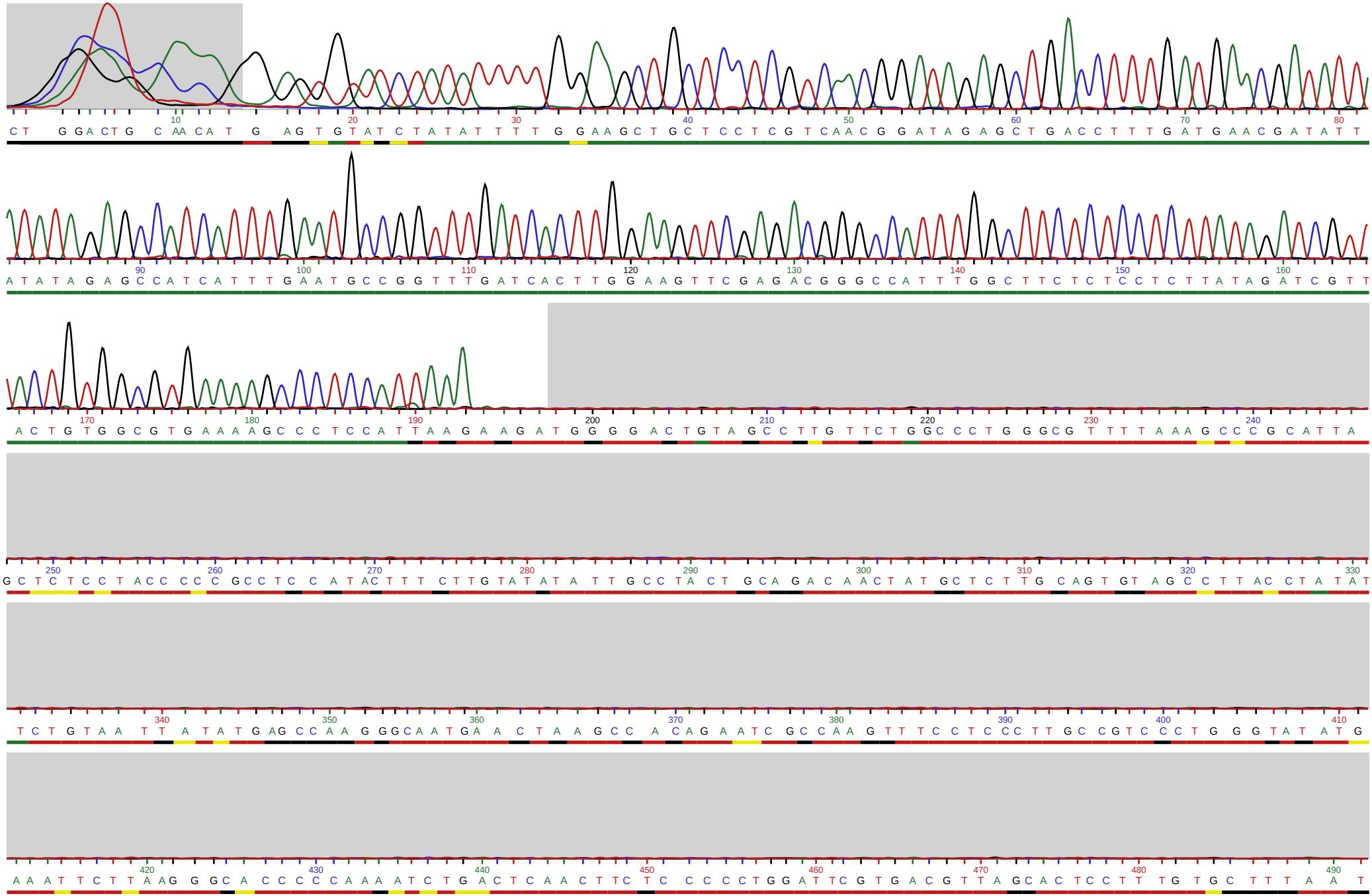

Clip. 1 BQ 20 WL 10 Sequence: RAT ISLET NETO 2_NETO-2.ab1

Clipped length:	183	Samples:	15510	Quality:	0 - 9
Left clip:	15	Bases:	496		10 - 19
Right clip:	197	Average spacing:	32.0		20 - 29
Avg. qual. in clip.:	53.79	Average quality >=	10: 231, 20: 28, 30: 169		>= 30